Biomaterials for manipulating mast cell activity

by

Shammy Raj

A thesis submitted in partial fulfillment of the requirements for the degree of

Doctor of Philosophy

in
Materials Engineering

Department of Chemical and Materials Engineering
University of Alberta

Abstract

Inflammation is a symphony of immune responses orchestrated by the different cells of immune system. The effect is soothing when the triggered immune response is healing against pathological invasions, tissue injuries, or an ailment. However, it becomes unpleasant when the immune response aggravates to allergies, autoimmune diseases, or when it complicates transplantations. The complexity of immune response is so vast that even after the given scientific advancements, only a few of the many discrete events pertaining to inflammations has been deciphered. Our understating of immune response is very specific, both with respect to the cells of immune system, and with respect to an inflammatory event; and that the interplay between these is yet to be comprehended. Having said that, it is incumbent upon engineers, to use these scientific understandings, however limited it may be, to better the lives of humankind.

Of various cells involved in an immune response, mast cells are the first responders. These cells are strategically located at the interface of a tissue and its external environment and get activated in response to a pathogenic agent. Activated mast cells release a plenty of biomolecules in their extracellular space, which act as chemoattractant for the downstream immune signaling. Immune mediators, as the released biomolecules are called, consists of cytokines, enzymes, biogenic amines, growth factors and reactive oxygen species (ROS). The premise of the thesis lies in designing materials, which would be useful in inflammation-targeted therapeutics. Since mast cells are de facto present as the first responders, emphasis has been put on designing materials which are responsive to mast cell functionality and characteristics.

Out of several mediators, ROS have been chosen as the primary mast cell specific mediator due to their immediate and localized release profiles. Furthermore, the selection of the stimulus mediator

was also governed by the easy synthesis of a ROS responsive molecules and its facile utilization in material design. A ROS responsive, bioactive thioketal (TK) molecule was synthesized and characterized. TK is cleaved into its parent molecules in ROS extensive environment. Synthesized TK was stable at physiological conditions (pH = 7.4). ROS activity of TK was ascertained by subjecting TK to Fenton's reagent. The in vitro biocompatibility and cell toxicity of TK was confirmed against islet cells. TK was deemed nontoxic to cells. TK was also used in *in vivo* transplantation of mouse islets where its biocompatibility was reaffirmed.

TK was then used to develop ROS responsive drug delivery platforms for the targeted delivery of anti-inflammatory dexamethasone (Dex) to the site of inflammation. Dex was successfully conjugated to the polyethylene glycol – polylactic acid (PEG-PLA) copolymer, and polyethylene glycol (PEG) through TK as a linker. ROS stimulated Dex release was confirmed in stimulated Fenton's reagent ROS solution. Both PEG-PLA and PEG systems responded to ROS by releasing cleaved Dex from the polymeric constructs. Nanoparticles were formed from the PEG-PLA construct through the film hydration method which showed a size of 14 nm and a –ve zeta potential. The nanoparticles were further subjected to Fenton's reagent to confirm Dex release.

Finally, a design rule to synthesize peptides specific to mast cell mas related G-protein receptor X2 (MRGPRX2) was devised, and a corresponding library of various peptides with differential mast cell activating potential was generated. Peptide activators of MRGPRX2 follows a generic rule of Xa-(Y)($n \geq 3$)-Xb where: Xa is an aromatic residue; Xb is a hydrophobic residue; and Y is a minimum 3 residue long sequence, containing a minimum of one positively charged residue with the remainder being uncharged residues. The design rule is an excellent tool to design inflammation targeted peptides with a desired mast cell activity. These could be very efficiently tethered on therapeutic systems to localize the therapy to the inflamed tissue.

Acknowledgement

I express my sincere gratitude to Dr. Larry D. Unsworth, my PhD supervisor for being an awesome mentor through my PhD. He has stood with me in my highs and lows and I cannot thank him enough. He has been a friend who has patiently listened to all my nonsensical ideas and my constant whinings. He has been my go-to man for both my scientific and non-scientific issues. Again, I cannot thank him enough.

I would like to thank Dr. Marianna Kulka for her help, support and guidance throughout my PhD.

I would like to thank Dr. Gary Eitzen, Dr. Peter Kwan, Dr. Jie Ding, Dr. Narcy Arizmendi, Mike Xia and Ashley Wagner for their help in conducting my research.

I thank my labmates - Mehdi, Dinuka, Markian, Shuhui, Rukhmani, Meng-Yi, Lei and Haleh. These guys were a treat to work with.

A big shout out to my friends - Aakanksha, Advaita, Angelica, Ankur, Antonio, Anupam, Dolly, Eleni, Fereshte, Hemant, Himanshi, Johnnson, Kasturi, Manika, Pallavi, Pratik, Puja, Rosmi, Ryan, Sachin, Sahil, Sarang, Satarupa, Shilpi, Shital, Shubham, Soumya, Sumalee, Syed, Upasana and Vineet for diluting the sufferings of PhD.

To the most beautiful and the most wonderful people in the world - maa, papa, Shashi and Summy. Thank you for supporting me, believing in me and standing by me.

Table of Contents

List of Tables

List of figures

Chapter 1. Introduction

1.1. Inflammation and mast cells

Immune response or inflammation is a protective mechanism through which a body protects itself from the physiologically unfavorable conditions, foreign entities and diseases. Broadly classified into innate and adaptive immune responses, the immune response is an intricate collaboration of different cells and tissue of the immune system to defend system against a foreign invasion. The innate immune response is a preexisting line of defense which is immediate and non-specific. It includes skin and mucus layer as anatomical barrier, temperature and pH as physiological barriers, activation of immune cells like tissue resident mast cells and macrophages, and a consecutive localization of serum proteins and neutrophils to the site of invasion. On contrary, the adaptive immune response is specific and succeeds innate immune response, in other words, the innate immune response activates the adaptive immune response. Adaptive immune response confers a long-lasting immunity against specific antigens. It is mediated by the B and T lymphocytes. The lymphocytes recognize the antigens, and secrets antibodies and proinflammatory cytokines to activate various pathways of immune system [1].

At the intersection of innate and adaptive immune responses lie the mast cell. Mast cells play an important role in both innate and adaptive immune response [2,3]. Mast cells are primarily located at the interface of a tissue and its external environment, and hence are the first responder in an inflammatory response. The cells are composed of granules, which contain preformed immunogenic mediators (Figure 1.1) [4]. The mediators range from tissue remodeling enzymes, antimicrobial enzymes, growth factors and proinflammatory biomolecules like histamines and cytokines among others. Once activated, mast cells degranulate to release the granular contents in

the extracellular space [4]. Table 1.1 lists several molecules that are released upon mast cell activation. Release of antimicrobial enzymes like β-hexosamindases, and proinflammtory molecules like interleukins and tumor necrosis factors that attract other inflammatory cells like neutrophils to the site of inflammation suggest the role of mast cell in innate immunity. Furthermore, the released molecules also serve as a chemoattractant for the antigen presenting cells and lymphocytes, which confirms their roles in adaptive immunity [3].

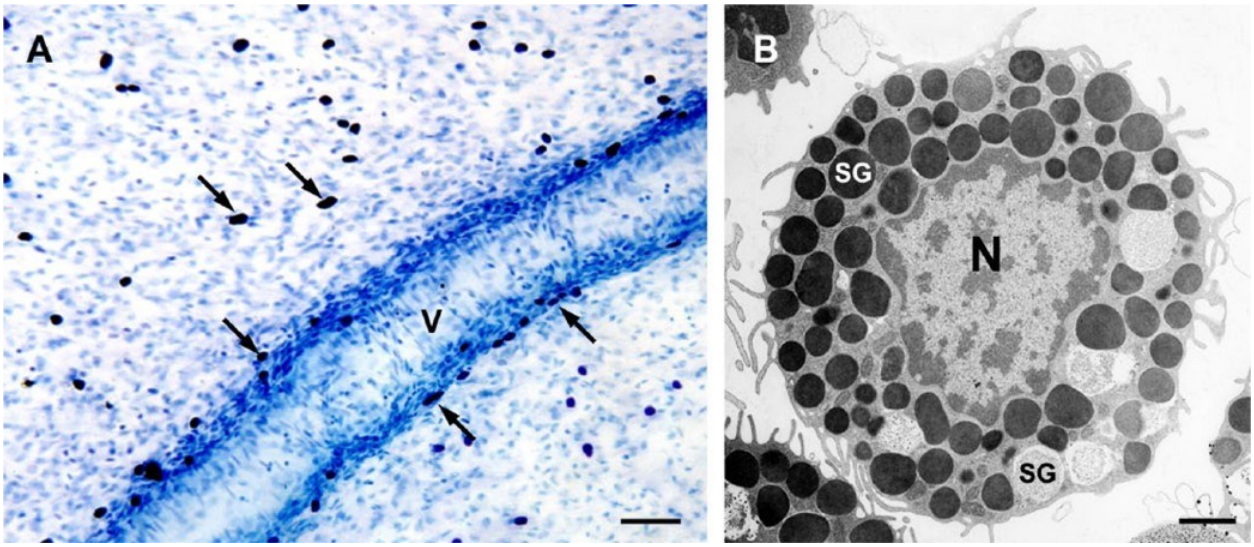

Figure 1.1. Mast cell location and structure. A) Toluidine blue stained mast cells (shown by arrow) along the wall of a blood vessel (shown by V); bar = 25 µm. (B) Transmission electron microscopy images of matured peritoneal mast cell with secretory granules (SG) and nucleus (N); bar = 1 µm. This image has been taken from [2] with permission.

1.2. Mast cell activation and pathological significance

Mast cell expresses several receptors on its surface, activation through which results in cell degranulation and release of stored mediators into the extracellular space. Of all the activation pathways, activation through surface expressed FcεR1 receptors are the best studied. FcεR1 based activation pathway is mediated by immunoglobulin E (IgE), a component of the adaptive immune response. Antigen specific IgE, produced by the B-lymphocytes, bind to FcεR1 receptor to form

IgE-FcεR1 complex. IgE specific antigen then binds to this IgE-FcεR1 complex and induces the crosslinking of the FcεR1 receptors. Crosslinking of the receptor subsequently initiates a cascade of downstream signaling that causes mast cell degranulation [5]. However, with the recent discovery of mas related G-protein receptor X2 (MRGPRX2) on mast cells, innate activation of mast cells through the direct binding of pathogenic entities to MRGPRX2 have also been reported [6]. MRGPRX2 is a membrane bound receptor which directly binds to antibacterial peptides, endogenous peptides, protein fragments and FDA approved drugs to activate and degranulate mast cells [7]. Apart from these, mast cells also express ligand specific receptors like Toll Like Receptors (TLRs), C5a and C3a complement receptors and KIT receptors causing cell degranulation [5,8].

Table 1.1. Mediators released from activated mast cells

Amines	Dopamine
	Histamine
	Polyamine
	Serotonin
Chemokines	CC-Chemokine ligand 2,3,4,5,11,20
	CXC-Chemokine ligand 1,2,8,9,10,11
Cytokines	Interferon α, β
	Interleukin 1,3,4,5,9,13,15,16
	Tumor necrosis factor
Enzymes	B-hexosaminidase
	Carboxypeptidase A
	Cathepsin G
	Chymase
	Tryptase
Growth factors	Vascular endothelial growth factor
Reactive oxygen species	Superoxide radicals

Table 1.1 has been adapted from [2,9].

Pathophysiologically, mast cells have been associated with several inflammatory and autoimmune diseases. Increased number of mast cells have been found in the airways and lungs of asthmatic patients and those suffering from pulmonary vascular diseases (PVD) [10,11]. Similarly, significant increment in mast cell number is seen in the synovial tissue of patients with osteoarthritis and in the skin of patients with atopic dermatitis [12,13]. Heart diseases, cancer and graft rejections have all witnessed an increase mast cell number [10,14,15]. Furthermore, direct involvement of mast cell MRGPRX2 receptor in acute allergies and drug side reactions has also been reported [7]. The involvement of mast cells in the pathogenesis of several diseases leverages the opportunity to locally target a disease through mast cell mediated therapeutics. Engineering materials responsive to mast cell released mediators could efficiently achieve targeted therapies. Adding to the mast cell released molecules, the overexpression of MRGPRX2 receptor on mast cells at the inflammatory sites could further be utilized to target therapies to inflamed tissues through MRGPRX2 ligands.

1.3. Strategies for targeted therapies

Targeted therapies are beneficial as they increase the bioavailability of the active therapeutics to the diseased tissue, and minimizes its unwanted adverse effect on other tissues. This has primarily been achieved by identifying disease specific cues as a stimulus and designing a bioactive material centered on it. Significant advancements have been made in this regard and materials sensitive to pH, temperature, oxidative environments and enzymes among others have been designed [16]. Furthermore, materials sensitive to stimuli like that of infrared light has been designed to externally guide the therapeutic systems to the targeted tissue [17]. Cell targeting peptides have also been used to help localize a therapeutic system to the diseased site [18]. The material design used in targeted therapies include nanoassemblies, gels, fibrous mats and liposomes, and have been used

for modalities like the delivery of drugs and genetic materials, imaging and detection among others [16].

1.4. Thesis statement and scope of thesis

Given that mast cell plays a crucial role in the pathogenesis of several inflammatory and autoimmune diseases, it would be advantageous to design therapies around mast cells. This could be facilitated by identifying mast cell released mediators as localized stimulus and designing materials around the stimulus for localized therapies. Present thesis consists of 6 chapters.

Chapter 1 is the introduction chapter which states the rationale for the thesis project.

Chapter 2 critically reviews various mast cell mediators and their corresponding substrates which could be used in the design of materials responsive to mast cell activation. The chapter further discusses various strategies around the bioresponsive materials which could find application in targeted therapies.

Chapter 3 shows the synthesis and characterization of reactive oxygen species (ROS) responsive thioketal molecule. ROS was selected as a mast cell specific stimulus for the design and development of mast cell responsive materials.

Chapter 4 shows the use of thioketal in the design of bioresponsive material. A ROS responsive drug delivery system was designed for the targeted delivery of anti-inflammatory dexamethasone.

Chapter 5 discusses the design rule for the synthesis of mast cell specific MRGPRX2 peptide ligands. A library of small peptide ligands with differential activity against mast cell was created for therapeutic applications.

Chapter 6 discusses the major conclusions and highlights the prospects for future work.

1.5. References

[1] J.A. Owen, J. Punt, S.A. Stranford, Kuby immunology, WH Freeman New York, NY, USA:, 2013.

[2] E.Z.M. da Silva, M.C. Jamur, C. Oliver, Mast cell function: a new vision of an old cell, Journal of Histochemistry & Cytochemistry. 62 (2014) 698–738.

[3] S.J. Galli, S. Nakae, M. Tsai, Mast cells in the development of adaptive immune responses, Nature Immunology. 6 (2005) 135.

[4] S. Wernersson, G. Pejler, Mast cell secretory granules: armed for battle, Nature Reviews Immunology. 14 (2014) 478.

[5] A.M. Gilfillan, C. Tkaczyk, Integrated signalling pathways for mast-cell activation, Nature Reviews Immunology. 6 (2006) 218–230. https://doi.org/10.1038/nri1782.

[6] B.D. McNeil, P. Pundir, S. Meeker, L. Han, B.J. Undem, M. Kulka, X. Dong, Identification of a mast-cell-specific receptor crucial for pseudo-allergic drug reactions, Nature. 519 (2015) 237–241. https://doi.org/10.1038/nature14022.

[7] H. Subramanian, K. Gupta, H. Ali, Roles of Mas-related G protein–coupled receptor X2 on mast cell–mediated host defense, pseudoallergic drug reactions, and chronic inflammatory diseases, Journal of Allergy and Clinical Immunology. 138 (2016) 700–710.

[8] T. Yoshimaru, Y. Suzuki, T. Inoue, S. Nishida, C. Ra, Extracellular superoxide released from mitochondria mediates mast cell death by advanced glycation end products, Biochimica et Biophysica Acta (BBA) - Molecular Cell Research. 1783 (2008) 2332–2343. https://doi.org/10.1016/j.bbamcr.2008.08.010.

[9] T.C. Moon, A. Dean Befus, M. Kulka, Mast cell mediators: Their differential release and the secretory pathways involved, Frontiers in Immunology. 5 (2014) 1–18. https://doi.org/10.3389/fimmu.2014.00569.

[10] H. Hamada, M. Terai, H. Kimura, K. Hirano, S. Oana, H. Niimi, Increased expression of mast cell chymase in the lungs of patients with congenital heart disease associated with early pulmonary vascular disease, American Journal of Respiratory and Critical Care Medicine. 160 (1999) 1303–1308. https://doi.org/10.1164/ajrccm.160.4.9810058.

[11] S. Balzar, M.L. Fajt, S.A.A. Comhair, S.C. Erzurum, E. Bleecker, W.W. Busse, M. Castro, B. Gaston, E. Israel, L.B. Schwartz, D. Curran-Everett, C.G. Moore, S.E. Wenzel, Mast cell phenotype, location, and activation in severe asthma: Data from the Severe Asthma Research Program, American Journal of Respiratory and Critical Care Medicine. 183 (2011) 299–309. https://doi.org/10.1164/rccm.201002-0295OC.

[12] M.G. Buckley, P.J. Gallagher, A.F. Walls, Mast cell subpopulations in the synovial tissue of patients with osteoarthritis: Selective increase in numbers of tryptase-positive, chymase- negative mast cells, Journal of Pathology. 186 (1998) 67–74. https://doi.org/10.1002/(SICI)1096-9896(199809)186:1<67::AID-PATH132>3.0.CO;2-D.

[13] A. Järvikallio, A. Naukkarinen, I.T. Harvima, M.L. Aalto, M. Horsmanheimo, Quantitative analysis of tryptase- and chymase-containing mast cells in atopic dermatitis and nummular eczema, British Journal of Dermatology. 136 (1997) 871–877. https://doi.org/10.1111/j.1365-2133.1997.tb03927.x.

[14] J.P. Kankkunen, I.T. Harvima, A. Naukkarinen, Quantitative analysis of tryptase and chymase containing mast cells in benign and malignant breast lesions, International Journal of Cancer. 72 (1997) 385–388. https://doi.org/10.1002/(SICI)1097-0215(19970729)72:3<385::AID-IJC1>3.0.CO;2-L.

[15] M. Yamada, M. Ueda, T. Naruko, S. Tanabe, Y.S. Han, Y. Ikura, M. Ogami, S. Takai, M. Miyazaki, Mast cell chymase expression and mast cell phenotypes in human rejected kidneys, Kidney International. 59 (2001) 1374–1381. https://doi.org/10.1046/j.1523-1755.2001.0590041374.x.

[16] S. Municoy, M.I. Álvarez Echazú, P.E. Antezana, J.M. Galdopórpora, C. Olivetti, A.M. Mebert, M.L. Foglia, M. v Tuttolomondo, G.S. Alvarez, J.G. Hardy, Stimuli-responsive materials for tissue engineering and drug delivery, International Journal of Molecular Sciences. 21 (2020) 4724.

[17] J. Li, C. Sun, W. Tao, Z. Cao, H. Qian, X. Yang, J. Wang, Photoinduced PEG deshielding from ROS-sensitive linkage-bridged block copolymer-based nanocarriers for on-demand drug delivery, Biomaterials. 170 (2018) 147–155. https://doi.org/10.1016/j.biomaterials.2018.04.015.

[18] F. Zhang, X. Huang, L. Zhu, N. Guo, G. Niu, M. Swierczewska, S. Lee, H. Xu, A.Y. Wang, K.A. Mohamedali, M.G. Rosenblum, G. Lu, X. Chen, Noninvasive monitoring of orthotopic glioblastoma therapy response using RGD-conjugated iron oxide nanoparticles, Biomaterials. 33 (2012) 5414–5422. https://doi.org/10.1016/j.biomaterials.2012.04.032.

Chapter 2. Targeting active sites of inflammation through the unique characteristics of mast cells

2.1. Introduction

Mast cells play a protective role against pathogenic invasions and infections [1,2], but are also complicit in allergic and autoimmune diseases [3,4]. Primarily localized in the tissues with close proximity to external environment (i.e., skin, mucosa), mast cells form the natural first line of defense against microbial infections [5]. That said, an increase in tissue resident mast cell population has been observed for a variety of inflammatory diseases, like in the airways and lungs of pulmonary vascular diseases (PVD) and asthmatic patients [6,7]; in the skin of atopic dermatitis patients [8]; in the synovial tissue of osteoarthritic patients [9]; and in the cancerous tissue during cancer metastasis [10,11]. Moreover, mast cells have also been shown to play crucial role in cardiovascular diseases and graft rejections [12,13].

Activated mast cells release an abundance of bioactive molecules from the secretory granules into the extracellular space [1,14]. Molecules released from activated mast cells includes [1,14–16]: pro-inflammatory cytokines (i.e., interleukin (IL)-4,5,6,15); TNF-α; vascular endothelial growth factors (VEGFs); biogenic amines (histamines); tissue remodeling and chemoattractant proteases (i.e., tryptase, chymase, and carboxypeptidases); and pathogen neutralizing hydrolases (i.e, β-hexosaminidase, β-hex). Apart from the preformed mediators, mast cell activation can lead to *de novo* synthesis of macromolecules (i.e., cytokines, chemokines, and enzymes). Additionally, reactive oxygen species (ROS) like superoxides and hydrogen peroxides (H_2O_2) are as well produced in the intracellular and extracellular spaces upon cell activation. All of these activities

work together to mitigate the presence of the immunogenetic entity, as well as function as signaling molecules that leads to the restoration of tissue function [17–19].

Several excellent reviews have detailed the mechanisms involved in mast cell activation [20,21]. Traditionally the activation of mast cells through FcεRI receptor, ligand specific receptors like Toll Like Receptors (TLR) receptor, KIT receptor, and C5a and C3a complement receptors are well-documented. Recent work has shown that the mass related G protein coupled receptor X2 (MRGPRX2) also initiates mast cell activation through a variety of peptides, and drugs [22,23]. It is not our intent to discuss cell signaling as a function of activation route, rather referring the reader to above cited reviews. However, the activation of mast cells leads to the release of a plethora of bioactive compounds that are spatiotemporally regulated to specific inflammatory processes; giving the unprecedented ability for the design of materials that can respond to these highly regulated stimuli in like kind.

The aim of the present review-cum-analysis is to highlight key mediators that are released from the mast cell during the progression of an inflammatory response which can be utilized as a stimulus in inflammatory targeted therapeutic applications. The article surveys the substrates for the corresponding stimulus for the express purpose of designing mast cell responsive materials with strategies offered for their therapeutic application. Further, simultaneous to mediator release, inflammatory diseases are also characterized by increased expression of MRGPRX2 receptor on mast cells in the diseased tissue like itch, allergy, psoriasis, atopic dermatitis and asthma [24,25]. In the context, MRGPRX2 receptor may be described as a characteristic of an inflamed tissue, and hence can be exploited in targeted therapies. In the later part of the review, peptide ligands of MRGPRX2 receptor has been identified and strategies on their use as homing peptides in

localizing therapeutic system to the inflamed tissue microenvironment through MRGPRX2 receptor has been discussed.

2.2. Mast cell specific enzymes as inflammatory stimulus

Mast cell activation results in the rapid releases of preformed granular enzymes like β-hex, tryptase, and chymase, which have a specific and well-defined activity against a limited set of substrates (Figure 2.1). Furthermore, mast cell activation also induces *de novo* synthesis and release of MMP-9 as shown in Figure 2.1, which is well known to process gelatins and denatured collagens. Herein, these enzymes and their substrates are discussed in terms of their use in developing bioactive materials to target regions of active inflammation.

2.2.1. Degranulated mast cell enzymes – β-hex, tryptase and chymase

2.2.1.1. Enzyme dependent tissue mast cell population and dynamics

β-hex is a key marker of mast cell activation and is routinely used to study inflammatory activation of mast cells against infections, drugs, and inhibitors among others [23,26]. Of its different isoforms, hexosaminidase A and hexosaminidase B are found in mast cells and are released from mast cells during activation [27]. It has been reported that a population of 10^6 lung mast cells contains 3.8 U of β-hex in their secretory granules, and up to 86% of the granulated β-hex is released upon activation. The maximum release occurs within minutes of cell activation and accounts for 45 – 62% of granular β-hex. β-hex release has been shown to be activation dependent and is directly proportional to the concentration of stimulator [27–29]. Furthermore, mast cells undergo re-activation in a 24-h period, whereby an equivalent amount of β-hex as in the first wave of activation is released [30].

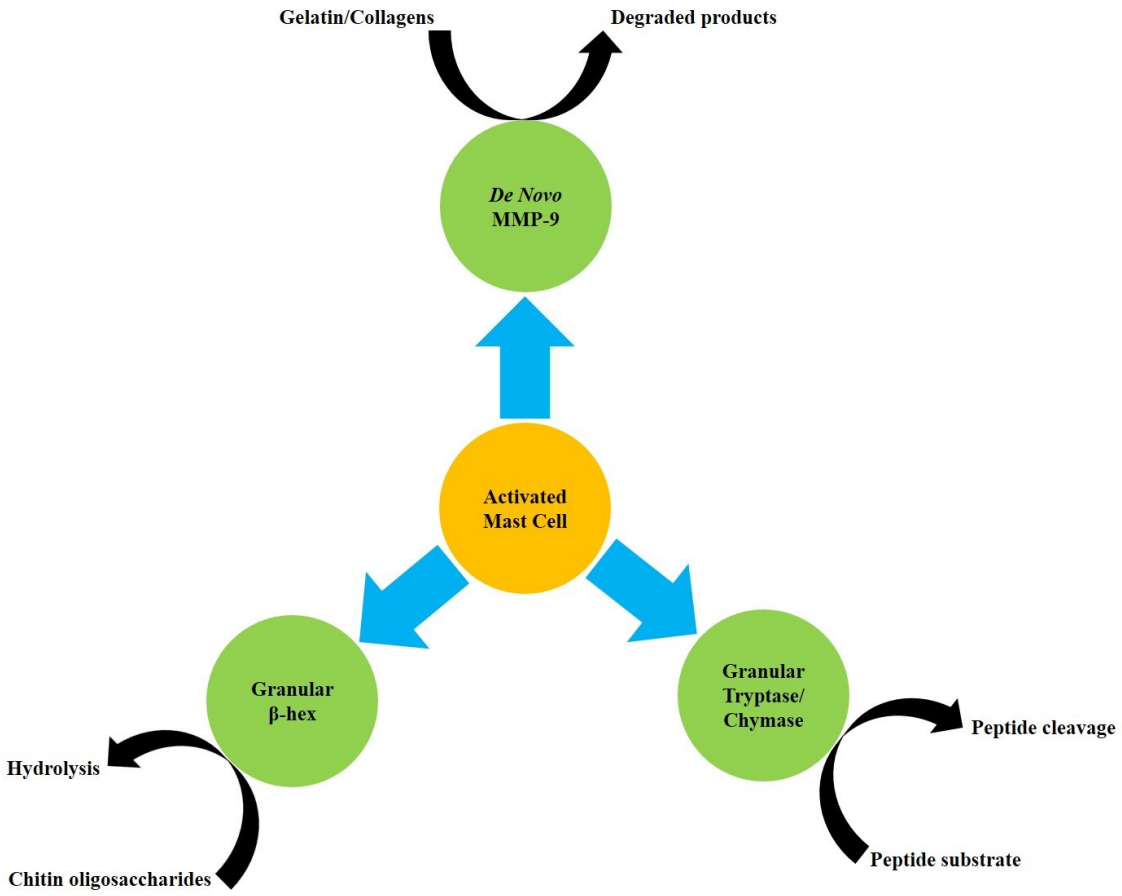

Figure 2.1. Physiochemical activity of various mass cell released enzymes. Mast cell secretes various enzymes and each exhibit specific catalytic activity on their substrates. Serine proteases and β-hex are preformed granular components of mast cell and exert their catalytic activities on peptide substrates and chitin oligomers respectively. MMP-9 is synthesized upon mast cell activation and degrades gelatin and denature collagens.

Concurrent to β-hex, mast cells also release preformed serine proteases - tryptase and chymase upon activation. In general, mast cells are classified into two subpopulations - (i) mast cell type containing both tryptase and chymase (MC_{TC}), and (ii) mast cells containing only tryptase (MC_T). For therapeutic purposes, it is important to recognize that mast cell populations are dynamic and vary with tissue, disease and disease severity [7–11,13]. For example, MC_{TC} are dominant mast cell population in skin and submucosa, accounting for 89 and 87% of the total mast cell population respectively. On the contrary, lung and intestinal mucosa mast cells are dominantly MC_T (~100%)

populations. Evaluation of granular composition of serine enzymes have shown that the skin mast cells (10^6 cells) contains 35 and 4.5 μg of tryptase and chymase [31], while the lung mast cells (10^6 cells) contains 10.8 and 0.3 μg of tryptase and chymase, respectively. Further, 79% of total tryptase is shown to be released upon the activation of lung mast cells [29]. Tryptase, however, has also been shown to be expressed by monocytes and basophils, though, monocytes predominantly release inactive α-tryptase, basophil tryptase is < 1% of that contained in mast cells [32,33]. These subtle differences in the relative composition of mast cells, and the respective presence and concentration of mast cell enzymes are therefore favorable considerations for the design of therapeutic strategies targeting a specific disease location and state.

The dynamics of tissue mast cell populations are further dependent on the disease (Table 2.1). For example, a change from MC_T to MC_{TC} mast cell population occurs in patients with asthma and pulmonary diseases relative to normal subjects [6,7,34–36]. This therefore provides an opportunity for a chymase based therapy during the progression of a lung disease. In addition, the change in phenotype from MC_T to MC_{TC} is also associated with pulmonary diseases severity [34,36]. In asthmatic patients, an increasing MC_{TC} trend with increasing asthma severity in the airway mucosa and in the epithelial cells from the airway was observed. Though a higher tryptase level in the Bronchoalveolar lavage (BAL) fluid as compared to control was reported, the relative level of tryptase with disease severity did not vary [34]. In contrast, an increased population of MC_T cells is observed in the synovial tissue of patients with osteoarthritis. Of the elevated populations of mast cell in patients with osteoarthritis (81 in patients *vs*. 24-32 cells/mm^2 in controls), 77% were MC_T subtype [9]. Similarly, scar tissue specimen from patients undergoing would healing showed a dramatic increase in the MC_T skin mast cells. MC_T population in scar tissue increased to 91%

from that in a normal skin tissue population of 11% [37], therefore opening doors for tryptase based therapeutic approach for such diseases.

Table 2.1. Dynamic changes in mast cell population through the progression of inflammatory diseases

Diseases	Physiological Anomaly	References
Asthma	Increased number of mast cell; increased MC_{TC} population	[6,7]
Pulmonary Vascular Diseases		[34-36]
Osteoarthritis	Increased number of mast cell; increased MC_T population	[9]
Wounds		[37]

2.2.1.2. Substrate consideration for β-hex

β-hex is a lysosomal enzyme which catalyzes the hydrolysis of glycosidic bonds in glycoconjugates [38]. β-hex degrades the structural component of microbial cell wall through the hydrolysis of 1-4 glycosidic bonds in glycosaminoglycans, thus exhibiting host defense by reducing the microbial load [39,40]. The transient release of β-hex from mast cell upon fungal infection with Candida Albicans is reported to reduce the microbial load by 30%, primarily through cell wall degradation [41,42]. Consequently, Chitin, a β-1,4 glucoside linked N-acetylglucosamine polysaccharide microbial cell wall component, theoretically, should be an excellent substrate for the enzyme. However, β-hex has been deemed ineffective against long chain chitin polymer, and its activity could only be established against hydrolyzed colloidaland ground chitin [43,44]. The catalytic activity of the enzyme increases as the chitin chain length decreases, resulting in sequential removal of monomers from the non-reducing end of the chain to furnish monomeric N-acetylglucosamine as the end product (Figure 2.2) [43,45,46]. Though the kinetic parameters for β-hex released from mast cells against chitinoligosachharides (COS) were not found, the kinetic studies of β-hex from other sources against COS with degree of polymerization, DP_n, n = 2 – 6,

illustrates varying yet definite activity. β-hex cloned from bacteria Stenotrophomonas maltophilia shows a K_{cat}/K_m values of 246 $M^{-1}s^{-1}$ respectively for the DP_6 chitin [46]. Similarly, β-Hex from Vibrio harveyi bacteria has its kinetic parameter standing at 166 $M^{-1}s^{-1}$ for K_{cat}/K_m [43]. β-hex from Vibrio furnissii showed the corresponding values of V_{max} and K_m for DP_6 chitin as 3.5 mM and 376 μmol $min^{-1}mg^{-1}$ respectively [47]. Adding to this, the activity of enzyme has shown to be best exhibited in the pH range of 5 - 8 and a temperature between 30 – 40 ℃, which makes β-hex a favorable inflammatory stimulus to be utilized in physiological conditions.

β-hex follows a 'substrate-assisted' mechanism wherein the hydrolysis is mediated by the 2-acetamide group in the monomer unit, and without which the enzymatic activity is inhibited (Figure 2.2a) [38,45]. Consequently, chitin derivative, chitosan in its acetylated form, and hyaluronic acid (HA) becomes an engineered substrate for the enzyme [48–50]. Chitin, chitosan and HA have regularly been used in drug delivery and biomaterial research and can easily be modified into β-hex mediated inflamed tissue mast cell responsive material. Furthermore, by varying the degree of acetylation in chitosan, the rate of enzymatic activity can be controlled and manipulated [51]. In the later sections, the recent research centered on COS as a biomaterial has been briefly discussed. COS are linear, low molecular weight homologues of chitin and chitosan, and are formed by chemical or enzymatic degradation of the parent chitin. They are nontoxic and hence could be very efficiently used as a platform for β-hex responsive materials [52,53].

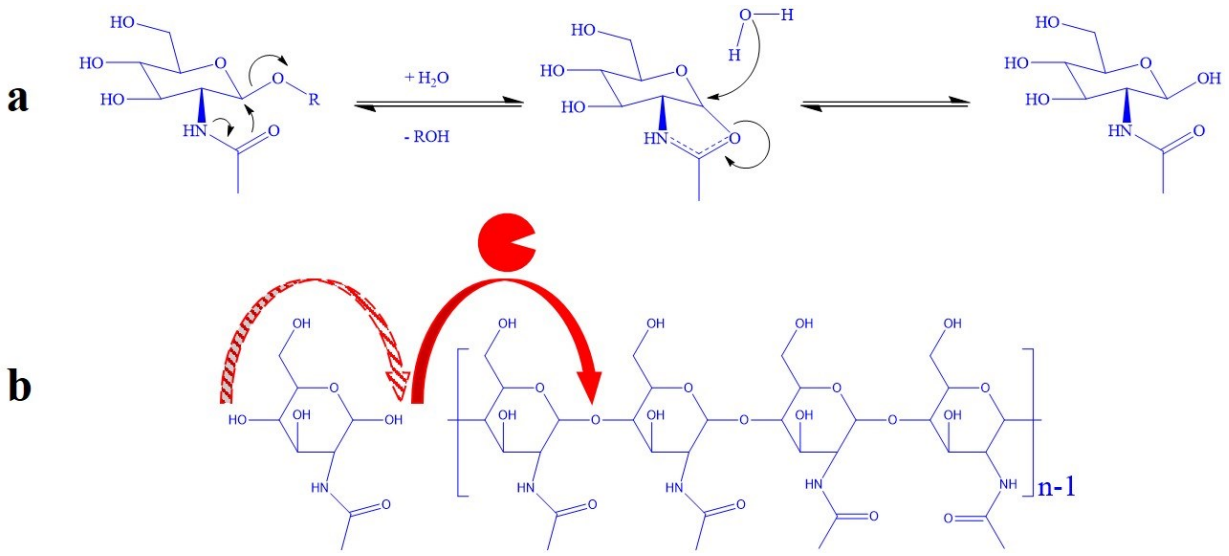

Figure 2.2. Substrate assisted mechanism of β-hexosaminidase. a) The monomers of chitin are removed successively by the hydrolysis of 1,4 glycosidic bond. The enzyme favours the carbonyl group on the acetamide of the monomer from non-reducing terminal to acts as a nucleophile, and attacks the C1 carbon of the terminal monomer. Thereafter the enzyme facilitates the attack of a water molecule at C1 causing the hydrolysis of the 1,4 glycosidic bond. The image has been adapted from [38]. b) A cartoon representation of sequential removal of monomers from the non-reducing terminal by the β-hex enzyme.

2.2.1.3. Tryptase substrate composition

It is evident that the spatiotemporally controlled release of tryptase upon mast cell activation is a cardinal event in an inflammatory condition; yet there is a dearth in the literature on utilizing this enzyme as a means to trigger latent functionalities programmed within a bioresponsive material. Scope of these materials in therapeutic applications are huge, be it for drug delivery, presentation of occult residues for cell signaling, destruction of cell signaling molecules, among others. Further consideration of these enzymes, their activity and inhibition are thought to provide design rules for the preparation of bioresponsive materials for biomedical applications.

Tryptase studies have shown that a basic residue at the C-terminal of the cleavage site facilitates peptide substrate cleavage (Figure 3b, P1) [54,55]. The conserved aspartic acid in the enzyme's

substrate binding domain interacts with the polar positively charged residues in the substrate, governing enzymatic activity. Combinatorial peptide screening, where amino acids are fixed at specific positions while other residues are varied, have shown Lysine and Arginine at P1 renders a greater tryptase catalytic activity (as seen from entries in Table 2.2) [56,57]. Arginine, with a longer side chain interacts directly with the Aspartic acid, while Lysine interaction is bridged by a water molecule [54].

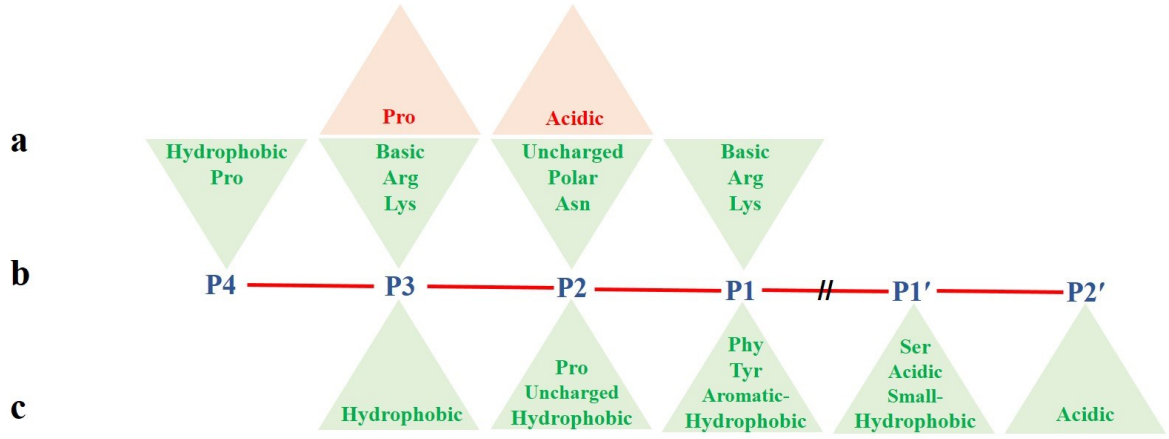

Figure 2.3. Optimized amino acids on each side of sessile bond in a peptide substrate for a) tryptase and c) chymase. Triangles facing towards the amino acid positions shows various amino acids and general group of amino acids that are favored at that position in a peptide substrate. Triangles facing away from the amino acid positions represent the amino acids or groups which are not favored at the position. Amino acid specificity for tryptase exists on the N-terminal side of the sessile bond while it exists on both the sides for chymase. b) General representation of amino acid positions in a peptide substrate. Two forward slashes denote the substrate cleavage site.

Tryptase exhibits an extended substrate specificity, where physio-chemical properties of the residues beyond P1 are also defined. Combinatorial experiments have shown a clear preference for Asparagine at P2, followed by other polar or uncharged residues at the position [54,56–58]. Replacing Asparagine at P2 with Threonine in peptide substrates caused more than a 30% decrease in catalytic activity of tryptase (Table 2.2, entry 11 vs 12, and entry 13 vs 14) [56]. However, it was found that tripeptide substrates containing positively charged residues at both P1 and P2 have

a high K_{cat}/K_M of $10^7 – 10^8$ $M^{-1}s^{-1}$ against human pituitary tryptase (Table 2.2, entry 22-24) [59]. These findings suggest that tryptase favors both positively charged and uncharged residues at P2, however, a negatively charged residue lowers the catalytic activity (Table 2.2, entry 19 with K_{cat}/K_M values 10 and 33-fold higher than entry 20 and 21 respectively) [59,60]. At P3, before mentioning what is favored, it is important to mention that Proline is not favored. A 100-fold decrease in the catalytic activity of the enzyme was observed when P3 was accommodated with Proline [61,62]. This was also evident in the combinatorial amino acid study of the substrates [56,58]. Almost all of the above studies have shown a clear preference for a basic charged residue Lysine and Arginine at P3 position (In Table 2.2, entry 1 with P3 Lysine was 100-fold more liable to be cleaved by tryptase than entry 4 with P3 Proline. Similarly, entry 6 was 100-fold more cleavable by tryptase than entry 9). Finally, Proline at P4, along with other hydrophobic residues is preferred for the enzyme activity [56–58]. Beyond P4, the broader specificity towards amino acid residues failed to draw a definite conclusion [57].

2.2.1.4. Chymase substrate composition

Human chymase also exhibits extended substrate specificity, however, in contrast to tryptase, chymase substrate selectivity extends to both the C- and the N- terminal of the scissile bond [63–65]. Physiologically, chymase is involved in the hydrolysis of Angiotensin I (Ang I) to Angiotensin II (Ang II), and hence Ang I has been widely used as a high affinity substrate to study the amino acid specificity for the enzyme [65–68]. Human heart chymase has shown strong P1 specificity for a hydrophobic residue bearing an aromatic ring, particularly Phenylalanine and Tyrosine. A hydrophobic residue devoid of an aromatic ring at P1 resulted in a loss of chymase (Table 2.3, entry 2 with K_{cat}/K_M of 0.81×10^6 $M^{-1}s^{-1}$ vs entry 5 with that of 0.024×10^6 $M^{-1}s^{-1}$) [64–66,69,70]. Hydrophobic, or uncharged, residues at P2 and P3 are also preferred for increased substrate

cleavage kinetics of chymase [63–66,69]. Proline at P2 has been deemed crucial if other substrate parameters are not met.

Human chymase hydrolyses the cleavage of Ang I (Asp-Arg-Val-Tyr-Ile-His-Pro-Phe-//-His-Leu) with 780-fold higher efficiency than Ang II (Asp-Arg-Val-Tyr-//-Ile-His-Pro-Phe) (Table 2.3, entry 10 and entry 14 respectively). The discrepancy in the catalytic activity of chymase against Ang I and Ang II, even though they have similar residue composition at the N-terminal of the scissile bond underscores the importance of C-terminal leaving groups (P1′, P2′,…,Pn′) in the human chymase catalyzed substrate hydrolysis [66]. Study with phage library of substrate peptides have shown a higher frequency of an acidic residue at either of P1′, P2′ or both, with slight preference for P2′. Frequent occurrence of Serine and small hydrophobic residues were also apparent at P′ [69]. It was shown that the presence of Arg-143 and Lys-192 in the substrate binding domain of chymase was facilitating the interaction of the enzyme with the P′ acidic residues of the substrate, resulting in efficient hydrolysis [69,71].

Table 2.2. Peptide substrates for human tryptase with varying enzyme kinetics

Entry	Peptide Substrate	K_{cat}/K_m (10^6 $M^{-1}s^{-1}$)	Source	Reference
1	Z-Lys-Gly-Arg-NA	0.46	Human Skin	[61]
2	Z-Lys-Phe-Arg-NA	0.048		
3	Z-Asn-Gly-Arg-NA	0.0387		
4	Z-Pro-Gly-Arg-NA	0.0063		
5	Z-Pro-Phe-Arg-NA	0.000464		
6	Z-Lys-Gly-Arg-NA	0.039	Human Lung	
7	Z-Asn-Gly-Arg-NA	0.0083		
8	Z-Lys-Phe-Arg-NA	0.0053		
9	Z-Pro-Gly-Arg-NA	0.00049		
10	Z-Pro-Phe-Arg-NA	0.00004		
11	Ac-Pro-Arg-Asn-Lys-AAC	1.89	Recombinant βII	[56]
12	Ac-Pro-Arg-Thr-Lys-AAC	1.27		
13	Ac-Pro-Arg-Asn-Lys-AAC	1.23	Recombinant βI	
14	Ac-Pro-Arg-Thr-Lys-AAC	0.78		
15	Pro-Ile-Arg-Asn-Lys-ANB-NH2	9.953	Human Mast Cell β Tryptase	[57]
16	Ala-Ala-Pro-Ile-Arg-Asn-Lys-ANB-NH2	4.746		
17	Ac-Arg-Asn-Lys-ANB-NH2	2.822		
18	Arg-Asn-Lys-ANB-NH2	1.587		
19	Boc-Phe-Ser-Arg-4-MCA	0.2757	Human Mast Cell β Tryptase	[60]
20	ABZ-Arg-Gln-Asp-Arg-ANB-NH2	0.0274		
21	ABZ-Arg-Gln-Asp-Lys-ANB-NH2	0.0067		
22	Z-Ala-Lys-Arg-AMC	238	Human Pituitary Tryptase	[59]
23	Z-Ala-Lys-Lys-AMC	103		
24	Z-Ala-Arg-Arg-AMC	49.9		
25	Boc-Val-Leu-Lys-AMC	1.78		

Z = benzyloxycarbonyl, NA = 4-nitroanilide, Ac = acetyl, AAC = 7-amino-4-carbamoylmethylcoumarin, ANB = 5-amino-2-nitrobenzoic acid, Boc = tert-butyloxycarbonyl, ABZ = 2-aminobenzoic acid, AMC = 4-methylcoumarin-7-amide.

Table 2.3. Peptide substrates for human chymase with varying enzyme kinetics

Entry	Peptide Substrate	K_{cat}/K_m (10^6 $M^{-1}s^{-1}$)	Source	Reference
1	Suc-Val-Pro-Pro-Phe-SBzl	8.3	Human Skin Chymase	[70]
2	Suc-Val-Pro-Phe-NA	0.81		
3	Ile-His-Pro-Phe-Suc-His-Pro-Phe-NA	0.13		
4	Suc-Val-Pro-Tyr-NA	0.11		
5	Suc-Val-Pro-Leu-NA	0.024		
6	Suc-Phe-Ser-Phe-NA	0.013		
7	Suc-Val-Pro-Met-NA	0.0073		
8	Suc-Phe-Glu-Phe-NA	0.006		
9	Asp-Arg-Val-Tyr-Ile-His-Pro-Phe//Gly-Gly-Gly	9	Human Heart Chymase	[66]
10	Asp-Arg-Val-Tyr-Ile-His-Pro-Phe-//-His-Leu	3.6		
11	Asp-Arg-Val-Tyr-Ile-His-Pro-Phe//Gly	0.12		
12	Asp-Arg-Val-Tyr-//-Ile-His-Pro-Phe	0.071		
13	Asp-Arg-Val-Tyr-//-Gly-Gly	0.051		
14	Asp-Arg-Val-Tyr-//-Ile-His-Pro-Phe	0.0046		
15	ABZ-Gly-Ile-Ala-Thr-Phe-//-Cys-Asp-Leu-Met-Pro-Glu-Gln-EDDnp	1.035	Human Mast Cell Chymase	[72]
16	ABZ-Gly-Ile-Ala-Thr-Phe-//-Cys-Met-Leu-Met-Pro-Glu-Gln-EDDnp	0.238		
17	ABZ-Gly-Ile-Ala-Thr-Phe-//-Trp-Met-Leu-Met-Pro-Glu-Gln-EDDnp	0.096		
18	Asp-Arg-Val-Tyr-Ile-His-Pro-Tyr-//-His-Leu	2.8	Human Heart Chymase	[65]
19	Asp-Arg-Val-Tyr-Ile-His-Pro-Phe-//-His-Leu	2.7		
20	Asp-Arg-Val-Tyr-Ile-His-Pro-Tyr-//-Ile-Leu	1.6		
21	Asp-Arg-Val-Tyr-Ile-His-Pro-Phe-//-His-Val	0.66		
22	Asp-Arg-Val-Tyr-Ile-His-HIs-Phe-//-His-Leu	0.33		
23	Asp-Arg-Val-Tyr-Ile-His-Pro-Leu-//-His-Leu	0.15		
24	Asp-Arg-Val-Tyr-Ile-His-Pro-Phe-//-His-Pro	0.14		
25	Asp-Arg-Val-Tyr-Ile-His-Pro-Phe-//-His	0.0035		

Suc = succinyl, SBzl = S-Benzyl, NA = 4-nitroanilide, ABZ = 2-aminobenzoic acid, EDDnp = N-(2,4-dinitrophenyl)-ethylenediamine. The two forward slashes represent the cleavage site of the substrate.

2.2.2. *De novo* synthesized mast cell MMP-9 as inflammatory stimulus

2.2.2.1. Release and pathophysiological significance

92-kDa metalloproteinase (MMP-9) is a key inflammatory regulator in diseases like neuroinflammation, peritonitis, rheumatoid arthritis, cancer, immunological graft rejections and wound healing [17,73–75]. Though neutrophils are the major MMP-9 secretory cells, mast cell activation induced the synthesis and release of MMP-9 into the extracellular space [76,77]. Mast cell MMP-9 then serves as the chemoattractant for the migration of neutrophils to the inflammatory site. The accumulation of neutrophil peaks at about 6-8 h after the initial inflammatory event and further increases the level of MMP-9 at the site of inflammation [74]. It has been reported that 65% of mast cells from the synovial tissue of patients with rheumatoid arthritis had stained for MMP-9 [17]. The level of MMP-9 in the inflamed fluid of the peritoneal cavity and in the wound fluid has been reported to be 0.3-0.4 ng/ml and 100 μg/ml respectively, which were significantly higher than the basal level [74,78]. Increased level of MMP-9 has also been shown at the site of islet transplantation, which resulted in initial inflammatory response and improper graft function [79]. The increased level of MMP-9 at an inflamed tissue site thus highlights another potential mast cell derived enzyme, which could be used as a stimulus in the design of bioresponsive materials for inflammatory targeted applications.

2.2.2.2. Substrate consideration for MMP-9

Gelatin is a natural substrate for MMP-9 and is ‘generally recognized as safe’ by the FDA. It is widely used in food, cosmetics, and pharmaceutical industry. Gelatin has been bestowed with equal attention in the drug delivery research, owing to its inexpensiveness and easy availability, biocompatibility, and low immunogenicity [80,81]. Apart from gelatin, several peptide substrates

specific to MMP-9 have also been identified. MMP-9, like all MMPs favors the Pro-X-X-//-Z motif in its substrates; where X is any amino acid, Z represent a hydrophobic residue, and // depict the cleavage site. However, it is the amino acids at position P2, P1 and P2′ that confers the distinctiveness to MMP-9 against other MMPs [82,83]. MMP-9 shows a strong preference for Arginine at P2, while small amino acids like Glycine, Alanine and Serine are favored at P1. Further, Serine and Threonine at P2′ of the peptide substrate has shown to be crucial in rendering MMP-9 specificity [84].

Several MMP-9 peptide substrates with their enzyme kinetics and comparative specificity to other MMPs have been derived computationally [83]. Table 2.4, however lists few of the peptides whose kinetics were determined experimentally through the fluorogenic substrates and recombinant MMP-9. Further, unlike tryptase and chymase discussed above, peptide substrates for MMP-9 are well established and have been regularly used for biomedical applications. Peptide Gly-glu-Arg-Gly-Pro-Pro-Gly-Pro-Gln-Gly-Ala-Arg-Gly-Phe-Pro-Gly-Thr-Pro-Gly-Leu and Cys-Gly-Pro-Gln-Gly-Ile-Trp-Gly-Gln-Gly-Cys-Arg have been used to localize drugs into MMP-9 extensive cancerous tissue [85,86]. Other MMP-9 peptide substrates that have been used in therapeutic applications are Pro-Leu-Gly-Val-Arg-Gly-Lys and Pro-Leu-Gly-Leu-Ala-Gly [75,87].

Table 2.4. Peptide substrate for MMP-9 with varying enzyme kinetics

Entry	Peptide Substrate	Kcat/Km (10^6 $M^{-1}s^{-1}$)	Source	Reference
1	Ser-Gly-Lys-Gly-Pro-Arg-Gln-//-Ile-Thr-Ala	0.19	Recombinant MMP-9	[84]
2	Ser-Gly-Lys-Ile-Pro-Arg-Arg-//-Leu-Thr-Ala	0.16		
3	Ser-Gly-Lys-Ile-Pro-Arg-Thr-//-Leu-Thr-Ala	0.07		
4	Ser-Gly-Pro-Arg-Ala-//-Val-Ser-Thr-Thr-Ala	0.06		
5	Ser-Gly-Pro-Leu-Phe-//-Tyr-Ser-Val-Thr-Ala	0.03		
6	Ser-Gly-Phe-Gly-Ser-Arg-Tyr-//-Leu-Thr-Ala	0.01		
7	Ser-Gly-Gln-Pro-His-Tyr-//-Leu-Thr-Thr-Ala	0.009		
8	Ser-Gly-Leu-Arg-Pro-Ala-Lys-//Ser-Thr-Ala	0.006		
9	Ser-Gly-Lys-Ile-Pro-Arg-Thr-//-Ala-Thr-Ala	0.002		
10	Ser-Gly-Arg-Arg-//-Leu-Leu-Ser-Arg-Thr-Ala	0.001		

The two forward slashes represent the cleavage site of the substrate.

2.2.3. System design strategies responsive to mast cell enzymes

2.2.3.1. Design strategies around COS as β-hex responsive platforms

COS are water-soluble molecules which facilitates its easy conjugation to other biologically relevant materials. The solubility, and hence hydrophobicity however can be easily modulated by varying the degree of acetylation [52,53,88]. Further, a fine balance between the hydrophilic COS and a conjugated hydrophobic domain can impart self-assembling property to the system. COS has been used as a backbone to graft PCL branches onto it. It was shown that by varying the length of the PCL branches, COS-PLC copolymers could be assembled into different nano morphologies including spherical, rod shaped and vesicles [89]. In another study, hydrophobic PCL was conjugated to COS through a disulphide bond to design a self-assembling system. The disulphide linkage rendered GSH responsiveness for the triggered delivery of DOX to cancerous cells [90]. Different hydrophobic domains like that of retinoic acid and stearic acids have been used with

COS for applications ranging from drug delivery, magnetic resonance imaging and chemotherapy [91,92].

COS, owed to its cationic amines, has found application as a coating-materials to enhance cellular uptake [91]. Drug laden liposomes and polymeric nanoparticles were coated with COS to increase stability and cellular uptake of the system [93,94]. The presence of cationic charges on COS also helps in condensing genetic materials for the effective transport of siRNAs into the cells [95]. Other than coatings, COS has also been used to develop injectable hydrogels, where the gelation properties and degradation has been controlled by its degree of acetylation [53]. As discussed in the preceding section, skin infection causes a burst release of β-hex, and hence β-hex substrate could be very efficiently used to develop fibrous wound dressing materials. COS was used as a cross linker for the electro-spun PCL fibers to impart both bioactivity and mechanical properties to the fibrous mats [96].

Adding to the wound healing materials, β-hex can be highly beneficial in targeting inflamed tissues, which are characterized by the development of a local charged microenvironment. For instance, the anionic mucus and the increased activity of β-hex in the blood serum of asthmatic patients can be synergistically used to localize and release respectively, the therapeutics for the respiratory diseases [40,97,98]. Chitosan, in this regard, which is both a substrate for β-hex and a preferred material for designing mucoadhesive systems, could provide an ideal platform for such an innovation [99]. In contrast, inflammatory bowel diseases are reported to be devoid of mucus layer consequently exposing a rather positively charged surface; which again, by using β-hex responsive COS can be used to localize and deliver therapeutics in the inflamed region [100].

2.2.3.2. Strategies around peptide substrates to design tryptase, chymase and MMP-9 responsive systems

Identification of enzyme cleavable substrates is an active area of research that has found wide application in biomedical research. Though tryptase and chymase peptide substrates, to the best of our knowledge have not been used in disease targeting, MMP-9 substrates have been considered in cancer research. PEG-MMP-9 peptide substrate (Cys-Gly-Pro-Gln-Gly-Ile-Trp-Gly-Gln-Gly-Cys-Arg) system was used to coat DOX loaded MSN particles in an effort to target MMP-9 rich cancerous tissue [99]. Similarly, MMP-9 responsive peptide Gly-Glu-Arg-Gly-Pro-Pro-Gly-Pro-Gln-Gly-Ala-Arg-Gly-Phe-Pro-Gly-Thr-Pro-Gly-Leu was conjugated to PEG-PLGA drug carrying nanoparticle system to expose the drug at the cancerous site [86]. In a modality different than drug targetting, MMP-9 substrate Pro-Leu-Gly-Val-Arg-Gly-Lys was used in cancer detection [68].

Peptide substrates with specificity to other MMPs have also been strategically used in designing bioresponsive materials; and such, can be used innovatively with mast cell enzyme substrates to devise inflammation-targeting systems. Our group coated cargo laden nanoparticles with peptides with varying MMP-2 cleavage kinetics, providing a handle on how to not only use enzymes to control the release profile of the loaded drug, but also the cleavage kinetics of the substrate in particular [54]. Enzyme cleavable domains of varying activities were also incorporated in a hydrogel system to modulate the degradation of the gel and hence, the release of incorporated drug [101,102]. Apart from MMP-2, peptide substrates with specificities towards MMP-1, MMP-8, MMP-7, and elastases, have also been used to crosslink and stabilize hydrogel systems [103–106]. However, the compact structure of crosslinked hydrogels restricts the accessibility of enzyme to the peptide substrates, which does affect the programmed degradation of the matrix [104,105].

On contrary to the hydrogel systems, enzyme sensitive peptide substrates have been used as a linker molecule in nano-assemblies [107,108]. A Polyethylene glycol (PEG) - Paclitaxel (PTX) self-assembling prodrug was synthesized using an MMP-2 peptide linker to release PTX in MMP-2 extensive tumor environment. The group later used the MMP-2 sensitive system for the co-delivery of PTX and SiRNA to cancerous cells [109,110]. Further, a triblock Polylactic acid (PLA)-peptide-PLA system was developed using MMP-2 sensitive peptide. The peptide cleavage resulted in a decrease in glass transition temperature which was used as a trigger for targeted cargo release at cancerous site [111]. In another study, curcumin, as an antitumor drug was sandwiched between two polycaprolactone (PCL) blocks through MMP-2 sensitive peptide for cancer treatment [112]. Cathepsin B sensitive peptide was used to conjugate drugs like Doxorubicin (DOX) and Gemcitabine to a dendrimer system for targeted drug delivery [107,113]. MMP-9 responsive peptide was conjugated to gold nanoclusters for cancer detection, with a rationale that upon enzyme activity in cancerous environment, the gold nanoclusters would pass through kidney to be detected in urine [75].

In contrast to material design strategies, where enzymatic cleavage has resulted in degradation or disassembly, cleavage of MMP sensitive peptides were used to decrease the hydrophilic - hydrophobic ratio which resulted in the targeted aggregation of the otherwise soluble amphiphilic system [87]. An MMP responsive peptide was used as a hydrophilic domain in an amphiphilic system where PTX formed the hydrophobic domain. MMP degradation of the outer shell resulted in the aggregation of hydrophobic drug at the cancerous site to exert its cytotoxicity [108]. The above discussed are only a few of the various ways in which mast cell enzyme sensitive peptide substrates can be used in designing mast cell responsive materials, and that the potential of these substrates are vast in therapies.

2.2.3.3. Strategies around gelatin to design MMP-9 responsive systems

As discussed above, gelatin has found varied applications in food and pharmaceutical industry [110,111]. In academic research, gelatin biomaterials ranging from hydrogels, nanostructures, electrospun mats and coatings have regularly been discussed [80]. Gelatin based systems however exhibit high water absorptivity and results in the immediate swelling and burst release of cargo [114,115]. This makes such systems inadequate for targeted application. Furthermore, gelatin possess large number of ionizable groups, electrostatic repulsion of which results in the unwanted release of the payload, again making it unsuitable for targeted therapies [116]. To circumvent these issues, crosslinking has been used. It has been shown that by varying the degree of crosslinking, the release profile at physiological conditions could be manipulated [117]. Pullulan dialdehyde was used to crosslink gelatin to form a high strength gelatin hydrogel which exhibited crosslink-dependent degradation profile in the presence of collagenase [118]. Another study used genipin as a crosslinker to prepare gelatin microspheres as a delivery system for the inflamed bones. The microspheres were then loaded with BMP-2 (bone morphogenic protein, promoting osteogenesis) as a therapeutic target [119].

Another efficient technique which holds promise, particularly in the design of MMP-9 stimulated release systems, is the use of gelatin as coatings. Gelatin was thermally adsorbed and crosslinked onto DOX loaded mesoporous silica nanoparticles (MSN). The nanoparticle-gelatin system remained stable exhibiting less than 4% drug release leased at physiological conditions [116]. To demonstrate a MMP-9 triggered release system, DOX was adsorbed onto aldehyde modified MSNs, which were then sealed with crosslinked gelatin. The system, which otherwise was stable in normal physiological condition over a range of pH, presence of MMP-9 in the *in vitro* condition resulted in burst release of DOX [120]. Gelatin coating also renders stability to drug loaded lipid

nanoparticles. The stability of these system over a wide range of pH could be used to target the site of high MMP-9 level which would facilitate localized cargo delivery [121].

2.3. Mast cell released ROS as localized inflammatory stimulus and design strategies for ROS responsive systems

ROS as an immune regulating molecule is primarily associated with macrophages [122]; however, mast cells have also been shown to release ROS upon activation. Intracellular ROS (ROS_{in}) is characteristic of mast cell activation. ROS within cell membrane is produced irrespective of mast cell activation mechanism. Antigens, thapsigargin and ionomycin, which activate immunologically through the FcεRI receptor, non-immunologically, and through the calcium transport respectively, have shown to induce ROS_{in} in mast cells [18,123,124]. Furthermore, compounds which activate mast cells through specific cell receptors, with the likes of advanced glycation end products and Galectin-3 have also been shown to induce ROS_{in} [22,125]. ROS_{in} is an immediate burst release, which occurs and peaks within the minutes of cell activation [18,123]. Superoxide radicals (O_2^-) radicals and Hydrogen peroxides (H_2O_2) are the two main constituents of ROS that have been identified within mast cells [126,127], and no intracellular nitric oxide could be detected in rat, mouse, and human mast cell upon antigen stimulation [123]. FcεRI mediated mast cell activation results in both O_2^- radicals and H_2O_2 production, however, by two independent pathways, and that they have been shown to inversely effect each other's release [128].

In contrast to ROS_{in}, a consensus does not exist on the release of ROS into the extracellular space (ROS_{ex}). *In vitro* study of the ROS_{ex} from the purified rat mast cells concluded that ROS_{ex} was primarily from the remnant macrophage impurity present in mast cell population [129]. However,

it was later shown that antigens, heavy metals like silver, and compound like epigallocatechin-3-gallate could induce release of ROS into the extracellular fluid [19,130]. The release of ROS_{ex} was immediate and like ROS_{in} consisted of O_2^- and H_2O_2. In addition to these, glycation products and galectin-3, which activates mast cell through their specific receptors have also been shown to induce ROS_{ex} upon cell activation, however, the release of ROS_{ex} in response to galectin-3 has been associated with mast cell apoptosis [22,125]. Apart from ROS_{ex} derived exclusively from mast cells, close proximity of mast cells to macrophages, which are well documented to release ROS in their extracellular matrix, also exposes the mast cells to ROS_{ex} [122]. As discussed, ROS_{in} and ROS_{ex} released upon mast cell activation are transient, and thus present themselves as an excellent stimulus for targeted therapeutics application. The recent advancement in the development of highly sensitive ROS sensitive molecules opens new avenue in the design and development of ROS stimulated inflammatory responsive materials.

Release of ROS upon mast cell activation, both within and in the extracellular space, offers an excellent stimulus to develop strategies centered around mast cells to target inflammations. Contemporary research on stimuli responsive materials has seen significant progress made in the design and development of ROS sensitive materials. ROS sensitive moieties within a material can be broadly classified into two – one, which in the presences of ROS undergoes a hydrophobic to hydrophilic phase switch, with the likes of sulphides, selenides and tellurides; and two, which undergo ROS based cleavage, with the likes of diselenides and thioketals among others (Figure 2.4) [131,132]. An extensive review of ROS sensitive molecules is beyond the motive for this review and readers are encouraged to read the reviews referenced above [131,132]. However, inhere only ROS sensitive thioketal (TK) molecule will be discussed because of its versatility in its susceptibility to several ROS molecules [133–135], synthesis of molecule with different

functional group and hence ease of conjugation to other biomaterials and biomolecules [134,136], stability across pH ranges, nontoxicity, and high reaction yields [137,138].

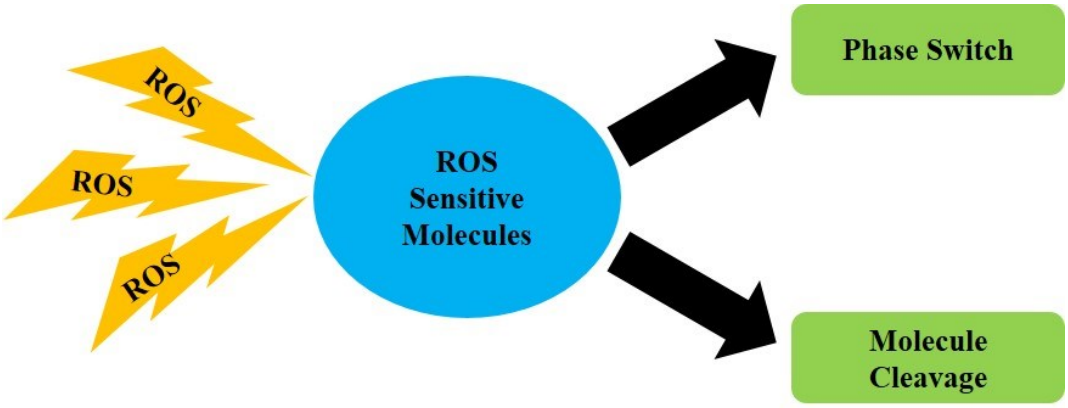

Figure 2.4. Generalized response of ROS sensitive molecules in the presence of ROS. Two classes of ROS sensitive molecules are being widely used. The first class, which includes sulphides, selenides and tellurides, respond by undergoing a hydrophobic to hydrophilic phase switch. The second class undergoes a ROS mediated cleavage, examples being diselenides and thioketals.

Susceptibility of TKs have been shown against O_2^-, hydroxyl radicals ($OH^\bullet$) and H_2O_2 [133–135,137]. TK undergoes hydrolysis in ROS extensive environment to get cleaved into a ketone and other reaction products [Figure 2.5] [135]. Because of its excellent ROS sensitivity, TKs have found varied applications in biomedical research ranging from chemotherapy, photodynamic therapy (PDT), to drug and therapeutic delivery [137,139,140]. Owed to its versatility, TKs with varied bi-functional groups have been synthesized to facilitate its incorporation and conjugation into biologically relevant material systems. Synthesis of TKs with bifunctional carboxylic groups, amine groups, hydroxyl, thio and allyl groups have been reported (Figure 2.5) [139,141]. Furthermore, bifunctional TK bearing an amine and a carboxyl group on either side of the molecule has also been synthesized [142].

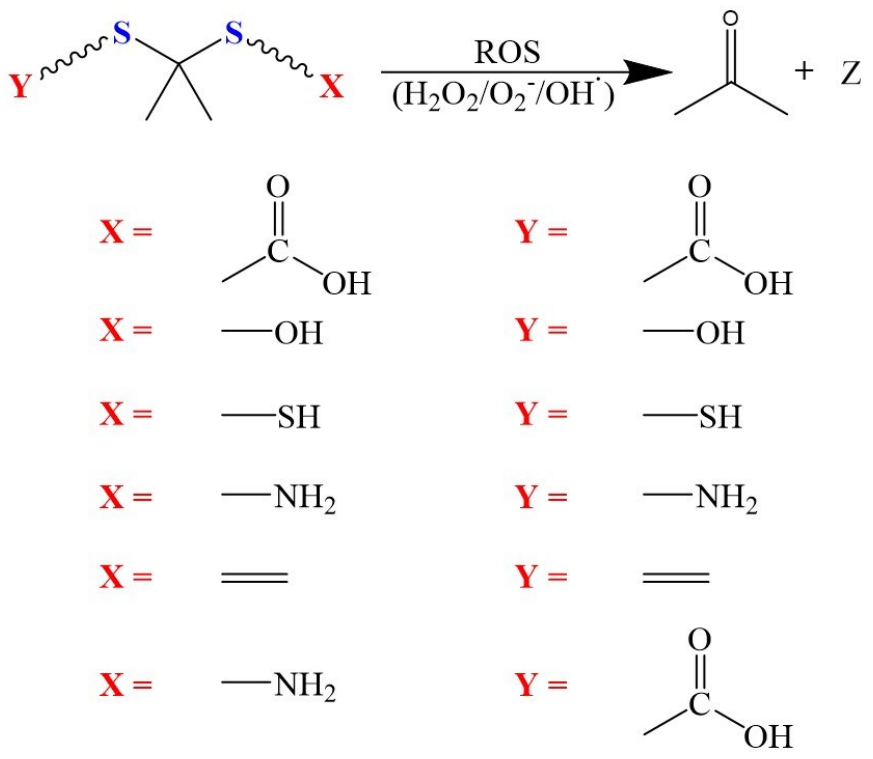

Figure 2.5. ROS triggered cleavage of TK molecule. It results in the formation of acetone and other reaction products (Z). The cleavage occurs in the presence of various types of ROS including O2−, OH• and H2O2. X, Y represent the various end functional groups that have been synthesized on TK to facilitate easy chemical conjugation to biological systems and drugs.

Pertinence of TK as a part of ROS sensitive system has mostly been explored, so far, as a drug/therapeutic delivery platform in cancer research. Cancerous cells have elevated level of ROS, which is being tapped to trigger the cargo release from the TK bearing materials. Having said that, these approaches are also applicable for inflamed tissues which as well exhibit high levels of ROS in their microenvironment. Incorporation of TK into the repeating unit of a polymer enables fast degradation and quick release of cargo at the target site. TK containing polymers have been used to deliver transfecting DNAs and chemotherapeutic drugs like PTX and DOX [134,140,143]. TK, as a part of copolymer system and as a crosslinker for polyethyleneimine has been used to enhance the efficiency of targeted siRNAs in gene silencing [137,141]. Interestingly in another approach,

TK was copolymerized with the cancer drug mitoxantrone (MTO) to form a polydrug molecule. It was then loaded into a polymeric nano-assembly containing cell recognition peptide motif for targeted delivery. High ROS levels in the cancerous cells triggered the release MTO form the polydrug exerting its cytotoxic properties [144]. This synergistic approach could be very well exploited for targeting inflammation through mast cells as the ligands for a very specific mast cells receptor have been identified (discussed in the next section). The discussed strategies show that the significant developments that has been made in engineering ROS responsive system would ease its repurposing to cater targeted inflammatory and allergic therapies.

2.4. Mast cell MRGPRX2 as inflamed tissue specific receptor for targeted therapies and MRGPRX2 peptide ligands for targeted delivery

Mas related G protein receptor X2 (MRGPRX2) is a mast cell specific cell surface receptor which has been shown to activate mast cells [23–25]. The expression profile of this receptor on mast cell has been shown to vary with anatomical sites in normal physiological conditions, as well with a diseased and a non-diseased conditions. Recent studies have identified several small molecules and peptide ligands which are specific to MRGPRX2 receptor [145,146]. The structures of peptides that activate mast cell through MRGPRX2 highlights a distinct physio-chemical motif within the peptide molecule. Conversely, the presence of the 'distinct core structure' within the amino acid sequence confers MRGPRX2 specificity to the molecule [147–149]. Taking this further, our group has proposed a generalized structure to design MRGPRX2 specific peptides with varied mast cell activating potential [150]. An optimized core peptide structure which can activate mast cell MRGPRX2 receptor can be deduced to X_a-$(Y)_{(n \geq 3)}$-X_b where: X_a is an aromatic residue; X_b is a hydrophobic residue; and Y is a minimum 3 residue long sequence, containing a minimum of one positively charged residue with the remainder being uncharged residues [150].

Table 2.5 lists several MRGPRX2 specific peptide with varying activity towards mast cells. The peptides coupled with the disparity in MRGPRX2 expression in mast cells from different anatomical sites; and between a healthy and diseased tissue, offers an excellent strategy to target specific tissues in an inflammatory episode [151,152]. Furthermore, since, the activity of mast cell through these peptides can be controlled; it gives a synergetic benefit to yield a desired mast cell response in immunotherapy, if and when needed [39,153,154]. The idea of targeting a diseased tissue through peptide ligand is already in practice and has been widely used in different shapes and form; in applications like cargo delivery, detection, and imaging [155]. Herein, few of the works on the use of synthetic tissue recognizing peptide in targeted biomedical applications will be discussed, to draw a parallel in strategies that can be employed to target inflammation through peptide ligands specific to mast cell MRGPRX2 receptor (Figure 2.6).

Tissue targeting through homing peptides has gained wide popularity in cancer research. Ideally, tissue-recognizing peptides are exposed on the delivery system to get recognized by the targeted cells. Several cell recognition peptides have been identified and are routinely being used in cancer research [155]. Tissue targeting peptide was attached on the surface of iron oxide nanoparticles to serve as a contrasting agent for the magnetic resonance imaging of cancerous tissue [156,157]. DOX loaded, gold coated silica nanoparticles were decorated with homing peptides for the NIR triggered release of drug at the cancerous site [158]. Similarly, receptor specific peptide ligands have been conjugated to polymeric nano-assemblies, liposomes and hydrogels to facilitate targeted release of cargo [159–162].

In addition to these, targeting peptides have also been used in synergy with other functionalities. As mentioned above, Arg-Gly-Asp has been used in conjugation with ROS sensitive TK molecule to localize the ROS dependent release chemotherapeutic drug to the cancerous tissue [138,144].

Furthermore, conjugation of cancerous cell penetrating peptide Arg-Gly-Asp and LyP-1 to MMP-9 sensitive nano-sensors has been discussed for the detection of small cancers through urine [163]. The discussed strategies are well developed and hence can be very efficiently used in targeting inflammations.

2.5. Limitations and challenges

Tryptase and chymase come from a family of serine proteases and hence have overlapping substrate specificities with other member of this family [54], and therefore it is imperative to test a given substrate against all relevant enzymes that may interfere with the respective therapeutic material. The most common and the most important enzymes that must be considered while designing a peptide substrate for tryptase and chymase are trypsin and chymotrypsin. Like tryptase, trypsin favors a basic residue at P1 [54], and similarly, like chymase, chymotrypsin prefers a hydrophobic amino acid with aromatic side chain [70]. It was found that enzymatic activity of human airway trypsin (HAT) on substrates simultaneously studied for tryptase was multifold higher, while HAT had a K_{cat}/K_M value of 0.454×10^6 $M^{-1}s^{-1}$ and 0.195 10^6 $M^{-1}s^{-1}$ for entry 20 and 21 in Table 2.2 respectively, tryptase had the same value at 0.027×10^6 $M^{-1}s^{-1}$ and 0.006×10^6 $M^{-1}s^{-1}$ respectively [60]. Substrate overlap of tryptase has also been studied with human plasma thrombin, and coagulant factor Xa [58]. In case of chymase, substrate overlap has been shown with chymotrypsin, cathepsin G and carboxypeptidase A [63,68,70]. A comparison of chymase activity with cathepsin G activity on thio-benzyl ester substrate (Table 2.3, entry 1) showed that chymase was only 7-fold more active than cathepsin G (K_{cat}/K_M value 8.3×10^6 $M^{-1}s^{-1}$ for human chymase vs 1.2×10^6 $M^{-1}s^{-1}$ for human leukocyte cathepsin G) [70]. Likewise, the substrate overlaps of MMP-9 should also be cross verified with other relevant MMPs present during the design of an MMP-9 responsive biomaterials to target inflammations.

Though several enzymes may compete for a given substrate, subtle changes in the substrate structure has shown to alters the enzyme activity. For example, C-terminal aldehyde analogous of substrates (Table 2.2, entry 20 and 21) have shown to reverse the enzymatic activity between HAT and tryptase [60]. The competitive activity of enzymes against a given substrates can also be modulated by using D- amino acids in the peptide structure [70]. Furthermore, since the serine enzymes have an extended substrate specificity, careful positioning of respective amino acids at a given substrate position may give a favorable substrate. For example, even though enzymes like human plasma thrombin and coagulant factor Xa favors a tryptase like basic amino acid residue at P1, the most favored amino acid at position P2 was proline for thrombin and phenylalanine for coagulant factor Xa, whereas for tryptase it was asparagine [58]. This was also apparent in competitive study of chymase with carboxypeptidase A against Ang I, where the activity of carboxypeptidase was deemed negligible in converting Ang I to Ang II [68]. Similarly, P2 Arginine and P2′ Serine/Threonine in peptide substrates impart MMP-9 specificity against other MMPs. Coupled to these, significant advancement and feasibility of computational methods has made it possible for a facile screening of substrates against various enzymes which could be used to test a substrate before bringing it to use [82].

Table 2.5. MRGPRX2 specific peptides ligands to be used as homing peptides for inflamed tissues

Entry	Peptide Ligand	Relative mast cell degranulation %	Model Cell	Reference
1	Trp-Lys-Lys-Lys-Trp	111	LAD 2 Cell; β-hex released upon stimulation with PAMP-12 is taken as 100 %	[150]
2	Phe-Arg-Lys-Lys-Trp	108		
3	Phe-Arg-Lys-Lys-Trp-Asn-Lys-Trp-Ala-Leu-Ser-Arg	100		
4	Tyr-Lys-Lys-Lys-Tyr	89		
5	Lys-Lys-Trp-Asn-Lys-Trp-Ala-Leu-Ser-Arg	75		
6	Lys-Trp-Asn-Lys-Trp-Ala-Leu-Ser-Arg	59		
7	Trp-Asn-Lys-Trp-Ala	52		
8	Asn-Lys-Trp-Ala-Leu-Ser-Arg	8		
9	Pro-Cys-Lys-Asn-Phe-Phe-Trp-Lys-Thr-Phe-Ser-Ser-Cys-Lys	100	MRGPRX2 transfected cell; calcium released upon stimulation with PAMP-12 and Cortistatin-14 is taken as 100 %	[147]
10	Ser-Glu-Phe-Arg-Lys-Lys-Trp-Asn-Lys-Trp-Ala-Leu-Ser-Arg	53		
11	Asp-Val-Ala-Ser-Glu-Phe-Arg-Lys-Lys-Trp-Asn-Lys-Trp-Ala-Leu-Ser-Arg	23		
12	Ala-Arg-Leu-Asp-Val	3		
13	Cyclic-Ala-Gly-Cys-Lys-Asn-Phe-Phe-Trp-(D)Lys-Thr-Phe-Thr-Ser-Cys	400	Rat peritoneal mast cell; histamine released upon stimulation with Somatostatin is taken as 100 %	[149]
14	Cyclic-Ala-Gly-Cys-Lys-Asn-Phe-Phe-Trp-Lys-Thr-Phe-Thr-Ser-Cys	100		
15	Non-Cyclic-Ala-Gly-Cys-Lys-Asn-Phe-Phe-Trp-Lys-Thr-Phe-Thr-Ser-Cys	33		

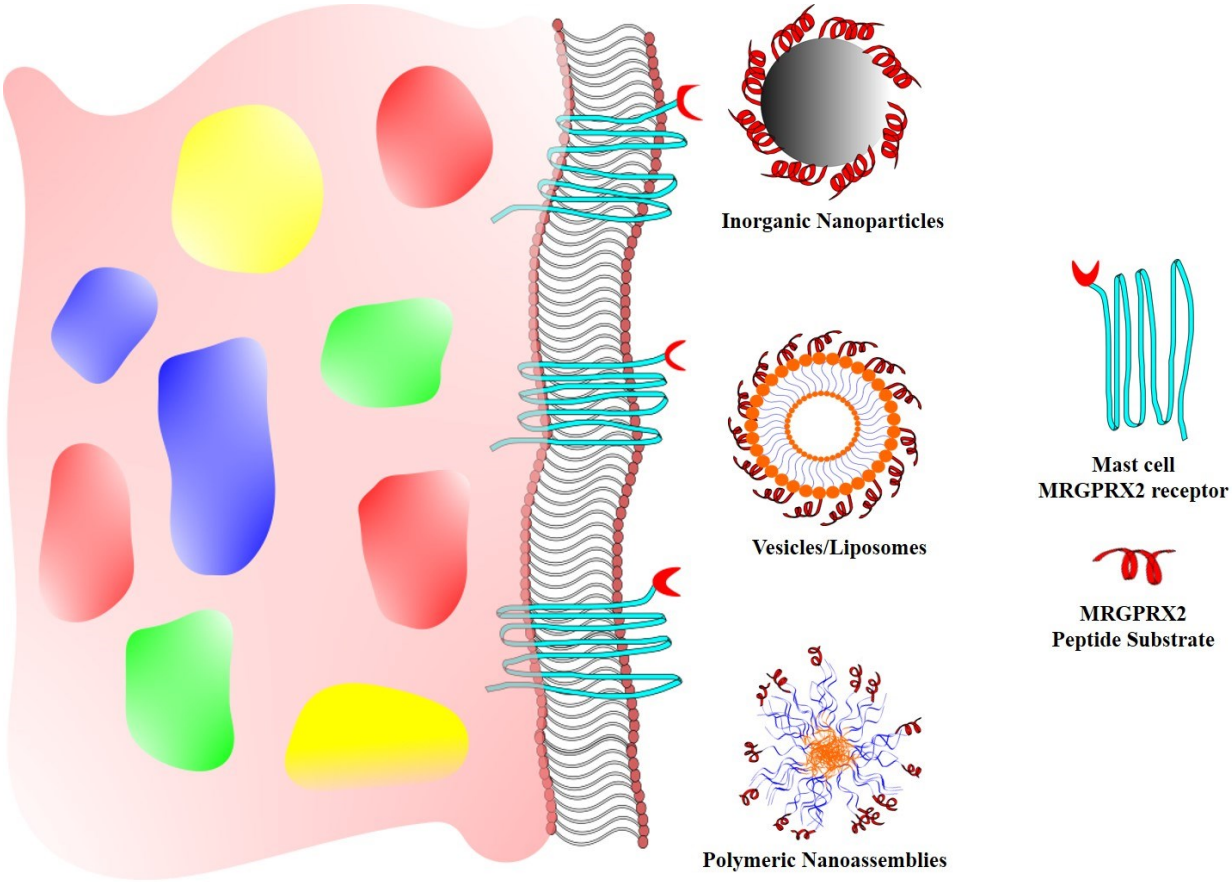

Figure 2.6. Cartoon representation of mast cell showing expression of MRGPRX2 receptor on its surface. MRGPRX2 can be used a cell specific receptor to specifically target mast cells. Several MRGPRX2 peptide substrates have been identified which can be exposed onto the surface of delivery systems to localize the delivery in and around inflammatory tissue.

Apart from substrate overlap, differences in the catalytic activity of an enzyme from different sources could hinder the development of a versatile substrate for all inflammatory disease (as shown in Table 2.2, entry 1-10, human skin tryptase was 10-fold more reactive for a given substrate than human lung tryptase). Adding to these, the ultimate diffusion of the enzymes in to the blood stream may hinder targeted therapeutic approach is [97,164]. Normally these enzymes are highly regulated to inhibit their widespread action throughout the host; however, enzymes eventually enter circulation. Blood levels of β-tryptase peaks within 15 – 20 min for an inflammatory response, increasing from < 1 ng/mL to > 10 ng/mL, before it declines with half-life of around 2

h [164]. Similarly, blood tryptase levels spike between 0.5 to 6 h at up to 2242 and 710 % for anaphylactic shock and anaphylactic reactions due to drug allergy respectively, before reaching to the physiological levels after 24 h [165]. Enzyme concentration kinetics are another feature of the system that should be considered when designing enzyme activated therapeutics.

Targeting an inflammatory disease through mast cell is in the use of mast cell specific MRGPRX2 receptor poses the risk of partial of complete mast cell activation. Though mast cell activation could be beneficial in certain cases [154], its activation could aggravate inflammatory conditions. Hence, the use of MRGPRX2 specific peptides in targeting a disease would entail a tradeoff between the therapeutic efficiency and the corresponding cell activation. It is therefore necessary to critically examine the therapeutic outcome while using MRGPRX2 specific peptides for cell targeting.

2.6. Conclusion

As and when the significance of mast cell becomes more and more evident, it would be advantageous to design and develop therapeutics around them. Furthermore, mast cells being the first responders of inflammatory and allergic diseases gives us the opportunity to control the disease form the early days of progression. Furthermore, various ways that inflammation could be targeted through mast cell has been shown. The substrates and strategies discussed here will open new avenues of therapies for inflammatory diseases.

2.7. References

[1] J.S. Marshall, Mast-cell responses to pathogens, Nature Reviews Immunology. 4 (2004) 787–799. https://doi.org/10.1038/nri1460.

[2] M. Urb, D.C. Sheppard, The role of mast cells in the defence against pathogens, PLoS Pathogens. 8 (2012) 2–4. https://doi.org/10.1371/journal.ppat.1002619.

[3] C. Benoist, D. Mathis, Mast cells in autoimmune disease, Nature. 420 (2002) 875–878.

[4] S.J. Galli, M. Tsai, IgE and mast cells in allergic disease, Nature Medicine. 18 (2012) 693–704. https://doi.org/10.1038/nm.2755.

[5] C. Zimmermann, D. Troeltzsch, V.A. Giménez-Rivera, S.J. Galli, M. Metz, M. Maurer, F. Siebenhaar, Mast cells are critical for controlling the bacterial burden and the healing of infected wounds, Proceedings of the National Academy of Sciences of the United States of America. 116 (2019) 20500–20504. https://doi.org/10.1073/pnas.1908816116.

[6] S. Balzar, H.W. Chu, M. Strand, S. Wenzel, Relationship of small airway chymase-positive mast cells and lung function in severe asthma, American Journal of Respiratory and Critical Care Medicine. 171 (2005) 431–439. https://doi.org/10.1164/rccm.200407-949OC.

[7] H. Hamada, M. Terai, H. Kimura, K. Hirano, S. Oana, H. Niimi, Increased expression of mast cell chymase in the lungs of patients with congenital heart disease associated with early pulmonary vascular disease, American Journal of Respiratory and Critical Care Medicine. 160 (1999) 1303–1308. https://doi.org/10.1164/ajrccm.160.4.9810058.

[8] A. Järvikallio, A. Naukkarinen, I.T. Harvima, M.L. Aalto, M. Horsmanheimo, Quantitative analysis of tryptase- and chymase-containing mast cells in atopic dermatitis and nummular eczema, British Journal of Dermatology. 136 (1997) 871–877. https://doi.org/10.1111/j.1365-2133.1997.tb03927.x.

[9] M.G. Buckley, P.J. Gallagher, A.F. Walls, Mast cell subpopulations in the synovial tissue of patients with osteoarthritis: Selective increase in numbers of tryptase-positive, chymase- negative mast cells, Journal of Pathology. 186 (1998) 67–74. https://doi.org/10.1002/(SICI)1096-9896(199809)186:1<67::AID-PATH132>3.0.CO;2-D.

[10] J.P. Kankkunen, I.T. Harvima, A. Naukkarinen, Quantitative analysis of tryptase and chymase containing mast cells in benign and malignant breast lesions, International Journal of Cancer. 72 (1997) 385–388. https://doi.org/10.1002/(SICI)1097-0215(19970729)72:3<385::AID-IJC1>3.0.CO;2-L.

[11] T. Ibaraki, M. Muramatsu, S. Takai, D. Jin, H. Maruyama, T. Orino, T. Katsumata, M. Miyazaki, The relationship of tryptase- and chymase-positive mast cells to angiogenesis in stage I non-small cell lung cancer, European Journal of Cardio-Thoracic Surgery. 28 (2005) 617–621. https://doi.org/10.1016/j.ejcts.2005.06.020.

[12] G. Varricchi, G. Marone, P.T. Kovanen, Cardiac Mast Cells: Underappreciated Immune Cells in Cardiovascular Homeostasis and Disease, Trends in Immunology. 41 (2020) 734–746. https://doi.org/10.1016/j.it.2020.06.006.

[13] M. Yamada, M. Ueda, T. Naruko, S. Tanabe, Y.S. Han, Y. Ikura, M. Ogami, S. Takai, M. Miyazaki, Mast cell chymase expression and mast cell phenotypes in human rejected kidneys,

Kidney International. 59 (2001) 1374–1381. https://doi.org/10.1046/j.1523-1755.2001.0590041374.x.

[14] S. Wernersson, G. Pejler, Mast cell secretory granules: armed for battle, Nature Reviews Immunology. 14 (2014) 478.

[15] J. Kalesnikoff, S.J. Galli, New developments in mast cell biology, Nature Immunology. 9 (2008) 1215–1223. https://doi.org/10.1038/ni.f.216.

[16] T.C. Moon, A. Dean Befus, M. Kulka, Mast cell mediators: Their differential release and the secretory pathways involved, Frontiers in Immunology. 5 (2014) 1–18. https://doi.org/10.3389/fimmu.2014.00569.

[17] N. di Girolamo, I. Indoh, N. Jackson, D. Wakefield, H.P. McNeil, W. Yan, C. Geczy, J.P. Arm, N. Tedla, Human Mast Cell-Derived Gelatinase B (Matrix Metalloproteinase-9) Is Regulated by Inflammatory Cytokines: Role in Cell Migration, The Journal of Immunology. 177 (2006) 2638–2650. https://doi.org/10.4049/jimmunol.177.4.2638.

[18] T. Inoue, Y. Suzuki, T. Yoshimaru, C. Ra, Reactive oxygen species produced up- or downstream of calcium influx regulate proinflammatory mediator release from mast cells: Role of NADPH oxidase and mitochondria, Biochimica et Biophysica Acta - Molecular Cell Research. 1783 (2008) 789–802. https://doi.org/10.1016/j.bbamcr.2007.12.004.

[19] T. Inoue, Y. Suzuki, C. Ra, Epigallocatechin-3-gallate induces cytokine production in mast cells by stimulating an extracellular superoxide-mediated calcium influx, Biochemical Pharmacology. 82 (2011) 1930–1939. https://doi.org/10.1016/j.bcp.2011.09.011.

[20] S.J. Galli, S. Nakae, M. Tsai, Mast cells in the development of adaptive immune responses, Nature Immunology. 6 (2005) 135.

[21] A.M. Gilfillan, C. Tkaczyk, Integrated signalling pathways for mast-cell activation, Nature Reviews Immunology. 6 (2006) 218–230. https://doi.org/10.1038/nri1782.

[22] T. Yoshimaru, Y. Suzuki, T. Inoue, S. Nishida, C. Ra, Extracellular superoxide released from mitochondria mediates mast cell death by advanced glycation end products, Biochimica et Biophysica Acta (BBA) - Molecular Cell Research. 1783 (2008) 2332–2343. https://doi.org/10.1016/j.bbamcr.2008.08.010.

[23] B.D. McNeil, P. Pundir, S. Meeker, L. Han, B.J. Undem, M. Kulka, X. Dong, Identification of a mast-cell-specific receptor crucial for pseudo-allergic drug reactions, Nature. 519 (2015) 237–241. https://doi.org/10.1038/nature14022.

[24] W. Manorak, C. Idahosa, K. Gupta, S. Roy, R. Panettieri, H. Ali, Upregulation of Mas-related G Protein coupled receptor X2 in asthmatic lung mast cells and its activation by the novel neuropeptide hemokinin-1, Respiratory Research. 19 (2018) 1–5.

[25] H. Subramanian, K. Gupta, H. Ali, Roles of Mas-related G protein–coupled receptor X2 on mast cell–mediated host defense, pseudoallergic drug reactions, and chronic inflammatory diseases, Journal of Allergy and Clinical Immunology. 138 (2016) 700–710.

[26] L. Lu, M.B. Parmar, M. Kulka, P. Kwan, L.D. Unsworth, Self-Assembling Peptide Nanoscaffold That Activates Human Mast Cells, ACS Applied Materials and Interfaces. 10 (2018) 6107–6117. https://doi.org/10.1021/acsami.7b14560.

[27] L.B. Schwartz, K.F. Austen, Enzymes of the mast cell granule, Journal of Investigative Dermatology. 74 (1980) 349–353.

[28] L.B. Schwartz, K.F. Austen, S.I. Wasserman, Immunologic release of β-hexosaminidase and β-glucuronidase from purified rat serosal mast cells, The Journal of Immunology. 123 (1979) 1445–1450.

[29] L.B. Schwartz, R.A. Lewis, D. Seldin, K.F. Austen, Acid hydrolases and tryptase from secretory granules of dispersed human lung mast cells., The Journal of Immunology. 126 (1981) 1290–1294.

[30] Z. Xiang, M. Block, C. Löfman, G. Nilsson, Ige-mediated mast cell degranulation and recovery monitored by time-lapse photography, Journal of Allergy and Clinical Immunology. 108 (2001) 116–121. https://doi.org/10.1067/mai.2001.116124.

[31] L.B. Schwartz, A.M. Irani, K. Roller, M.C. Castells, N.M. Schechter, Quantitation of histamine, tryptase, and chymase in dispersed human T and TC mast cells., The Journal of Immunology. 138 (1987) 2611–2615.

[32] L.B. Schwartz, H.-K. Min, S. Ren, H.-Z. Xia, J. Hu, W. Zhao, G. Moxley, Y. Fukuoka, Tryptase Precursors Are Preferentially and Spontaneously Released, Whereas Mature Tryptase Is Retained by HMC-1 Cells, Mono-Mac-6 Cells, and Human Skin-Derived Mast Cells, The Journal of Immunology. 170 (2003) 5667–5673. https://doi.org/10.4049/jimmunol.170.11.5667.

[33] S. Jogie-Brahim, H.K. Min, Y. Fukuoka, H.Z. Xia, L.B. Schwartz, Expression of α-tryptase and β-tryptase by human basophils, Journal of Allergy and Clinical Immunology. 113 (2004) 1086–1092. https://doi.org/10.1016/j.jaci.2004.02.032.

[34] S. Balzar, M.L. Fajt, S.A.A. Comhair, S.C. Erzurum, E. Bleecker, W.W. Busse, M. Castro, B. Gaston, E. Israel, L.B. Schwartz, D. Curran-Everett, C.G. Moore, S.E. Wenzel, Mast cell phenotype, location, and activation in severe asthma: Data from the Severe Asthma Research Program, American Journal of Respiratory and Critical Care Medicine. 183 (2011) 299–309. https://doi.org/10.1164/rccm.201002-0295OC.

[35] A. Zanini, A. Chetta, M. Saetta, S. Baraldo, R. D'Ippolito, A. Castagnaro, M. Neri, D. Olivieri, Chymase-positive mast cells play a role in the vascular component of airway remodeling in asthma, Journal of Allergy and Clinical Immunology. 120 (2007) 329–333. https://doi.org/10.1016/j.jaci.2007.04.021.

[36] C.K. Andersson, M. Mori, L. Bjermer, C.G. Löfdahl, J.S. Erjefält, Alterations in lung mast cell populations in patients with chronic obstructive pulmonary disease, American Journal of Respiratory and Critical Care Medicine. 181 (2010) 206–217. https://doi.org/10.1164/rccm.200906-0932OC.

[37] B. Hermes, I. Feldmann-Böddeker, P. Welker, B. Algermissen, M.U. Steckelings, J. Grabbe, B.M. Henz, Altered expression of mast cell chymase and tryptase and of c-Kit in human cutaneous scar tissue, Journal of Investigative Dermatology. 114 (2000) 51–55. https://doi.org/10.1046/j.1523-1747.2000.00837.x.

[38] R. Zhang, V.L.Y. Yip, S.G. Withers, Mechanisms of enzymatic glycosyl transfer, (2010).

[39] I.C. Koo, Y.M. Ohol, P. Wu, J.H. Morisaki, J.S. Cox, E.J. Brown, Role for lysosomal enzyme β-hexosaminidase in the control of mycobacteria infection, Proceedings of the National Academy of

Sciences of the United States of America. 105 (2008) 710–715. https://doi.org/10.1073/pnas.0708110105.

[40] N. Fukuishi, S. Murakami, A. Ohno, N. Yamanaka, N. Matsui, K. Fukutsuji, S. Yamada, K. Itoh, M. Akagi, Does β-Hexosaminidase Function Only as a Degranulation Indicator in Mast Cells? The Primary Role of β-Hexosaminidase in Mast Cell Granules, The Journal of Immunology. 193 (2014) 1886–1894. https://doi.org/10.4049/jimmunol.1302520.

[41] E. Trevisan, F. Vita, N. Medic, M.R. Soranzo, G. Zabucchi, V. Borelli, Mast Cells Kill Candida albicans in the Extracellular Environment but Spare Ingested Fungi from Death, Inflammation. 37 (2014) 2174–2189. https://doi.org/10.1007/s10753-014-9951-9.

[42] J.P. Lopes, M. Stylianou, G. Nilsson, C.F. Urban, Opportunistic pathogen Candida albicans elicits a temporal response in primary human mast cells, Scientific Reports. 5 (2015) 1–14. https://doi.org/10.1038/srep12287.

[43] W. Suginta, D. Chuenark, M. Mizuhara, T. Fukamizo, Novel β-N-acetylglucosaminidases from Vibrio harveyi 650: Cloning, expression, enzymatic properties, and subsite identification, BMC Biochemistry. 11 (2010). https://doi.org/10.1186/1471-2091-11-40.

[44] N. Konno, H. Takahashi, M. Nakajima, T. Takeda, Y. Sakamoto, Characterization of β-N-acetylhexosaminidase (LeHex20A), a member of glycoside hydrolase family 20, from Lentinula edodes (shiitake mushroom), AMB Express. 2 (2012) 1–7. https://doi.org/10.1186/2191-0855-2-29.

[45] Q. Yang, T. Liu, F. Liu, M. Qu, X. Qian, A novel β-N-acetyl-d-hexosaminidase from the insect Ostrinia furnacalis (Guenée), FEBS Journal. 275 (2008) 5690–5702. https://doi.org/10.1111/j.1742-4658.2008.06695.x.

[46] S. Katta, S. Ankati, A.R. Podile, Chitooligosaccharides are converted to N-acetylglucosamine by N-acetyl-β-hexosaminidase from stenotrophomonas maltophilia, FEMS Microbiology Letters. 348 (2013) 19–25. https://doi.org/10.1111/1574-6968.12237.

[47] N.O. Keyhani, S. Roseman, The chitin catabolic cascade in the marine bacterium vibrio furnissii: Molecular cloning, isolation, and characterization of a periplasmic β-N-acetylglucosaminidase, Journal of Biological Chemistry. 271 (1996) 33425–33432. https://doi.org/10.1074/jbc.271.52.33425.

[48] F. Nanjo, R. Katsumi, K. Sakai, Purification and characterization of an Exo-β-D-glucosaminidase, a novel type of enzyme, from nocardia orientalis, Journal of Biological Chemistry. 265 (1990) 10088–10094. https://doi.org/10.1016/s0021-9258(19)38783-6.

[49] L. Gushulak, R. Hemming, D. Martin, V. Seyrantepe, A. Pshezhetsky, B. Triggs-Raine, Hyaluronidase 1 and β-hexosaminidase have redundant functions in hyaluronan and chondroitin sulfate degradation, Journal of Biological Chemistry. 287 (2012) 16689–16697. https://doi.org/10.1074/jbc.M112.350447.

[50] S.M. Lim, D.K. Song, S.H. Oh, D.S. Lee-Yoon, E.H. Bae, J.H. Lee, In vitro and in vivo degradation behavior of acetylated chitosan porous beads, Journal of Biomaterials Science, Polymer Edition. 19 (2008) 453–466. https://doi.org/10.1163/156856208783719482.

[51] F. Liaqat, R. Eltem, Chitooligosaccharides and their biological activities: A comprehensive review, Carbohydrate Polymers. 184 (2018) 243–259.

[52] C. Chatelet, O. Damour, A. Domard, Influence of the degree of acetylation on some biological properties of chitosan films, Biomaterials. 22 (2001) 261–268. https://doi.org/10.1016/S0142-9612(00)00183-6.

[53] L.F. Boesel, R.L. Reis, J.S. Román, Innovative approach for producing injectable, biodegradable materials using chitooligosaccharides and green chemistry, Biomacromolecules. 10 (2009) 465–470. https://doi.org/10.1021/bm801332u.

[54] D.N. Gosalia, C.M. Salisbury, J.A. Ellman, S.L. Diamond, High throughput substrate specificity profiling of serine and cysteine proteases using solution-phase fluorogenic peptide microarrays, Molecular and Cellular Proteomics. 4 (2005) 626–636. https://doi.org/10.1074/mcp.M500004-MCP200.

[55] J.J. Perona, C.S. Craik, Structural basis of substrate specificity in the serine proteases, Protein Science. 4 (1995) 337–360.

[56] J.L. Harris, A. Niles, K. Burdick, M. Maffitt, B.J. Backes, J.A. Ellman, I. Kuntz, M. Haak-Frendscho, C.S. Craik, Definition of the Extended Substrate Specificity Determinants for β-Tryptases I and II, Journal of Biological Chemistry. 276 (2001) 34941–34947. https://doi.org/10.1074/jbc.M102997200.

[57] B. Spichalska, A. Lesner, M. Wysocka, M. Śledź, A. Łęgowska, A. Jaśkiewicz, H. Miecznikowska, K. Rolka, The influence of substrate peptide length on human β-tryptase

specificity, Journal of Peptide Science: An Official Publication of the European Peptide Society. 14 (2008) 917–923.

[58] S.T. Furlong, R.C. Mauger, A.M. Strimpler, Y.P. Liu, F.X. Morris, P.D. Edwards, Synthesis and physical characterization of a P1 arginine combinatorial library, and its application to the determination of the substrate specificity of serine peptidases, Bioorganic and Medicinal Chemistry. 10 (2002) 3637–3647. https://doi.org/10.1016/S0968-0896(02)00174-8.

[59] J.A. Cromlish, N.G. Seidah, M. Marcinkiewicz, J. Hamelin, D.A. Johnson, M. Chrétien, Human pituitary tryptase: Molecular forms, NH2-terminal sequence, immunocytochemical localization, and specificity with prohormone and fluorogenic substrates, Journal of Biological Chemistry. 262 (1987) 1363–1373. https://doi.org/10.1016/s0021-9258(19)75795-0.

[60] M. Wysocka, B. Spichalska, A. Lesner, M. Jaros, K. Brzozowski, A. Łęgowska, K. Rolka, Substrate specificity and inhibitory study of human airway trypsin-like protease, Bioorganic & Medicinal Chemistry. 18 (2010) 5504–5509.

[61] T. Tanaka, B.J. McRae, K. Cho, R. Cook, J.E. Fraki, D.A. Johnson, J.C. Powers, Mammalian Tissue Trypsin-like Enzymes, Journal of Biological Chemistry. 258 (1983) 13552–13557.

[62] M. Poe, C.D. Bennett, W.E. Biddison, J.T. Blake, G.P. Norton, J.A. Rodkey, N.H. Sigal, R. v. Turner, J.K. Wu, H.J. Zweerink, Human cytotoxic lymphocyte tryptase. Its purification from granules and the characterization of inhibitor and substrate specificity, Journal of Biological Chemistry. 263 (1988) 13215–13222. https://doi.org/10.1016/s0021-9258(18)37694-4.

[63] W.W. Raymond, S. Waugh Ruggles, C.S. Craik, G.H. Caughey, Albumin is a substrate, of human chymase: Prediction by combinatorial peptide screening and development of a selective inhibitor

based on the albumin cleavage site, Journal of Biological Chemistry. 278 (2003) 34517–34524. https://doi.org/10.1074/jbc.M304087200.

[64] M. Bastos, N.J. Maeji, R.H. Abeles, Inhibitors of human heart chymase based on a peptide library, Proceedings of the National Academy of Sciences of the United States of America. 92 (1995) 6738–6742. https://doi.org/10.1073/pnas.92.15.6738.

[65] A. Kinoshita, H. Urata, F.M. Bumpus, A. Husain, Multiple determinants for the high substrate specificity of an angiotensin II-forming chymase from the human heart, Journal of Biological Chemistry. 266 (1991) 19192–19197. https://doi.org/10.1016/s0021-9258(18)54981-4.

[66] S. Sanker, U.M. Chandrasekharan, D. Wilk, M.J. Glynias, S.S. Karnik, A. Husain, Distinct multisite synergistic interactions determine substrate specificities of human chymase and rat chymase-1 for angiotensin II formation and degradation, Journal of Biological Chemistry. 272 (1997) 2963–2968. https://doi.org/10.1074/jbc.272.5.2963.

[67] H. Urata, A. Kinoshita, K.S. Misono, F.M. Bumpus, A. Husain, Identification of a highly specific chymase as the major angiotensin II-forming enzyme in the human heart, Journal of Biological Chemistry. 265 (1990) 22348–22357. https://doi.org/10.1016/s0021-9258(18)45712-2.

[68] S. Ahmad, K.N. Wright, X. Sun, L. Groban, C.M. Ferrario, Mast cell peptidases (carboxypeptidase A and chymase)-mediated hydrolysis of human angiotensin-(1–12) substrate, Biochemical and Biophysical Research Communications. 518 (2019) 651–656. https://doi.org/10.1016/j.bbrc.2019.08.098.

[69] M.K. Andersson, M. Enoksson, M. Gallwitz, L. Hellman, The extended substrate specificity of the human mast cell chymase reveals a serine protease with well-defined substrate recognition profile, International Immunology. 21 (2009) 95–104. https://doi.org/10.1093/intimm/dxn128.

[70] J.C. Powers, T. Tanaka, J.W. Harper, Y. Minematsu, L. Barker, D. Lincoln, K. v Crumley, J.E. Fraki, N.M. Schechter, Mammalian chymotrypsin-like enzymes. Comparative reactivities of rat mast cell proteases, human and dog skin chymases, and human cathepsin G with peptide 4-nitroanilide substrates and with peptide chloromethyl ketone and sulfonyl fluoride inhibitors, Biochemistry. 24 (1985) 2048–2058.

[71] M.K. Andersson, M. Thorpe, L. Hellman, Arg143 and Lys192 of the human mast cell chymase mediate the preference for acidic amino acids in position P2′ of substrates, FEBS Journal. 277 (2010) 2255–2267. https://doi.org/10.1111/j.1742-4658.2010.07642.x.

[72] B. Korkmaz, G. Jégot, L.C. Lau, M. Thorpe, E. Pitois, L. Juliano, A.F. Walls, L. Hellman, F. Gauthier, Discriminating between the activities of human cathepsin G and chymase using fluorogenic substrates, The FEBS Journal. 278 (2011) 2635–2646.

[73] N. Lingwal, M. Padmasekar, B. Samikannu, R.G. Bretzel, K.T. Preissner, T. Linn, Inhibition of gelatinase B (matrix metalloprotease-9) activity reduces cellular inflammation and restores function of transplanted pancreatic islets, Diabetes. 61 (2012) 2045–2053. https://doi.org/10.2337/db11-1143.

[74] E. Kolaczkowska, B. Arnold, G. Opdenakker, Gelatinase B/MMP-9 as an inflammatory marker enzyme in mouse zymosan peritonitis: Comparison of phase-specific and cell-specific production

by mast cells, macrophages and neutrophils, Immunobiology. 213 (2008) 109–124. https://doi.org/10.1016/j.imbio.2007.07.005.

[75] C.N. Loynachan, A.P. Soleimany, J.S. Dudani, Y. Lin, A. Najer, A. Bekdemir, Q. Chen, S.N. Bhatia, M.M. Stevens, Renal clearable catalytic gold nanoclusters for in vivo disease monitoring, Nature Nanotechnology. 14 (2019) 883–890. https://doi.org/10.1038/s41565-019-0527-6.

[76] J. Pugin, M.C. Widmer, S. Kossodo, C.M. Liang, H.L. Preas, A.F. Suffredini, Human neutrophils secrete gelatinase B in vitro and in vivo in response to endotoxin and proinflammatory mediators, American Journal of Respiratory Cell and Molecular Biology. 20 (1999) 458–464. https://doi.org/10.1165/ajrcmb.20.3.3311.

[77] N. Kanbe, A. Tanaka, M. Kanbe, A. Itakura, M. Kurosawa, H. Matsuda, Human mast cells produce matrix metalloproteinase 9, European Journal of Immunology. 29 (1999) 2645–2649.

[78] H. Trøstrup, P. Holstein, T. Karlsmark, C. Moser, M.S. Ågren, Uncontrolled gelatin degradation in non-healing chronic wounds, Journal of Wound Care. 27 (2018) 724–734. https://doi.org/10.12968/jowc.2018.27.11.724.

[79] N. Lingwal, M. Padmasekar, B. Samikannu, R.G. Bretzel, K.T. Preissner, T. Linn, Inhibition of gelatinase B (matrix metalloprotease-9) activity reduces cellular inflammation and restores function of transplanted pancreatic islets, Diabetes. 61 (2012) 2045–2053.

[80] M. Santoro, A.M. Tatara, A.G. Mikos, Gelatin carriers for drug and cell delivery in tissue engineering, Journal of Controlled Release. 190 (2014) 210–218.

[81] D. Olsen, C. Yang, M. Bodo, R. Chang, S. Leigh, J. Baez, D. Carmichael, M. Perälä, E.-R. Hämäläinen, M. Jarvinen, Recombinant collagen and gelatin for drug delivery, Advanced Drug Delivery Reviews. 55 (2003) 1547–1567.

[82] U. Eckhard, P.F. Huesgen, O. Schilling, C.L. Bellac, G.S. Butler, J.H. Cox, A. Dufour, V. Goebeler, R. Kappelhoff, U. auf dem Keller, Active site specificity profiling of the matrix metalloproteinase family: Proteomic identification of 4300 cleavage sites by nine MMPs explored with structural and synthetic peptide cleavage analyses, Matrix Biology. 49 (2016) 37–60.

[83] B.I. Ratnikov, P. Cieplak, K. Gramatikoff, J. Pierce, A. Eroshkin, Y. Igarashi, M. Kazanov, Q. Sun, A. Godzik, A. Osterman, Basis for substrate recognition and distinction by matrix metalloproteinases, Proceedings of the National Academy of Sciences. 111 (2014) E4148–E4155.

[84] S.J. Kridel, E. Chen, L.P. Kotra, E.W. Howard, S. Mobashery, J.W. Smith, Substrate hydrolysis by matrix metalloproteinase-9, Journal of Biological Chemistry. 276 (2001) 20572–20578.

[85] N. Singh, A. Karambelkar, L. Gu, K. Lin, J.S. Miller, C.S. Chen, M.J. Sailor, S.N. Bhatia, Bioresponsive mesoporous silica nanoparticles for triggered drug release, Journal of the American Chemical Society. 133 (2011) 19582–19585. https://doi.org/10.1021/ja206998x.

[86] B. Grünwald, J. Vandooren, E. Locatelli, P. Fiten, G. Opdenakker, P. Proost, A. Krüger, J.P. Lellouche, L.L. Israel, L. Shenkman, M. Comes Franchini, Matrix metalloproteinase-9 (MMP-9) as an activator of nanosystems for targeted drug delivery in pancreatic cancer, Journal of Controlled Release. 239 (2016) 39–48. https://doi.org/10.1016/j.jconrel.2016.08.016.

[87] M.M. Nguyen, A.S. Carlini, M.P. Chien, S. Sonnenberg, C. Luo, R.L. Braden, K.G. Osborn, Y. Li, N.C. Gianneschi, K.L. Christman, Enzyme-Responsive Nanoparticles for Targeted

Accumulation and Prolonged Retention in Heart Tissue after Myocardial Infarction, Advanced Materials. 27 (2015) 5547–5552. https://doi.org/10.1002/adma.201502003.

[88] P. Sorlier, A. Denuzière, C. Viton, A. Domard, Relation between the degree of acetylation and the electrostatic properties of chitin and chitosan, Biomacromolecules. 2 (2001) 765–772. https://doi.org/10.1021/bm015531+.

[89] C. Wang, G. Li, R. Guo, Multiple morphologies from amphiphilic graft copolymers based on chitooligosaccharides as backbones and polycaprolactones as branches, Chemical Communications. 1 (2005) 3591–3593. https://doi.org/10.1039/b504428f.

[90] Y. Xu, L. Wang, Y.K. Li, C.Q. Wang, Reduction and pH dual-responsive nanoparticles based chitooligosaccharide-based graft copolymer for doxorubicin delivery, Colloids and Surfaces A: Physicochemical and Engineering Aspects. 497 (2016) 8–15. https://doi.org/10.1016/j.colsurfa.2016.01.049.

[91] J. Zhang, J. Han, X. Zhang, J. Jiang, M. Xu, D. Zhang, J. Han, Polymeric nanoparticles based on chitooligosaccharide as drug carriers for co-delivery of all-trans-retinoic acid and paclitaxel, Carbohydrate Polymers. 129 (2015) 25–34. https://doi.org/10.1016/j.carbpol.2015.04.036.

[92] C. Xin, X. Yao, B. Du, W. Yang, L. Wang, L. Ma, W. Weng, Stearic Acid-Grafted Chitooligosaccharide Nanomicelle System with Biocleavable Gadolinium Chelates as a Multifunctional Agent for Tumor Imaging and Drug Delivery, Pharmaceutical Research. 36 (2019). https://doi.org/10.1007/s11095-018-2530-2.

[93] J.S. Seong, M.E. Yun, S.N. Park, Surfactant-stable and pH-sensitive liposomes coated with N-succinyl-chitosan and chitooligosaccharide for delivery of quercetin, Carbohydrate Polymers. 181 (2018) 659–667. https://doi.org/10.1016/j.carbpol.2017.11.098.

[94] X. Hu, S. Chen, H. Yin, Q. Wang, Y. Duan, L. Jiang, L. Zhao, Chitooligosaccharides-modified PLGA nanoparticles enhance the antitumor efficacy of AZD9291 (Osimertinib) by promoting apoptosis, International Journal of Biological Macromolecules. 162 (2020) 262–272. https://doi.org/10.1016/j.ijbiomac.2020.06.154.

[95] X. Liu, L. Chen, Y. Zhang, X. Xin, L. Qi, M. Jin, Y. Guan, Z. Gao, W. Huang, Enhancing anti-melanoma outcomes in mice using novel chitooligosaccharide nanoparticles loaded with therapeutic survivin-targeted siRNA, European Journal of Pharmaceutical Sciences. 158 (2021) 105641. https://doi.org/10.1016/j.ejps.2020.105641.

[96] P. Chandika, G.W. Oh, S.Y. Heo, S.C. Kim, T.H. Kim, M.S. Kim, W.K. Jung, Electrospun porous bilayer nano-fibrous fish collagen/PCL bio-composite scaffolds with covalently cross-linked chitooligosaccharides for full-thickness wound-healing applications, Materials Science and Engineering C. 121 (2021) 111871. https://doi.org/10.1016/j.msec.2021.111871.

[97] M.M. Tomasiak, M. Tomasiak, Z. Zietkowski, R. Skiepko, A. Bodzenta-Lukaszyk, N-acetyl-beta-hexosaminidase activity in asthma, International Archives of Allergy and Immunology. 146 (2008) 133–137. https://doi.org/10.1159/000113516.

[98] A.K. Thakur, B. Kaundle, I. Singh, Mucoadhesive drug delivery systems in respiratory diseases, in: Targeting Chronic Inflammatory Lung Diseases Using Advanced Drug Delivery Systems, Elsevier, 2020: pp. 475–491.

[99] A.S. Balijepalli, R.C. Sabatelle, M. Chen, B. Suki, M.W. Grinstaff, A synthetic bioinspired carbohydrate polymer with mucoadhesive properties, Angewandte Chemie. 132 (2020) 714–720.

[100] S. Zhang, J. Ermann, M.D. Succi, A. Zhou, M.J. Hamilton, B. Cao, J.R. Korzenik, J.N. Glickman, P.K. Vemula, L.H. Glimcher, An inflammation-targeting hydrogel for local drug delivery in inflammatory bowel disease, Science Translational Medicine. 7 (2015) 300ra128-300ra128.

[101] K. Koss, C. Tsui, L.D. Unsworth, Induced Neural Differentiation of MMP-2 Cleaved (RADA)4 Drug Delivery Systems, Journal of Controlled Release. 243 (2016) 204–213. https://doi.org/10.1016/j.jconrel.2016.09.037.

[102] K.M. Koss, C. Tsui, L.D. Unsworth, Enzymatic Activity in Fractal Networks of Self-Assembling Peptides, Biomacromolecules. 20 (2019) 422–434. https://doi.org/10.1021/acs.biomac.8b01496.

[103] Y. Wang, Y. Luo, Q. Zhao, Z. Wang, Z. Xu, X. Jia, An Enzyme-Responsive Nanogel Carrier Based on PAMAM Dendrimers for Drug Delivery, ACS Applied Materials and Interfaces. 8 (2016) 19899–19906. https://doi.org/10.1021/acsami.6b05567.

[104] E. Secret, S.J. Kelly, K.E. Crannell, J.S. Andrew, Enzyme-responsive hydrogel microparticles for pulmonary drug delivery, ACS Applied Materials and Interfaces. 6 (2014) 10313–10321. https://doi.org/10.1021/am501754s.

[105] M. Najafi, H. Asadi, J. van den Dikkenberg, M.J. van Steenbergen, M.H.A.M. Fens, W.E. Hennink, T. Vermonden, Conversion of an Injectable MMP-Degradable Hydrogel into Core-Cross-Linked Micelles, Biomacromolecules. 21 (2020) 1739–1751. https://doi.org/10.1021/acs.biomac.9b01675.

[106] L. Massi, A. Najer, R. Chapman, C.D. Spicer, V. Nele, J. Che, M.A. Booth, J.J. Doutch, M.M. Stevens, Tuneable peptide cross-linked nanogels for enzyme-triggered protein delivery, Journal of Materials Chemistry B. 8 (2020) 8894–8907. https://doi.org/10.1039/d0tb01546f.

[107] C. Zhang, D. Pan, K. Luo, W. She, C. Guo, Y. Yang, Z. Gu, Peptide dendrimer-doxorubicin conjugate-based nanoparticles as an enzyme-responsive drug delivery system for cancer therapy, Advanced Healthcare Materials. 3 (2014) 1299–1308. https://doi.org/10.1002/adhm.201300601.

[108] C.E. Callmann, C. v. Barback, M.P. Thompson, D.J. Hall, R.F. Mattrey, N.C. Gianneschi, Therapeutic Enzyme-Responsive Nanoparticles for Targeted Delivery and Accumulation in Tumors, Advanced Materials. 27 (2015) 4611–4615. https://doi.org/10.1002/adma.201501803.

[109] L. Zhu, F. Perche, T. Wang, V.P. Torchilin, Matrix metalloproteinase 2-sensitive multifunctional polymeric micelles for tumor-specific co-delivery of siRNA and hydrophobic drugs, Biomaterials. 35 (2014) 4213–4222. https://doi.org/10.1016/j.biomaterials.2014.01.060.

[110] L. Zhu, T. Wang, F. Perche, A. Taigind, V.P. Torchilin, Enhanced anticancer activity of nanopreparation containing an MMP2-sensitive PEG-drug conjugate and cell-penetrating moiety, Proceedings of the National Academy of Sciences of the United States of America. 110 (2013) 17047–17052. https://doi.org/10.1073/pnas.1304987110.

[111] R. Dorresteijn, N. Billecke, M. Schwendy, S. Pütz, M. Bonn, S.H. Parekh, M. Klapper, K. Müllen, Polylactide-block-polypeptide-block-polylactide copolymer nanoparticles with tunable cleavage and controlled drug release, Advanced Functional Materials. 24 (2014) 4026–4033. https://doi.org/10.1002/adfm.201304074.

[112] N. Padmavathy, L. das Ghosh, S.R.K. Meka, K. Chatterjee, Synthesis of a Block Copolymer Exhibiting Cell-Responsive Phytochemical Release for Cancer Therapy, ACS Applied Materials & Interfaces. 10 (2018) 21816–21824. https://doi.org/10.1021/acsami.8b03521.

[113] C. Zhang, D. Pan, J. Li, J. Hu, A. Bains, N. Guys, H. Zhu, X. Li, K. Luo, Q. Gong, Z. Gu, Enzyme-responsive peptide dendrimer-gemcitabine conjugate as a controlled-release drug delivery vehicle with enhanced antitumor efficacy, Acta Biomaterialia. 55 (2017) 153–162. https://doi.org/10.1016/j.actbio.2017.02.047.

[114] H. Qi, Q. Chen, H. Ren, X. Wu, X. Liu, T. Lu, Electrophoretic deposition of dexamethasone-loaded gelatin nanospheres/chitosan coating and its dual function in anti-inflammation and osteogenesis, Colloids and Surfaces B: Biointerfaces. 169 (2018) 249–256. https://doi.org/10.1016/j.colsurfb.2018.05.029.

[115] A.A. Dongargaonkar, G.L. Bowlin, H. Yang, Electrospun blends of gelatin and gelatin-dendrimer conjugates as a wound-dressing and drug-delivery platform, Biomacromolecules. 14 (2013) 4038–4045. https://doi.org/10.1021/bm401143p.

[116] Z. Zou, D. He, X. He, K. Wang, X. Yang, Z. Qing, Q. Zhou, Natural gelatin capped mesoporous silica nanoparticles for intracellular acid-triggered drug delivery, Langmuir. 29 (2013) 12804–12810. https://doi.org/10.1021/la4022646.

[117] Z.X. Meng, X.X. Xu, W. Zheng, H.M. Zhou, L. Li, Y.F. Zheng, X. Lou, Preparation and characterization of electrospun PLGA/gelatin nanofibers as a potential drug delivery system, Colloids and Surfaces B: Biointerfaces. 84 (2011) 97–102. https://doi.org/10.1016/j.colsurfb.2010.12.022.

[118] L. Zhang, J. Liu, X. Zheng, A. Zhang, X. Zhang, K. Tang, Pullulan dialdehyde crosslinked gelatin hydrogels with high strength for biomedical applications, Carbohydrate Polymers. 216 (2019) 45–53. https://doi.org/10.1016/j.carbpol.2019.04.004.

[119] R.T. Annamalai, P.A. Turner, W.F. Carson, B. Levi, S. Kunkel, J.P. Stegemann, Harnessing macrophage-mediated degradation of gelatin microspheres for spatiotemporal control of BMP2 release, Biomaterials. 161 (2018) 216–227. https://doi.org/10.1016/j.biomaterials.2018.01.040.

[120] J.H. Xu, F.P. Gao, L.L. Li, H.L. Ma, Y.S. Fan, W. Liu, S.S. Guo, X.Z. Zhao, H. Wang, Gelatin-mesoporous silica nanoparticles as matrix metalloproteinases- degradable drug delivery systems in vivo, Microporous and Mesoporous Materials. 182 (2013) 165–172. https://doi.org/10.1016/j.micromeso.2013.08.050.

[121] S. Jain, P.U. Valvi, N.K. Swarnakar, K. Thanki, Gelatin coated hybrid lipid nanoparticles for oral delivery of Amphotericin B, Molecular Pharmaceutics. 9 (2012) 2542–2553. https://doi.org/10.1021/mp300320d.

[122] H. Blaser, C. Dostert, T.W. Mak, D. Brenner, TNF and ROS crosstalk in inflammation, Trends in Cell Biology. 26 (2016) 249–261.

[123] E.J. Swindle, D.D. Metcalfe, J.W. Coleman, Rodent and human mast cells produce functionally significant intracellular reactive oxygen species but not nitric oxide, Journal of Biological Chemistry. 279 (2004) 48751–48759. https://doi.org/10.1074/jbc.M409738200.

[124] H.S. Kuehn, E.J. Swindle, M.-S. Kim, M.A. Beaven, D.D. Metcalfe, A.M. Gilfillan, The Phosphoinositide 3-Kinase-Dependent Activation of Btk Is Required for Optimal Eicosanoid

Production and Generation of Reactive Oxygen Species in Antigen-Stimulated Mast Cells, The Journal of Immunology. 181 (2008) 7706–7712. https://doi.org/10.4049/jimmunol.181.11.7706.

[125] Y. Suzuki, T. Inoue, T. Yoshimaru, C. Ra, Galectin-3 but not galectin-1 induces mast cell death by oxidative stress and mitochondrial permeability transition, Biochimica et Biophysica Acta - Molecular Cell Research. 1783 (2008) 924–934. https://doi.org/10.1016/j.bbamcr.2008.01.025.

[126] E.J. Swindle, J.W. Coleman, F.R. DeLeo, D.D. Metcalfe, FcεRI- and Fcγ Receptor-Mediated Production of Reactive Oxygen Species by Mast Cells Is Lipoxygenase- and Cyclooxygenase-Dependent and NADPH Oxidase-Independent, The Journal of Immunology. 179 (2007) 7059–7071. https://doi.org/10.4049/jimmunol.179.10.7059.

[127] Y. Suzuki, T. Yoshimaru, T. Matsui, T. Inoue, O. Niide, S. Nunomura, C. Ra, FcεRI Signaling of Mast Cells Activates Intracellular Production of Hydrogen Peroxide: Role in the Regulation of Calcium Signals, The Journal of Immunology. 171 (2003) 6119–6127. https://doi.org/10.4049/jimmunol.171.11.6119.

[128] Y. Suzuki, T. Yoshimaru, T. Inoue, C. Ra, Discrete generations of intracellular hydrogen peroxide and superoxide in antigen-stimulated mast cells: Reciprocal regulation of store-operated Ca2+ channel activity, Molecular Immunology. 46 (2009) 2200–2209. https://doi.org/10.1016/j.molimm.2009.04.013.

[129] E.J. Swindle, J.A. Hunt, J.W. Coleman, A Comparison of Reactive Oxygen Species Generation by Rat Peritoneal Macrophages and Mast Cells Using the Highly Sensitive Real-Time Chemiluminescent Probe Pholasin: Inhibition of Antigen-Induced Mast Cell Degranulation by

Macrophage-Derived Hydrogen Pero, The Journal of Immunology. 169 (2002) 5866–5873. https://doi.org/10.4049/jimmunol.169.10.5866.

[130] T. Yoshimaru, Y. Suzuki, T. Inoue, O. Niide, C. Ra, Silver activates mast cells through reactive oxygen species production and a thiol-sensitive store-independent Ca2+ influx, Free Radical Biology and Medicine. 40 (2006) 1949–1959. https://doi.org/10.1016/j.freeradbiomed.2006.01.023.

[131] G. Saravanakumar, J. Kim, W.J. Kim, Reactive-Oxygen-Species-Responsive Drug Delivery Systems: Promises and Challenges, Advanced Science. 4 (2017). https://doi.org/10.1002/advs.201600124.

[132] W.C. Ballance, E.C. Qin, H.J. Chung, M.U. Gillette, H. Kong, Reactive oxygen species-responsive drug delivery systems for the treatment of neurodegenerative diseases, Biomaterials. 217 (2019) 119292. https://doi.org/10.1016/j.biomaterials.2019.119292.

[133] A.K. Shukla, M. Verma, K.N. Singh, Superoxide induced deprotection of 1,3-dithiolanes: A convenient method of dedithioacetalization, Indian Journal of Chemistry - Section B Organic and Medicinal Chemistry. 43 (2004) 1748–1752. https://doi.org/10.1002/chin.200449059.

[134] M.S. Shim, Y. Xia, A reactive oxygen species (ROS)-responsive polymer for safe, efficient, and targeted gene delivery in cancer cells, Angewandte Chemie - International Edition. 52 (2013) 6926–6929. https://doi.org/10.1002/anie.201209633.

[135] B. Liu, S. Thayumanavan, Mechanistic Investigation on Oxidative Degradation of ROS-Responsive Thioacetal/Thioketal Moieties and Their Implications, Cell Reports Physical Science. 1 (2020) 100271. https://doi.org/10.1016/j.xcrp.2020.100271.

[136] J. Li, C. Sun, W. Tao, Z. Cao, H. Qian, X. Yang, J. Wang, Photoinduced PEG deshielding from ROS-sensitive linkage-bridged block copolymer-based nanocarriers for on-demand drug delivery, Biomaterials. 170 (2018) 147–155. https://doi.org/10.1016/j.biomaterials.2018.04.015.

[137] D.S. Wilson, G. Dalmasso, L. Wang, S. v. Sitaraman, D. Merlin, N. Murthy, Orally delivered thioketal nanoparticles loaded with TNF-α-siRNA target inflammation and inhibit gene expression in the intestines, Nature Materials. 9 (2010) 923–928. https://doi.org/10.1038/nmat2859.

[138] Y. Yuan, J. Liu, B. Liu, Conjugated-polyelectrolyte-based polyprodrug: Targeted and image-guided photodynamic and chemotherapy with on-demand drug release upon irradiation with a single light source, Angewandte Chemie - International Edition. 53 (2014) 7163–7168. https://doi.org/10.1002/anie.201402189.

[139] C. Yue, Y. Yang, C. Zhang, G. Alfranca, S. Cheng, L. Ma, Y. Liu, X. Zhi, J. Ni, W. Jiang, J. Song, J.M. de la Fuente, D. Cui, ROS-responsive mitochondria-targeting blended nanoparticles: Chemo- and photodynamic synergistic therapy for lung cancer with on-demand drug release upon irradiation with a single light source, Theranostics. 6 (2016) 2352–2366. https://doi.org/10.7150/thno.15433.

[140] D. Chen, G. Zhang, R. Li, M. Guan, X. Wang, T. Zou, Y. Zhang, C. Wang, C. Shu, H. Hong, L.J. Wan, Biodegradable, Hydrogen Peroxide, and Glutathione Dual Responsive Nanoparticles for Potential Programmable Paclitaxel Release, Journal of the American Chemical Society. 140 (2018) 7373–7376. https://doi.org/10.1021/jacs.7b12025.

[141] J. Wang, X. He, S. Shen, Z. Cao, X. Yang, ROS-Sensitive Cross-Linked Polyethylenimine for Red-Light-Activated siRNA Therapy, ACS Applied Materials and Interfaces. 11 (2019) 1855–1863. https://doi.org/10.1021/acsami.8b18697.

[142] X. Ling, S. Zhang, P. Shao, P. Wang, X. Ma, M. Bai, Synthesis of a reactive oxygen species responsive heterobifunctional thioketal linker, Tetrahedron Letters. 56 (2015) 5242–5244. https://doi.org/10.1016/j.tetlet.2015.07.059.

[143] L. Xu, M. Zhao, W. Gao, Y. Yang, J. Zhang, Y. Pu, B. He, Polymeric nanoparticles responsive to intracellular ROS for anticancer drug delivery, Colloids and Surfaces B: Biointerfaces. 181 (2019) 252–260. https://doi.org/10.1016/j.colsurfb.2019.05.064.

[144] X. Xu, P.E. Saw, W. Tao, Y. Li, X. Ji, S. Bhasin, Y. Liu, D. Ayyash, J. Rasmussen, M. Huo, J. Shi, O.C. Farokhzad, ROS-Responsive Polyprodrug Nanoparticles for Triggered Drug Delivery and Effective Cancer Therapy, Advanced Materials. 29 (2017) 1–6. https://doi.org/10.1002/adma.201700141.

[145] H. Subramanian, K. Gupta, D. Lee, A.K. Bayir, H. Ahn, H. Ali, β-Defensins activate human mast cells via Mas-related gene X2, The Journal of Immunology. 191 (2013) 345–352.

[146] M. Kamohara, A. Matsuo, J. Takasaki, M. Kohda, M. Matsumoto, S. Matsumoto, T. Soga, H. Hiyama, M. Kobori, M. Katou, Identification of MrgX2 as a human G-protein-coupled receptor for proadrenomedullin N-terminal peptides, Biochemical and Biophysical Research Communications. 330 (2005) 1146–1152.

[147] H.-P. Nothacker, Z. Wang, H. Zeng, S.K. Mahata, D.T. O'Connor, O. Civelli, Proadrenomedullin N-terminal peptide and cortistatin activation of MrgX2 receptor is based on a common structural motif, European Journal of Pharmacology. 519 (2005) 191–193.

[148] L. Lu, M. Kulka, L.D. Unsworth, Peptide-mediated mast cell activation: ligand similarities for receptor recognition and protease-induced regulation, Journal of Leukocyte Biology. 102 (2017) 237–251.

[149] T.C. Theoharides, W.W. Douglas, Mast cell histamine secretion in response to somatostatin analogues: structural considerations, European Journal of Pharmacology. 73 (1981) 131–136.

[150] L. Lu, S. Raj, N. Arizmendi, J. Ding, G. Eitzen, P. Kwan, M. Kulka, L.D. Unsworth, Identification of short peptide sequences that activate human mast cells via mas-related g-protein coupled receptor member x2, Acta Biomaterialia. 136 (2021) 159–169.

[151] G. Varricchi, A. Pecoraro, S. Loffredo, R. Poto, F. Rivellese, A. Genovese, G. Marone, G. Spadaro, Heterogeneity of human mast cells with respect to MRGPRX2 receptor expression and function, Frontiers in Cellular Neuroscience. 13 (2019) 299.

[152] W. Manorak, C. Idahosa, K. Gupta, S. Roy, R. Panettieri, H. Ali, Upregulation of Mas-related G Protein coupled receptor X2 in asthmatic lung mast cells and its activation by the novel neuropeptide hemokinin-1, Respiratory Research. 19 (2018) 1–5. https://doi.org/10.1186/s12931-017-0698-3.

[153] S. Willows, M. Kulka, Harnessing the power of mast cells in unconventional immunotherapy strategies and vaccine adjuvants, Cells. 9 (2020) 2713.

[154] J.B. McLachlan, C.P. Shelburne, J.P. Hart, S. v Pizzo, R. Goyal, R. Brooking-Dixon, H.F. Staats, S.N. Abraham, Mast cell activators: a new class of highly effective vaccine adjuvants, Nature Medicine. 14 (2008) 536–541.

[155] E. Ruoslahti, Peptides as targeting elements and tissue penetration devices for nanoparticles, Advanced Materials. 24 (2012) 3747–3756. https://doi.org/10.1002/adma.201200454.

[156] F. Zhang, X. Huang, L. Zhu, N. Guo, G. Niu, M. Swierczewska, S. Lee, H. Xu, A.Y. Wang, K.A. Mohamedali, M.G. Rosenblum, G. Lu, X. Chen, Noninvasive monitoring of orthotopic glioblastoma therapy response using RGD-conjugated iron oxide nanoparticles, Biomaterials. 33 (2012) 5414–5422. https://doi.org/10.1016/j.biomaterials.2012.04.032.

[157] M. Lewin, N. Carlesso, C.H. Tung, X.W. Tang, D. Cory, D.T. Scadden, R. Weissleder, Tat peptide-derivatized magnetic nanoparticles allow in vivo tracking and recovery of progenitor cells, Nature Biotechnology. 18 (2000) 410–414. https://doi.org/10.1038/74464.

[158] X. Li, L. Xing, Y. Hu, Z. Xiong, R. Wang, X. Xu, L. Du, M. Shen, X. Shi, An RGD-modified hollow silica@Au core/shell nanoplatform for tumor combination therapy, Acta Biomaterialia. 62 (2017) 273–283. https://doi.org/10.1016/j.actbio.2017.08.024.

[159] F. Danhier, B. Vroman, N. Lecouturier, N. Crokart, V. Pourcelle, H. Freichels, C. Jérôme, J. Marchand-Brynaert, O. Feron, V. Préat, Targeting of tumor endothelium by RGD-grafted PLGA-nanoparticles loaded with Paclitaxel, Journal of Controlled Release. 140 (2009) 166–173. https://doi.org/10.1016/j.jconrel.2009.08.011.

[160] N. Yonenaga, E. Kenjo, T. Asai, A. Tsuruta, K. Shimizu, T. Dewa, M. Nango, N. Oku, RGD-based active targeting of novel polycation liposomes bearing siRNA for cancer treatment, Journal of Controlled Release. 160 (2012) 177–181. https://doi.org/10.1016/j.jconrel.2011.10.004.

[161] H.A. Kim, K. Nam, S.W. Kim, Tumor targeting RGD conjugated bio-reducible polymer for VEGF siRNA expressing plasmid delivery, Biomaterials. 35 (2014) 7543–7552. https://doi.org/10.1016/j.biomaterials.2014.05.021.

[162] C. Shu, R. Li, Y. Yin, D. Yin, Y. Gu, L. Ding, W. Zhong, Synergistic dual-targeting hydrogel improves targeting and anticancer effect of Taxol in vitro and in vivo, Chemical Communications. 50 (2014) 15423–15426. https://doi.org/10.1039/c4cc05614k.

[163] E.J. Kwon, J.S. Dudani, S.N. Bhatia, Ultrasensitive tumour-penetrating nanosensors of protease activity, Nature Biomedical Engineering. 1 (2017). https://doi.org/10.1038/s41551-017-0054.

[164] L.B. Schwartz, Diagnostic Value of Tryptase in Anaphylaxis and Mastocytosis, Immunology and Allergy Clinics of North America. 26 (2006) 451–463. https://doi.org/10.1016/j.iac.2006.05.010.

[165] E. Ordoqui, J.M. Zubeldia, A. Aranzábal, M. Rubio, T. Herrero, P. Tornero, V.M. Rodriguez, A. Prieto, M.L. Baeza, Serum tryptase levels in adverse drug reactions, Allergy: European Journal of Allergy and Clinical Immunology. 52 (1997) 1102–1105. https://doi.org/10.1111/j.1398-9995.1997.tb00182.x.

Chapter 3. Effect of thioketal antioxidants on islet cell transplantation

Preface

This chapter has been submitted titled, “Effect of thioketal antioxidants on islet cell transplantation”. Shammy Raj, Kosala D. Waduthanthri, Purushothaman Kuppan, Gregory S. Korbutt, Larry D. Unsworth and Andrew R. Pepper are the coauthors of the manuscript. Kosala D. Waduthanthri and I share the 1st co-authorship. Shammy Raj designed and conducted all thioketal synthesis and ROS functional testing, analyzed results, and participated in writing the manuscript. Kosala D. Waduthanthri and Purushothaman Kuppan designed and conducted all cell-based experiments, analyzed the data, and participated in writing the manuscript. Gregory S. Korbutt, Larry D. Unsworth and Andrew R. Pepper guided the research design, analyzed and reviewed the data, reviewed and edited the manuscript.

3.1. Introduction

Diabetes is a major global health crisis with about 500 million adults enduring an impaired glucose metabolism. 10% of the diabetic individuals are type 1 diabetes mellitus (T1DM) patients who suffer from limited or no insulin secretion. Limited insulin secretion is owed to the autoimmune destruction of the insulin producing native pancreatic β-cells [1]. The quality of life, vascular complications, organ failure and mortality of T1DM patients therefore depends on external insulin administration. However, while insulin delivery techniques have improved for the last century, they are fraught with complications such as noncompliance, lipodystrophy, and peripheral hyperinsulinemia [2,3]. Furthermore, only a fraction of patients using a biomechanical insulin delivery system achieve satisfactory glycemic control [4]. β-cell replacement therapy, such as islet transplantation, is the only way to endogenously restore regulated glucose homeostasis. Islet transplantation has been shown to be less invasive than whole pancreas transplantation with improved clinical outcomes, while increasing the potential donor pool by having less stringent donor selection criteria [5].

Phase III clinicals trials have demonstrated that islet transplantation restores glucose homeostasis, improves HbA1c levels, eliminates hypoglycemic unawareness [6], and stabilizes secondary complications [7]. A post-transplantation insulin independence of 100 and 28% has been realized after 1 and 10 years, respectively [5,6,8]. After 10 years it was shown that 78% of the subjects have continued graft function with improved glycemic control and reduced insulin requirements [9]. Transplantation efficacy depends on several factors including graft revascularization, and the inflammatory and immune response to the graft [10]. Graft failure has been linked to the fact that more than two thirds of the transplanted islet mass does not survive the process from isolation to intrahepatic engraftment [11]. The presence of reactive oxygen species (ROS) during organ

procurement, islet isolation, cell culture, and within the transplanted site has been highlighted as a major reason for reduced islet number and viability that has yielded a lower engraftment efficiency [12]. The deleterious effects of ROS are further aggravated by the low expression of endogenous antioxidant enzymes by islet cells (i.e., glutathione peroxidases and catalases) [13].

Strategies utilizing exogenous ROS scavengers or the overexpression of ROS processing proteins have been used to mitigate the effects of ROS on islet survival [14,15]. After transplantation anti-inflammatory drugs and vascularization agents, among others, are applied to improve the outcome of islet transplantation [16]. ROS scavengers, like Bilirubin (BR), have been shown to reduce the effect of ROS on islets [14]. However promising, BR has an extremely short half-life (~ 5 min) and has been shown to be cytotoxic (at concentrations > 60 μM) [17]. Another molecule, the cysteine-rich antioxidant protein, metallothionein (MT) has also been shown to expedite the restoration of physiological glycemic level after islet transplantation [18]. Furthermore, BMX-001, a metallo-porphyrine superoxide dismutase (SOD) mimic, has been used to enhance the recovery and improvement of islet functions [19]. However, despite having a high activity in catalysing superoxides, SOD mimics exhibit an extremely low catalase like activity for hydrogen peroxide. The catalase-like activity of Mn porphyrins have reported to be 10^4 orders less than the catalase enzyme [20].

Alternatively, thioketals (TK) are small molecules that undergo bond cleavage in ROS extensive environment. TKs are widely used chemical modifications in protecting the ketones during a chemical reaction. Subsequent to reaction, compounds are deprotected to furnish the nascent ketonic groups. Among several reagents used for deprotection, oxidative environment is reported to be highly efficient in facilitating the desired transformation [21]. In the process, the highly toxic ROS are transformed into non-toxic, biocompatible molecules [22]. Herein, the inherent property

of TKs to convert detrimental ROS into non-toxic molecules have been employed to shield porcine islets from the oxidative damage. TK treated islets showed enhanced viability and preserved cellular functionalities. These results were translated to the mouse models, where diabetic mice were syngrafted with TK-treated mouse islets. The survival analysis indicated an improved graft survival in the group receiving TK-treated islet in comparison to the controls. Glucose tolerance results confirmed long-term graft function *via* rapid glucose clearance upon metabolic challenge. It is thought that TK as a ROS scavenger provides a clinical advantage to other anti-oxidants for enhancing islet survival during isolation, transplantation, and engraftment.

3.2. Materials and methods

3.2.1. Synthesis and characterization of thioketal (TK) molecule

American chemical society (ACS) grade acetone (Sigma Aldrich) (3g, 0.052 mole, 1 equivalent) was reacted with 3-mercaptapropionic acid (3-MPA) (Sigma Aldrich) (12g, 0.113 mole, 2.2 equivalent) in the presence of a catalytic amount of trifluoracetic acid (TFA) (Sigma Aldrich) at room temperature, overnight. Obtained white solid crystals were washed with hexane (ACS grade, Fischer Chemicals) and dried overnight in a vacuum oven. This compound was dissolved in a sparing amount of dichloromethane (HPLC grade, Sigma Aldrich), excess hexane added, and kept at -20 ℃ to recrystallize. Crystals were filtered and dried overnight in a vacuum oven. TK was dissolved in chloroform-D (Sigma Aldrich) at 1 mg/mL and characterized using nuclear magnetic resonance spectroscopy (NMR, Varian). TK was further dissolved in acetonitrile (ACN) (HPLC grade, Fischer Chemicals) at 1 mg/mL and analysed for purity using high performance liquid chromatography (HPLC, Agilent 1260) as well as mass using a mass spectrometer (Agilent 1100) (detailed procedure in supporting information).

3.2.1.1. Stability and activity of TK

TK at 1 mg/mL in PBS was incubated at 37 ℃ for 7 days, and 200 µL was removed and stored at -20 ℃ until HPLC analysis could be conducted. Area under the curve was compared to test the stability (detailed procedure in supporting information). ROS induced activity was determined by subjecting TK (4 mM) to H_2O_2 (ACS, EMD Chemicals, 16 mM, 4 equivalents) and iron (II) sulfate heptahydrate (Sigma Aldrich, 1.6 mM) in methanol-D (Sigma Aldrich) in a sealed NMR tube, and acetone evolution monitored using NMR. Chlorotrimethylsilane (TMS-Cl) (Sigma Aldrich) was used as an internal reference (detailed procedure in supporting information).

3.2.1.2. Purity, mass determination and stability studies

TK at 1 mg/ml was analyzed using HPLC with Agilent Zorbax 5 µm, 4.6 X 250 mm, C-18 column. Elution was monitored using a DAD detector at 242 nm wavelength. The compound was eluted using DI water + 1% ACN + 0.1% TFA as aqueous phase (A) and ACN + 0.1% TFA as organic phase (B). Solvent B was varied from 25% to 70% in 15 min, with a stop time of 3 min between successive runs. Same method and column were used during mass identification and stability studies. Percentage purity was determined by the % area under the curve.

3.2.1.3. ROS activity studies

In a typical experiment, three solutions were prepared in methanol-D (Sigma Aldrich): (i) 6 mM TK; (ii) 96 mM H_2O_2, 30% H_2O_2 (ACS, EMD Chemicals); and (iii) 0.003 volume% TMS-Cl (Sigma Aldrich). These solutions combined to a final volume of 600 µL (400 µL (i), 100 µL (ii), 100 µL (iii)). In a control experiment, 100 µL methanol-D was added instead of (ii). Readings were then taken in an NMR spectrophotometer. To generate hydroxyl radicals, 10 µL of 96 mM of iron (II) sulfate heptahydrate (Sigma Aldrich) in 0.01M HCl was added. NMR readings were taken at predetermined time interval to monitor the acetone formation.

3.2.2. Neonatal porcine islet preparation

Animal experiments were performed in accordance with the guidelines established by Canadian Council on Animal Care. Donor pancreases were obtained from 1 to 3 days old sacrificed neonatal piglets from the University of Alberta Swine Research Centre (1.5 - 2.0 kg body weight). Neonatal porcine islets (NPIs) were isolated as described previously [23]. A minimum of three independent NPI isolations were used for islet experiments reported in this study. Isolated NPIs were maintained in Ham's tissue culture medium at standard cell culture conditions (37 ℃, 5% CO_2 and 95% air). On the third day of culture, the incubation medium was switched to DMEM F12 (Thermo Fisher) supplemented with 1% pig serum (heat inactivated), 0.2 mM insulin, 7 µmol/L transferrin, 4 µmol/L sodium selenite (ITS; Thermo Fisher), 100 U/mL penicillin, 0.1 mg/mL streptomycin (Cedarlane), 10 mM nicotinamide (Sigma-Aldrich) and 10 nmol/L of exendin-4 (Sigma-Aldrich). Islets were maintained in cultures 4-6 days prior to experimentations.

3.2.3. Islet viability assessment

Neonatal porcine pancreatic islets were co-cultured with TK and cell membrane integrity (e.g. viability) was evaluated based on Calcein AM (Ex 488 nm/Em 515 nm) and BOBO 3-Iodide (Ex 570 nm/Em 602 nm) fluorescent dyes using Live/Dead Cell Imaging Kit (Invitrogen). Isolated islets were cultured in DMEM F12 media for 48 h in the presence of TK at a final concentration of 100 and 200 µM. Equivolume PBS served as controls. To induce ROS, islets incubated with TK for 48 h were exposed to 400 µM H_2O_2 for an additional 4 h 37 ℃. 0 µM H_2O_2 (PBS only) treatment served as the control. Aliquots of 100 neonatal porcine islets per isolation were assayed for membrane integrity according to the manufacturer's instructions. Fluorescent images were captured under 20X magnification using a Zeiss Axioscope 5 fluorescence microscope (Carl Zeiss, Germany). To quantify the number of live (green) and dead (red) islet cells from the fluorescence micrographs, cells were assigned into three categories by visual observation: (i) few or no cells are green, and the majority are red (average viability = 0%, counted as 0); (ii) ~50% of the cells are red (average viability = 50%, counted as 0.5); (iii) few or no cells are red (average viability = 100%, counted as 1). Percent viability was calculated by dividing the overall count of each category (sum of 0, 0.5 or 1 for each treatment) by the sum of all categories (sum of 0, 0.5 or 1 for all treatments), multiplied by 100.

3.2.4. Measurement of oxygen consumption rate

Oxygen consumption rate (OCR) was assessed with islets obtained from 3-4 separate isolations, with an aliquot of 1,000 islets per replicate. Islets were co-cultured with TK (200 µM) for 48 h at standard cell culture conditions. Cultures treated with PBS were used as controls. For H_2O_2 treated group, TK treated islets were exposed to 800 µM exogenous H_2O_2 and incubated at standard cell

culture conditions for 4h. OCR was measured using a fiber optic sensor (Instech Laboratories, Plymouth Meeting, PA) and oxygen partial pressure (pO2) was monitored over time [24]. OCR data were normalized to the amount of DNA in each sample (nmol/min-mg DNA), determined using a Quant-iT PicoGreen dsDNA kit (Molecular Probes, Eugene, OR).

3.2.5. Quantification of lipid peroxidation in monolayer cell cultures

Beta-TC-6 cells (β-TC6) were purchased from ATCC, Manassas, VA, USA (cat. no. CRL 11506) and studies were repeated 6 times with cell passages 14-16. Monolayer cultures were prepared with initial seeding density of $3x10^5$ cells per well with DMEM culture medium supplemented with 15% fetal bovine serum. Cultures were maintained at standard cell culture conditions with media changes every 48 h. Seven days post-culture β-TC6 were treated with TK at 200 μM final concentration or equivolume PBS (control) and were incubated for 48 h at standard cell culture conditions. To induce intracellular lipid peroxidation, half of the culture was treated with H_2O_2 at 800 μM final concentration for 4 h. The other half served as control.

Malondialdehyde (MDA) analysis was performed with monolayer cultures. Cells were washed twice with PBS and were treated with Trypsin-EDTA for 1 min to detach form the culture substrate. Cells from three wells were pooled together to prepare individual samples for the analysis. Harvested cells were then pelleted out and washed twice in PBS, with brief centrifugation steps at 92 x g for 7 min and stored at -800C until used for MDA assay. Intracellular lipid peroxidase content was then determined using the modified thiobarbituric acid assay through measuring the amount of MDA using MDA assay kit (cat. no. ab118970, Abcam, Cambridge, UK), according to the manufacturer's instructions. Briefly, cells after thawing were treated with 300 μL MDA lysis buffer and 3 μL 100X butylated hydroxytoluene followed by pulse sonication

(20 pulses) in ice. Samples were then centrifuged at 13,000 x g for 10 min at 40 ºC to remove the insoluble materials. 200 µL supernatant was transferred to a new tube and 600 µL TBA solution was added. TBA-sample mixture was then incubated at 95 ºC for 60 min and then cooled to room temperature in an ice bath for 10 min. The solution was then filtered through 0.20 µm syringe filter (Whatman, Maidstone, UK). 200 µL of the filtrate solution was transferred to a 96-well microplate. Absorbance was measured on a microplate reader at OD 532 nm. MDA quantification was done using a standard curve. MDA content was normalized to the amount of DNA in each sample (µmol MDA/µg DNA), which was determined using a Quant-iT PicoGreen dsDNA kit (Molecular Probes, Eugene, OR).

3.2.6. Mouse islet isolation

Animal studies were conducted in accordance with the Canadian Council of Animal Care. Donor BALB/c mice (Jackson Laboratory) were maintained in a clean, sterile, and pathogen-free environment and had access to water and food ad libitum. Donors were between 6 and 8 weeks of age male mice and weighed between 22 and 27 g. Islet isolation and purification were performed according to a previously described methodology [25]. Islets were washed in Hank's Balanced Salt Solution (HBSS) after isolation and cultured in Connaught Medical Research Laboratories (CMRL-1066, Mediatech, Manasses, VA) media at pH 7.4 supplemented with 10% fetal bovine serum, L-glutamine (100 mg/L), penicillin (112 kU/L), streptomycin (112 mg/L), and HEPES (25 mM) for 1 h prior to transplantation.

3.2.7. Diabetic induction

Diabetes was chemically induced in 6 - 8 weeks old BALB/c male recipient mice (Jackson Laboratory) via a single intraperitonially injected with 185 mg/kg streptozotocin (STZ, Sigma-

Aldrich) in acetate buffer (pH 4.5). Induction was conducted one week prior to islet transplantation [25]. Blood glucose levels in recipient mice were recorded using UltraMini glucose meter (LifeScan, Burnaby, BC, Canada). Animals with blood glucose levels >18 mM for two consecutive days were considered diabetic and used for subsequent transplant studies.

3.2.8. Marginal islet mass transplantation

Diabetic BALB/c mice were transplanted with either 48 h TK treated islets (200 μM TK; 200 islets per mouse; n = 7) or non-TK treated control islets (0 μM TK; 200 islets per mouse; n = 7) under the kidney capsule. Three separate islet isolation were conducted. After transplantation, recipient's non-fasting blood glucose was monitored 3 times per week using OneTouch UltraMini glucose meter (LifeScan, Burnaby, BC, Canada). At 30-day post-transplantation, mice were subjected to an intraperitoneal glucose tolerance test (IPGTT). Overnight fasted mice were injected with 3 g/kg of glucose (DMVet, Coaticook, QC, Canada) intraperitonially and blood glucose levels were measured at time intervals of 0, 15, 30, 60, 90, and 120 min. Area under the curve (AUC) values were used to determine the glucose clearance. Subsequently, survival nephrectomies were performed on all the recipients and the blood glucose levels were monitored for three consecutive days post-nephrectomy to confirm the graft dependent function. Graft bearing kidneys were fixed in 10% formalin (Thermo-Fisher, Ottawa, ON, Canada) for histological assessment.

3.2.9. Immunohistochemistry

Immunofluorescence with anti-insulin antibodies was used to identify the presence of pancreatic β-cells in the islet grafts. Briefly, following deparaffinization, graft sections were washed with PBS supplemented with 1% normal goat serum (Jackson ImmunoResearch, West Grove, PA), followed by blocking with 20% normal goat serum in PBS for 1 h. Sections were washed with

PBS and stained with anti-guinea pig α-insulin (prepared in 5% normal goat serum; 1:5, Dako) primary antibodies for 1 h, followed by PBS washing and incubation with goat anti-guinea pig Alexa fluor488 (1:200, Thermo-Fisher Scientific) secondary antibodies for 1 h at room temperature. Slides were rinsed with PBS and counterstained with DAPI in antifade mounting medium (ProLong; Life Technologies). Fluorescent microscope was used to capture microphotographs using the appropriate filter with AxioVision imaging software.

3.2.10. Statistical analysis

Data are represented as mean ± standard error of the mean (SEM). All experiments have been confirmed with a minimum of 3 replicates Statistical analysis between treatment groups was calculated by 2-tailed unpaired *t* test. Comparison of Kaplan-Meier survival function curves were done using the Gehan-Breslow-Wilcoxon statistical analysis. A 95% confidence interval was used as a threshold for significance, $p < 0.05$.

3.3. Results

3.3.1. Synthesis and characterization of TK

Crude product was formed with 12 g of 3-MPA reacted overnight with 3 g of acetone for a yield 11.3 g. TK was recrystallized from the crude and washed with hexane. The structure was characterized using NMR (Figure 3.1A). It was purified to 95%+ purity as assessed using HPLC with a gradient elution of ACN-water solvent system (Figure 3.2), and mass spectroscopy with a mass to charge (m/z) ratio of 251 in the negative scan mode that corresponded to the theoretical mass of 252 g/mol (Figure 3.3). TK structure was confirmed using ^{1}H-NMR (Figure 3.1A): characteristic resonance peak at 2.84 ppm (4H, protons labelled as ‘a’), 2.61 ppm (4H, protons labelled as ‘b’) and 1.53 ppm (6H, protons labelled as ‘c’) confirmed the structure.

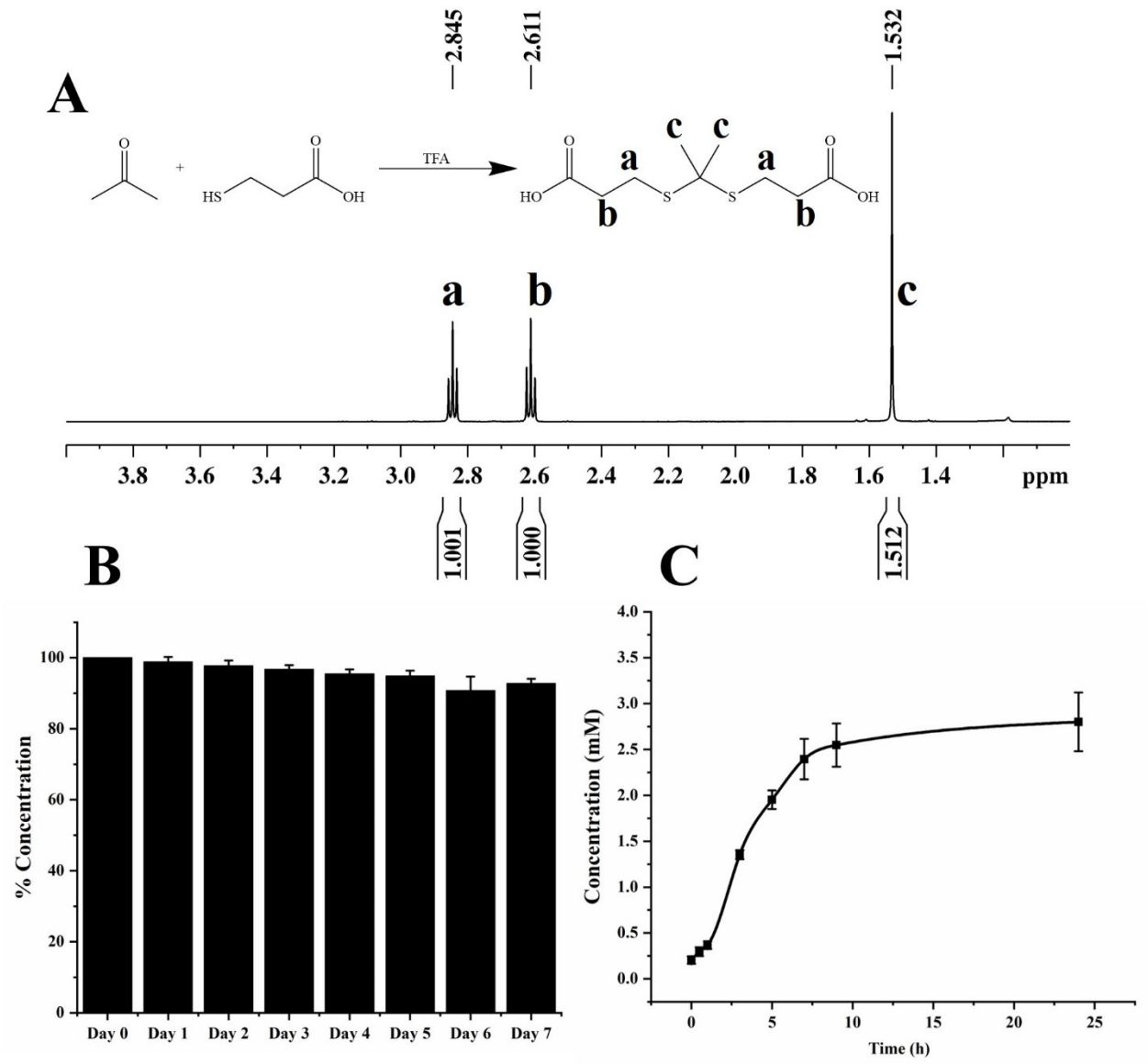

Figure 3.1. Synthesis and characterization of TK. (A) ^{1}H-NMR resonance spectrum of TK in $CDCl_3$ with characteristics peak at 1.53 (6H, s), 2.61 (4H, t) and 2.84 (4H, t) ppm; (B) stability of TK at pH of 7.4 determined using HPLC; (C) concentration (mean ± SEM) of acetone generated upon ROS stimulated TK degradation, quantified using area under the ^{1}H-NMR resonance.

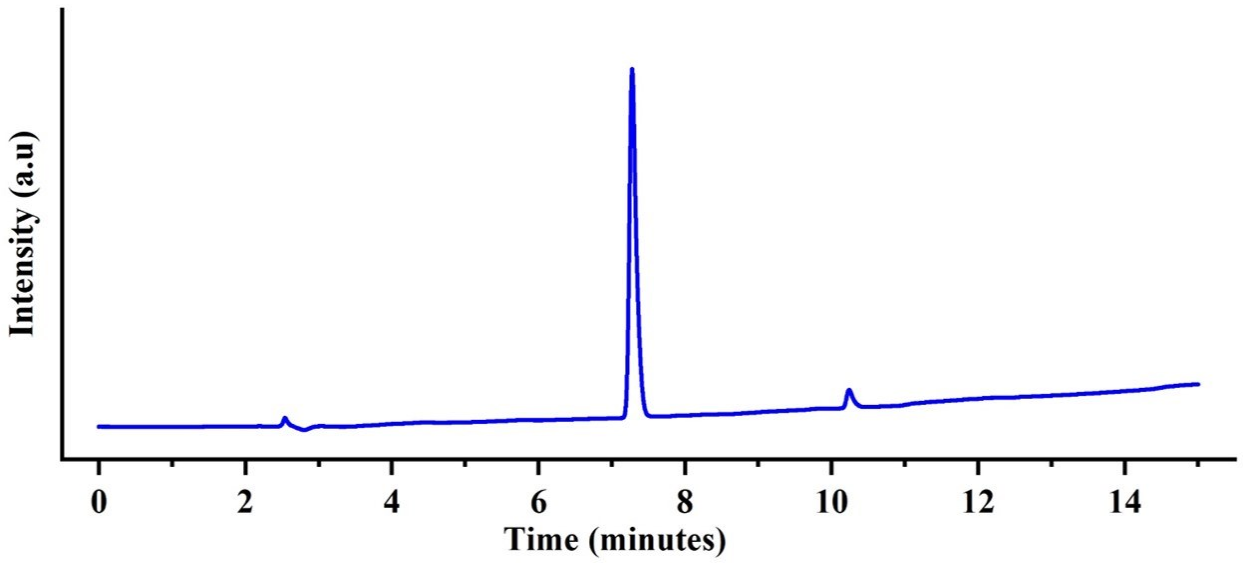

Figure 3.2. HPLC elution chromatogram of TK. TK was detected using 242 nm DAD detector. 95.29 % purity was determined by the percentage of the peak area

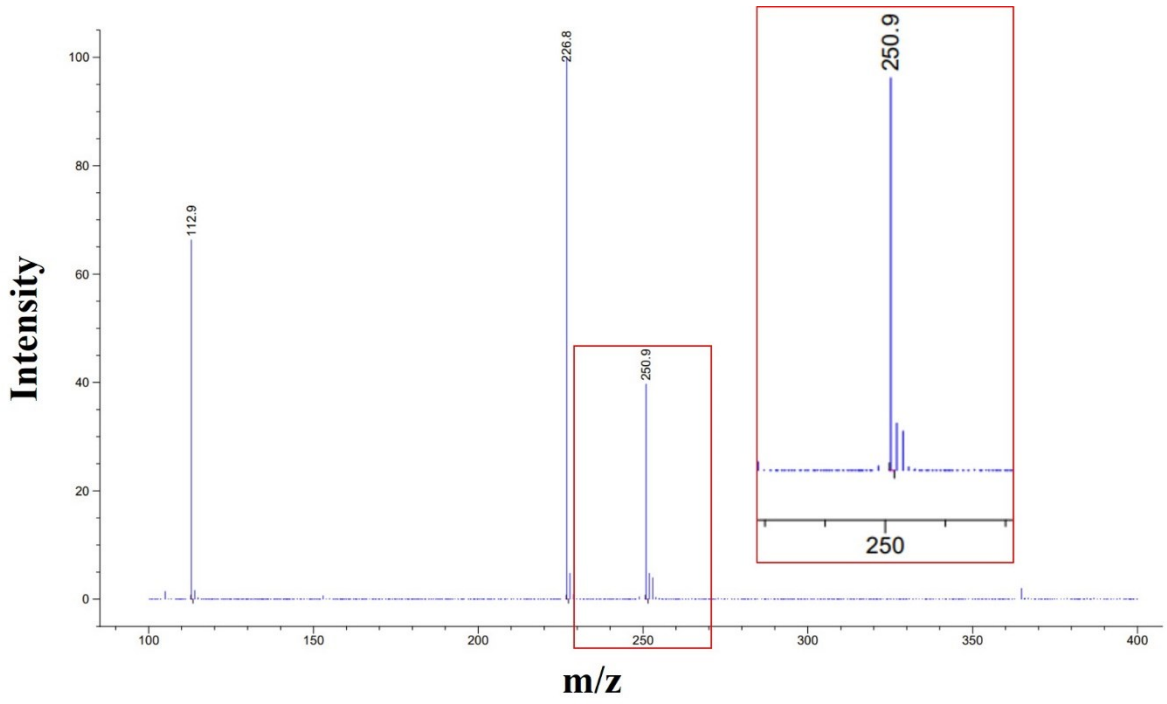

Figure 3.3. Mass spectroscopic, m/z spectrum of TK. The spectrum was averaged between 7.12 and 7.22 min of elution as shown in HPLC. The [M-H] mass of 251 g/mol in -ve scan mode against a theoretical mass of 252 g/mol was confirmed.

3.3.2. Stability and ROS mediated degradation of TK

A seven-day incubation of TK in 1X-PBS (pH = 7.4, 37 ºC) resulted in less than a 10 % decrease in chromatogram peak area (Figure 3.1B). To test TK's activity in the presence of ROS, acetone formation upon incubation with Fenton reagent (H_2O_2-Fe^{+2}) was monitored for 24 h using ^{1}H-NMR (Figure 3.4). It was observed that acetone (2.18 ppm) concentration increased with the incubation time in Fenton reagent, with a subsequent decrease in characteristics TK peaks. However, no acetone peak was observed in the control experiment with no Fenton reagent over a 24 h timeframe (Figure 3.5). Acetone concentration was quantified using TMS-Cl as an internal ^{1}H-NMR reference and its concentration was found to be 2.8 ± 0.32 mM after 24 h (Figure 3.1C).

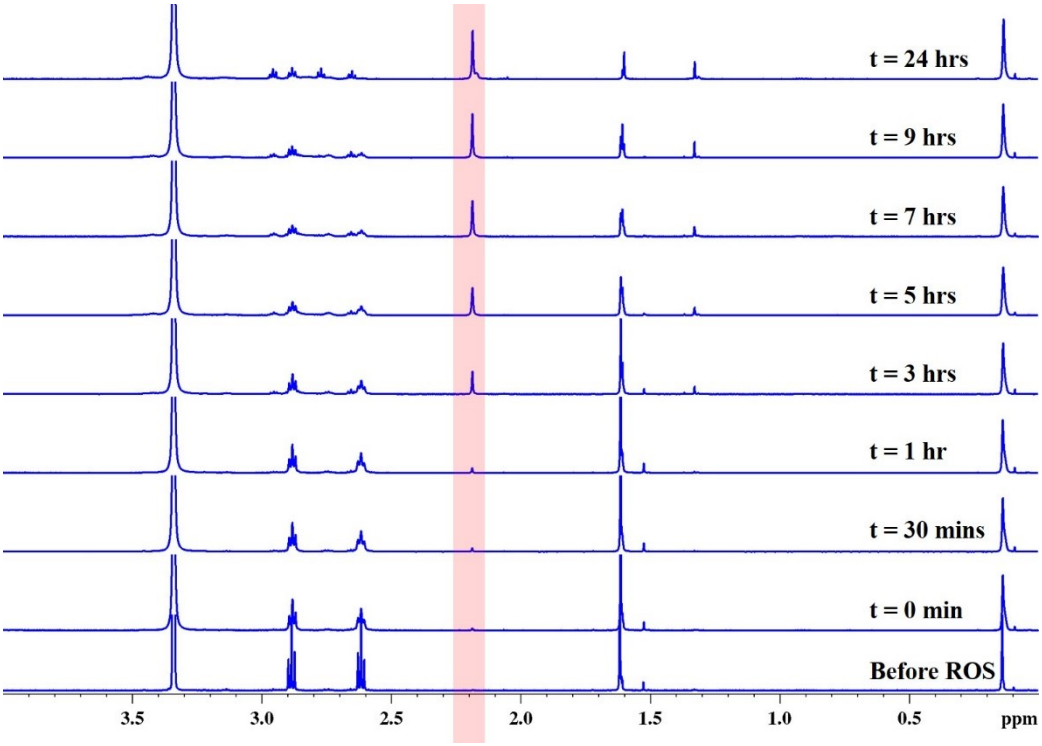

Figure 3.4. ROS activity of TK in Fenton's reagent. Time dependent ^{1}H-NMR spectra for OH$^{\bullet}$ mediated cleavage of TK as characterized through the evolution of the acetone peak (2.18 ppm).

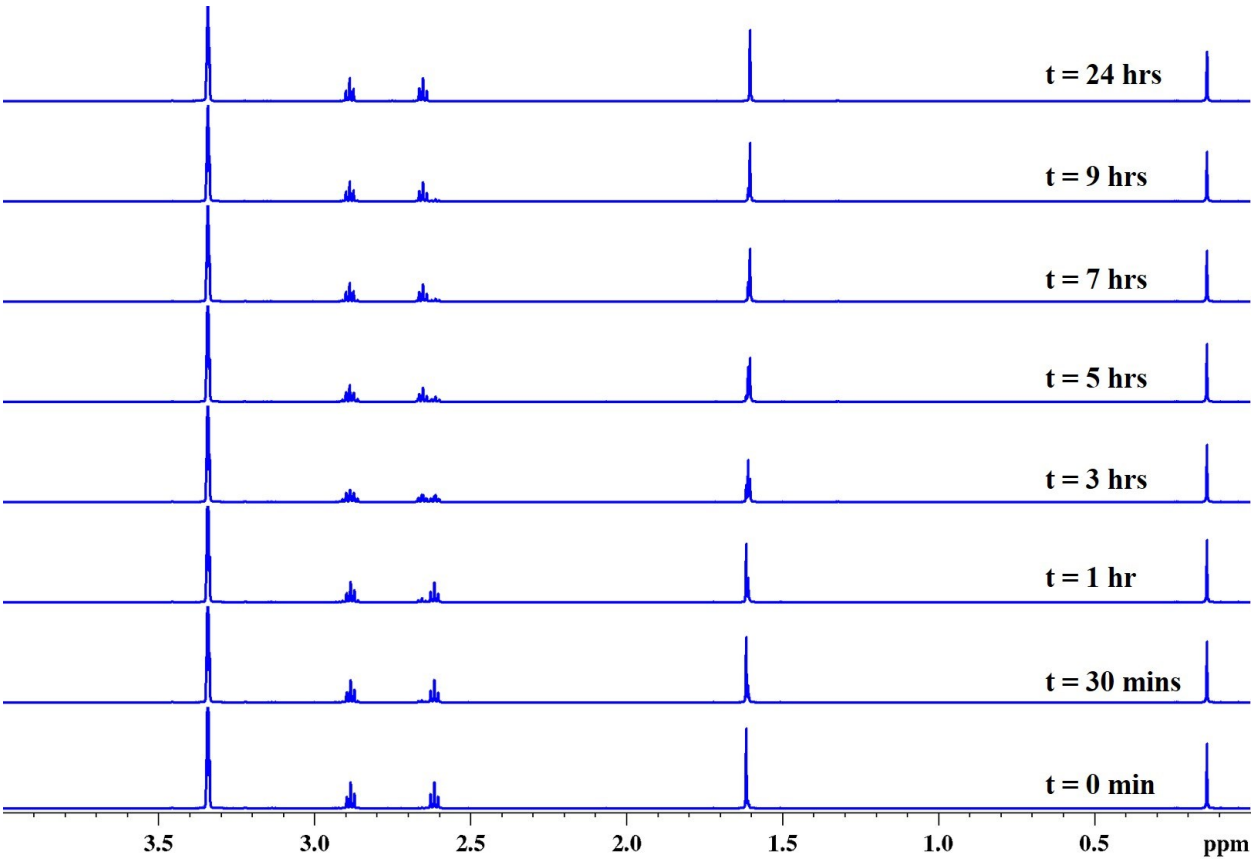

Figure 3.5. ROS activity of TK in the absence of Fenton's reagent. Time dependent control ^{1}H-NMR study showing no acetone evolution in the absence of Fenton reagent.

3.3.3. Effect of TK on cell toxicity and cell viability

Cell membrane integrity was evaluated using the Calcein-AM and BOBO 3-Iodide staining of the porcine islet cells. Islets treated with 100 or 200 µM of TK for 48 h showed no toxicity (Figure 3.6A-C). As a result, all further experiments were done with 200 µM of TK. The viability counts of islets incubated with 0 µM (88 ± 3%) and 200 µM (80 ± 4%) TK for 48 h were statistically similar (Figure 3.6A and C, $p>0.05$). Further, cells were exposed to exogenous H_2O_2 (400 µM, 4 h). The cell viability in TK-treated cells were maintained at greater than 53.6% as compared to the non-TK treated cells, whose viability decreased to less than 31.6 % (Figure 3.6D and E).

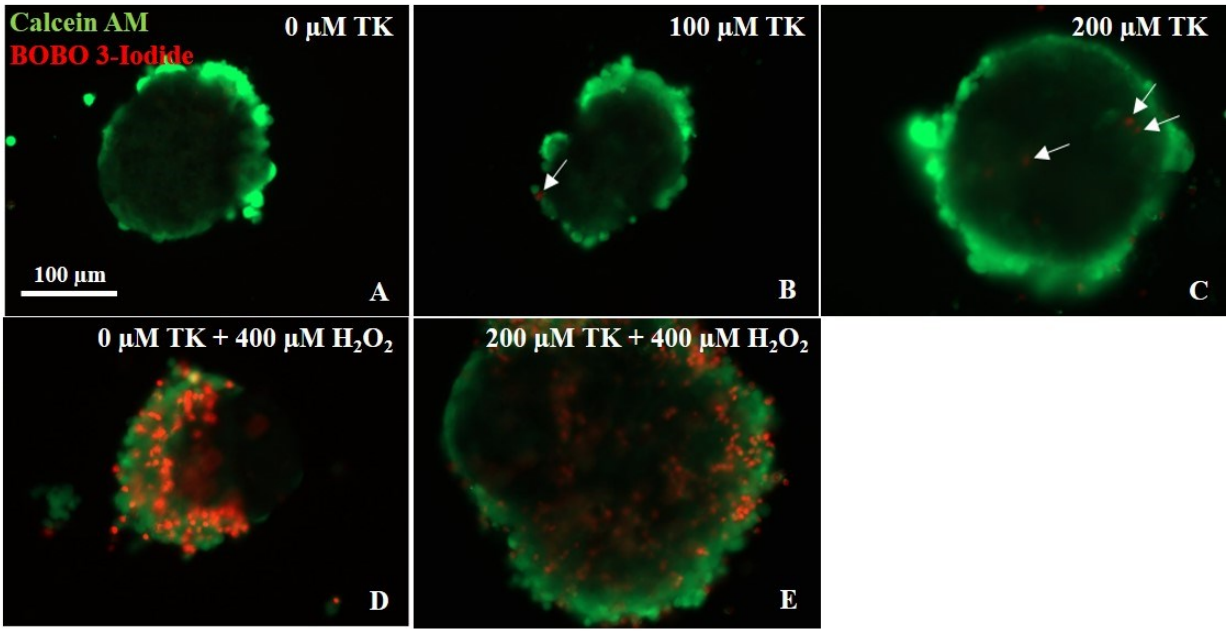

Figure 3.6. Florescence micrographs of NPI islets. NPI islets were treated with Calcein AM and BOBO 3-Iodide to detect live (green) and dead (red) cells respectively. Islet preparations were co-cultured with, (A) PBS (0 µM TK; control), (B) 100 µM TK, (C) 200 µM TK, (D) 0 µM TK+ 400 µM H_2O_2 and (E) 200 µM TK+ 400 µM H_2O_2. White arrows in A, B and C indicate the dead cells.

3.3.4. Oxygen consumption rate

The oxygen consumption rate (OCR) is indicative of the overall cellular responses to metabolic demand, mitochondrial potency and, hence, is a measure of overall cell function [26]. Respective OCR levels in islets incubated (48 h) with 0 or 200 µM TK was 212.8 ± 26.1 or 221.4 ± 8.6 nmol/(min-mg DNA), with no significant difference observed between the two groups (Figure 3.7A, $p>0.05$). Further, islets, pre-incubated with 200 µM of TK for 48 h were exposed to 800 µM H_2O_2 in the culture to study the effect TK pre-incubation has on ROS-induced cell stress. As expected, OCR values in cells without TK pre-incubation dropped significantly from 86.3 to 21.3 nmol/(min-mg DNA)) ($p<0.05$) upon exposure to H_2O_2. On the contrary, cells pre-incubation with 200 µM of TK for 48 h showed no change in cellular metabolism upon H_2O_2 exposure (Figure 3.7B, $p>0.05$).

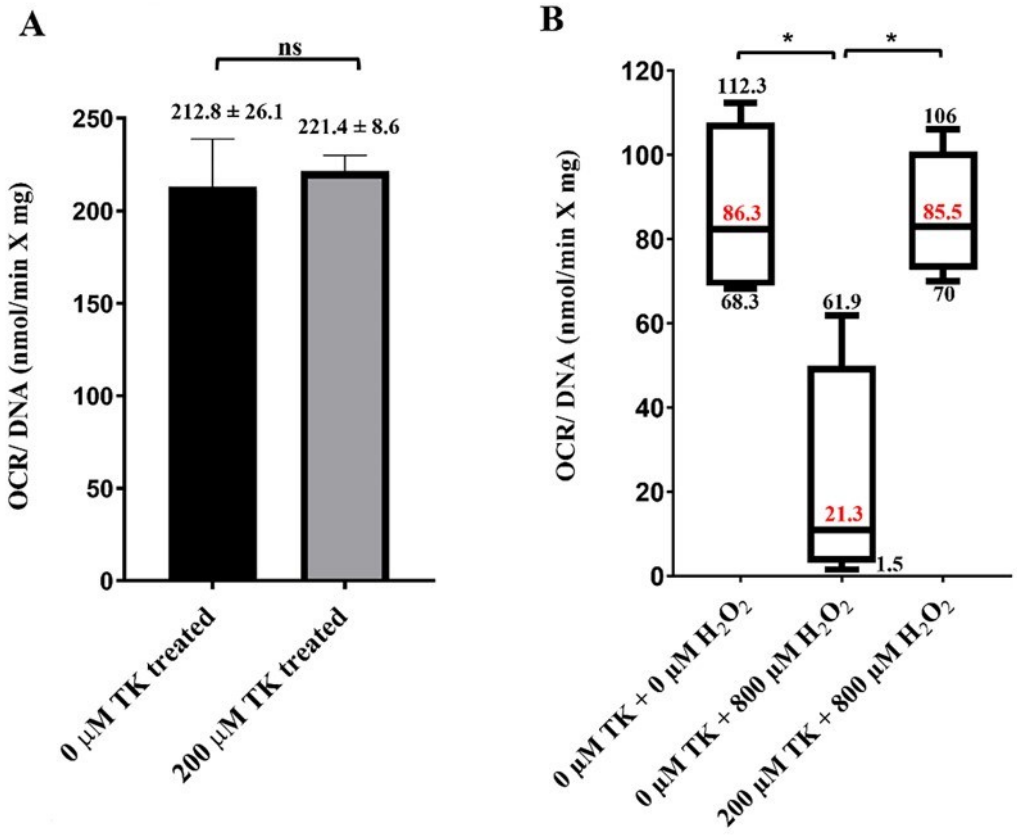

Figure 3.7. Oxygen consumption rates of NPI after 48 h TK incubation. (A) OCR of islets treated with 0 and 200 μM TK (n=3). Mean ± SEM of each treatment are shown above the relevant data group. (B) Boxplot for the OCR of islets treated with 0 and 200 μM TK for 48 h and exposed to 800 μM H_2O_2 for 4 h. Numbers are represented as the mean (red), median (black) and minimum and maximum values (black). For A and B; *=$p<0.05$, ns=nonsignificant (paired two-tailed t test). Data for each treatment group were generated with 3 biological replicates (from 3 individual pigs; n=3) in A and with 4 biological replicates (from 4 individual pigs; n=4) in B.

3.3.5. Lipid peroxidation assay

Lipid peroxidation reflects the oxidative cellular injury and is characterized by the oxidative degradation of polyunsaturated lipids, resulting in the formation of malondialdehyde (MDA) [27]. MDA levels in β-TC-6 cells incubated with 200 μM TK for 48 h was equivalent to the control (0.020 and 0.017 μmol/(μg DNA) ($p>0.05$) respectively, (Figure 3.8). Further, when 800 μM of H_2O_2 was added to the cell monolayers for 4 h, a significantly enhanced lipid peroxidation (0.027 μmol/μg DNA, $p<0.05$) was observed in the controls. However, when H_2O_2 was added to the cells

incubated with 200 µM of TK, the oxidative damaged was reduced by a significant 22%, with an MDA content of 0.021 µmol/µg DNA ($p<0.05$) as compared to the control (Figure 3.8).

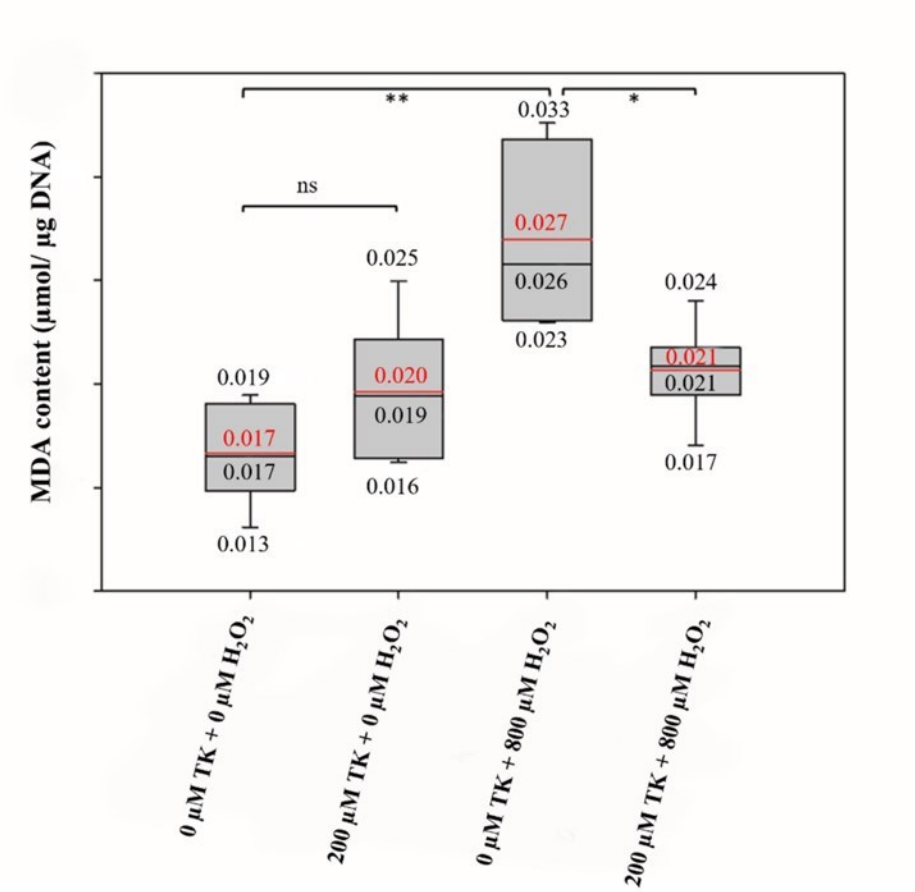

Figure 3.8. Lipid peroxidation in β-TC6 cells. MDA assay for the quantification of lipid peroxidation in β-TC6 cells in the presence and absence of 200 µM TK. The extent of lipid peroxidation upon addition of 800 µM H_2O_2 to TK-treated β-TC6 monolayer cultures were significantly reduced when compared to the non-treated cells. Shown numbers are the mean (red), median (black) and minimum and maximum values (black). **p<0.005, *p<0.05, ns=nonsignificant (paired two-tailed t test). Data for each treatment group were generated with 6 biological replicates (from 6 individual pigs; n=6).

3.3.6. Co-culturing islets with TK for enhancing islet survival after transplantation

Three cohorts of diabetic mice were transplanted with islets pre-incubated with 200 µM of TK (n = 7). The average blood glucose levels in the recipients of TK treated islets reached euglycemia (blood glucose <11.1 mM) within two days after transplantation. On the contrary, recipients of

non-TK treated islets never attained normoglycemic status (average) during the course of the study (Figure 3.9A).

Kaplan-Meier survival analysis of the islet recipients showed that the percent euglycemia in the group receiving TK-treated islets reached ~63% five days after transplantation, whereas the control group could only be maintained at ~30% (Figure 3.9B). Diabetes reversal rates in the control group (0 μM TK treated islets) plateaued at 60% at 18 days until graft retrieval. In contrast, a diabetes reversal rate of 82% ($p<0.05$) was achieved only in 13 days in the group receiving TK treated islets (Figure 3.9B).

Furthermore, long-term syngeneic graft function was characterized by metabolically challenging islet recipients by IPGTT (Figure 3.9C) and AUC analysis (Figure 3.9D), conducted at 30 days post-transplantation. TK-treated islet recipients showed a relatively faster glucose clearance profile compared to the control group (Figure 3.9C), however no significance difference from the control was observed Histological examination (H&E) as well as insulin-stained tissue sections confirmed the retention of islet graft within the kidney capsule (Figure 3.10A-D).

3.4. Discussion

TK is cleaved in ROS environments to yield free thiol (RSH) groups (Figure 3.11), resulting in the formation of the parent ketone groups. Conversely, TKs function as a highly sensitive ROS scavenger, effective in scavenging ROS *viz*. superoxide radicals, hydroxyl radicals, and hydrogen peroxides (H_2O_2) [21,22,28]. Furthermore, the free thiols (RSH) generated during the process are further oxidized to sulfenic (RSOH), sulfinic (RSO_2H), and finally to sulfonic (RSO_3H) acids in the presence of H_2O_2 (Figure 3.11), successively scavenging many more toxic ROS molecules in the process [29]. Thioketals as a ROS sensitive entity has found wide applicability in targeted drug

delivery systems [28]. However, its effectiveness as an antioxidant molecule is underreported. It is demonstrated here that TK acts a very promising antioxidant molecule, with it's effectiveness in neutralising several kinds of ROS.

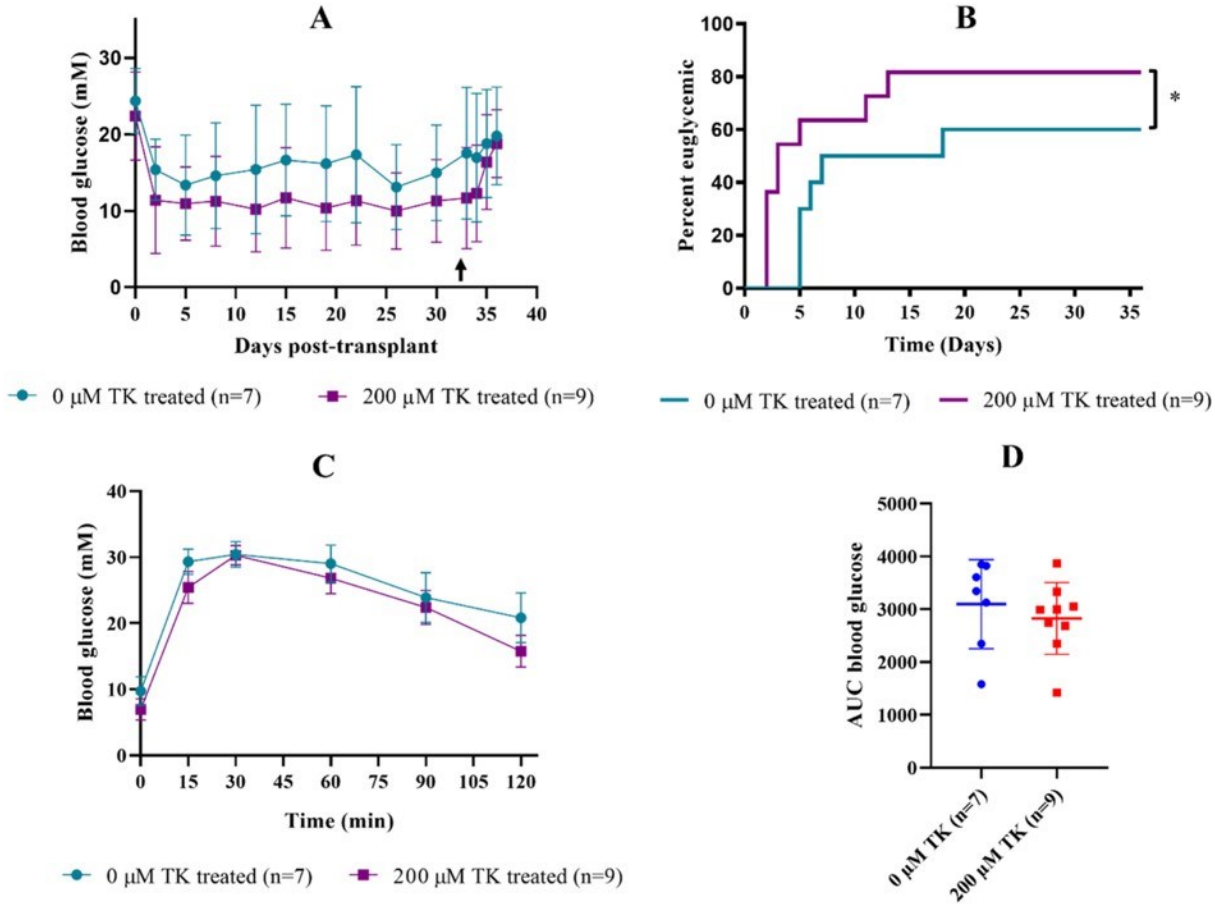

Figure 3.9. Syngeneic islet graft functional outcomes after transplantation of TK treated islets under the kidney capsule of diabetic BALB/c male mice. (A) Post-transplant blood glucose measurements of PBS treated islets (n = 7) and 200 µM TK treated islets (n = 9) recipients. Arrow represents time of survival nephrectomy. (B) Islet graft survival, Kaplan-Meier survival analysis of mouse recipients transplanted with PBS treated islets (blue; n = 7) and 200 µM TK treated islets (green; n = 9). (C) IPGTT of PBS treated islets recipients (n = 7) and 200 µM TK treated islets recipients (n = 9), at 30 days posttransplant. (D) IPGTT area under the curve data of individual mouse. *p<0.05.

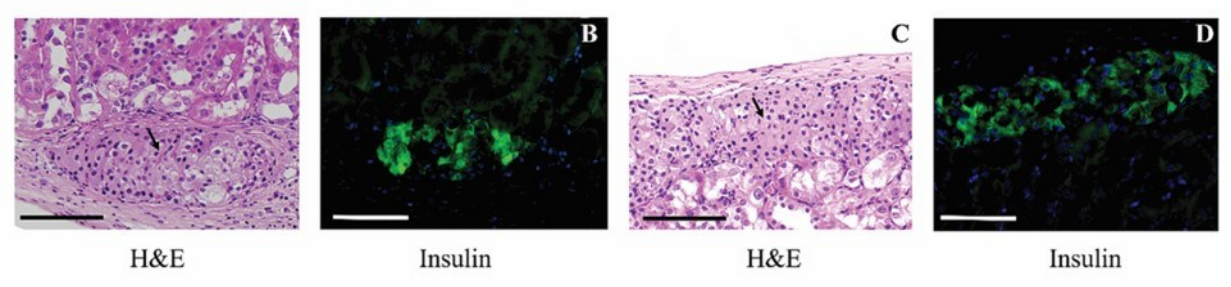

Figure 3.10. Immunochemistry of syngrafted islets. Hematoxylin and Eosin (H&E) staining, and immunohistochemistry of syngeneic PBS treated islets (A and B) and 200 µM TK treated islets (C and D); Green = insulin, blue = DAPI stained nuclei. Arrows in H&E-stained images indicate the area where the islets grafts under the kidney capsule is located. Scale bars represent 100 µm.

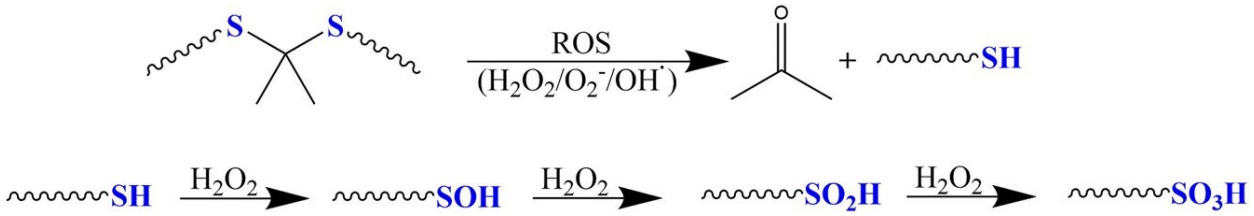

Figure 3.11. Reaction showing ROS mediated cleavage of TK. Top: TK consumes several ROS molecules to yield acetone and free thiol (RSH) groups. Bottom: RSH, in the presence of H_2O_2 can successively get oxidized to sulfenic (RSOH), sulfinic (RSO_2H) and finally to sulfonic (RSO_3H) acids.

TK was successfully synthesized and characterized and, as expected, was stable at physiological pH (Figure 3.1B) [28] with ROS activity in the presence of Fenton's reagent (Figure 3.1C). The in vitro attributes of TK were evaluated using porcine islets, where intact membrane integrity and viability count (80% against 88% in control) of the porcine islets incubated with 200 µM TK confirmed that TK was non-toxic to cells at this high concentration (Figure 3.6). The cytoprotective properties of TK was then studied against oxidative insults. Cells pre-incubated with TK (200 µM) were exposed to four equivalents (800 µM) of H_2O_2. OCR as a measure of cell functionality and MDA as a measure of oxidative damage was analysed on porcine islets and β-TC-6 cells, respectively. DNA normalized OCR consumption rate in the untreated (control) and TK treated cells showed no differences, further affirming the nontoxicity of TK at 200 µM (Figure 3.7a). Further, when islets were exposed to 800 µM H_2O_2, cells preincubated with TK showed no

significant decrease in metabolic activity and the OCR remained comparable to the control (no TK, no H_2O_2) with an OCR of 85.5 and 86.3 nmol/min-mg DNA respectively. However, when H_2O_2 was added to the non-TK treated cells, the OCR exhibited a 75% reduction in cell viability (Figure 3.7B). These results demonstrate that not only TK is biocompatible, it protects these complex cells against oxidative stress.

MDA analysis of a β-TC-6 cell monolayer pre-incubated with TK showed that TK limited the oxidative damage; or conversely, incubating cells with TK protected them from the deleterious effects of ROS. Addition of H_2O_2 to β-TC-6 cell monolayer increased the oxidative damage by 59 % (0.017 µmol/µg-DNA in no TK + no H_2O_2 group vs 0.027 µmol/µg-DNA in no TK + 800 µM H_2O_2 group. However, when H_2O_2 was added to the cells preincubated with TK, the oxidative damage was reduced by a significant 22% (0.021 µmol/µg-DNA in 200 µM TK + 800 µM H_2O_2 group) (Figure 3.8). These results are in accordance with our other experimental data and thus substantiate that TK molecule protects the cells against the ill effects of free radicals. Furthermore, the MDA levels in the control group (no TK, no H_2O_2) and TK incubated cells (200 µM TK, no H_2O_2 were comparable (0.017, 0.020 and 0.021 µmol/µg-DNA), affirming the non-toxic effects of TK.

TK is a small (252 g/mole), slightly hydrophobic molecule with two carboxylic groups; properties that may allow for their internalization within cells. Based on these postulates and the results of our cytoprotective studies, it could be possible that the protective effect of TK is a synergistic role-play of both extracellular, and intracellular activity against a myriad of free radicals that are generated within the cell. The *in vitro* results of TK were translated *in vivo* through the syngeneic BALB/c mouse-marginals islet transplant model. Three cohorts of mice transplanted with islets pre-incubated with 200 µM of TK (n = 7) showed that TK-treatment expedites the restoration of

physiological glucose levels and yields an improved glycemic control which is maintained through to the graft nephrectomy (Figure 3.9A). These results were also evident through the Kaplan-Meier survival analysis of the islet recipients as where 63% of TK-treated islet recipients reached euglycemia in five days post transplantation while the control group could only be maintained at ~30% (Figure 3.9B). Further, nephrectomy promptly restored a hyperglycemic state in the TK-treated islet recipients, confirming a graft dependent glycemic control (Figure 3.9A). The long-term graft functions in the islet recipients through were assessed through IPGTT and subsequent AUC analysis. Though these data did not show a significant difference, the general trend suggests that the TK treatment of islets during culturing enhanced efficient long-term graft function (Figure 3.9C, D) and graft retention (Figure 3.10).

Results demonstrated here are very promising and puts TK in comparison with other molecules that are being investigated as an antioxidant in islet transplantation. Metallothionein (MT), owed to its cysteine rich protein structure has been used as a ROS scavenger to protect islets from the oxidative damage during IT. However, a transgenic mouse model with β-cells that expressed 30-fold more MT in mice were only successful in delaying hyperglycemia in response to exogenous streptozotocin [15]. The group later isolated the islets from the transgenic mouse model and allografted 400 islets under the kidney capsule of diabetic mice. Mice receiving islets that overexpressed MT maintained normal glucose levels for an average of 16.2 days as compared to 8.36 days in control animals [30]. However, overexpression of a protein was deemed clinically unviable, and to enhance the clinical applicability, MT was genetically fused with a cell permeating peptide to facilitate cell internalization into isolated rat islet cells. Results showed that MT internalization was protective against both externally induced nitric oxide and superoxide anions [18,31]. The group then xenografted the rat islets into mouse to test their efficacy. The results

showed that a high number of islets (1200 IEQ) was needed to maintain the normal glucose level in the recipient and to withstand immune rejection. When a lower number (350 IEQ) of rat islets were transplanted into the mouse, the glucose level showed a hyperglycemic trend before they were immunologically rejected. The hyperglycemic trend was also apparent with administration of immunosuppressant, though graft was preserved throughout the study [18,31]. In contrast, our results show that transplantation of only 200 TK-treated islets into diabetic recipients were sufficient to maintain a normal glucose level with significantly increased graft retrieval after more than 30 days (total time of our study) post-transplantation. Our survival analysis demonstrated a promising functional graft retention compared to the control group and was well aligned with the outcome of the IPGTT. However, it is noteworthy that xenotransplantation, in the above-mentioned studies, is more prone to immune rejection as compared to allotransplantation [18,31].

Bilirubin (BR) is another antioxidant molecule which has found utility in islet transplantation. Administration of BR before islet isolation has shown to minimize oxidative damage, and enhance functionality (an *in vitro* insulin secretion index of 1.93 in islets isolated from BR administered group vs 1.55 in controls) post-isolation [14]. Protective effect of BR has also been shown post-isolation in cell preservation. It was shown that islets preserved with 1 µg/mL BR could maintain more than 90% islet viability as compared to 60% for controls after 72 h [32]. However, BR induced apoptosis and was toxic at higher concentrations (>34 µM). Apart from toxicity, extremely short half-life (5 min) and water insolubility are other factors which limit the use of BR. To overcome these challenges, BR was loaded into cyclodextrin (CD) supramolecule. However, this approach did not alter the toxicity of BR, and both free BR and equivalent BR loaded CD molecule exhibited islet toxicity at concentration above 60 µM. Further, conjugation of BR to a hydrophilic polyethylene glycol (PEG), which facilitated its self-assembly into a nanoparticle, could only show

a marginal decrease in BR toxicity; where free BR was toxic at 60 μM, BR nanoparticles elicited toxicity at 80 μM equivalent BR concentration [17]. As opposed to BR, TK remains stable both in solid form, Fenton-based cleavage experiments of TK (Figure 3.4 and Figure 3.5) were repeated four months after synthesis and NMR showed no additional peaks that were indicative of degradation.

Finally, the results obtained for TK were compared with SOD mimic metalloporphyrins, BMX-001. BMX-001 administration during mouse islet isolation and culture has shown to reduce extracellular ROS in isolated mouse cells: 1.65-fold vs 2.6-fold ROS in islets from non-BMX-001 treated mouse. However, BMX-001 administration during isolation alone did not have a significant effect on cell viability, and it need BMX-001 administration both during islet isolation and cell culture for improved cell survival [19,33]. Further, transplantation studies showed that BMX-001 administration during isolation and culture helped 71% of recipients reach euglycemia after 12 days, while the same number was achieved in 14 days for the control [33]. In contrast, with respect to TK, only 48 h incubation was able to show promising transplantation results. In addition to these enzyme mimics, several metal-oxide nanoparticles exhibiting ROS scavenging properties are also being studied [34,35]. These are however limited by their cell cytotoxicity and precise control of their nanostructure during synthesis, which affects their functionality [36].

3.5. Conclusion

In conclusion, the applicability of thioketals as a ROS scavenging molecule is reported for the first time. TK exhibits excellent cell compatibility and protects cells from oxidative stress induced damage. These attributes of TK were used as therapeutics in islet cell transplantation. TK was highly efficient in maintaining cell viability and functionality. Further, *in vivo* results showed that

incubation of islets pre-transplantation enhances graft survival and insulin metabolism. These are crucial findings which will help improve the outcomes of islet cell transplantation. Furthermore, TK, owed to its excellent ROS sensitivity and ROS scavenging properties, can be utilised as a bifunctional moiety in drug delivery and tissue engineering platforms.

3.6. References

[1] I.D.F.D. Atlas, 463 PEOPLE LIVING WITH DIABETES million, 2019.

[2] R. Shah, M. Patel, D. Maahs, V. Shah, Insulin delivery methods: Past, present and future, International Journal of Pharmaceutical Investigation. 6 (2016) 1. https://doi.org/10.4103/2230-973x.176456.

[3] H. Thabit, R. Hovorka, Coming of age: the artificial pancreas for type 1 diabetes, Diabetologia. 59 (2016) 1795–1805. https://doi.org/10.1007/s00125-016-4022-4.

[4] E. Latres, D.A. Finan, J.L. Greenstein, A. Kowalski, T.J. Kieffer, Navigating two roads to glucose normalization in diabetes: automated insulin delivery devices and cell therapy, Cell Metabolism. 29 (2019) 545–563.

[5] A.M.J. Shapiro, M. Pokrywczynska, C. Ricordi, Clinical pancreatic islet transplantation, Nature Reviews Endocrinology. 13 (2017) 268–277. https://doi.org/10.1038/nrendo.2016.178.

[6] B.J. Hering, W.R. Clarke, N.D. Bridges, T.L. Eggerman, R. Alejandro, M.D. Bellin, K. Chaloner, C.W. Czarniecki, J.S. Goldstein, L.G. Hunsicker, D.B. Kaufman, O. Korsgren, C.P. Larsen, X. Luo, J.F. Markmann, A. Naji, J. Oberholzer, A.M. Posselt, M.R. Rickels, C. Ricordi, M.A. Robien, P.A. Senior, A.M. James Shapiro, P.G. Stock, N.A. Turgeon, Phase 3 trial of transplantation of human islets in type 1 diabetes complicated by severe hypoglycemia, Diabetes Care. 39 (2016) 1230–1240. https://doi.org/10.2337/dc15-1988.

[7] A. Citro, E. Cantarelli, L. Piemonti, Anti-inflammatory strategies to enhance islet engraftment and survival, Current Diabetes Reports. 13 (2013) 733–744.

[8] D.C. Brennan, H.A. Kopetskie, P.H. Sayre, R. Alejandro, E. Cagliero, A.M.J. Shapiro, J.S. Goldstein, M.R. Desmarais, S. Booher, P.J. Bianchine, Long-Term Follow-Up of the Edmonton Protocol of Islet Transplantation in the United States, American Journal of Transplantation. 16 (2016) 509–517. https://doi.org/10.1111/ajt.13458.

[9] M.C. Vantyghem, M. Chetboun, V. Gmyr, A. Jannin, S. Espiard, K. le Mapihan, V. Raverdy, N. Delalleau, F. Machuron, T. Hubert, M. Frimat, E. van Belle, M. Hazzan, P. Pigny, C. Noel, R. Caiazzo, J. Kerr-Conte, F. Pattou, Erratum: Ten-year outcome of islet alone or islet after kidney transplantation in type 1 diabetes: A prospective parallel-arm cohort study.(Diabetes care(2019)42(2042–2049)Doi:10.2337/dc19-0401), Diabetes Care. 43 (2020) 1164. https://doi.org/10.2337/dc20er05.

[10] J.A. Emamaullee, A.M.J. Shapiro, Factors influencing the loss of β-cell mass in islet transplantation, Cell Transplantation. 16 (2007) 1–8.

[11] E.A. Ryan, J.R.T. Lakey, B.W. Paty, S. Imes, G.S. Korbutt, N.M. Kneteman, D. Bigam, R. v Rajotte, A.M.J. Shapiro, Successful islet transplantation: continued insulin reserve provides long-term glycemic control, Diabetes. 51 (2002) 2148–2157.

[12] N.R. Barshes, S. Wyllie, J.A. Goss, Inflammation-mediated dysfunction and apoptosis in pancreatic islet transplantation: implications for intrahepatic grafts, Journal of Leukocyte Biology. 77 (2005) 587–597.

[13] A. Miki, C. Ricordi, Y. Sakuma, T. Yamamoto, R. Misawa, A. Mita, R.D. Molano, N.D. Vaziri, A. Pileggi, H. Ichii, Divergent antioxidant capacity of human islet cell subsets: A potential cause

of beta-cell vulnerability in diabetes and islet transplantation, PLoS ONE. 13 (2018) 1–16. https://doi.org/10.1371/journal.pone.0196570.

[14] H.Q. Zhu, Y. Gao, H.R. Guo, Q.Z. Kong, Y. Ma, J.Z. Wang, S.H. Pan, H.C. Jiang, W.J. Dai, Pretreatment with bilirubin protects islet against oxidative injury during isolation and purification, in: Transplantation Proceedings, Elsevier, 2011: pp. 1810–1814.

[15] H. Chen, E.C. Carlson, L. Pellet, J.T. Moritz, P.N. Epstein, Overexpression of metallothionein in pancreatic β-cells reduces streptozotocin-induced DNA damage and diabetes, Diabetes. 50 (2001) 2040–2046.

[16] J.M. Barra, H.M. Tse, Redox-dependent inflammation in islet transplantation rejection, Frontiers in Endocrinology. 9 (2018) 175.

[17] M.J. Kim, Y. Lee, S. Jon, D.Y. Lee, PEGylated bilirubin nanoparticle as an anti-oxidative and anti-inflammatory demulcent in pancreatic islet xenotransplantation, Biomaterials. 133 (2017) 242–252. https://doi.org/10.1016/j.biomaterials.2017.04.029.

[18] H.S. Jung, K.S. Lim, M.J. Kim, Y.H. Hwang, C. Yoo, Y. Lee, Y.-H. Kim, D.Y. Lee, Hypoxic resistance of hypodermically transplanted pancreatic islets by using cell-absorbable antioxidant Tat-metallothionein, Journal of Controlled Release. 172 (2013) 1092–1101.

[19] A. Bruni, A.R. Pepper, R.L. Pawlick, B. Gala-Lopez, A. Gamble, T. Kin, A.J. Malcolm, C. Jones, J.D. Piganelli, J.D. Crapo, A.M.J. Shapiro, BMX-001, a novel redox-active metalloporphyrin, improves islet function and engraftment in a murine transplant model, American Journal of Transplantation. 18 (2018) 1879–1889. https://doi.org/10.1111/ajt.14705.

[20] A. Tovmasyan, C.G.C. Maia, T. Weitner, S. Carballal, R.S. Sampaio, D. Lieb, R. Ghazaryan, I. Ivanovic-Burmazovic, G. Ferrer-Sueta, R. Radi, A comprehensive evaluation of catalase-like activity of different classes of redox-active therapeutics, Free Radical Biology and Medicine. 86 (2015) 308–321.

[21] A.K. Shukla, M. Verma, K.N. Singh, Superoxide induced deprotection of 1,3-dithiolanes: A convenient method of dedithioacetalization, Indian Journal of Chemistry - Section B Organic and Medicinal Chemistry. 43 (2004) 1748–1752. https://doi.org/10.1002/chin.200449059.

[22] B. Liu, S. Thayumanavan, Mechanistic Investigation on Oxidative Degradation of ROS-Responsive Thioacetal/Thioketal Moieties and Their Implications, Cell Reports Physical Science. 1 (2020) 100271.

[23] G.S. Korbutt, J.F. Elliott, Z. Ao, D.K. Smith, G.L. Warnock, R. v Rajotte, Large scale isolation, growth, and function of porcine neonatal islet cells., The Journal of Clinical Investigation. 97 (1996) 2119–2129.

[24] K.K. Papas, A. Pisania, H. Wu, G.C. Weir, C.K. Colton, A stirred microchamber for oxygen consumption rate measurements with pancreatic islets, Biotechnology and Bioengineering. 98 (2007) 1071–1082.

[25] A.R. Pepper, B. Gala-Lopez, R. Pawlick, S. Merani, T. Kin, A.M.J. Shapiro, A prevascularized subcutaneous device-less site for islet and cellular transplantation, Nature Biotechnology. 33 (2015) 518–523.

[26] I.R. Sweet, G. Khalil, A.R. Wallen, M. Steedman, K.A. Schenkman, J.A. Reems, S.E. Kahn, J.B. Callis, Continuous measurement of oxygen consumption by pancreatic islets, Diabetes Technology & Therapeutics. 4 (2002) 661–672.

[27] D.L. Tribble, T.Y. Aw, D.P. Jones, The pathophysiological significance of lipid peroxidation in oxidative cell injury, Hepatology. 7 (1987) 377–386.

[28] D.S. Wilson, G. Dalmasso, L. Wang, S. v. Sitaraman, D. Merlin, N. Murthy, Orally delivered thioketal nanoparticles loaded with TNF-α-siRNA target inflammation and inhibit gene expression in the intestines, Nature Materials. 9 (2010) 923–928. https://doi.org/10.1038/nmat2859.

[29] L.A.H. van Bergen, G. Roos, F. de Proft, From thiol to sulfonic acid: Modeling the oxidation pathway of protein thiols by hydrogen peroxide, The Journal of Physical Chemistry A. 118 (2014) 6078–6084.

[30] X. Li, H. Chen, P.N. Epstein, Metallothionein Protects Islets from Hypoxia and Extends Islet Graft Survival by Scavenging Most Kinds of Reactive Oxygen Species, Journal of Biological Chemistry. 279 (2004) 765–771. https://doi.org/10.1074/jbc.M307907200.

[31] M.J. Kim, Y.H. Hwang, Y.H. Kim, D.Y. Lee, Immunomodulation of cell-penetrating tat-metallothionein for successful outcome of xenotransplanted pancreatic islet, Journal of Drug Targeting. 25 (2017) 350–359.

[32] Q. Yao, X. Jiang, Z.-W. Huang, Q.-H. Lan, L.-F. Wang, R. Chen, X.-Z. Li, L. Kou, H.-L. Xu, Y.-Z. Zhao, Bilirubin improves the quality and function of hypothermic preserved islets by its antioxidative and anti-inflammatory effect, Transplantation. 103 (2019) 2486–2496.

[33] A. Bruni, A.R. Pepper, B. Gala-Lopez, R. Pawlick, N. Abualhassan, J.D. Crapo, J.D. Piganelli, A.M.J. Shapiro, A novel redox-active metalloporphyrin reduces reactive oxygen species and inflammatory markers but does not improve marginal mass engraftment in a murine donation after circulatory death islet transplantation model, Islets. 8 (2016). https://doi.org/10.1080/19382014.2016.1190058.

[34] N.J. Abuid, K.M. Gattás-Asfura, E.A. Schofield, C.L. Stabler, Layer-by-Layer Cerium Oxide Nanoparticle Coating for Antioxidant Protection of Encapsulated Beta Cells, Advanced Healthcare Materials. 8 (2019) 1–10. https://doi.org/10.1002/adhm.201801493.

[35] A.A. Vernekar, D. Sinha, S. Srivastava, P.U. Paramasivam, P. D'Silva, G. Mugesh, An antioxidant nanozyme that uncovers the cytoprotective potential of vanadia nanowires, Nature Communications. 5 (2014). https://doi.org/10.1038/ncomms6301.

[36] S. Raj, S. Kumar, K. Chatterjee, Facile synthesis of vanadia nanoparticles and assessment of antibacterial activity and cytotoxicity, Materials Technology. 31 (2016) 562–573.

Chapter 4. Synthesis and characterization of reactive oxygen species responsive dexamethasone delivery systems

Preface

Shammy Raj designed and conducted all synthesis and functional testing work detailed in this chapter, analyzed the results, and wrote the chapter. Larry D. Unsworth guided the research design, analyzed and reviewed the data, reviewed and edited the document.

4.1. Introduction

Reactive oxygen species (ROS) are important regulators of immune response. Elevated levels of ROS have been found in several inflammatory and autoimmune diseases including respiratory and lung diseases like asthma and chronic obstructive pulmonary diseases (COPD); diabetes, organ transplantation, and cancer, among others [1,2]. ROS at the site of inflammation are primarily generated by the first responders of immune system viz. mast cells and macrophages, and consecutively elicit varied effects [3,4]. In a defensive role, ROS protects against the pathogenic microbial invasions [5]. ROS manifests itself in an anti-inflammatory role by suppressing T cell proliferation and activation [6]**.** However, in contrast to its protecting effects, ROS also serves as regulatory molecules in the downstream signalling of immunogenic pathways, aggravating the inflammation and allergic reaction [7]. High level of ROS further causes oxidative stress mediated cell apoptosis [8], and has been shown to trigger inflammation and graft rejection post transplantation [9].

ROS being central to inflammation, has been explored as a stimulus to design ROS sensitive materials, for its application in tissue repair, drug delivery and cancer therapeutic [10]. As discussed in the preceding chapters, ROS sensitive systems can be categorized into two categories. First category includes the ones which oxidize and undergo a phase transition from a hydrophobic to a hydrophilic system in ROS extensive environment. The phase transition triggers the release of encapsulated cargo. Elements from the oxygen family namely sulphur, selenium and tellurium exhibit such characteristics and thus have been explored to develop ROS sensitive materials [11–13]. The second category includes molecule which undergoes cleavage in oxidative environments. These molecules are generally embedded within the system, and the cleavage of which alters the hydrophobic-hydrophilic balance, causing a dissociation or aggregation of the materials.

Diselenides, thioketals and phenyl boronic esters are representative molecules of this category and been extensively used in designing ROS sensitive materials [14–16].

In the previous chapter, the synthesis and characterization of the ROS sensitive thioketal (TK) molecule was shown. TK exhibits excellent ROS sensitivity, and is both biocompatible and bioactive. TKs, in the presence of ROS gets cleaved at two positions to furnish the corresponding ketonic group and sulphide containing reaction products [17]. TK shows versatility in its sensitivity against various ROS molecules including superoxide radicals (O_2^-), hydroxyl radicals ($OH^\bullet$) and hydrogen peroxide (H_2O_2). Owed to its versatile ROS responsiveness, TKs have widely been used in the design of drug delivery systems, where the cleave of TK results in the release of encapsulated/conjugated cargo exclusively at the site of elevated ROS [14,17]. In the present study, TK has been used to design delivery platforms to release anti-inflammatory drug Dexamethasone (Dex) in the ROS intensive environment.

Dex is an anti-inflammatory steroidal drug which is commonly used in the treatment of auto immune and inflammatory disease. Dex exerts its therapeutic effects both by down regulating the transcription of genes which encodes for inflammatory mediators, and by upregulating anti-inflammatory genes like Annexin-1 and Interleukin – 10 (IL-10). In the mechanism, Dex is internalized into the cytoplasm through cell membrane to bind and activate the cytoplasmic Glucocorticoid Receptor (GR). Activation of GR exposes the GR domain needed to diffuse nuclear membrane and facilitates the diffusion of GR-Dex complex into the nucleus. In the nucleus, the GR-Dex complex forms a homodimer and binds to the targeted sequences of the glucocorticoid responsive anti-inflammatory genes. This results in an increase in the transcription of the corresponding genes. Alternatively, activated GRs have also been reported to repress genes through transrepression, wherein, activated GRs directly bind to the pro-inflammatory

transcription factors and coactivator molecules, and inhibit their activity, thus repressing the transcription of inflammatory genes [18,19].

GRs are ubiquitous across tissues and cell lines, however, the cascade of events following GR activation differ accordingly. Dex activation of GR in eyes prevent vascularization and angiogenesis; while that in osteoblasts and osteocytes has shown to induces cell apoptosis [20]. In immune cells, the administration of Dex during macrophage differentiation has shown to increase ROS production, with a simultaneous reduction in immunogenic IL-6 cytokine production. The result was also extended to dendritic cells (DC). The *in vitro* results were also translated to *in vivo* rat model, where Dex administered macrophages supressed T cell mediated IFN-γ and IL-4 production [6]. Furthermore, Dex has shown to upregulate macrophage mediated phagocytosis of neutrophils, prevent T cell proliferation, restrict T cell migration; and induce T cell apoptosis [20,21].

In mast cells, Dex supresses the expression of FcεRI receptor on the cell surface, with a similar effect on mast cell development, maturation and proliferation [22]. Studies with antigen activated rat mast cell line, RBL-2H3 cells have shown that Dex administration results in significant reduction in phosphatidylinositol 4,5-bisphosphate (PIP2), a key signaling molecule in the Inositol trisphosphate (IP3) pathway. The down regulation of IP3 pathway was mediated by the GR receptor in a dose dependent manner. The decreases in IP3 activity causes a decrease in cytosolic calcium release which subsequently decreases degranulation [23]**.** Furthermore, since mast cells are also activated through the recently discovered mas related G-protein receptor X2 (MRGPRX2), studies have shown that Dex supresses the expression of MRGPRX2 receptor, as well mast cell degranulation when activated with known MRGPRX2 ligand [22,24].

In the present study, TK was used as a linker to conjugate Dex to polyethylene glycol (PEG) and polyethylene glycol – polylactic acid (PEG-PLA) copolymer. The results showed that Dex was successfully conjugated to the polymeric material and were released when exposed to ROS. Furthermore, Dex conjugated to PEG-PLA copolymers exhibited self assembly and assembled into nanoparticles when dispersed in an aqueous environment.

4.2. Materials and methods

4.2.1. Synthesis and characterization of TK

Detailed procedure for the synthesis and characterization of TK has been described in the previous chapter.

4.2.2. Synthesis of PEG-PLA block copolymer

PEG-PLA block copolymer with a targeted PLA block of 2000 g/mole (PLA-2K) was synthesized using ring opening polymerization of L-lactide (Sigma Aldrich). PEG methyl ether (m-PEG, 2000 g/mole) (Sigma Aldrich) was used as a macroinitiator, and stannous octoate ($Sn(Oct)_2$ (Sigma Aldrich) was used as a catalyst. In atypical reaction, m-PEG (7.5 g) and L-lactide (7.5 g) was introduced in a dried 3-neck glass round bottom flask (RBF). The temperature of the reaction flask was then stabilized to 160 ^oC under inert N_2 atmosphere. Once temperature had stabilized, 0.038 g of stannous octoate catalyst dissolved in little amount of anhydrous dichloromethane (DCM, Sigma Aldrich) was injected in to the reaction vessel and the reaction was continued for 90 min. After reaction, the flask was immediately immersed in ice to quench the reaction. A white viscous substance was obtained, which was dissolved in DCM (ACS, Fischer Scientific) and precipitated thrice in cold di-ethyl ether (Sigma Aldrich) to obtain the PEG-PLA block copolymer (PLA-2K).

4.2.3. Synthesis of PLA-2K-TK-Dex and PEG-TK-Dex

PLA-2K-TK-Dex (PLA-TD) and PEG-TK-Dex (PEG-TD) were synthesized in a two-step process. In the first step TK was conjugated to PLA-2K and PEG, and then in the second step, Dex was conjugated to the corresponding PLA-2K-TK and PEG-TK respectively. For the conjugation of TK to PLA-2K, PLA-2K (1 g), TK (0.630 g), N-(3-Dimethylaminopropyl)-N′-ethylcarbodiimide hydrochloride (EDC, Sigma Aldrich) (0.096 g), and 4-(dimethylamino) pyridine (DMAP, Aldrich) (0.015g) were dissolved in anhydrous DCM and were simultaneously introduced into a reaction vessel maintained at 37 ºC and inert N_2 atmosphere. Final volume of DCM was adjusted to 40 mL. The reaction was run for 48 h. After reaction, the product was successively washed with 1N hydrogen chloride (HCl, Sigma Aldrich) and DI water. The product was then extracted thrice with DCM and was dried over Na_2SO_4. The polymer solution was then filtered, concentrated using a rotary evaporator, and precipitated in cold diethyl ether. The precipitate was then filtered, dried overnight in a vacuum oven, and dialysed overnight in a 3500 MWCO regenerated cellulose dialysis tube (Thermo Fischer) against acetonitrile (ACN, ACS grade, Fischer Scientific) overnight. The polymer solution was again concentrated, precipitated, filtered and dried to get PLA-2K-TK polymer.

In a similar reaction, for the conjugation of TK to PEG, m-PEG (5000 g/mole) (1 g), TK (0.5 g), EDC (0.08 g) and DMAP (0.012 g) dissolved in 40 mL anhydrous DCM were added to a reaction vessel in inert atmosphere and at 37 ºC. Reaction was then run for 48 h. After reaction, the polymer was washed with 1N HCl and DI water, extracted with DCM, dried with Na_2SO_4, filtered and precipitated in cold diethyl ether. White colour polymer was obtained which was filtered and dried overnight in vacuum oven. Polymers were then dialysed against ACN in 3500 MWCO, precipitated and dried as discussed above to get PEG-TK polymer.

In the second step, formed PLA-2K-TK and PEG-TK, each with a free TK carboxyl end group, was conjugated to the hydroxyl group of Dexamethasone through ester bond. PLA-2K-TK (0.650 g), EDC (0.065 g) and DMAP (0.010 g) were dissolved in anhydrous DCM and added to the reaction vessel at 37 ºC, N_2 atmosphere. Final volume of DCM was adjusted to 40 mL. After 1 h of stirring, Dex (0.133 g) (TCI America) dissolved in little amount of DMSO (HPLC grade, Sigma Aldrich) was added to the reaction vessel. The reaction was run for 48 h. After reaction, DCM was removed using rotary evaporator, while DMSO was removed through successive dilutions and freeze drying. After DMSO was removed, the polymer was purified as discussed above to get the PLA-TD construct. Same procedure as that of PLA-TD was employed for the synthesis of PEG-TD. PEG-TK (1g), EDC (0.08 g), and DMAP (0.012 g) were dissolved in 40 mL DCM and introduced into a reaction vessel at 37 ºC, N_2 atmosphere. After one 1 h of stirring, 0.157 g of Dex was added into the vessel and reaction was run for 48 h. Further processing of polymers after reaction was done as described before. The resultant polymer was PEG-TD

As a control system, non-ROS responsive, dicarboxylic sebacic acid (SA, Sigma Aldrich) was used and reacted in a similar way as that of TK. It was dissolved in DMSO and introduced in the reaction vessel. DMSO was removed in a method describe above. The corresponding polymers are mentioned as PLA-SD and PEG-SD.

4.2.4. Characterization of the synthesized polymers

Synthesised polymers and their corresponding constructs were confirmed using NMR (Varian). Unless mentioned, the polymers were dissolved in $CDCl_3$ (Sigma Aldrich) for NMR spectroscopy. For comparisons, the NMR spectra of TK, SA and Dex were obtained as well. Their NMR spectra were recorded in CD_3OD (Sigma Aldrich).

The mass of PEG-TD and PEG-SD was also confirmed through matrix-assisted laser desorption ionisation (MALDI) mass spectrometer. m-PEG (5000 g/mole), and PEG-TD and PEG-SD after dialysis, were dissolved in ACN at a concentration of 1 mg/ml. 1 uL of polymer solution was then mixed with 1 µL of saturated of NaCl (Sigma Aldrich) in methanol (ACS, Sigma Aldrich). The solution was then mixed with 10 µL of trans-2-[3-(4-tert-Butylphenyl)-2-methyl-2-propenylidene] malononitrile (DCTB, 10 mg/ml in DCM, Sigma Aldrich) as matrix. The solution mixture was then dropped and crystallized onto a clean and dry MALDI plate and the spectrum was acquired on ABSciex Voyager Elite MALDI MS.

4.2.5. ROS stimulated Dex release from the polymer-drug systems

ROS triggered release of Dex from the dispersed polymer systems was studied under stimulated ROS conditions with the Fenton's reagent. 1 mL, 1 mg/mL solution of PLA-TD, PLA-SD, PEG-TD and PEG-SD in DI water was incubated with 4 µL, 1M H_2O_2 (ACS, EMD Chemicals) and 40 µL, 20 mM of Fe^{+2} (ferrous sulfate heptahydrate, Sigma Aldrich) solution in 0.01 N HCl for 24 h. Dex released in the solution was monitored through HPLC over time. At the predetermined time points of 1, 3, 5, 9 and 24 h of incubation, 200 µL of solution was removed and equal volume of fresh ROS solution was added to the sample vials. Removed sample was then filtered trough 0.22 µm syringe filter and stored in -20 ºC refrigerator until HPLC analysis. HPLC analysis was done as described before using gradient elution of ACN-water solvent system through C-18 reversed phase column. Prior to HPLC analysis, 2 uL of a known concentration of benzophenone (Sigma Aldrich) was added to 50 µL of samples, including pure Dex standards, as an internal reference. 15 µL of sample was injected into the column. Analysis was done taking the ratio of the area under the peak of the sample to that of the benzophenone. Experiment was repeated in triplicates.

4.2.6. Nanoparticle formation by film hydration method

PLA-TD and PLA-SD particles was assembled into nanoparticles using film hydration method. In a typical method, known amount of PLA-TD or PLA-SD polymer was dissolved in DCM in an RBF. DCM was then removed using rotary evaporator to form a film on the RBF surface. The film was further dried overnight in a vacuum oven. DI water was then added into the RBF to make a 1mg/mL concentration of the polymer. Formed nanoparticles were further incubated at 4 ºC overnight before use.

4.2.7. Nanoparticle characterization

Size and zeta potential of the formed nanoparticles were measured using DLS. Confirmatory drug release experiment from the nanoparticles were done as described above. Precisely, ROS were generated in 1 ml, 1 mg/mL nanoparticle dispersion using Fenton's reagent. 200 uL sample was then removed at 6 and 24 h without replenishing the removed liquid. The drug elution was quantified using HPLC using Dex standards, as described above.

4.2.8. Statistics

Statistical analysis has been done using Origin (OriginLab Corporation) and Microsoft Excel. All experiments have been repeated in triplicates. Data are represented as mean ± standard error of the mean (SEM).

4.3. Results

4.3.1. Synthesis and characterization of PLA-2K block copolymer

Figure 4.1a shows the reaction scheme for the ring opening polymerization of L-lactide using m-PEG as an initiator. Synthesis of PEG-PLA (PLA-2K) block copolymer was confirmed using ^{1}H-NMR spectrum. As shown in Figure 4.2, characteristics ^{1}H-NMR PLA block peaks at 5.10 ppm (peak c) and 1.50 ppm (peak d) corresponding to -CH and -CH_3 protons respectively, confirm the synthesis of PLA block. End group analysis using the end group -CH_3 peak (peak a) of the PEG-PLA block copolymer and either of the PLA peaks (peak c or peak d) gave a degree of polymerization, DP_n of 27 for the PLA block and a corresponding number average molecular weight, M_n of 1500 g/mole. As a result, overall molecular weight of the PLA-2K block copolymer was taken to be around 3500 g/mole.

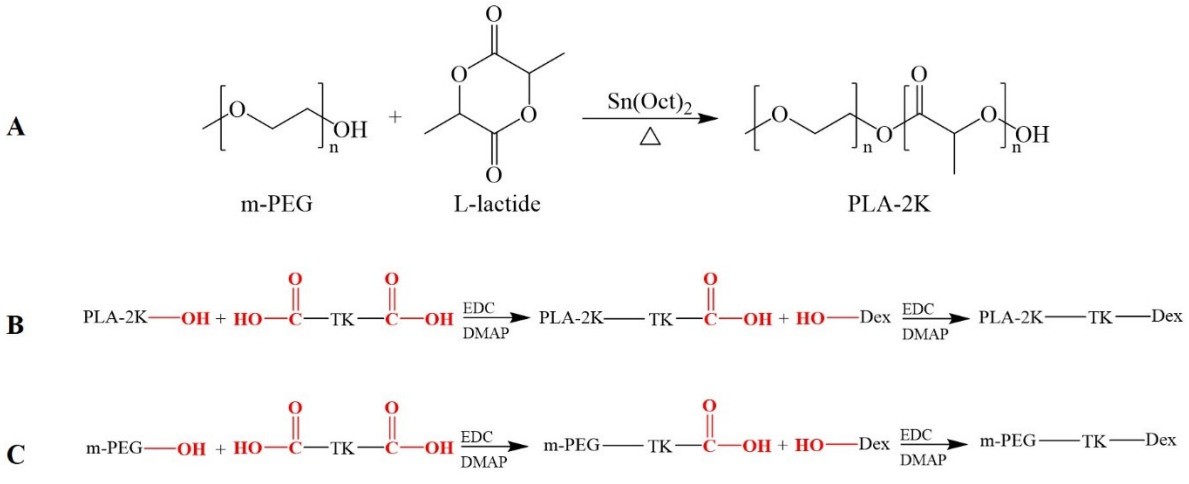

Figure 4.1. Reaction scheme for the synthesis of PLA-2K, PLA-TD and PEG-TD. A) Ring opening polymerization of L-lactide using m-PEG as an initiator; B) reaction scheme for the synthesis of PLA-TD, and C) reaction scheme for the synthesis of PEG-TD.

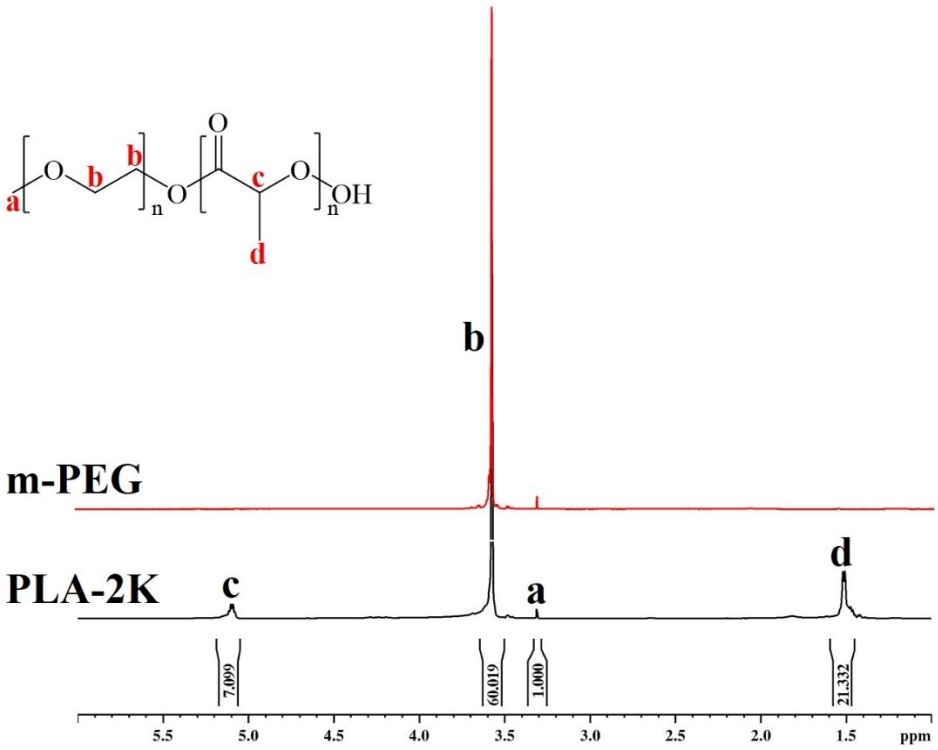

Figure 4.2. ^{1}H-NMR of m-PEG and PEG-PLA block copolymer in $CDCl_3$. Peaks 'a' at 3.31 ppm and 'b' at 3.57 ppm corresponds to -CH_3 and -CH_2 protons in the PEG block, while peaks 'c' and 'd' at 5.10 ppm and 1.50 ppm corresponds to -CH and -CH_3 peaks of PLA block. Peak integral for the end group peak 'a' vs that of PLA block peak 'c' or 'd' gave a DP_n of 27 for the PLA block, corresponding to PLA M_n of 1500 g/mole.

4.3.2. Synthesis and characterization of PLA-TD and PLA-SD polymer constructs

PLA-TD and PLA-SD were synthesized in a two-step process. A representative reaction scheme is shown in Figure 4.1B. In the first step, one of the carboxylic end group of bifunctional TK or SA was conjugated to the hydroxyl group of the PLA-2K block copolymer to form PLA-2K-TK or PLA-2K-SA intermediates, respectively. Figure 4.3B shows the ^{1}H-NMR of PLA-2K-TK. Comparing the ^{1}H-NMR spectrum of PLA-2K-TK with that of PLA-2K (Figure 4.3A), emergence of new peaks at 2.82 ppm and 2.57 ppm (shown by arrow) is observed. These peaks correspond to the characteristic peaks of TK (Figure 4.4A). These data therefore confirm the successful conjugation of TK to PLA-2K. In the next step of synthesis, the free carboxyl group of PLA-2K-

TK was conjugated to the hydroxyl group of Dex through ester bond, to form PLA-TD (Figure 4.1B). Figure 4.3C shows the ^{1}H-NMR spectrum of PLA-TD. Comparing the ^{1}H-NMR spectrum of PLA-TD with that of PLA-2K-TK (Figure 4.3B), new peaks at 6.26 ppm and 6.04 ppm (shown by arrow), which are characteristic peaks of Dex (Figure 4.4C), is observed. This data therefore confirms the successful synthesis of PLA-TD system.

Similar to PLA-TD, PLA-SD was synthesized in two steps, except TK was replaced by non-ROS responsive SA. Figure 4.5B shows the ^{1}H-NMR spectrum of PLA-2K conjugated to SA. NMR peaks at 2.25 ppm and 1.25 ppm (marked by arrow), which are characteristic SA peaks (Figure 4.4B), confirm the synthesis of PLA-2K-SA. Figure 4.5C shows the ^{1}H-NMR spectrum of PLA-SD, with characteristic Dex peaks at 6.26 and 6.04 ppm, confirming the successful synthesis of non-ROS responsive control PLA-SD.

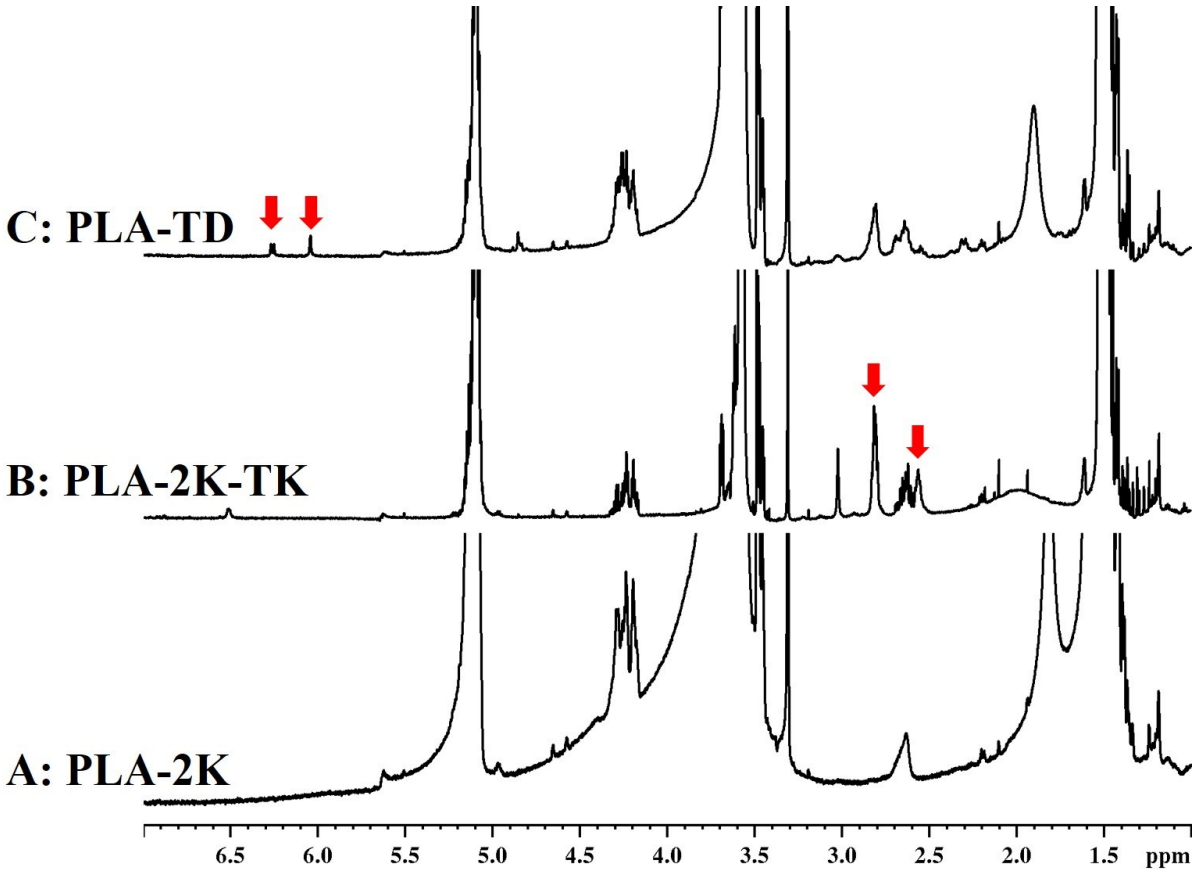

Figure 4.3. ^{1}H-NMR spectrum of PLA-TD and its intermediates. A) PLA-2K, B) PLA-2K-TK, and C) PLA-TD. The spectra were recorded in $CDCl_3$. Arrows in B and C shows the respective addition of TK and Dex.

4.3.3. Synthesis and characterization of PEG-TD and PEG-SD polymeric constructs

Like PLA-TD/PLA-SD systems, PEG-TD/PEG-SD were synthesized in a two-step process (Figure 4.1C). Comparing Figure 4.6B with 4.6A, the emergence of characteristics TK peaks at 2.82 and 2.57 ppm in PEG-TK confirms successful conjugation of TK to PEG. Further, as compared to Figure4.6B, Figure 4.6C shows two new peaks at 6.26 and 6.04 ppm corresponding to Dex, thus confirming successful synthesis of PEG-TK construct. Similarly, Figure 4.7B shows the ^{1}H-NMR of the formed PEG-SA polymer with characteristic SA peaks at 2.25 ppm, 1.57 ppm and 1.25 ppm. In Figure 4.7C, the characteristic Dex peaks at 6.26 and 6.04 ppm confirms the

conjugation of Dex to PEG-SA in the second step of synthesis, and hence confirms the successful synthesis of PEG-SD.

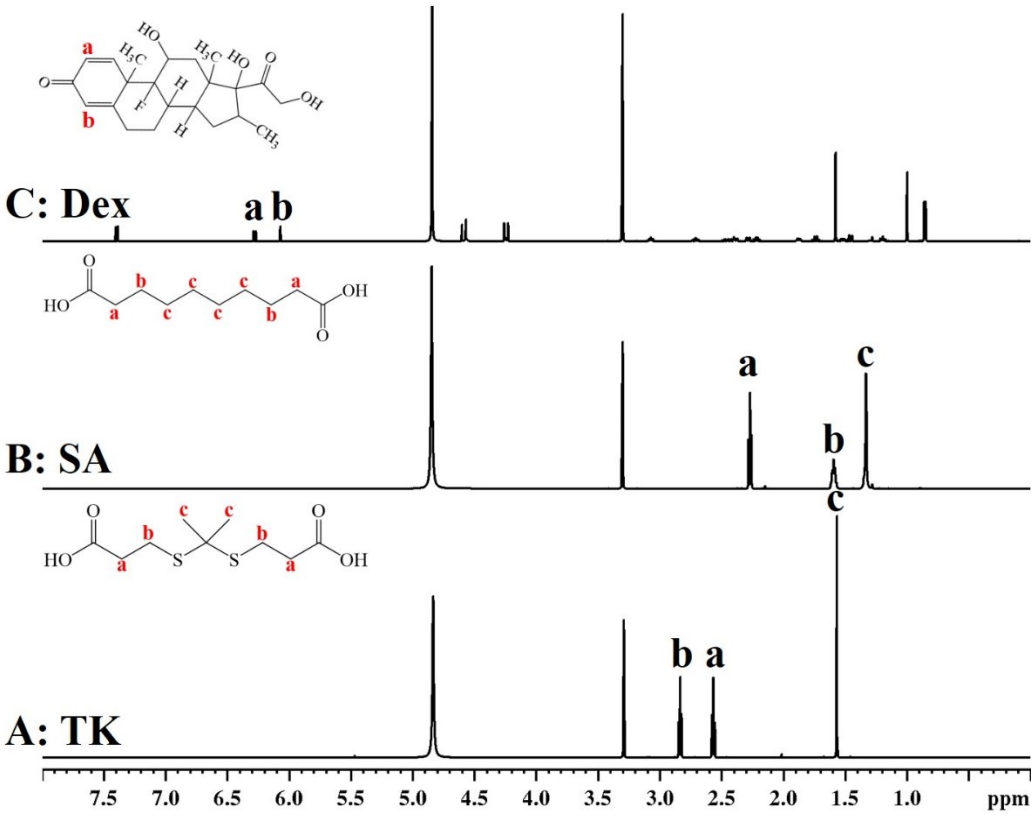

Figure 4.4. ^{1}H-NMR spectrum of A) TK, B) SA, and C) Dexamethasone. The spectra were recorded in CD_3OD.

The mass of the synthesized PEG-TD and PEG-SD were also confirmed using MALDI-TOF mass spectrometer. As shown in Figure 4.8, A m/z shift of 608 is observed in PEG-TD (Figure 4.8B) which corresponds to the successive addition of TK and Dex to the end of PEG chain (Figure 4.8A). Taking a representative m/z of 5079 on PEG (Figure 4.8A), a corresponding m/z of 5687 is observed on PEG-TD (Figure 4.8B). Similarly, a m/z shift of 558 is seen on PEG-SD (Figure 4.8C), which corresponds to the successive addition of SA and Dex to PEG chain. Taking the

representative m/z of 5079 on PEG, a m/z of 5637 on PEG-SD confirms the formation of PEG-SD. These data along with the NMR confirms the synthesis of PEG-TD and PEG-SD polymers.

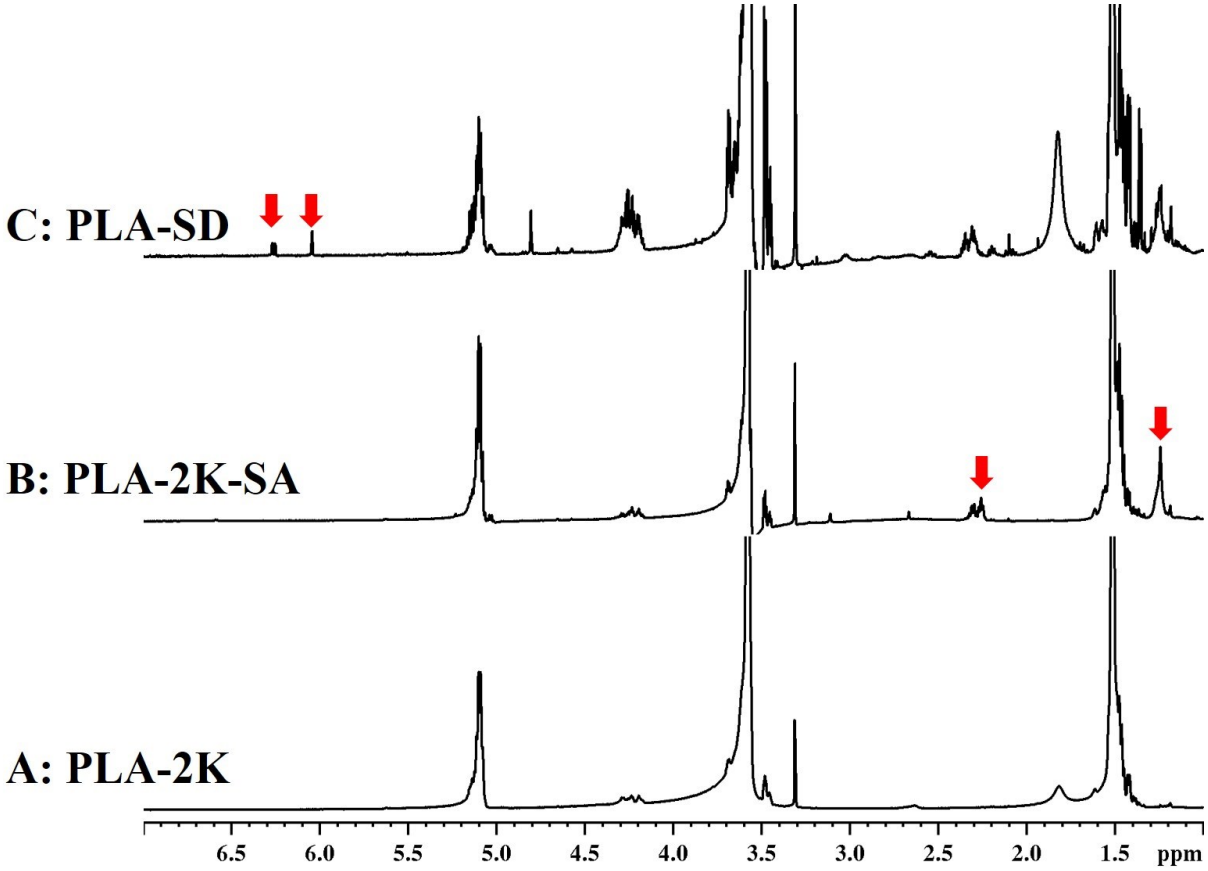

Figure 4.5. ^{1}H-NMR spectrum of PLA-SD and its intermediates. A) PLA-2K, B) PLA-2K-SA, and C) PLA-SD. The spectra were recorded in $CDCl_3$. Arrows in B and C shows the respective addition of SA and Dex.

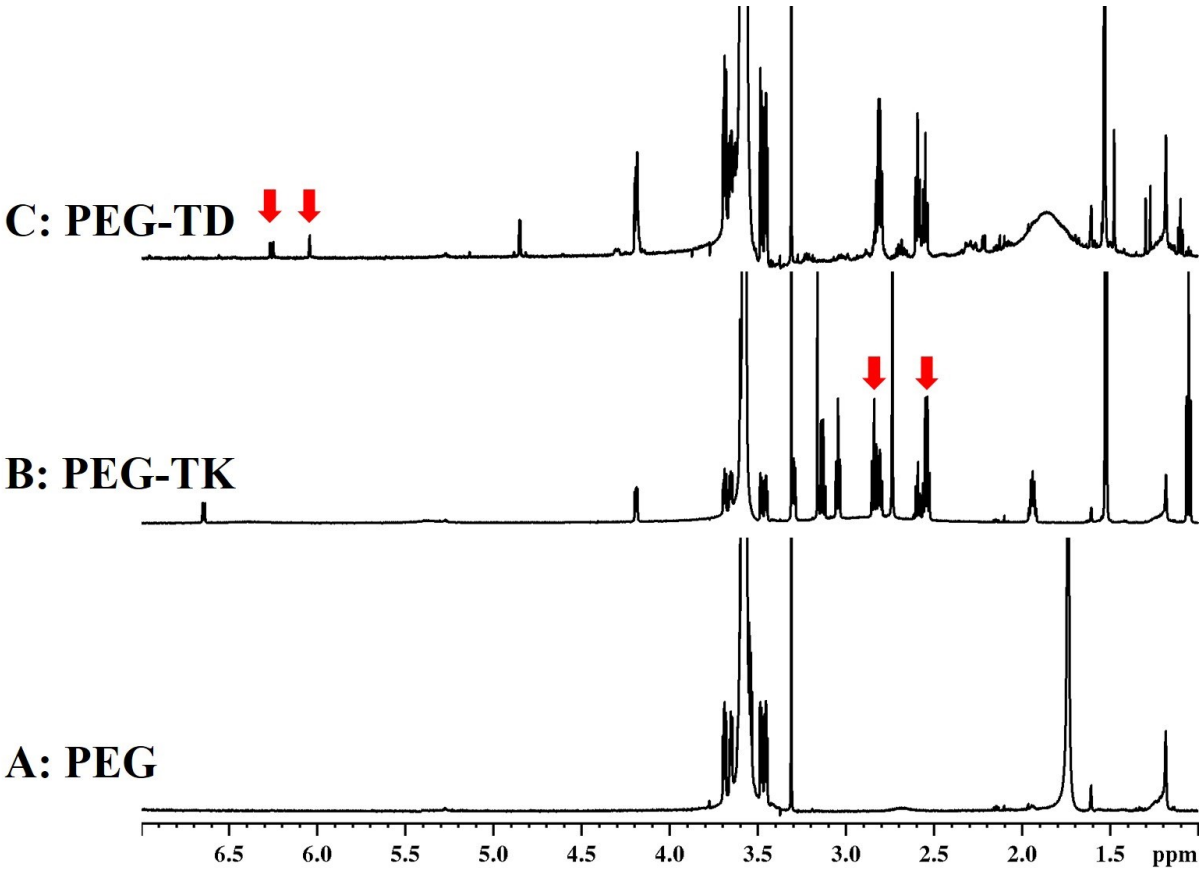

Figure 4.6. ^{1}H-NMR spectrum of PEG-TD and its intermediates. A) PEG, B) PEG-TK, and C) PEG-TD. The spectra were recorded in $CDCl_3$. Arrows in B and C shows the respective addition of TK and Dex.

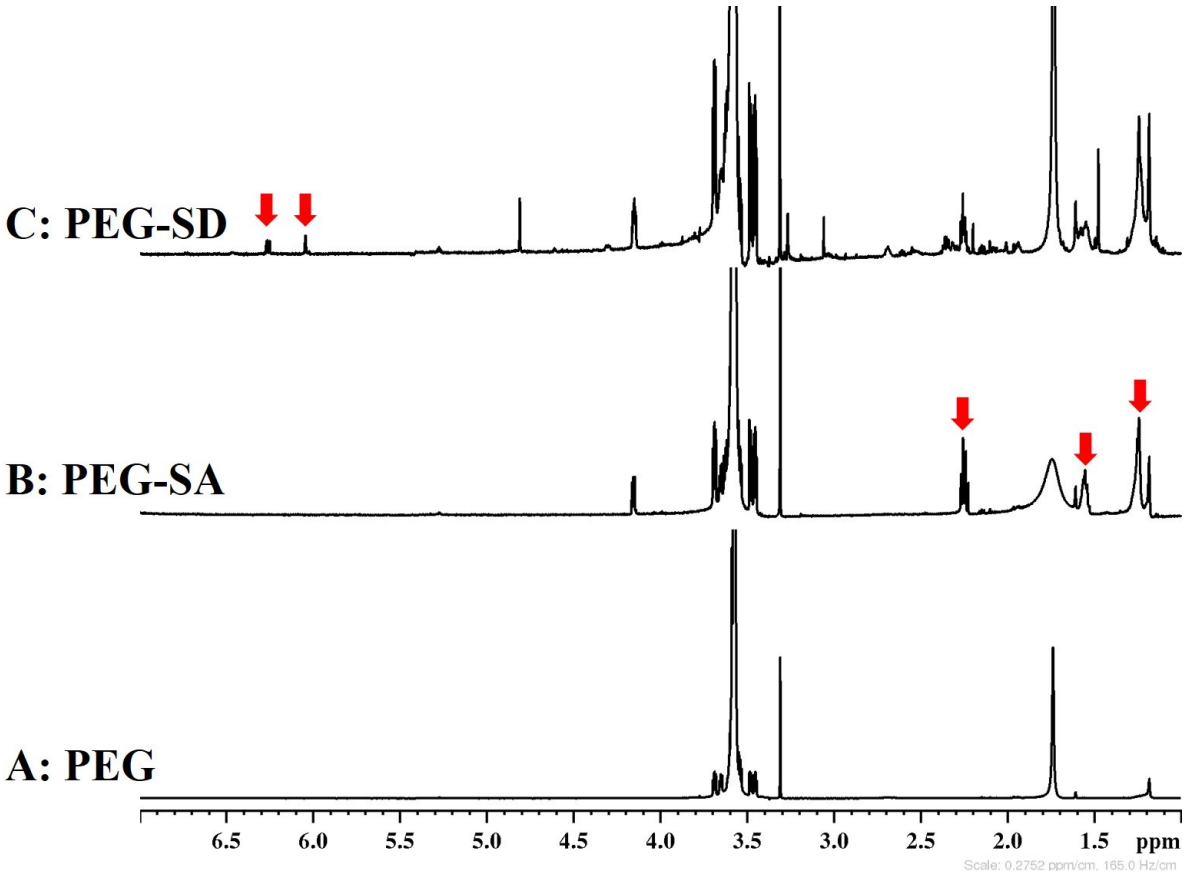

Figure 4.7. ^{1}H-NMR of PEG-SD and its intermediates. A) PEG, B) PEG-SA, and C) PEG-SD. The spectra were recorded in $CDCl_3$. Arrows in B and C shows the respective addition of SA and Dex.

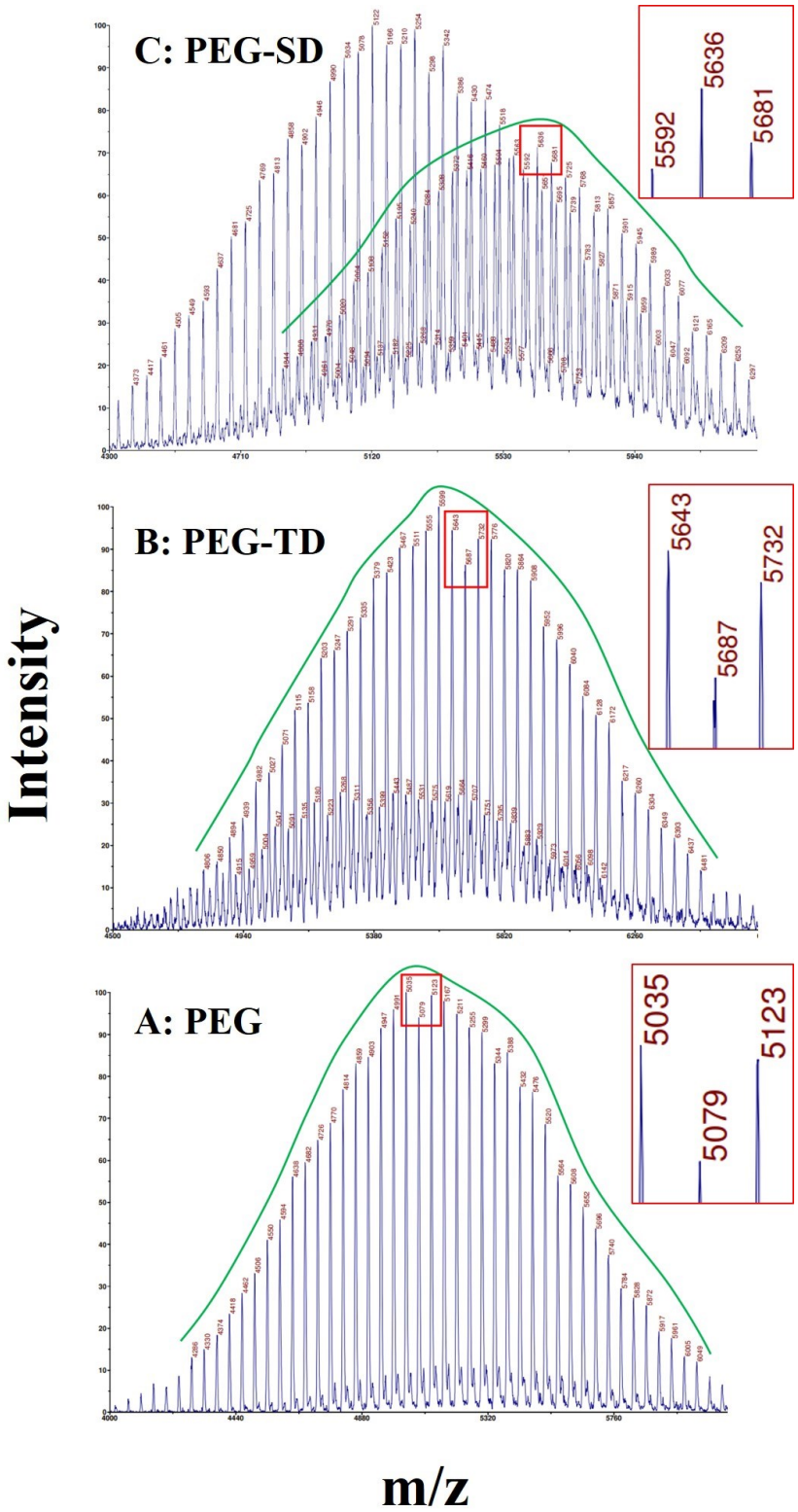

Figure 4.8. MALDI-TOF m/z spectra for A) PEG, B) PEG-TD, and C) PEG-SD. m/z of the respective polymer constructs have been highlighted with a curve. With respect to PEG, a m/z shift of 608 and 558 in observed in PEG-TD and PEG-SD respectively.

4.3.4. ROS stimulated Dex release from the polymer systems.

ROS stimulated release of Dex from the polymeric systems was studied. Polymer dispersion was subjected to Fenton's reagent and Dex release monitored using HPLC over time. Figure 4.9A and Figure 4.9B shows the HPLC elution of the release media of PLA-TD and PLA-SD respectively, from different time points. As time increased, the area under the elution peak at ~ 5.7 min increased (Figure 4.9A). However, no such peak was apparent for PLA-SD (Figure 4.9B). To identify the mass of the eluting compound, the sample was run on mass spectrometer using same column and at solvent gradient profile. As shown in Figure 4.10, the m/z for the eluting compound was found to be 529, which belongs to the cleaved Dex which has undergone oxidation in the presence of H_2O_2 (Figure 4.10, reaction scheme). The peak at time ~ 8.6 min corresponds to free Dex. Dex released were further quantified using Dex standards and cumulative release is shown in Figure 4.11A. Mean Dex released at 1, 3, 5, 9 and 25 h are 0 (undetectable by HPLC), 0.4, 1, 1.8 and 2 nmole respectively.

Similarly, Figure 4.9B and 9C shows the HPLC chromatogram of the Dex released from the PEG-TD and PEG-SD systems. As expected, PEG-SD did not show any Dex release. Cumulative Dex release from the PEG-TD dispersion has been shown in Figure 4.11B. Mean Dex released at 1, 3, 5, 9 and 25 h are 8.3, 12.3, 14.6, 16.6 and 18 nmole respectively (Figure 4.11B).

4.3.5. Nanoparticle formation and Dex release

Nanoparticles were formed out of PLA-2K, PLA-TD and PLA-SD polymers using film hydration method. The size and zeta potential of the nanoparticle were evaluated using DLS. The sizes of the nanoparticles were found to be 132.8 ± 21.6, 14.2 ± 2 and 11.9 ± 60 respectively (Figure 4.12A), while their respective zeta potentials were -5.38, -0.8 and -2.28 mV. To confirm that ROS

activity is preserved upon nanoparticle formation, PLA-TD and PLA-SD particles were subjected to ROS and Dex released was measured at 6 and 24 h. As shown in Figure 4.12B, the concentration of Dex released in the release media increased from 7.5 ± 0.37 μM at 6 h to 9 ± 0.37 μM at 24 h. However, the concentration of free Dex remained constant at 6.4 ± 0.2 and 6.13 ± 0.1 μM at 6 and 24 h respectively.

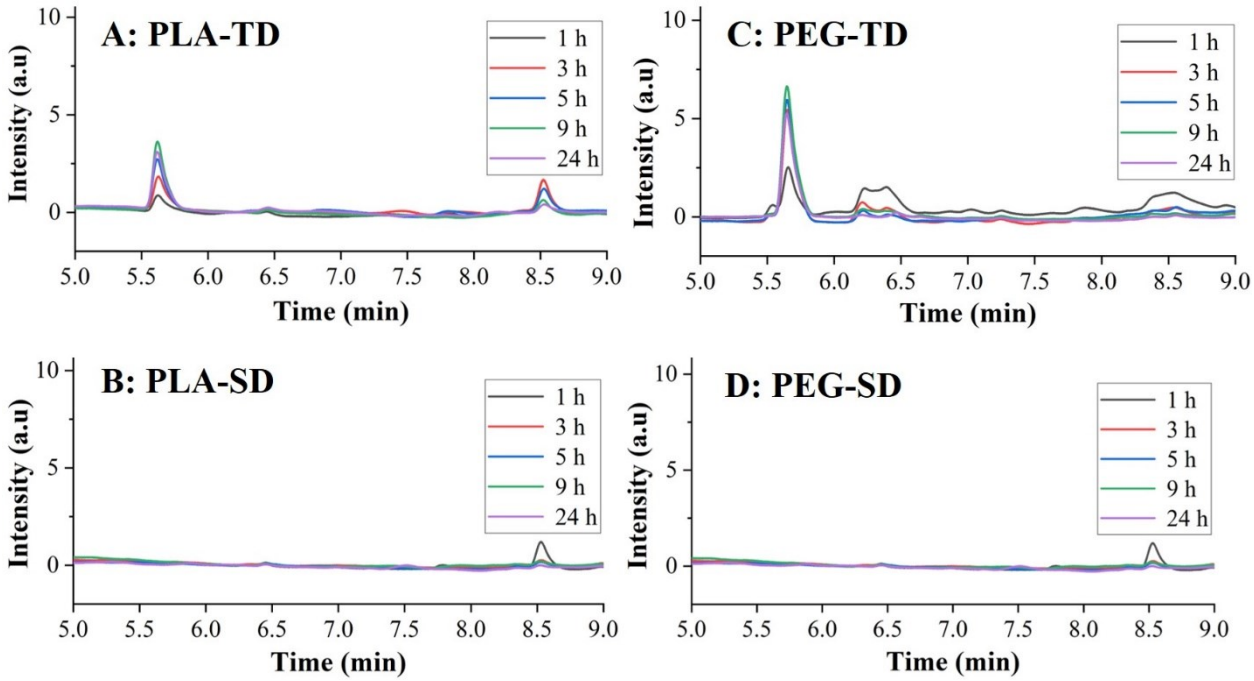

Figure 4.9. HPLC elution of cleaved Dex in medium at various time points. A) corresponds to PLA-TD, and C) corresponds to PEG-TD. The peak at t ~ 5.7 min corresponds to released Dex. While the peak at ~ 8.6 corresponds to free Dex. B) corresponds to PLA-SD control and D) corresponds to PEG-SD. SA being the non ROS responsive linker, these construct do not show any Dex release.

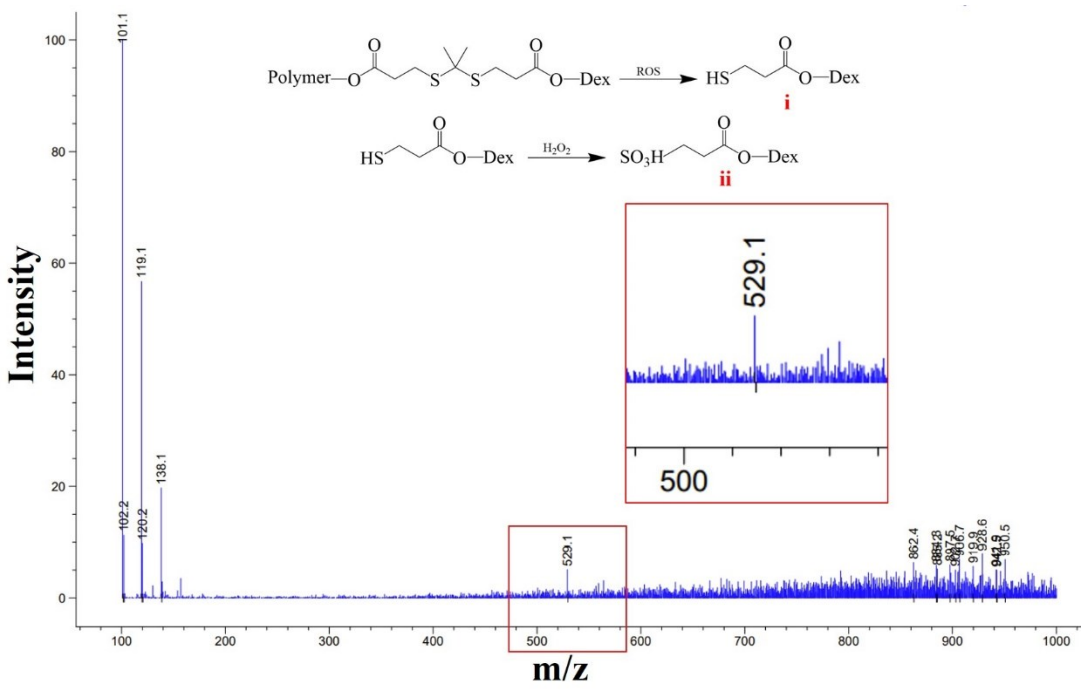

Figure 4.10. Mass spectrum of cleaved Dex. Dex is released from the polymer-Dex conjugate with an active -SH group (Compound i). Thiol group is however prone to oxidation in the presence of H_2O_2 and hence get oxidised to its sulfonic acid derivative (Compound ii). An m/z peak of 529 corresponds to the corresponding M+H peak in the +ve scan mode. The mass spectrum was averaged between the times 5.6 – 5.7 min which was the elution time for the released Dex.

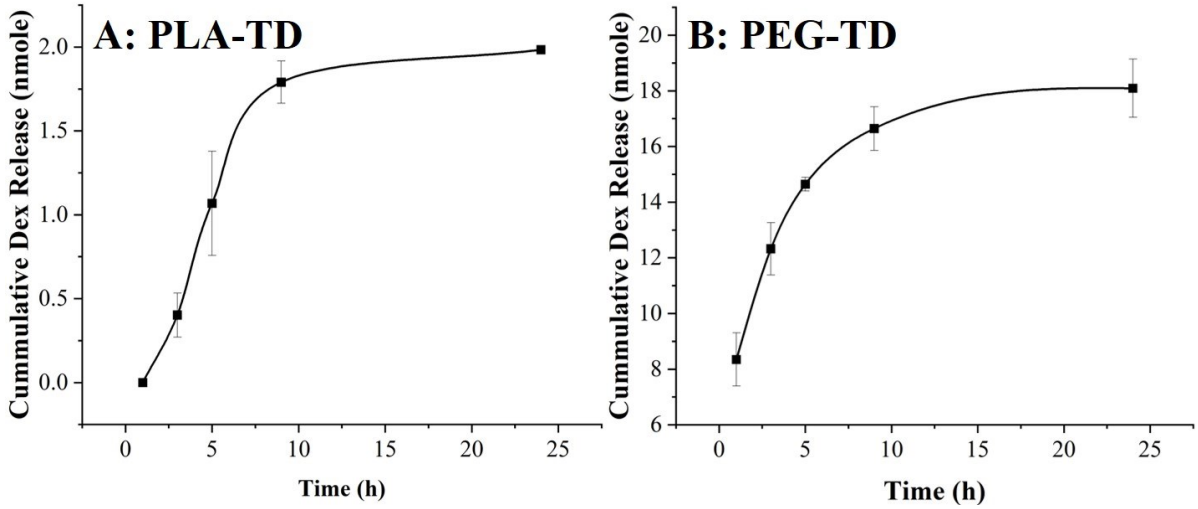

Figure 4.11. Cumulative release of cleaved Dex. Cumulative Dex released from the A) PLA and B) PEG-TD polymer constructs. Area under the curve for the released Dex was quantified using Dex standards. Data is represented as Mean ± SEM. Free Dex was released within the 1st h of ROS incubation. Free Dex released from the PLA-TD polymer stood 1.13 ± 0.3 nmole. Free Dex from PLA-SD was only detected in one experimental repeat and stood at 0.15 nmole.

Similarly, free Dex from PEG-TD was also detected in only one of the experimental repeats with an amount of 6.6 nmole. No free Dex was detected in PEG-SD samples.

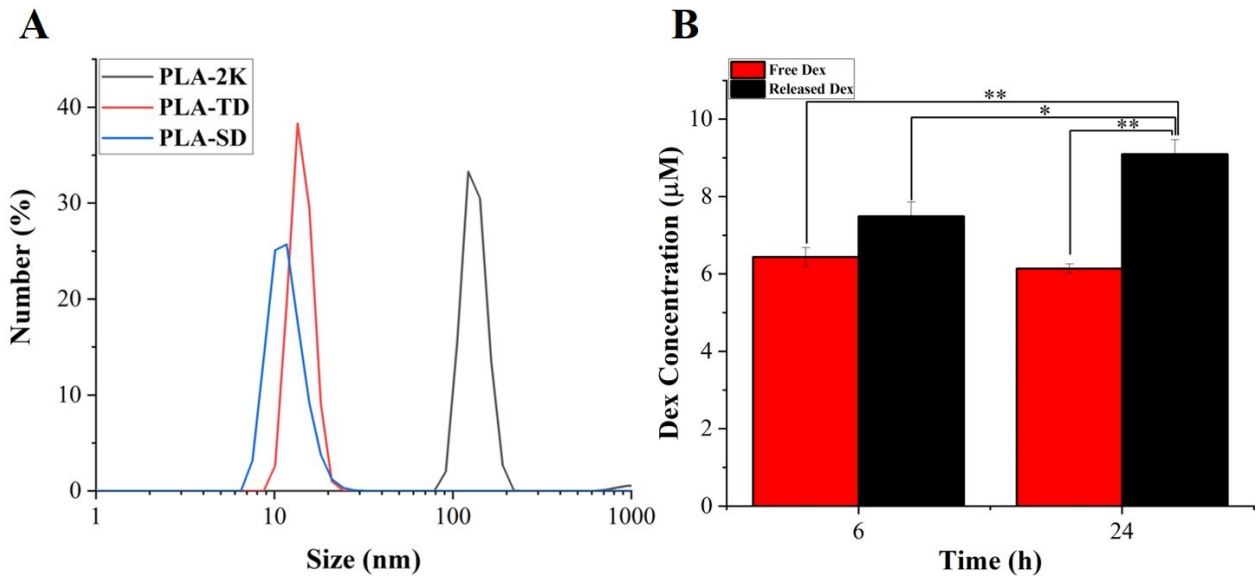

Figure 4.12. Characterization of nanoparticles. A) Number distribution of PLA-2K, PLA-TD and PLA-SD nanoparticles as detected by DLS. B) Dex released from PLA-TD nanoparticles in ROS environment. Data are represented as mean ± SEM. Mean was compared between the data set. * represents $p \leq 0.05$, ** represents $p < 0.005$. No significance was assigned at $p \geq 0.05$.

4.4. Discussion

PEG-PLA based polymer systems are the first-line biocompatible polymeric material for biomedical application [25]. The polymer system however lacks bioresponsiveness and efforts have been made to impart bioresponsiveness through the inclusion of stimuli responsive moieties into the polymer constructs [26]. Herein, PEG-PLA block copolymer and PEG were conjugated with ROS responsive TK molecule; and then, the bioresponsive constructs were used to design inflammatory targeted delivery platform for the administration of anti-inflammatory Dex. In the previous chapter it was shwon that TK can be easily synthesized, is non-toxic and shows effectiveness in scavenging ROS both *in vitro* and in *in vivo* systems. In the present study, the applicability of TK in therapeutic formulations in shown.

PEG-PLA block copolymer was synthesized through the ring opening polymerization (ROP) of l-lactide using m-PEG as an initiator and $(Sn(Oct)_2$ as a catalyst. The ROP is considered to be controlled polymerization technique where DP_n is about equal to the ratio of the concentration of the monomer to that of initiator [27]. For a targeted PLA block of weight 2000 g/mole, a 14-mole equivalent of L-lactide was reacted to 1 mole equivalent of m-PEG. The NMR result however showed that the weight of the PLA block was 1500 g/mole. The discrepancy in the theoretical and the experimental PLA block length could be due the high viscosity of the resultant polymer melt. The increasing chain length could have restricted further propagation of polymerization.

Since ROS is a hallmark of various inflammatory diseases, PEG-PLA platform was used to develop a ROS responsive delivery system for the delivery of Dex to the ROS extensive inflamed tissue microenvironment. A ROS cleavable PEG conjugate of Dex was also synthesized. Diacid TK was successfully attached to the terminal –OH group of the PEG-PLA and PEG polymers through one its the -COOH group, while the other -COOH was used to attach an anti-inflammatory Dex (Figure 4.1B, C). The synthesis resulted in the formation of ROS responsive PLA-TD and PEG-TD systems. The ROS based Dex release from both PLA-TD and PEG-TD systems was then studied. Under exogenous ROS, both PEG-PLA and PEG systems showed biphasic Dex release (Figure 4.11). An expediated release was observed until 5 h, which was then followed by a sustained release. The cumulative Dex released by the PLA-TD at 24 h was 9-fold less than that of PEG-TD. This could be explained on the basis of amphiphilicity of systems. Both PLA-TD and PEG-TD, because of their amphiphilic nature (PLA-DEX and Dex being the respective hydrophobic domains) would self assemble into a micelle. However, the hydrophobic domain of PLA-TD is stronger than that of PEG-TD and thus the hydrophobic core of PLA-TD would be more strongly held than that of PEG-TD. This would therefore restrict the access of ROS molecule

to the cleavage site and vis a vis slows the diffusion of Dex into the solution, resulting in low Dex release.

Next, nanoparticles were formed of the PEG-PLA system using film hydration method. Nanoparticles formed by PLA-TD and PLA-SD were smaller than those formed by PLA-2K (132.8 nm for PLA-2K vs 14.2 nm for PLA-TD and 11.9 nm for PLA-SD). This is due to the stronger hydrophobic interaction between the Dex molecules in the core, which is absent in PLA-2K particles. The zeta potentials for PLA-TK, PLA-TD and PLA-SD were found to be -ve (-5.38, -0.8 and -2.28 mV respectively) which are characteristics of PEG shell [28]. The nanoparticles formed by film hydration method were subjected to Fenton's reagent and Dex released was confirmed through HPLC (Figure 4.12B). Dex released by the nanoparticles (9 nmole) in 24 h was greater than those released by a mere dispersion (2 nmole) in Figure 4.11A. This is due to the regular removal of solution in case of Figure 4.11A which simultaneous results in loss of nanoparticle from the solution.

PEG-PLA copolymers are widely used to encapsulate hydrophobic drug in its core [25]. The conjugation of PEG to a hydrophobic domain imparts amphiphilicity to the construct. PEG conjugation also restricts the immune response against the polymer nano-assembly and thereby increases the blood circulation time of the drug-laden nanoparticles [29]. Dex stands at the forefront of anti-inflammatory treatments, however, its poor solubility and side effects often entails the support of a drug carrier for its regulated delivery [30,31]. Dexamethasone was loaded into PLGA micro-particles to study the mechanism and release in vitro. It was shown that by varying the loaded drug, the rate and pattern of release could be modulated. Low drug loading showed controlled release, while high drug loading showed a triphasic Dex release profile - burst release followed by a controlled phase, and finally an expedited final release [32]. Another polyester based

amphiphilic system that has been used to deliver Dex is that of PEG-Polycaprolactone (PEG-PCL). Dex was encapsulated in to its hydrophobic core to target autoimmune rheumatoid arthritis. *In vitro* results showed a slow and sustained Dex release from the polymer micelles, accounting for only 50% of encapsulated Dex in 3 days. The slow release of Dex increased the bioavailability of the drug to the targeted tissue, and decreased toxicity. Further, the long circulation time increased the availability to the inflamed joints as seen in the arthritic rat models [30].

Another strategy that has been used to regulate the Dex release is by incorporating Dex into a matrix. PLGA-PEG-PLGA tri-block copolymer was designed such that it remained in solution phase at room temperature but formed a gel at body temperature of 37 ^{o}C. The gel exhibited a sustained release of Dex, which lasted for 10 days. The release profile, like Dex encapsulated self assemblies, was dependent on the drug loading. Dex laden polymer solution was administered to the vitreous of a rabbit eye. Dex incorporated gel was retained until 11 days as opposed to normal solution which was rapidly cleared. Dex released from the hydrogels were slow and remained above the effective concentration until 9 days of administration [33]. Furthermore, a strategy combining drug loaded nanoassembly and its incorporation in a gel matrix has also been studied. Dex loaded PLGA nanoparticles were embedded in to a thermos-responsive gel made up of Poloxamer. By doing this, the initial *in vitro* burst release was controlled such that only 20% and 46% of loaded drug was released within 1 and 24 h respectively [34].

In comparison to encapsulation, conjugation offers a better control over release profile. In this regard, polysaccharides have been widely used as they offer an abundance of free functional groups, which could be used to conjugate Dex into the structure [35]. Dex was conjugated onto the glycol modified chitosan which could self assemble into nanoparticles. *In vitro* drug release studies showed a faster release till 8 h which was followed by the control release till the next 48 h

resulting in 80% of the drug release [36]. Delivery strategies discussed so far are governed primarily by the diffusion of drug due to weakening of the polymer nanoassembly, swelling [32], hydrolysis [36] or polymer degradation, and hence they are not effective in targeting a specific diseased tissue based on local cues, unless specifically administered, for example in the vitreous of the eye [33], implantation of a drug incorporated fibers [37], or simultaneous loading of Dex with the insulin secreting islet cells during islet transplantation [38]. These may seem feasible for easily accessible tissues, but it will be a challenge to localize them to internal organs. In the context, stimuli responsive systems will prove to be helpful.

In an effort to localize Dex into the posterior segment of the eye, peptide substrate for a transporter protein was exposed onto Dex loaded Chitosan based micelle [39]. A pH responsive Dex delivery system was developed using the commercially available methacrylate polymers and cellulose based polymers for delivery into skin inflammations. At the slightly acidic pH of the skin, the nanoparticles swelled to release the loaded drug. The drug release was primarily a function of dissolution and swelling of nanoparticles at their effective pH [40]. With the recent advancement in the design of ROS responsive molecules, Dex delivery systems prone to release in ROS extensive environment has also been explored. Dexamethasone was encapsulated into the multi-shell core of nanocarriers, the hydrophobic domain of which contained sulphur in its structure. Oxidation of sulphur in oxidative environment transformed the hydrophobic domain into a hydrophilic domain, triggering the release of encapsulated Dex [41]. Similarly, ROS responsive TK was used in a micellar structure to destabilized the micelle in ROS environment, and cause a subsequent release of loaded Dex [42].

A direct comparison of the stimuli responsive system discussed above with that of the developed PLA-TD system in this study shows that the mechanism involved in drug release could be well

regulated for PLA-TD. The release of Dex would be very selective and highly sensitive to ROS environment. Further, the diffusion kinetics for the release of cleaved drug can also be optimized to confer dual control over release profile. Thus, PLA-TD developed in the study will prove to be an excellent formulation for inflammation targeted delivery of anti-inflammatory Dex.

4.5. Conclusion

In conclusion, ROS responsive Dex releasing system for varied therapeutic applications is shown. Dex is a most commonly used anti-inflammatory drug, however it is often associated with unwanted side effects. The system engineered here will allow for the slow and controlled release of Dex into the diseased tissue microenvironment, thereby avoiding the harmful side effects of the otherwise highly therapeutic drug.

4.6. References

[1] I.-T. Lee, C.-M. Yang, Role of NADPH oxidase/ROS in pro-inflammatory mediators-induced airway and pulmonary diseases, Biochemical Pharmacology. 84 (2012) 581–590.

[2] J.M. Barra, H.M. Tse, Redox-dependent inflammation in islet transplantation rejection, Frontiers in Endocrinology. 9 (2018) 175.

[3] E.J. Swindle, D.D. Metcalfe, The role of reactive oxygen species and nitric oxide in mast cell-dependent inflammatory processes, Immunological Reviews. 217 (2007) 186–205.

[4] C. Kohchi, H. Inagawa, T. Nishizawa, G.-I. Soma, ROS and innate immunity, Anticancer Research. 29 (2009) 817–821.

[5] E. Shekhova, Mitochondrial reactive oxygen species as major effectors of antimicrobial immunity, PLoS Pathogens. 16 (2020) e1008470.

[6] M.D. Kraaij, S.W. van der Kooij, M.E.J. Reinders, K. Koekkoek, T.J. Rabelink, C. van Kooten, K.A. Gelderman, Dexamethasone increases ROS production and T cell suppressive capacity by anti-inflammatory macrophages, Molecular Immunology. 49 (2011) 549–557.

[7] H. Blaser, C. Dostert, T.W. Mak, D. Brenner, TNF and ROS crosstalk in inflammation, Trends in Cell Biology. 26 (2016) 249–261.

[8] H.-U. Simon, A. Haj-Yehia, F. Levi-Schaffer, Role of reactive oxygen species (ROS) in apoptosis induction, Apoptosis. 5 (2000) 415–418.

[9] N.R. Barshes, S. Wyllie, J.A. Goss, Inflammation-mediated dysfunction and apoptosis in pancreatic islet transplantation: implications for intrahepatic grafts, Journal of Leukocyte Biology. 77 (2005) 587–597.

[10] G. Saravanakumar, J. Kim, W.J. Kim, Reactive-Oxygen-Species-Responsive Drug Delivery Systems: Promises and Challenges, Advanced Science. 4 (2017). https://doi.org/10.1002/advs.201600124.

[11] M.K. Gupta, T.A. Meyer, C.E. Nelson, C.L. Duvall, Poly (PS-b-DMA) micelles for reactive oxygen species triggered drug release, Journal of Controlled Release. 162 (2012) 591–598.

[12] P. Han, N. Ma, H. Ren, H. Xu, Z. Li, Z. Wang, X. Zhang, Oxidation-responsive micelles based on a selenium-containing polymeric superamphiphile, Langmuir. 26 (2010) 14414–14418.

[13] W. Cao, Y. Gu, T. Li, H. Xu, Ultra-sensitive ROS-responsive tellurium-containing polymers, Chemical Communications. 51 (2015) 7069–7071.

[14] D.S. Wilson, G. Dalmasso, L. Wang, S. v Sitaraman, D. Merlin, N. Murthy, Orally delivered thioketal nanoparticles loaded with TNF-α–siRNA target inflammation and inhibit gene expression in the intestines, Nature Materials. 9 (2010) 923–928.

[15] Y. Liu, Y. Liu, J. Zang, A.A.I. Abdullah, Y. Li, H. Dong, Design strategies and applications of ROS-responsive phenylborate ester-based nanomedicine, ACS Biomaterials Science & Engineering. 6 (2020) 6510–6527.

[16] C. Wei, Y. Zhang, H. Xu, Y. Xu, Y. Xu, M. Lang, Well-defined labile diselenide-centered poly (ε-caprolactone)-based micelles for activated intracellular drug release, Journal of Materials Chemistry B. 4 (2016) 5059–5067.

[17] B. Liu, S. Thayumanavan, Mechanistic Investigation on Oxidative Degradation of ROS-Responsive Thioacetal/Thioketal Moieties and Their Implications, Cell Reports Physical Science. 1 (2020) 100271.

[18] P.J. Barnes, How corticosteroids control inflammation: quintiles prize lecture 2005, British Journal of Pharmacology. 148 (2006) 245–254.

[19] A.E. Coutinho, K.E. Chapman, The anti-inflammatory and immunosuppressive effects of glucocorticoids, recent developments and mechanistic insights, Molecular and Cellular Endocrinology. 335 (2011) 2–13.

[20] M. Kadmiel, J.A. Cidlowski, Glucocorticoid receptor signaling in health and disease, Trends in Pharmacological Sciences. 34 (2013) 518–530.

[21] A.J. Giles, M.-K.N.D. Hutchinson, H.M. Sonnemann, J. Jung, P.E. Fecci, N.M. Ratnam, W. Zhang, H. Song, R. Bailey, D. Davis, Dexamethasone-induced immunosuppression: mechanisms and implications for immunotherapy, Journal for Immunotherapy of Cancer. 6 (2018) 1–13.

[22] K. Yamada, H. Sato, K. Sakamaki, M. Kamada, Y. Okuno, N. Fukuishi, K. Furuta, S. Tanaka, Suppression of IgE-independent degranulation of murine connective tissue-type mast cells by dexamethasone, Cells. 8 (2019) 112.

[23] M.V.M. Andrade, T. Hiragun, M.A. Beaven, Dexamethasone suppresses antigen-induced activation of phosphatidylinositol 3-kinase and downstream responses in mast cells, The Journal of Immunology. 172 (2004) 7254–7262.

[24] B.D. McNeil, P. Pundir, S. Meeker, L. Han, B.J. Undem, M. Kulka, X. Dong, Identification of a mast-cell-specific receptor crucial for pseudo-allergic drug reactions, Nature. 519 (2015) 237–241. https://doi.org/10.1038/nature14022.

[25] R.Z. Xiao, Z.W. Zeng, G.L. Zhou, J.J. Wang, F.Z. Li, A.M. Wang, Recent advances in PEG–PLA block copolymer nanoparticles, International Journal of Nanomedicine. 5 (2010) 1057.

[26] J. Li, C. Sun, W. Tao, Z. Cao, H. Qian, X. Yang, J. Wang, Photoinduced PEG deshielding from ROS-sensitive linkage-bridged block copolymer-based nanocarriers for on-demand drug delivery, Biomaterials. 170 (2018) 147–155. https://doi.org/10.1016/j.biomaterials.2018.04.015.

[27] O. Dechy-Cabaret, B. Martin-Vaca, D. Bourissou, Controlled ring-opening polymerization of lactide and glycolide, Chemical Reviews. 104 (2004) 6147–6176.

[28] R. Ghasemi, M. Abdollahi, E. Emamgholi Zadeh, K. Khodabakhshi, A. Badeli, H. Bagheri, S. Hosseinkhani, mPEG-PLA and PLA-PEG-PLA nanoparticles as new carriers for delivery of recombinant human Growth Hormone (rhGH), Scientific Reports. 8 (2018) 1–13.

[29] R. Gref, M. Lück, P. Quellec, M. Marchand, E. Dellacherie, S. Harnisch, T. Blunk, R.H. Müller, 'Stealth'corona-core nanoparticles surface modified by polyethylene glycol (PEG): influences of the corona (PEG chain length and surface density) and of the core composition on phagocytic uptake and plasma protein adsorption, Colloids and Surfaces B: Biointerfaces. 18 (2000) 301–313.

[30] Q. Wang, J. Jiang, W. Chen, H. Jiang, Z. Zhang, X. Sun, Targeted delivery of low-dose dexamethasone using PCL–PEG micelles for effective treatment of rheumatoid arthritis, Journal of Controlled Release. 230 (2016) 64–72.

[31] L. Lu, E.A. Armstrong, J.Y. Yager, L.D. Unsworth, Sustained Release of Dexamethasone from Sulfobutyl Ether β-cyclodextrin Modified Self-Assembling Peptide Nanoscaffolds in a Perinatal Rat Model of Hypoxia–Ischemia, Advanced Healthcare Materials. 8 (2019) 1900083.

[32] H. Gasmi, F. Siepmann, M.C. Hamoudi, F. Danede, J. Verin, J.-F. Willart, J. Siepmann, Towards a better understanding of the different release phases from PLGA microparticles: Dexamethasone-loaded systems, International Journal of Pharmaceutics. 514 (2016) 189–199.

[33] L. Zhang, W. Shen, J. Luan, D. Yang, G. Wei, L. Yu, W. Lu, J. Ding, Sustained intravitreal delivery of dexamethasone using an injectable and biodegradable thermogel, Acta Biomaterialia. 23 (2015) 271–281.

[34] D.-H. Kim, T.N. Nguyen, Y.-M. Han, P. Tran, J. Rho, J.-Y. Lee, H.-Y. Son, J.-S. Park, Local drug delivery using poly (lactic-co-glycolic acid) nanoparticles in thermosensitive gels for inner ear disease treatment, Drug Delivery. 28 (2021) 2268–2277.

[35] J. Urbańska, A. Karewicz, M. Nowakowska, Polymeric delivery systems for dexamethasone, Life Sciences. 96 (2014) 1–6.

[36] A. Yu, H. Shi, H. Liu, Z. Bao, M. Dai, D. Lin, D. Lin, X. Xu, X. Li, Y. Wang, Mucoadhesive dexamethasone-glycol chitosan nanoparticles for ophthalmic drug delivery, International Journal of Pharmaceutics. 575 (2020) 118943.

[37] N.M. Vacanti, H. Cheng, P.S. Hill, J.D.T. Guerreiro, T.T. Dang, M. Ma, S. Watson, N.S. Hwang, R. Langer, D.G. Anderson, Localized delivery of dexamethasone from electrospun fibers reduces the foreign body response, Biomacromolecules. 13 (2012) 3031–3038.

[38] K. Jiang, J.D. Weaver, Y. Li, X. Chen, J. Liang, C.L. Stabler, Local release of dexamethasone from macroporous scaffolds accelerates islet transplant engraftment by promotion of anti-inflammatory M2 macrophages, Biomaterials. 114 (2017) 71–81.

[39] X. Xu, L. Sun, L. Zhou, Y. Cheng, F. Cao, Functional chitosan oligosaccharide nanomicelles for topical ocular drug delivery of dexamethasone, Carbohydrate Polymers. 227 (2020) 115356.

[40] F.F. Sahle, C. Gerecke, B. Kleuser, R. Bodmeier, Formulation and comparative in vitro evaluation of various dexamethasone-loaded pH-sensitive polymeric nanoparticles intended for dermal applications, International Journal of Pharmaceutics. 516 (2017) 21–31.

[41] K. Rajes, K.A. Walker, S. Hadam, F. Zabihi, J. Ibrahim-Bacha, G. Germer, P. Patoka, B. Wassermann, F. Rancan, E. Rühl, Oxidation-sensitive core–multishell nanocarriers for the controlled delivery of hydrophobic drugs, ACS Biomaterials Science & Engineering. 7 (2021) 2485–2495.

[42] Q. Meng, H. Hu, X. Jing, Y. Sun, L. Zhou, Y. Zhu, B. Yu, H. Cong, Y. Shen, A modular ROS-responsive platform co-delivered by 10-hydroxycamptothecin and dexamethasone for cancer treatment, Journal of Controlled Release. 340 (2021) 102–113.

Chapter 5. Identification of short peptides activating human mast cells *via* Mas-related G-protein coupled receptor member X2

Preface

This chapter has been published in 'Acta Biomaterialia' titled, 'Identification of short peptide sequences that activate human mast cells via Mas-related G-protein coupled receptor member X2'. Lei Lu, Shammy Raj, Narcy Arizmendi, Jie Ding, Gary Eitzen, Peter Kwan, Marianna Kulka, and Larry D. Unsworth are the coauthors of the manuscript. Lei Lu and Shammy Raj share the 1st co-authorship. Shammy Raj designed and conducted HEK cell experiments, analyzed the data, and participated in writing the manuscript. Lei Lu designed the peptide experiments, analyzed the data, and participated in writing the manuscript. Narcy Arizmendi and Jie Ding conducted LAD2 experiments, analyzed the data, and reviewed the manuscript. Gary Eitzen helped design the HEK experiments, and participated in writing the manuscript. Peter Kwan helped design skin experiments, analyzed the data, and edited the manuscript. Marianna Kulka, and Larry D. Unsworth guided the research design, analyzed and reviewed the data, reviewed and edited the manuscript.

Chapter 5, in parts, has also been published in 'Journal of Visualized Experiments: JoVE' titled, "Screening peptides that activate MRGPRX2 using engineered HEK cells". Shammy Raj, Lei Lu and Larry D. Unsworth are the coauthors of the manuscript. Shammy Raj selected the experiments to highlight, conducted the experiments, analyzed the data, wrote the manuscript, and shot and edited the accompanying video. Lei Lu edited the manuscript. Larry D. Unsworth guided the research design, analyzed and reviewed the data, reviewed and edited the manuscript and reviewed the experimental video.

5.1. Introduction

Tissue resident mast cells play a significant role in innate and adaptive immune responses [1]. In immune-initiated allergic inflammation, mast cell activation is mediated through antigen crosslinking of FcεRI receptors that rapidly cause mast cell degranulation [2, 3]. However, various unrelated endogenous peptides, basic secretagogues, and clinically approved drugs have been shown to activate mast cells independent of the FcεRI pathway and through Mas-related G-protein coupled receptor X2 (MRGPRX2) [4, 5].

MRGPRX2 is pivotal in itch, allergy, and other inflammatory diseases, and its overexpression has been associated with asthma, atopic dermatitis, and psoriasis [6, 7]. A variety of peptide stimuli, including peptide toxins, neuropeptides, antibacterial peptides, and endogenous peptide fragments have been shown to activate mast cells *via* MRGPRX2 [8, 9]. Moreover, peptide drugs including icatibant, cetrorelix, octreotide, and leuprolide have been shown to be potent MRGPRX2 activators inducing mast cell activation to varying degree [4, 10-14]. Thus, elucidating the correlation between peptide structure and activation potential on mast cells *via* MRGPRX2 may inform general peptide design limitations as well as application specific peptide design where only mast cell activation is desired, like in the case of host defense against microbial infections [15, 16].

The structural similarity among most of the known peptide ligands of MRGPRX2 has been summarized. Abundance of positively charged, aromatic, and hydrophobic residues were observed to be essential for MRGPRX2 recognition. Similar properties were also evident in non-peptide drugs like compound 48/80, atracurium, and tubocurarine [17]. Recent site-specific mutagenesis studies as well as the interaction of MRGPRX2 with opioid molecules have indicated a key role of Glu164 and Asp184 in ligand coordination and receptor activation [18, 19]. Negatively charged

residues have been hypothesized to mediate the ionic interaction of MRGPRX2 with cationic ligands. Synthetic opioid molecules contain a positively charged tertiary amine and a phenolic ring at a fixed distance; similar to the above-mentioned fundamental structure of the ligands binding MRGPRX2 receptor [18]. It was, therefore, of interest to study the crucial role of physiochemical properties of amino acids within a peptide molecule in MRGPRX2 activation. To elucidate the molecular basis for peptide-MRGPRX2 interactions, a peptide library based on Proadrenomedullin N-terminal 12 (PAMP-12) was used to identify amino acid residues responsible for MRGPRX2 induced activation of mast cells [4, 9]. PAMP-12 based peptide library was developed using common screening techniques: N and C-terminal truncations, and alanine scanning. MRGPRX2 expressing HEK-293 (HEK-X2) and LAD2 human mast cells were used to screen the activation potential of these peptides. Selected peptides were further tested on epidermis-free human skin biopsies to test their efficacy in activating tissue resident mast cells. Based on these results, and previously published studies [17], a generalized principle for peptides was observed that can activate mast cells through MRGPRX2 with varying potency. The activating potential of these artificial peptides were similarly evaluated using HEK-X2 and LAD2 human mast cells. The results show that MRGPRX2 can be affected by 5-mer peptides, and that by varying the physiochemical nature of amino acids, peptides with distinct activating potentials can be generated.

5.2. Materials and methods

5.2.1. Screening of peptide library with MRGPRX2 transfected HEK cells

Peptides (≥95% purity) were purchased from RS Synthesis (Louisville, KY, USA) and peptide solutions were prepared in PBS (1×, pH 7.4). The N-terminal of the peptide was modified with an acetyl group while the C-terminal was modified to an amide group. In a typical experiment, wild type HEK-293 cells (HEK-WT) and MRGPRX2 transfected HEK-293 cells (HEK-X2, a stably transfected HEK cell line described in previous work [4]) were seeded in the alternate rows of a 96 well, clear bottom, black polystyrene microplate (Corning®, Corning, NY) at a density of 4×10^4 cells per well in 200 µL DMEM (high glucose, pyruvate, Gibco, Thermo Fisher) culture media supplemented with 10% fetal bovine serum (FBS, Gibco, Thermo Fischer), 2 mM L-Glutamine (Gibco, Thermo Fisher Scientific, Waltham, MA) and 100 U/mL of penicillin and 100 µg/mL of streptomycin (Pen Strep Gibco, Thermo Fisher Scientific, Waltham, MA). The cells were grown for 24 h at 37 ^oC in 5% CO_2. Culture medium was replaced with fresh media loaded with 1 µM of Fura-2 AM dye (Gibco, Thermo Fisher Scientific, Waltham, MA) and incubated for 45 min at 37 ^oC in 5% CO_2. After incubation, cells were washed with HTB buffer (25 mM HEPES buffer (Gibco, Thermo Fisher Scientific, Waltham, MA), 120 mM NaCl, 5 mM KCl, 1 mg/mL glucose, 1 mg/mL bovine serum albumin (BSA) and freshly added 1.8 mM $CaCl_2$ (all from Sigma Aldrich, Oakville, ON, Canada)) and re-suspended in 100 µL of HTB buffer. Fluorescence was measured using FlexStation 3 (Molecular Devices, San Jose, CA) at dual excitation wavelength of 340 and 380 nm, and an emission wavelength of 510 nm, excitation and emission slits 9 and 15 nm, respectively. After generating a baseline, 50 µL of 3 µM peptide solution was added into the wells to make a final peptide concentration of 1 µM. Data is represented as the ratio of fluorescence at 340 nm and 380 nm (F_{340} / F_{380}).

5.2.2. Determination of intracellular calcium concentration upon activation by peptides

Similar experimental protocol as mentioned above was followed to determine the intracellular calcium upon peptide activation. [Ca^{2+}] was quantified using the below equation [20]:

$$[Ca^{2+}] = K_d \frac{F_{380min}}{F_{380max}} \frac{(R - R_{min})}{(R_{max} - R)}$$

Where, K_d is the dissociation constant of Fura 2 (135 nM, as per supplier), R is the F_{340} / F_{380} ratio for respective peptides. R_{max} is the maximum fluorescence ratio observed by the addition of 50 µL of 30 µM ionomycin and R_{min} is the minimum fluorescence observed by the addition of 50 µL of 100 mM, 2.5% EGTA – Triton X-100 (Sigma Aldrich, Oakville, ON, Canada) solution. F_{380min} and F_{380max} are the absolute fluorescence intensity of Fura 2 in bound and free state respectively. R_{max}, R_{min}, F_{380min} and F_{380max} was calculated for each column of the microplate and was averaged over the entire plate. Data is represented after base line correction followed by blank correction.

5.2.3. Evaluation of LAD2 degranulation – β-hexosaminidase (β-hex) release assay

β-hex, a preformed inflammatory mediator stored in mast cell granule is a well-known marker of mast cell degranulation, the experimental protocol is similar to the one described in our previous work [21]. The LAD2 cells were gifted by Dr. Dean Metcalfe and Dr. Arnold Kirshenbaum under a Material Transfer Agreement (MTA) with the National Institutes of Health-National Institute of Allergy and Infectious Diseases (NIH-NIAID). LAD2 mast cells were cultured in StemPro-34 SFM medium (Life Technologies, Rockville, MD) containing 2 mM L-glutamine, 100 U/mL penicillin, 50 µg/mL streptomycin, and 100 ng/mL recombinant human stem cell factor (SCF, Peprotech, Rocky Hill, NJ). Cells were maintained at a density of 0.1 $\times 10^6$ cells/mL at 37 ºC in 5% CO_2. Fresh media was added to the cultures every 3-7 days. For β-hex assay, 0.25 $\times 10^5$ LAD2

cells/well were washed and resuspended in 90 µL prewarmed 10 mM HEPES buffer supplemented with 0.4% BSA (pH 7.4). Cells were activated by adding 10 µL peptide solutions for 30 min at 37 ºC. β-hex release was quantified using the analysis of p-nitrophenyl-N-acetyl-b-D-glucosamide (Sigma Aldrich, Oakville, ON, Canada) hydrolysis in 0.1 M sodium citrate buffer (pH 4.5) with both supernatant and cell lysates solubilized in 0.01% Triton X-100 at 37 ºC, for 90 min. Glycine buffer (pH 10.7) was used to stop the reaction. Absorbance was read at 405 nm with 620 nm reference filter. β-hex released in the supernatant was calculated as a percentage with respect to total β-hex (combined β-hex in cell lysate and supernatant). Degranulation study on BMMCs as control experiment was done as previously described method [22].

5.2.4. *Ex-vivo* activation of skin mast cells

Discarded abdominoplasty surgical specimen obtained upon written consent of the individual as per the University of Alberta research ethics board was used as the skin model for the study. In a typical experiment, 8 mm punches were made in the epidermis removed skin biopsies as described previously [21]. Skin punches were immersed in 1.5 mL of 10 µM of peptides solutions in PBS and were incubated for 2 h at 37 ºC in 5% CO_2. After incubation, tissue was washed with PBS and snap frozen in liquid nitrogen and stored at -80 ºC until further processing. Peptide treated skin biopsies were powdered using Mikro Dismenbrator (B. Braun Biotech, Allentown, PA) and was lysed using TRIzol reagent (Invitrogen, Carlsbad, CA). Total RNA was isolated and purified using a RNeasy Mini kitPlus Kit (Qiagen Sciences, Germantown, MD) according to the manufacturer's protocol. 200 ng RNA were used to synthetize cDNA by M-MLV reverse transcriptase (Invitrogen, Waltham, MA) according to the manufacturer's instructions. The gene expression levels of tryptase (TSAPB1) enzyme were analyzed by a StepOnePlus real-time PCR system (Applied Biosystems, Thermofisher Scientific, Waltham, MA) with gene-specific primers and probe set

(Integrated DNA Technologies, Coralville IA). PrimeTime qPCR oligonucleotides for TPSAB1 and a reference gene, HPRT1 (Supplementary Information, Table 1), were obtained from Integrated DNA Technologies (Coralville, IA). PCR mixture (20 μL total volume) consisted of template, primers, probe for each gene, and the PrimeTime® Gene expression Master Mix (Integrated DNA Technologies, Coralville IA). Real-time PCR amplification was carried out as follows: initial denaturation cycle at 95 ºC for 10 min, followed by 40 cycles of denaturation at 95 ºC for 15 s, and annealing and elongation at 60 ºC for 1 min, with a final extension at 97 ºC for 10 min. The results were analyzed using the 2-ΔΔCT method. HPRT1 was used to normalize the gene expression. Data were obtained from three independent measurements performed in duplicates.

5.2.5. Statistical analysis

All experiments were conducted in at least triplicates with independent repeats and presented as average ± standard error of the mean (SEM). The statistical significance of differences between mean values was determined using one-way ANOVA, followed by two-tailed Student's t-test for analysis of variance, where significance was evaluated for * $p < 0.05$, ** $p < 0.01$, *** $p < 0.001$ and NS (non-significance) $p > 0.05$.

5.3. Results

5.3.1. Specificity of PAMP-12 towards MRGPRX2 receptor

MRGPRX2 receptor binding of PAMP-12 is known to activate human mast cells [4, 9]. Calcium flux kinetics were monitored upon PAMP-12 incubation with MRGPRX2 transfected HEK cells (HEK-X2) or associated wild type HEK cells (HEK-WT) (Figure 5.1a, b). The effect of PAMP-12 on HEX-X2 activation was characterized using calcium mobilization (Figure 5.1a); on average a stepwise increase in Ca^{2+} flux from 0.01 to 1 μM PAMP-12 concentrations was observed and it saturated beyond 1 μM. Therefore, a 1 μM peptide concentration was used to compare the inter-peptide mast cell activation potential. Further, HEK-X2 stimulated with 1 μM PAMP-12 yielded a substantial release of Ca^{2+}, while the HEK-WT remained at basal levels (Figure 5.1b).

This control was also conducted using the human MRGPRX2 expressing mast cell LAD2, used as a model human cell line to verify peptide activity prior to human skin tests. Non-MRGPRX2 expressing BMMCs (murine mast cell) were used as negative controls. As with Ca^{2+} release from HEX-X2 cells, β-hex release upon mast cell activation is indicative of the extent of degranulation. PAMP-12 was shown to have a concentration dependent β-hex release from LAD2 cells (Figure 5.1c); a saturation of which was found at 10 μM PAMP-12 concentration. As a result, a 10 μM peptide concentration was used to compare their activation potentials. Similar to Ca^{2+} flux in HEK-X2 cells, exposure to 10 μM of PAMP-12 yielded a 69 ± 1% β-hex release in LAD2 cells while the control BMMCs showed no β-hex release upon activation by the same concentration of PAMP-12 (Figure 5.1d).

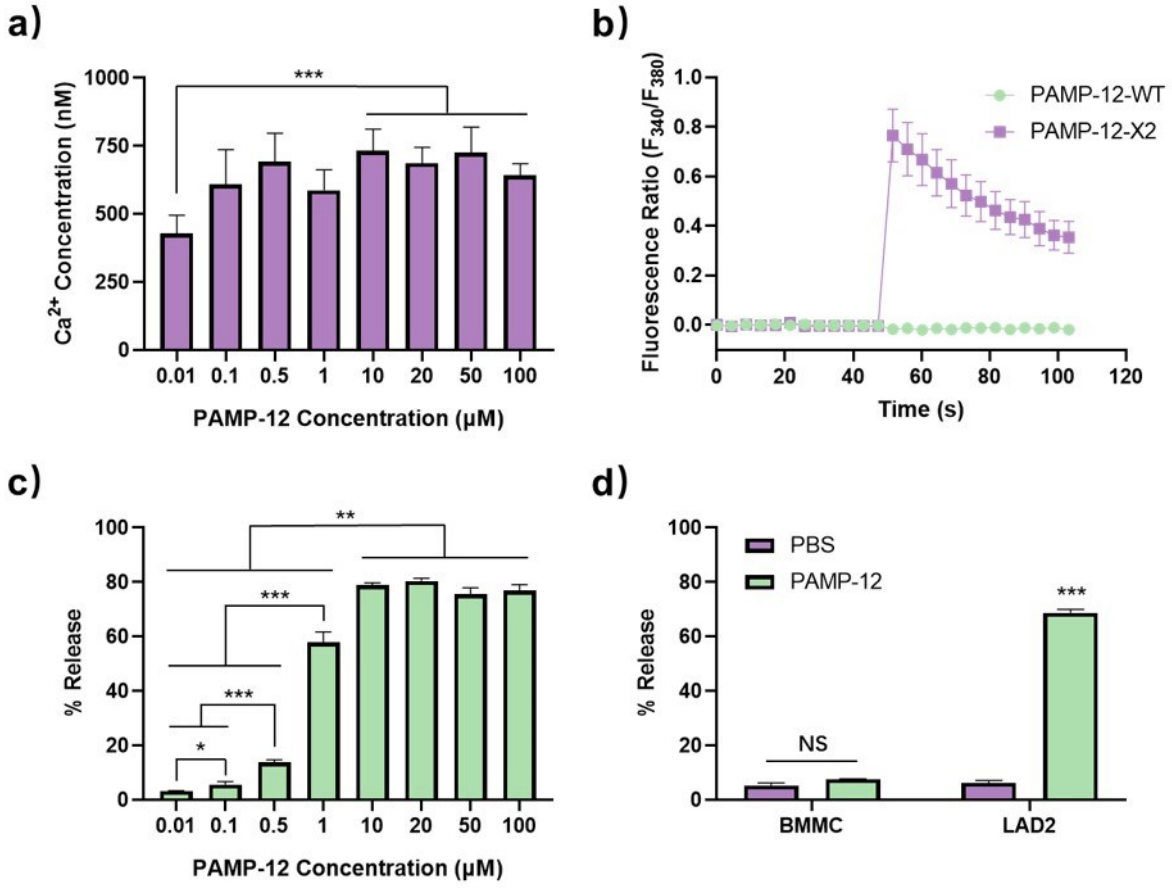

Figure 5.1. Specificity of PAMP-12 towards MRGPRX2 receptor. a) dose dependent calcium release from HEK-X2 with increasing PAMP-12 concentration; b) calcium mobilization in HEK-X2 and HEK-WT cells upon incubation with 1 µM PAMP-12; c) concentration dependent β-hex release in LAD2 cells upon incubation with PAMP-12; and d) β-hex release from LAD2 cells versus BMMCs upon incubation with 10 µM PAMP-12. Data are represented as mean ± SEM, $n \geq 6$. The significance was evaluated for * $p < 0.05$, ** $p < 0.01$, *** $p < 0.001$, and NS $p > 0.05$.

5.3.2. PAMP-12 has two mast cell activating domains

To identify amino acid domains within PAMP-12 that activates MRGPRX2, a series of truncated sequences (TS) were derived from N-(TS-Nx), C-(TS-Cy), and N+C-truncation (TS-NxCy) of PAMP-12 (Supplementary Information, Table 2) and were screened using HEK-X2 and LAD2 cells (Figure 5.2). Similar to PAMP-12 induced activation (Figure 5.1b), all derived peptides

induced calcium mobilization in HEK-X2 but not in HEK-WT; confirming truncated peptides exhibit their activity through MRGPRX2.

Calcium released upon incubation with truncated peptides was quantified using the Grynkiewicz equation [20]. As shown in Figure 5.3a, TS-N1 to TS-N5 showed a Ca^{2+} release of 719 ± 128, 538 ± 72, 453 ± 55, 625 ± 76, and 167 ± 19 nM, respectively. There was no significant difference between PAMP-12 (538 ± 27 nM) and TS-N1 to TS-N4, whereas TS-N5 resulted in a significant decrease in Ca^{2+} flux. Calcium released by TS-N5 was only 31% of PAMP-12 and 27% of TS-N4. Similar results were observed using LAD2 cells (Figure 5.3b), *viz*., PAMP-12 and truncated sequence TSN1 to TS-N4 showed a respective β-hex release of 69 ± 1, 65 ± 4, 52 ± 1, 40 ± 3, and 66 ± 2% respectively, while TS-N5 showed only 5% β-hex release. Results from the calcium mobilization and β-hex release showed that in the library of N-truncated sequences, TS-N4 is the minimum sequence that has a similar activation potential as PAMP-12 for the MRGPRX2 receptor. Further removal of residues from the N-terminal (TS-N5) resulted in a significant reduction in activation potential.

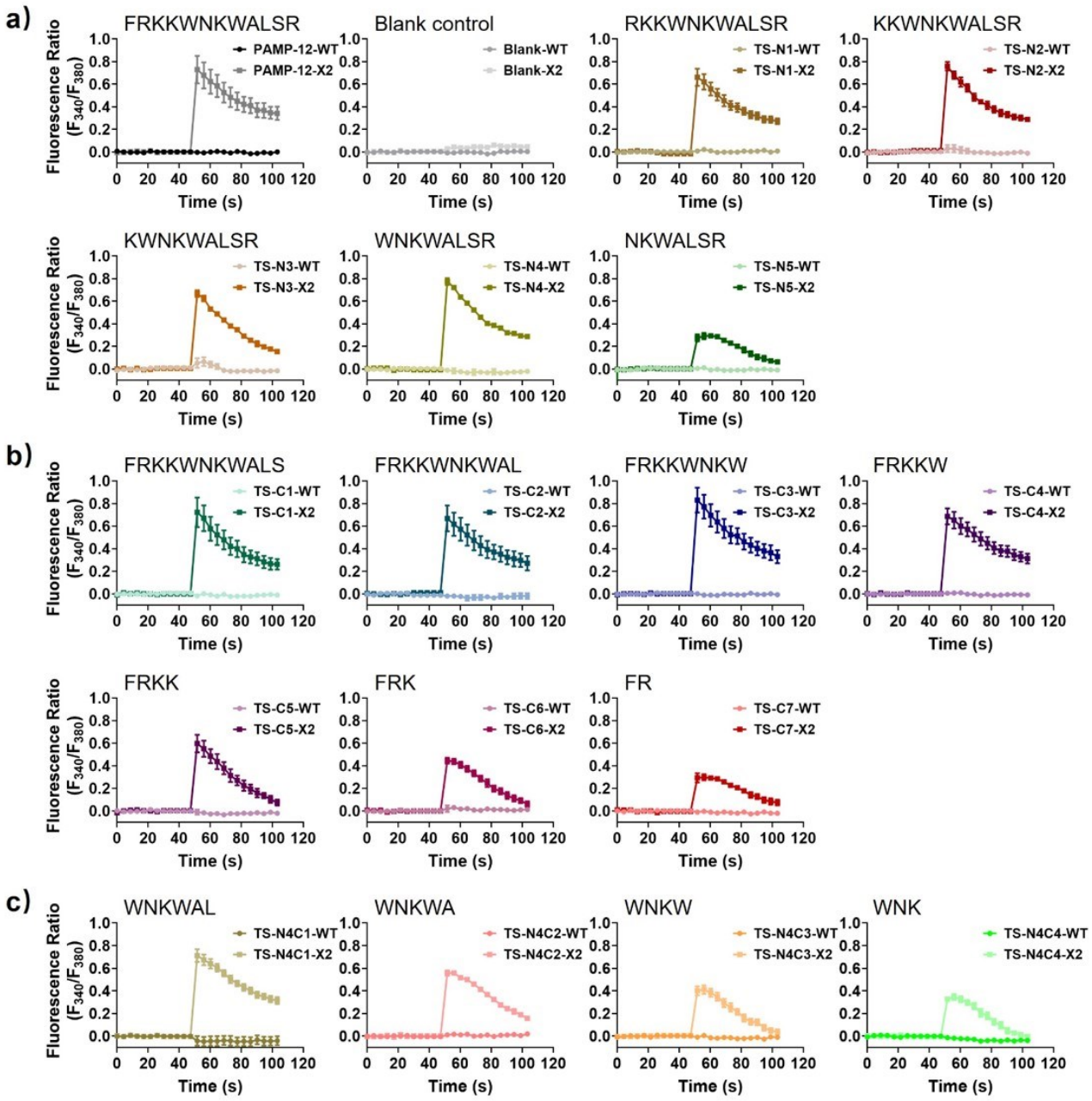

Figure 5.2. Truncated peptide activity towards MRGPRX2 receptor as confirmed using calcium mobilization in HEK-X2 and HEK-WT cells. a) PAMP-12, blank control, and N-truncated peptides; b) C-truncated peptides; and c) N+C-truncated peptides. Data are represented as mean ± SEM, n ≥ 6.

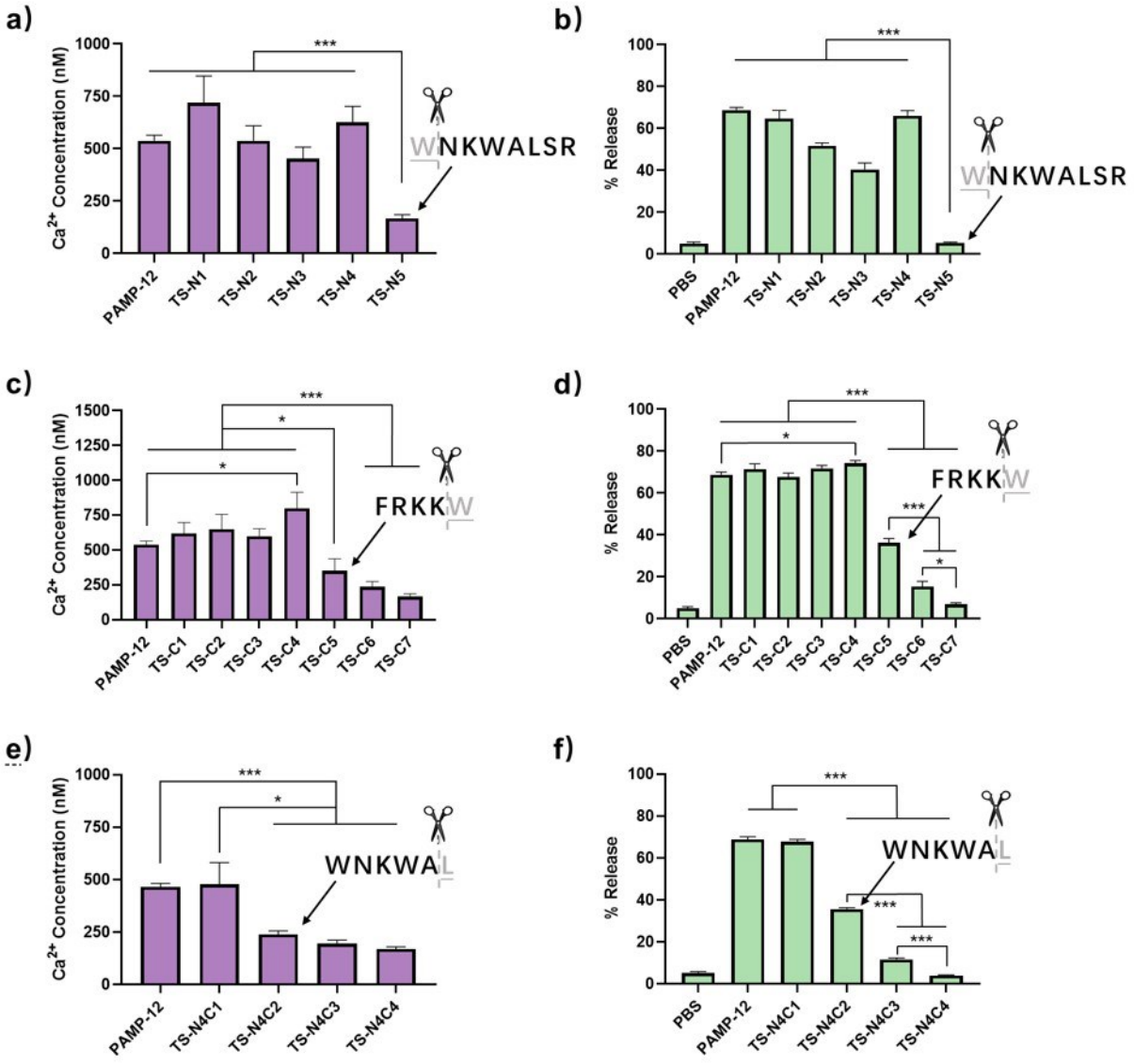

Figure 5.3. Activation of MRGPRX2 receptor by N, C, and N+C-truncated peptides. Calcium flux measured using ratiometric Fura-2 dye in HEK-X2 cells upon incubation with 1 μM peptide concentration. a) N-truncated peptides, c) C-truncated peptides, and e) N+C-truncated peptides. β-hex release from LAD2 cells upon stimulation by 10 μM of b) N-truncated peptides, d) C-truncated peptides, and f) N+C-truncated peptides. Data are represented as mean ± SEM, n ≥ 6. The significance was evaluated for * $p < 0.05$, ** $p < 0.01$, *** $p < 0.001$.

The effect of C-terminal truncation on PAMP-12 activity against HEK-X2 cells showed a Ca^{2+} release of 618 ± 80, 651 ± 106, 599 ± 54, and 799 ± 116 nM for TS-C1 to TS-C4, respectively (Figure 5.3c). TS-C1 to TS-C3 peptides induced a similar calcium release as PAMP-12 (538 ± 27 nM), whereas TS-C4 was significantly higher. HEK-X2 incubation with TS-C5 through TS-C7

showed an on average stepwise decrease in calcium release. TS-C5 showed a Ca^{2+} concentration of 352 ± 85 nM, 44% of TS-C4 and 65% of PAMP-12. TS-C6 and TS-C7 showed a calcium release of 237 ± 37 and 166 ± 21 nM, respectively. The trend in LAD2 activation was similar to that observed for HEK-X2 (Figure 5.3d). PAMP-12 and TS-C1 to TS-C4 showed β-hex release in the range of 68-74%; while TS-C5 showed a significant decrease in activity to 36%. Consistent with Ca^{2+} flux data, TS-C6 and TS-C7 showed a decreased β-hex release, both being at 15% and 7%, respectively. These results suggest that TS-C4 is the minimum sequence in the library of C-truncated sequences that can activate mast cells with a potential comparable to that of PAMP-12.

Further, residues at both ends of PAMP-12 were sequentially truncated (TS-NxCy) and their activity evaluated using HEK-X2 and LAD2 cells. PAMP-12 and TS-N4C1 showed (Figure 5.3e) a comparable calcium mobilization of 466 ± 17 and 478 ± 103 nM, respectively. Removal of one more C-terminal residue from TS-N4C1 resulted in a decrease in Ca^{2+} flux to 238 ± 17 nM (TS-N4C2). This concentration was 51and 50% of PAMP-12 and TS-N4C1, respectively. Analogous to HEK-X2 activation, activation against LAD2 cells showed that while PAMP-12 and TS-N4C1 caused a respective release of 69 ± 1 and 68 ± 1%, β-hex released by TS-N4C2 was reduced to 36%; a 48 and 47% decrease relative to PAMP-12 and TS-N4C1, respectively (Figure 5.3f).

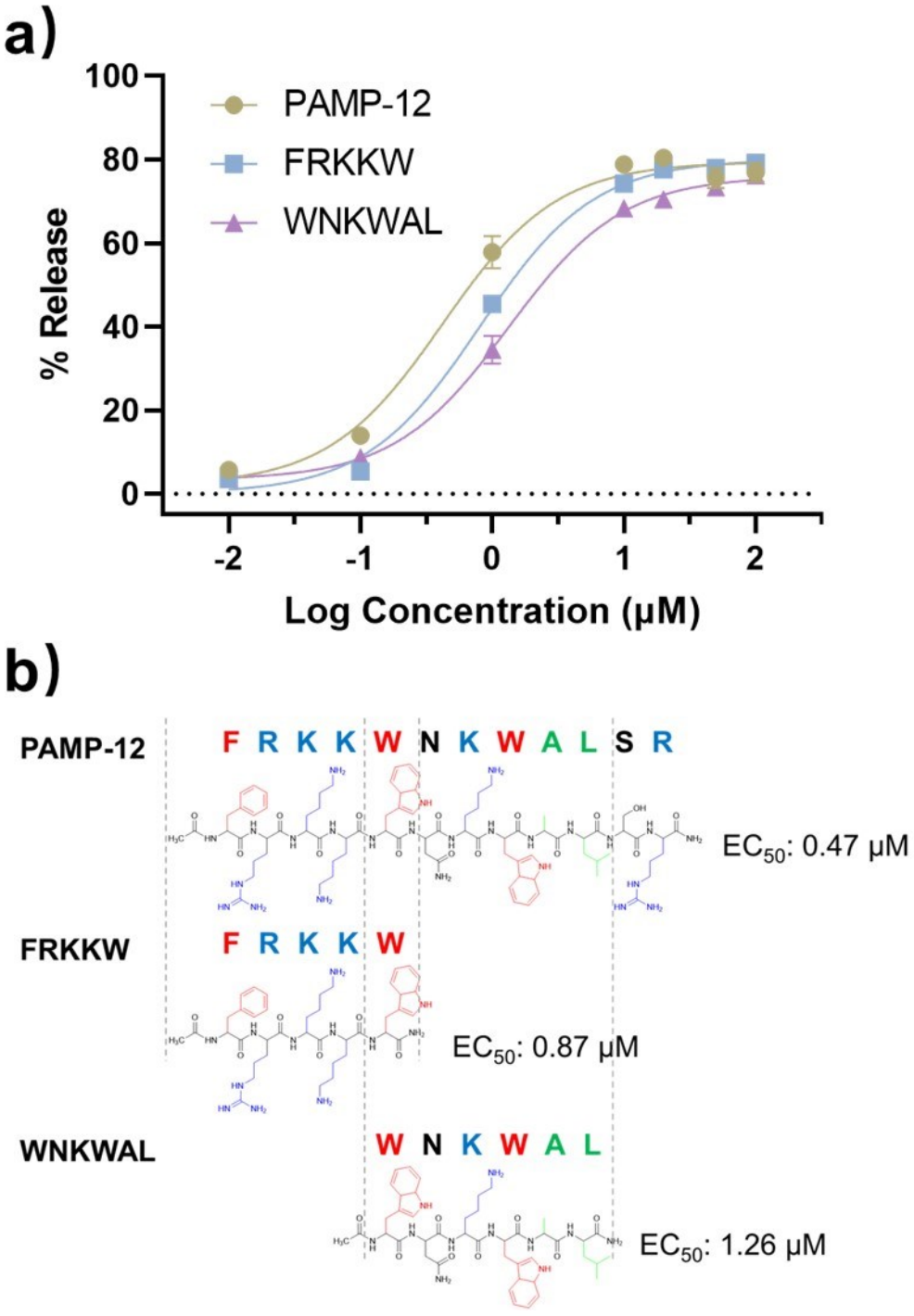

Figure 5.4. Dose dependent activation of LAD2 cells by PAMP-12 and core motifs. a) Dose dependent β-hex response of PAMP-12 and the two identified core motifs, FRKKW and WNKWAL on LAD2 mast cells; b) sequence, structure and activity of PAMP-12 and its core motifs. Red - aromatic residues, blue - positively charged residues; green - hydrophobic residues, black -polar uncharged residues. Note that aromatic residues are hydrophobic as well. Data are represented as mean ± SEM, n ≥ 6.

5.3.3. Significance of amino acid residues in mast cell activation through MRGPRX2

Alanine scanning (ASn) of PAMP-12 was used to establish the significance of individual amino acids in activating mast cells (Supplementary Information, Table 3). All peptides caused calcium flux in HEK-X2 but not in HEK-WT cells, but no significant difference among alanine altered peptides in flux was observed (Figure 5.5). However, β-hex release from LAD2 degranulation experiments indicated the significance of specific residues in receptor activation (Figure 5.5c). AS5 tryptophan to alanine replacement in PAMP-12 caused a significant decrease in β-hex release to 50 ± 2% from the 69 ± 1% seen in PAMP-12 controls.

5.3.4. Activation potential for a fully artificial peptide

The smallest amino acid sequence that retained an activity similar to PAMP-12 had the structure X_a-$(Y)_{(n \geq 3)}$-X_b: where X_a is an aromatic residue, and X_b is a hydrophobic residue, and that X_a and X_b are flanked by a peptide group ($n \geq 3$) containing at least 1-3 basic polar amino acid (i.e. positively charged side chain) with the remaining being uncharged residues. A series of artificial peptides that were not biomimetic but only based upon this structural constraint were synthesized (CSTx, Supplementary Information, Table 4). CSTx peptides induced activity in HEK-X2 cells but not wild type controls (Figure 5.6a), confirming an MRGPRX2 affinity. Calcium flux upon incubation of HEX-X2 with PAMP-12, CST5, and CST7 to CST10 was 546 ± 25, 418 ± 33, 471 ± 52, 770 ± 73, 638 ± 72, and 498 ± 53 nM, respectively (Figure 5.6b). Sequences CST1 to CST4, CST6, and CST11 showed minimal activity. On the contrary, peptides CST8 (WKKKW) and CST9 (FKKKF) had mean values 141% and 117% of PAMP-12. These results were further supported by the degranulation assay (Figure 5.6c), where β-hex released by LAD2 cells upon

activation by 10 μM peptide concentration of PAMP-12, and CST7 to CST10 was 69 ± 1, 61 ± 1, 77 ± 1, 73 ± 2, and 42 ± 2%, respectively.

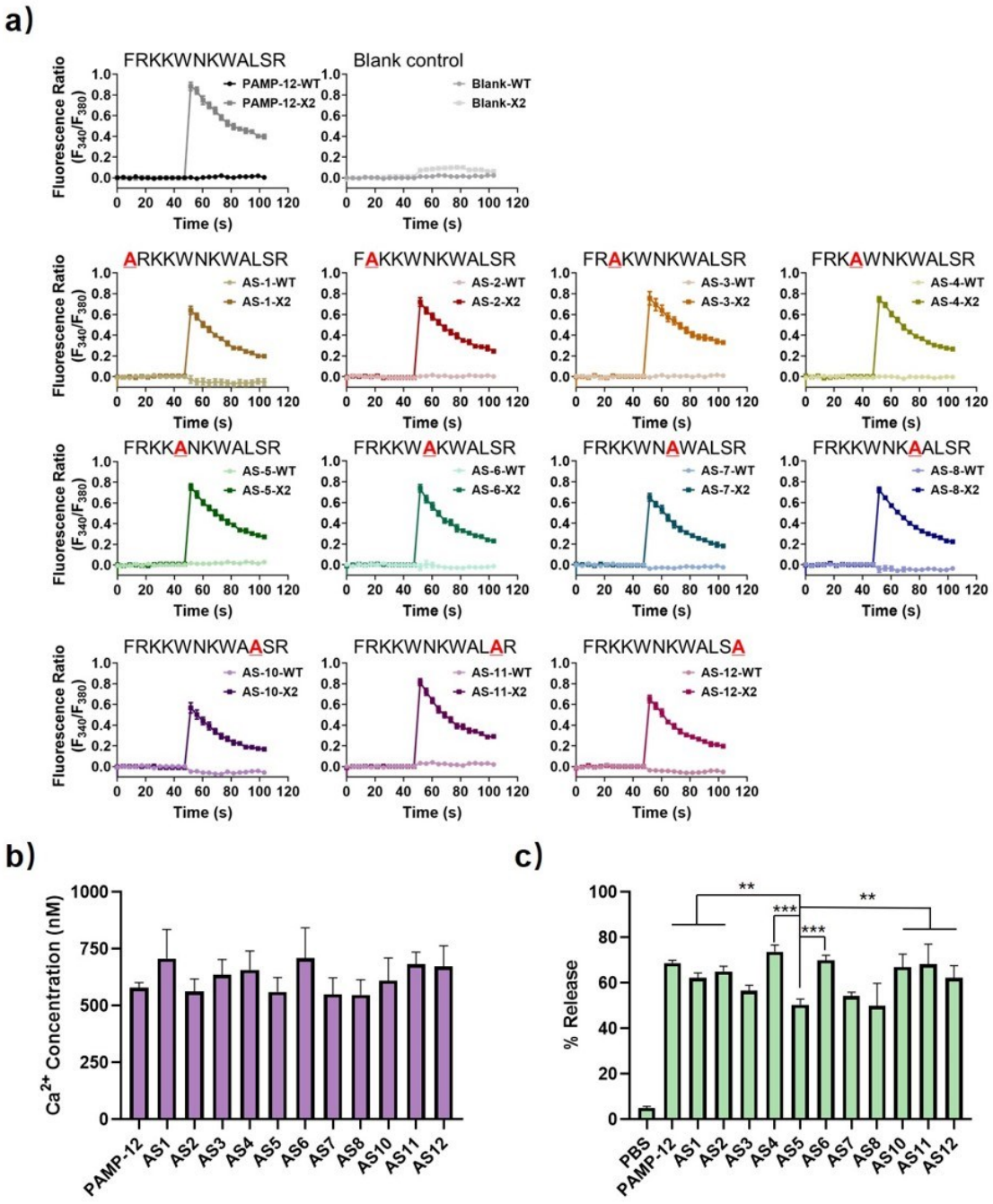

Figure 5.5. Activation of MRGPRX2 receptor by PAMP-12 derived peptides. a) Calcium mobilization in HEK-X2 and HEK-WT cells; b) calcium flux measured using ratiometric Fura-2 dye in HEK-X2 cells upon incubation with 1 μM concentration; and c) β-hex release study on LAD2 cells upon stimulation by 10 μM peptide concentration. Data are represented as mean ± SEM, n ≥ 6. Significance was evaluated for * $p < 0.05$, ** $p < 0.01$, *** $p < 0.001$.

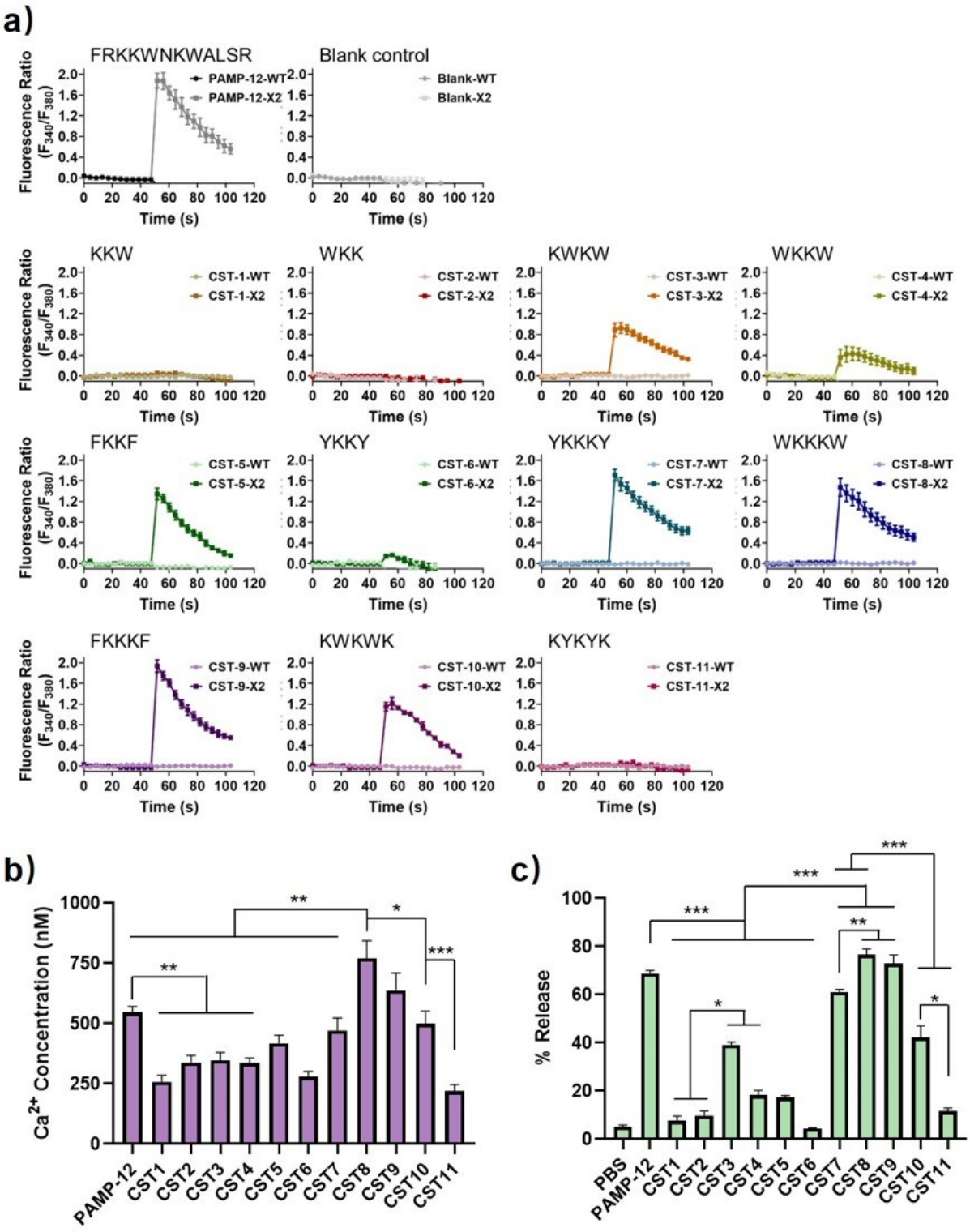

Figure 5.6. Activation of MRGPRX2 receptor by customized peptides. a) Calcium mobilization in HEK-X2 and HEK-WT cells; b) calcium flux measured using ratiometric Fura-2 dye in HEK-X2 cells upon incubation with 1 μM peptides. c) β-hex release study on LAD2 cells upon stimulation by 10 μM peptide concentration. Data are represented as mean ± SEM, n ≥ 6. The significance was evaluated for * $p < 0.05$, ** $p < 0.01$, *** $p < 0.001$.

5.3.5. Peptides of varying activation potential against MRGPRX2

To test the effect of these peptides on MRGPRX2 expressing mast cells within the skin tissue, the epidermis was removed, and the skin tissue incubated with a 10 μM solution of PAMP-12 (control) or peptides with a greater (FRKKW, FKKKF), similar (WNKWAL), or lower (KWKWK) activation potential than PAMP-12. Mast cell specific activation was evaluated using RNA expression for tryptase after 2 h of incubation, quantified using RT-qPCR and normalized against the HPRT1 housekeeping gene (Figure 5.7). Positive control, PAMP-12, showed a 1.54-fold increase in tryptase expression relative to HPRT1. FRKKW and WNKWAL caused a mean of 2.13 and 1.78-fold increase in tryptase expression upon incubation. Similarly, the highly potent sequence based on the devised format, FKKKF showed an expression level of 1.02-fold. KWKWK, which failed to activate LAD2 and HEK-X2, caused a 0.58-fold tryptase expression, which was significantly ($p<0.001$) less than the PAMP-12 control.

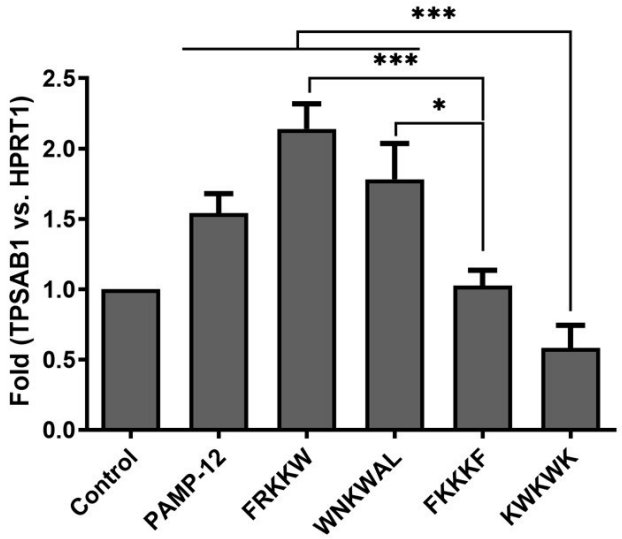

Figure 5.7. Effect of peptide administration to human skin tissue on tryptase (TPSAB1) expression. HPRT1 was used to normalize gene expression. Data is represented as mean ± SEM, n ≥ 3. The significance was evaluated for * $p < 0.05$, ** $p < 0.01$, *** $p < 0.001$.

5.4. Discussions

MRGPRX2 is a low-affinity receptor, differentially expressed on mast cells depending on the tissue of origin; connective tissue mast cells express high levels of MRGPRX2 receptor, mucosal mast cells in the lung and heart have limited receptor expression [5, 23]. PAMP-12 controls showed a dose dependent activity against both the MRGPRX2 expressing HEK and human LAD2 cells (Figure 5.1a, c) [4]. On the contrary, wild type HEK cells and murine mast cells that do not express MRGPRX2 receptors were unaffected by PAMP-12 (Figure 5.1b, d).

Fragments of degraded proteins have been reported to be more potent activators of MRGPRX2 than whole proteins [9, 10]. Calcium mobilization in MRGPRX2 transfected Chinese hamster ovary cells stimulated with PAMP-12 and PAMP yielded an EC_{50} values of 41 and 223 nM respectively; suggesting PAMP-12 has a higher mast cell activating potential than PAMP [9]. It was, therefore, of interest to find if smaller sequences within PAMP-12 could potentially activate mast cells. These results show that FRKKW and WNKWAL are the smallest peptides that can activate mast cells with statistically similar potency as PAMP-12. Relative to PAMP-12 controls the Ca^{2+}flux in HEK-X2 was 148% and 102%, and LAD2 β-hex release was 107% and 99% for FRKKW and WNKWAL, respectively. These results were similar to previously published -activity values of 97 ± 5 % for WNKWALSR and 100 ± 12 % for PAMP-12 as compared to cortistatin-14 [24]. Since, MRGPRX2 ligands have shown a concentration dependent activation profile, dose dependent response of FRKKW and WNKWAL on β-hex was also evaluated (Figure 5.4a). Using dose dependent results on LAD2 cells, EC_{50} values for PAMP-12, FRKKW, and WNKWAL were found to be 0.47, 0.87, and 1.26 μM, respectively.

As discussed above, PAMP-12, FRKKW, and WNKWAL, have comparable activity towards MRGPRX2 expressing mast cells. Similarly, Cortistatin-17 has been shown to induce a calcium response in MRGPRX2 transfected HEK cells with an EC_{50} value of 0.099 μM, while its smaller analog cortistatin-14 had an EC_{50} value of 0.025 μM [10]. Cathelicidin, LL-37 and its derived peptide FK-13 (FKRIVQRIKDFLR) showed equivalent degranulation in LAD2 mast cells [25]. Following a similar trend, the fragments of albumin and chaperonin proteins have also shown a calcium response in MRGPRX2 expressing HEK cells and degranulation in mast cells [8, 26]. These data suggest that the size of ligand molecules has an important role in their activation potential towards MRGPRX2 [18].

The significance of individual amino acid residues in PAMP-12 on MRGPRX2 activation was studied using alanine scanning techniques. Tryptophan at the 5th position from N-terminal of PAMP-12 showed a significant decrease in β-hex release when replaced with alanine (Figure 5.5c). This was also seen for the N and N+C truncated sequences (Figure 5.3a-d), both identified sequences (FRKKW and WNKWAL) include this tryptophan. Residues outside these core sequences also impacted cell activity: AS3, AS7 (replacement of 3rd lysine from N-terminal, positively charged), and AS8 (replacement of 8th tryptophan from N-terminal, aromatic) showed a similar reduction in β-hex release as AS5. These data suggest that for longer sequences these amino acids would have an effect on MRGPRX2 mediated activation of mast cells (Figure 5.5).

Altering, or removing, the tryptophan at 5th position from the N-terminal in PAMP-12 significantly reduced the peptide's activation potential. Also, the presence of an N-terminal aromatic residues (i.e., F in PAMP-12 and TS-C4; W in TS-N4C1) was vital for MRGPRX2-based activation. Results obtained in our study are in accordance with other published reports, where the activity of PAMP [10-20] lacking an N-terminal hydrophobic residue decreased by 15% compared to PAMP-

12. Similarly, cortistatin-14 with an N-terminal proline was four times more potent than cortistatin-17, which has a negatively charged aspartic acid at its N-terminal [24]. The albumin fragment TKKVPQVSTPTL, with threonine (polar, uncharged) at the N-terminal, failed to cause both Ca^{2+} release in MRGPRX2 transfected HEK cells and β-hex release in LAD2 cells. However, albumin fragments LLVRYTKKVPQVSTPTL, LVRYTKKVPQVSTPTL, and VRYTKKVPQVSTPTL with underlined N-terminal hydrophobic residues activated both MRGPRX2 transfected HEK cells and LAD2 cells [8]. Falling in line, cathelicidin, LL-37 and its derived peptide FK-13 (LL-37 [17-19]) having a sequence FKRIVQRIKDFLR showed equivalent degranulation in LAD2; both these peptides contain hydrophobic N-terminal residues [25].

Peptide sequences that activate mast cells through the MRGPRX2 receptor contained a general chemical structure (Supplementary Information, Table 5, 6), which were also observed (i.e., FRKKW and WNKWAL). By manipulating these structures mast cell activation can be likewise manipulated. It is observed that the optimized amino acid sequence retained an activity similar to that of PAMP-12 and follows a format of X_a-$(Y)_{(n \geq 3)}$-X_b: where X_a is an aromatic residue, and X_b is a hydrophobic residue, and that X_a and X_b are flanked by a peptide group ($n \geq 3$) containing at least 1-3 basic polar amino acid (i.e. positively charged side chain) with the remaining being uncharged residues. Structure of PAMP-12 and associated short motifs (Figure 5.4b) seem to support the above structure: wherein aromatic, hydrophobic residues (F, W, and L) flank a group of positively charged amino acids (R and K). CST8 and CST9 sequences held to this general peptide structure, with an N-terminal hydrophobic group bearing an aromatic ring, C-terminal is a hydrophobic group, and these are flanked by polar basic lysine group. Replacing the terminal groups with tyrosine, CST7 (YKKKY) decreased the mean by 14% of that of PAMP-12. This is likely due to the presence of the -OH group in the side chain of tyrosine as compared to

phenylalanine, which reduces the hydrophobicity of tyrosine. Peptide sequences (CST1, CST2, CST3, CST4, and CST6) and scrambled sequences (CST10 and CST11) that did not satisfy the hypothesis, showed lower calcium mobilization. YKKKY with the less hydrophobic tyrosine at 61 ± 1% was less than PAMP-12, WKKKW, and FKKKF.

Similarity between ligand structures that activate MRGPRX2 expressing mast cells have been discussed, including between PAMP-12 and cortisatin-14 [17, 24]. MRGPRX2 is known to consist of a large number of hydrophobic and negatively charged Glu164 and Asp184 residues that contribute to ligand binding. A mutation of negatively charged Glu164 with positively charged arginine inhibited the activation by substance P and compound 48/80 [18, 19]. In case of opioids, it has been proposed that the aromatic ring within the opioids guides the molecule towards the binding pocket, while free tertiary amine group facilitate electrostatic interactions [18]. Similarly, non-peptide molecules that bind MRGPRX2 also contain an aromatic ring and amine groups in their structure [17, 27]. In accordance with the above results, the presence of a terminal hydrophobic residue in the generalized motif, X_a - $(Y)_{(n \geq 3)}$ -X_b, indicates the hydrophobic effect that assists in the localization of the ligand within the binding pocket of the receptor. Polar basic groups, with positively charged side chains, within this structure will facilitate in an electrostatic interaction with Glu164 and/or Asp184 of the receptor. In contrast to these findings, authors in a recently published article have argued that the activation of MRGPRX2 receptor largely depends on the net positive charge of the peptide molecule and that the sequence of amino acids has a minimal effect on receptor activation [28]. However, it could be observed that most of the peptides studied by these authors contained this proposed amino acid structure.

Peptides which can elicit a controlled immune response through mast cell activation have a broad therapeutic interest. These results show that the activity of synthetic peptides against MRGPRX2

expressing LAD2 mast cells are in the following order: FRKKW = WKKKW = FKKKF (72-76%) > PAMP-12 = WNKWAL (67%) > YKKKY (61%) > FRKKANKWALSR = FRKKWNKAALSR (49%) >KWKWK (42%) > FRKK = WNKWA (36%) > KYKYK (11%) > NKWALSR = YKKY = WNK (5%). These are very important findings; especially as antibiotic resistant microbes are on the rise. Peptides that specifically target this receptor may provide an alternate route to confer protection against such pathogens [29, 30]. Whereas, limited activation compared to controls was observed for peptide sequences lacking tryptophan at the 5th position from the N-terminus of PAMP-12 (NKWALSR, TS-N5; FRKK, TS-C5), WNKWA, andTS-N4C2. Also, peptides which did not follow the general chemical structure (i.e., WKKW, FKKF, YKKY and KYKYK) failed to cause significant mast cell degranulation.

The peptides were then studied in physiologically relevant, epidermis removed, human skin tissue. Skin tissue possess MRGPRX2 expressing mast cells belonging to the CT (chymase – tryptase) subclass [23, 31]. The quantification of TPSAB1 (tryptase) mRNA levels in human tissue is a convenient method to determine the degree of mast cell activation, which usually need more than 30 min for expression [21, 32-34]. Thus, 2 h incubation selected in this study is long enough for gene expression and short enough to evaluate the immediate stimulation. Results showed that PAMP-12, FRKKW, and WNKWAL, had a similar trend in activation of skin resident mast cells as LAD2 cell culture. Though the expression's mean value was lower compared to PAMP-12, statistical analysis showed no significant difference between the two groups. Peptide KWKWK, which did not adhere to the generalized sequence, failed to activate skin mast cell, in accordance with the HEK-X2 and LAD2 results. Skin results supported the observation from the *in vitro* LAD2 and HEK-X2 results in that this subset of peptides initiated a mast cell response in a complex cellular environment and with a varied activation potential.

5.5. Conclusion

In conclusion, short peptide structures were found that can activate MRGPRX2 expressing mast cells with similar potency as PAMP-12. Also, it was observed that a range of peptides with differing activation potential were identified for the first time. This provides fundamental information on the possible limits of peptide design that should be considered early in the development of peptide-based materials or drugs for *in vivo* application. Moreover, a series of peptides were identified that have a range of activation potentials for mast cells that could be used to develop immunotherapies where controlled mast cell activation, in very complex cellular environments, is the desired outcome.

5.6. References

[1] S.J. Galli, S. Nakae, M. Tsai, Mast cells in the development of adaptive immune responses, Nature immunology 6(2) (2005) 135-142.

[2] S. Wernersson, G. Pejler, Mast cell secretory granules: armed for battle, Nature Reviews Immunology 14(7) (2014) 478-494.

[3] J. Kalesnikoff, S.J. Galli, New developments in mast cell biology, Nature immunology 9(11) (2008) 1215.

[4] B.D. McNeil, P. Pundir, S. Meeker, L. Han, B.J. Undem, M. Kulka, X. Dong, Identification of a mast-cell-specific receptor crucial for pseudo-allergic drug reactions, Nature 519(7542) (2015) 237-241.

[5] K. Tatemoto, Y. Nozaki, R. Tsuda, S. Konno, K. Tomura, M. Furuno, H. Ogasawara, K. Edamura, H. Takagi, H. Iwamura, Immunoglobulin E-independent activation of mast cell is mediated by Mrg receptors, Biochemical and biophysical research communications 349(4) (2006) 1322-1328.

[6] H. Subramanian, K. Gupta, H. Ali, Roles of Mas-related G protein–coupled receptor X2 on mast cell–mediated host defense, pseudoallergic drug reactions, and chronic inflammatory diseases, Journal of Allergy and Clinical Immunology 138(3) (2016) 700-710.

[7] W. Manorak, C. Idahosa, K. Gupta, S. Roy, R. Panettieri, H. Ali, Upregulation of Mas-related G Protein coupled receptor X2 in asthmatic lung mast cells and its activation by the novel neuropeptide hemokinin-1, Respiratory research 19(1) (2018) 1-5.

[8] T. Karhu, K. Akiyama, O. Vuolteenaho, U. Bergmann, T. Naito, K. Tatemoto, K.-H. Herzig, Mast cell degranulation via MRGPRX2 by isolated human albumin fragments, Biochimica et Biophysica Acta (BBA)-General Subjects 1861(11) (2017) 2530-2534.

[9] M. Kamohara, A. Matsuo, J. Takasaki, M. Kohda, M. Matsumoto, S.-i. Matsumoto, T. Soga, H. Hiyama, M. Kobori, M. Katou, Identification of MrgX2 as a human G-protein-coupled receptor for proadrenomedullin N-terminal peptides, Biochemical and biophysical research communications 330(4) (2005) 1146-1152.

[10] N. Robas, E. Mead, M. Fidock, MrgX2 is a high potency cortistatin receptor expressed in dorsal root ganglion, Journal of Biological Chemistry 278(45) (2003) 44400-44404.

[11] Y. Yu, Y. Zhang, Y. Zhang, Y. Lai, W. Chen, Z. Xiao, W. Zhang, M. Jin, B. Yu, LL-37-induced human mast cell activation through G protein-coupled receptor MrgX2, International Immunopharmacology 49 (2017) 6-12.

[12] H. Subramanian, K. Gupta, D. Lee, A.K. Bayir, H. Ahn, H. Ali, β-Defensins activate human mast cells via Mas-related gene X2, The Journal of Immunology 191(1) (2013) 345-352.

[13] K. Gupta, A. Kotian, H. Subramanian, H. Daniell, H. Ali, Activation of human mast cells by retrocyclin and protegrin highlight their immunomodulatory and antimicrobial properties, Oncotarget 6(30) (2015) 28573.

[14] A. Navinés-Ferrer, E. Serrano-Candelas, A. Lafuente, R. Muñoz-Cano, M. Martín, G. Gastaminza, MRGPRX2-mediated mast cell response to drugs used in perioperative procedures and anaesthesia, Scientific reports 8(1) (2018) 1-11.

[15] A. Di Nardo, A. Vitiello, R.L. Gallo, Cutting edge: mast cell antimicrobial activity is mediated by expression of cathelicidin antimicrobial peptide, The Journal of Immunology 170(5) (2003) 2274-2278.

[16] N. Fukuishi, S. Murakami, A. Ohno, N. Yamanaka, N. Matsui, K. Fukutsuji, S. Yamada, K. Itoh, M. Akagi, Does β-hexosaminidase function only as a degranulation indicator in mast cells? The primary role of β-hexosaminidase in mast cell granules, The Journal of Immunology 193(4) (2014) 1886-1894.

[17] L. Lu, M. Kulka, L.D. Unsworth, Peptide-mediated mast cell activation: ligand similarities for receptor recognition and protease-induced regulation, Journal of Leukocyte Biology 102(2) (2017) 237-251.

[18] K. Lansu, J. Karpiak, J. Liu, X.-P. Huang, J.D. McCorvy, W.K. Kroeze, T. Che, H. Nagase, F.I. Carroll, J. Jin, In silico design of novel probes for the atypical opioid receptor MRGPRX2, Nature chemical biology 13(5) (2017) 529.

[19] V.B. Reddy, T.A. Graham, E. Azimi, E.A. Lerner, A single amino acid in MRGPRX2 necessary for binding and activation by pruritogens, Journal of Allergy and Clinical Immunology 140(6) (2017) 1726-1728.

[20] G. Grynkiewicz, M. Poenie, R.Y. Tsien, A new generation of Ca2+ indicators with greatly improved fluorescence properties, Journal of biological chemistry 260(6) (1985) 3440-3450.

[21] L. Lu, M.B. Parmar, M. Kulka, P. Kwan, L.D. Unsworth, Self-assembling peptide nanoscaffold that activates human mast cells, ACS applied materials & interfaces 10(7) (2018) 6107-6117.

[22] L. Lu, N. Arizmendi, M. Kulka, L.D. Unsworth, The Spontaneous Adhesion of BMMC onto Self-Assembled Peptide Nanoscaffold without Activation Inhibits Its IgE-Mediated Degranulation, Advanced Healthcare Materials 6(18) (2017) 1700334.

[23] G. Varricchi, A. Pecoraro, S. Loffredo, R. Poto, F. Rivellese, A. Genovese, G. Marone, G. Spadaro, Heterogeneity of human mast cells with respect to MRGPRX2 receptor expression and function, Frontiers in cellular neuroscience 13 (2019) 299.

[24] H.-P. Nothacker, Z. Wang, H. Zeng, S.K. Mahata, D.T. O'Connor, O. Civelli, Proadrenomedullin N-terminal peptide and cortistatin activation of MrgX2 receptor is based on a common structural motif, European journal of pharmacology 519(1-2) (2005) 191-193.

[25] K. Gupta, H. Subramanian, H. Ali, Modulation of host defense peptide-mediated human mast cell activation by LPS, Innate immunity 22(1) (2016) 21-30.

[26] K. Tatemoto, Y. Nozaki, R. Tsuda, S. Kaneko, K. Tomura, M. Furuno, H. Ogasawara, K. Edamura, H. Takagi, H. Iwamura, Endogenous protein and enzyme fragments induce immunoglobulin E-independent activation of mast cells via a G protein-coupled receptor, MRGPRX 2, Scandinavian journal of immunology 87(5) (2018) e12655.

[27] L. Malik, N.M. Kelly, J.-N. Ma, E.A. Currier, E.S. Burstein, R. Olsson, Discovery of non-peptidergic MrgX1 and MrgX2 receptor agonists and exploration of an initial SAR using solid-phase synthesis, Bioorganic & medicinal chemistry letters 19(6) (2009) 1729-1732.

[28] J. Grimes, S. Desai, N.W. Charter, J. Lodge, R. Moita Santos, A. Isidro-Llobet, A.M. Mason, Z. Wu, L.A. Wolfe III, L. Anantharaman, MrgX2 is a promiscuous receptor for basic peptides

causing mast cell pseudo-allergic and anaphylactoid reactions, Pharmacology research & perspectives 7(6) (2019) e00547.

[29] R. Malaviya, T. Ikeda, E. Ross, S.N. Abraham, Mast cell modulation of neutrophil influx and bacterial clearance at sites of infection through TNF-α, Nature 381(6577) (1996) 77-80.

[30] R. Malaviya, S.N. Abraham, Mast cell modulation of immune responses to bacteria, Immunological reviews 179(1) (2001) 16-24.

[31] A. Irani, T.R. Bradford, C.L. Kepley, N.M. Schechter, L.B. Schwartz, Detection of MCT and MCTC types of human mast cells by immunohistochemistry using new monoclonal anti-tryptase and anti-chymase antibodies, Journal of Histochemistry & Cytochemistry 37(10) (1989) 1509-1515.

[32] A.L. Christy, M.E. Walker, M.J. Hessner, M.A. Brown, Mast cell activation and neutrophil recruitment promotes early and robust inflammation in the meninges in EAE, Journal of autoimmunity 42 (2013) 50-61.

[33] K.S.H. Blatman, N. Gonsalves, I. Hirano, P.J. Bryce, Expression of mast cell–associated genes is upregulated in adult eosinophilic esophagitis and responds to steroid or dietary therapy, The Journal of allergy and clinical immunology 127(5) (2011) 1307.

[34] C.V. Velasquez, A.D. Roman, N.T.P. Lan, N.T. Huy, E.S. Mercado, F.E. Espino, M.L.M. Perez, V.T.Q. Huong, T.T. Thuy, V.D. Tham, Alpha tryptase allele of tryptase 1 (TPSAB1) gene associated with dengue hemorrhagic fever (DHF) and dengue shock syndrome (DSS) in Vietnam and Philippines, Human immunology 76(5) (2015) 318-323.

Chapter 6. Conclusion

6.1. Thesis conclusion

In the research described in the thesis, efforts have been made to design materials to respond to and alter the inflammatory cascade using mast cell characteristics. Since mast cells are one of the primary immune cells involved in both innate and adaptive immune response, the material design could be used for a variety of applications including, but not limited to, therapeutic delivery, wound dressing, transplant scaffolds and so on an so forth.

The extensive literature search on mast cell released mediators helped identify several mast cell degranulated biomolecules that are differentially released dependent on stimulant, tissue, diseases and disease severity. Enzymes like tryptase, chymase and β-hexosaminidase are the main enzyme that are secreted by activated mast cells. Each of these enzymes have a well-defined catalytic activity against one or more of their substrate. For example, several peptide substrates were identified on which the tryptase and chymase exerted their activity. Similarly, β-hexosaminidase exerts its activity on colloidal chitin, collagens and hyaluronic acids. Adding to these enzymes, activated mast cells are involved in the *de novo* synthesis of gelatinase, which are involved in the degradation of denatured collagens and gelatins. Apart from enzymes, mast cells also triggers the release of reactive oxygen species (ROS), both within the cells and outside into the extracellular space. ROS are short-lived molecules and hence are always localized around the inflamed tissue.

The mediators identified here are an excellent mast cell derived inflammatory stimuli and such their corresponding substrates offer excellent platform to design inflammatory targeted therapeutic systems. To this effect, ROS was selected as a mast cell derived stimulus in the current project, and emphasis was made to design bioactive materials responsive to ROS. ROS responsive

thioketal (TK) molecule was synthesized and its ROS based activity was studied both *in vitro* and *in vivo*.

TK is a small molecule which was easily synthesized in an overnight reaction with acetone and 3-mercaptopropionic acid. Results showed that TK was stable at physiological pH and exhibited excellent sensitivity to ROS. As explained in the mechanism, TK is cleaved in the presence of ROS to non-toxic molecules. In happening so, the toxic ROS is converted to nontoxic molecules. Consequently, TK exhibits both bioresponive and bioactive traits, in sense that it is cleaved in ROS extensive environment and simultaneously dissipates the deleterious ROS, respectively. The *in vitro* study of TK was done against islets cells, which are highly prone to ROS mediated oxidative damage. Results show that TK was non-cytotoxic to porcine islet cells. TK mitigated the oxidative damage of the cells and maintaining the regular cell functionalities even in the presence of exogenous ROS. Efficacy of TK was further showed *in vivo* where TK incubated islets were syngenically transplanted into mouse models. Transplanted graft restored glycemic control in otherwise diabetic mice and showed improved graft survival rates.

After successful synthesis and characterization, TK was incorporated into biologically inactive polyethylene glycol – polylactic acid (PEG-PLA) copolymer, and polyethylene glycol (PEG) to impart bioresponsiveness to the resulting polymer systems. The formed bioresponsive polymer construct was then used develop a ROS responsive drug delivery platform to deliver the anti-inflammatory dexamethasone (Dex). Dex was conjugated to PEG-PLA block copolymer and PEG through TK as a linker molecule. After successful synthesis and characterization of the constructs, ROS stimulated Dex release was confirmed in stimulated Fenton's reagent ROS solution. Results showed that both PEG-PLA and PEG systems responded to hydroxyl radicals by releasing cleaved Dex from the polymer construct. The release profile was characterized by an expedited release till

5 h, which was then followed by a rather controlled release till 24 h. Nanoparticles were formed from the PEG-PLA constructs. The size of the nanoparticles of the naked PEG-PLA was 132.8 nm while the sizes of Dex conjugated PEG-PLA and its corresponding non-ROS responsive control was 14.2 and 11.9 nm respectively. Zeta potential measurement of all the nanoparticles gave a -ve potential, which is characteristics of the PEG shell. The nanoparticles were further subjected to Fenton's reagent to confirm Dex release. Where, control did not show any release, Dex concentration in the release medium from the ROS responsive constructs were found to be 7.5 and 9 μM respectively. With the proof of concept study, the designed system is an excellent platform to be used for the targeted delivery of anti-inflammatory drug in varied therapeutic applications.

The goal of targeted therapies, apart from designing bioresponsive materials specific to the tissue microenvironment, can also be achieved by specific cell targeting peptides. Since mast cells specifically expresses mas related G-protein receptor X2 (MRGPRX2), a design rule was derived for peptide ligands which would specifically bind to the mast cell MRGPRX2 receptor. Peptide ligands specific to MRGPRX2 follows a generic rule of X_a-$(Y)_{(n \geq 3)}$-X_b where: X_a is an aromatic residue; X_b is a hydrophobic residue; and Y is a minimum 3 residue long sequence, containing a minimum of one positively charged residue with the remainder being uncharged residues. Through modulation of the design rule, several peptides with varying mast cell activity was designed for therapeutic applications. These peptides can serve as excellent mast cell targeting peptides with an additional benefit of regulated mast cell activation [1].

6.2. Future work and recommendations

Design of materials to stimulus other than ROS

This study explored ROS as mast cell specific stimulus. However, as discussed in Chapter 1, other mast cell released mediators like tryptase, chymase, β-hexosamindase and gelatinase could also be used as inflammatory stimulus and can be used to design inflammatory responsive material for different modalities.

Modification of TK with varying functional groups

In the present study, TK with carboxylic acid functional groups was synthesized. TK was used to link PEG-PLA and PEG with Dex through their respective hydroxyl groups. Esterification between the carboxyl group of the TK and hydroxyl group of PEG-PLA, PEG and Dex facilitated the conjugation. However, esterification may not be a versatile bioconjugation approach, and a need may arise to incorporate other functional groups in modified TK for other therapeutic drugs. In the interest, TK with functional groups like hydroxyl, thiol, amines, and double bonds have been synthesized and used in varying applications (Figure 2.5) [2–4]. In addition, TK with one carboxylic and one amine group has also been synthesized [5].

Design of bioresponsvie platforms

ROS responsive TK was used to design nanoassemblies in the present study. However, TK is versatile in the sense it could be used to design other platforms as well. The bifunctional TK could be very efficiently used as cross linker to design ROS responsive hydrogels. Similarly, it can be incorporated in fibrous mats to impart bioresponsiveness. TK has also been used as a monomer to design a polymeric material [6].

Therapeutic use of ROS responsive dexamethasone delivery system

Dex sits at the cornerstone of anti-inflammatory drugs. It is prescribed for almost every inflammatory complications, be it eye disease, ear disease, asthma, skin allergies or transplantation [7]. However, Dex is often associated with unwanted side effects. In this regards, the designed PLA-TD nanoassembly would have high therapeutic importance. It would not only target the inflamed tissue but also control the release of Dex to minimize the side effects. Further, the conjugation of PEG to Dex increases the solubility of otherwise insoluble Dex in water.

Co-delivery of multiple therapeutics

PLA-TD is an excellent amphiphilic system where PLA, together with Dex forms the hydrophobic core and PEG forms the hydrophilic shell. Consequently, the hydrophobic core could be used to encapsulate one or more of other therapeutics for the simultaneous delivery of Dex and the loaded active component.

6.3. References

[1] L. Lu, S. Raj, N. Arizmendi, J. Ding, G. Eitzen, P. Kwan, M. Kulka, L.D. Unsworth, Identification of short peptide sequences that activate human mast cells via mas-related g-protein coupled receptor member x2, Acta Biomaterialia. 136 (2021) 159–169.

[2] C. Yue, Y. Yang, C. Zhang, G. Alfranca, S. Cheng, L. Ma, Y. Liu, X. Zhi, J. Ni, W. Jiang, J. Song, J.M. de la Fuente, D. Cui, ROS-responsive mitochondria-targeting blended nanoparticles: Chemo- and photodynamic synergistic therapy for lung cancer with on-demand drug release upon irradiation with a single light source, Theranostics. 6 (2016) 2352–2366. https://doi.org/10.7150/thno.15433.

[3] D. Chen, G. Zhang, R. Li, M. Guan, X. Wang, T. Zou, Y. Zhang, C. Wang, C. Shu, H. Hong, L.J. Wan, Biodegradable, Hydrogen Peroxide, and Glutathione Dual Responsive Nanoparticles for Potential Programmable Paclitaxel Release, Journal of the American Chemical Society. 140 (2018) 7373–7376. https://doi.org/10.1021/jacs.7b12025.

[4] J. Wang, X. He, S. Shen, Z. Cao, X. Yang, ROS-Sensitive Cross-Linked Polyethylenimine for Red-Light-Activated siRNA Therapy, ACS Applied Materials and Interfaces. 11 (2019) 1855–1863. https://doi.org/10.1021/acsami.8b18697.

[5] X. Ling, S. Zhang, P. Shao, P. Wang, X. Ma, M. Bai, Synthesis of a reactive oxygen species responsive heterobifunctional thioketal linker, Tetrahedron Letters. 56 (2015) 5242–5244. https://doi.org/10.1016/j.tetlet.2015.07.059.

[6] D.S. Wilson, G. Dalmasso, L. Wang, S. v. Sitaraman, D. Merlin, N. Murthy, Orally delivered thioketal nanoparticles loaded with TNF-α-siRNA target inflammation and inhibit gene expression in the intestines, Nature Materials. 9 (2010) 923–928. https://doi.org/10.1038/nmat2859.

[7] P.J. Barnes, How corticosteroids control inflammation: quintiles prize lecture 2005, British Journal of Pharmacology. 148 (2006) 245–254.

Reference

Chapter 1

[1] J.A. Owen, J. Punt, S.A. Stranford, Kuby immunology, WH Freeman New York, NY, USA:, 2013.

[2] E.Z.M. da Silva, M.C. Jamur, C. Oliver, Mast cell function: a new vision of an old cell, Journal of Histochemistry & Cytochemistry. 62 (2014) 698–738.

[3] S.J. Galli, S. Nakae, M. Tsai, Mast cells in the development of adaptive immune responses, Nature Immunology. 6 (2005) 135.

[4] S. Wernersson, G. Pejler, Mast cell secretory granules: armed for battle, Nature Reviews Immunology. 14 (2014) 478.

[5] A.M. Gilfillan, C. Tkaczyk, Integrated signalling pathways for mast-cell activation, Nature Reviews Immunology. 6 (2006) 218–230. https://doi.org/10.1038/nri1782.

[6] B.D. McNeil, P. Pundir, S. Meeker, L. Han, B.J. Undem, M. Kulka, X. Dong, Identification of a mast-cell-specific receptor crucial for pseudo-allergic drug reactions, Nature. 519 (2015) 237–241. https://doi.org/10.1038/nature14022.

[7] H. Subramanian, K. Gupta, H. Ali, Roles of Mas-related G protein–coupled receptor X2 on mast cell–mediated host defense, pseudoallergic drug reactions, and chronic inflammatory diseases, Journal of Allergy and Clinical Immunology. 138 (2016) 700–710.

[8] T. Yoshimaru, Y. Suzuki, T. Inoue, S. Nishida, C. Ra, Extracellular superoxide released from mitochondria mediates mast cell death by advanced glycation end products, Biochimica et

Biophysica Acta (BBA) - Molecular Cell Research. 1783 (2008) 2332–2343. https://doi.org/10.1016/j.bbamcr.2008.08.010.

[9] T.C. Moon, A. Dean Befus, M. Kulka, Mast cell mediators: Their differential release and the secretory pathways involved, Frontiers in Immunology. 5 (2014) 1–18. https://doi.org/10.3389/fimmu.2014.00569.

[10] H. Hamada, M. Terai, H. Kimura, K. Hirano, S. Oana, H. Niimi, Increased expression of mast cell chymase in the lungs of patients with congenital heart disease associated with early pulmonary vascular disease, American Journal of Respiratory and Critical Care Medicine. 160 (1999) 1303–1308. https://doi.org/10.1164/ajrccm.160.4.9810058.

[11] S. Balzar, M.L. Fajt, S.A.A. Comhair, S.C. Erzurum, E. Bleecker, W.W. Busse, M. Castro, B. Gaston, E. Israel, L.B. Schwartz, D. Curran-Everett, C.G. Moore, S.E. Wenzel, Mast cell phenotype, location, and activation in severe asthma: Data from the Severe Asthma Research Program, American Journal of Respiratory and Critical Care Medicine. 183 (2011) 299–309. https://doi.org/10.1164/rccm.201002-0295OC.

[12] M.G. Buckley, P.J. Gallagher, A.F. Walls, Mast cell subpopulations in the synovial tissue of patients with osteoarthritis: Selective increase in numbers of tryptase-positive, chymase- negative mast cells, Journal of Pathology. 186 (1998) 67–74. https://doi.org/10.1002/(SICI)1096-9896(199809)186:1<67::AID-PATH132>3.0.CO;2-D.

[13] A. Järvikallio, A. Naukkarinen, I.T. Harvima, M.L. Aalto, M. Horsmanheimo, Quantitative analysis of tryptase- and chymase-containing mast cells in atopic dermatitis and nummular

eczema, British Journal of Dermatology. 136 (1997) 871–877. https://doi.org/10.1111/j.1365-2133.1997.tb03927.x.

[14] J.P. Kankkunen, I.T. Harvima, A. Naukkarinen, Quantitative analysis of tryptase and chymase containing mast cells in benign and malignant breast lesions, International Journal of Cancer. 72 (1997) 385–388. https://doi.org/10.1002/(SICI)1097-0215(19970729)72:3<385::AID-IJC1>3.0.CO;2-L.

[15] M. Yamada, M. Ueda, T. Naruko, S. Tanabe, Y.S. Han, Y. Ikura, M. Ogami, S. Takai, M. Miyazaki, Mast cell chymase expression and mast cell phenotypes in human rejected kidneys, Kidney International. 59 (2001) 1374–1381. https://doi.org/10.1046/j.1523-1755.2001.0590041374.x.

[16] S. Municoy, M.I. Álvarez Echazú, P.E. Antezana, J.M. Galdopórpora, C. Olivetti, A.M. Mebert, M.L. Foglia, M. v Tuttolomondo, G.S. Alvarez, J.G. Hardy, Stimuli-responsive materials for tissue engineering and drug delivery, International Journal of Molecular Sciences. 21 (2020) 4724.

[17] J. Li, C. Sun, W. Tao, Z. Cao, H. Qian, X. Yang, J. Wang, Photoinduced PEG deshielding from ROS-sensitive linkage-bridged block copolymer-based nanocarriers for on-demand drug delivery, Biomaterials. 170 (2018) 147–155. https://doi.org/10.1016/j.biomaterials.2018.04.015.

[18] F. Zhang, X. Huang, L. Zhu, N. Guo, G. Niu, M. Swierczewska, S. Lee, H. Xu, A.Y. Wang, K.A. Mohamedali, M.G. Rosenblum, G. Lu, X. Chen, Noninvasive monitoring of orthotopic glioblastoma therapy response using RGD-conjugated iron oxide nanoparticles, Biomaterials. 33 (2012) 5414–5422. https://doi.org/10.1016/j.biomaterials.2012.04.032.

Chapter 2

[1] J.S. Marshall, Mast-cell responses to pathogens, Nature Reviews Immunology. 4 (2004) 787–799. https://doi.org/10.1038/nri1460.

[2] M. Urb, D.C. Sheppard, The role of mast cells in the defence against pathogens, PLoS Pathogens. 8 (2012) 2–4. https://doi.org/10.1371/journal.ppat.1002619.

[3] C. Benoist, D. Mathis, Mast cells in autoimmune disease, Nature. 420 (2002) 875–878.

[4] S.J. Galli, M. Tsai, IgE and mast cells in allergic disease, Nature Medicine. 18 (2012) 693–704. https://doi.org/10.1038/nm.2755.

[5] C. Zimmermann, D. Troeltzsch, V.A. Giménez-Rivera, S.J. Galli, M. Metz, M. Maurer, F. Siebenhaar, Mast cells are critical for controlling the bacterial burden and the healing of infected wounds, Proceedings of the National Academy of Sciences of the United States of America. 116 (2019) 20500–20504. https://doi.org/10.1073/pnas.1908816116.

[6] S. Balzar, H.W. Chu, M. Strand, S. Wenzel, Relationship of small airway chymase-positive mast cells and lung function in severe asthma, American Journal of Respiratory and Critical Care Medicine. 171 (2005) 431–439. https://doi.org/10.1164/rccm.200407-949OC.

[7] H. Hamada, M. Terai, H. Kimura, K. Hirano, S. Oana, H. Niimi, Increased expression of mast cell chymase in the lungs of patients with congenital heart disease associated with early pulmonary vascular disease, American Journal of Respiratory and Critical Care Medicine. 160 (1999) 1303–1308. https://doi.org/10.1164/ajrccm.160.4.9810058.

[8] A. Järvikallio, A. Naukkarinen, I.T. Harvima, M.L. Aalto, M. Horsmanheimo, Quantitative analysis of tryptase- and chymase-containing mast cells in atopic dermatitis and nummular eczema, British Journal of Dermatology. 136 (1997) 871–877. https://doi.org/10.1111/j.1365-2133.1997.tb03927.x.

[9] M.G. Buckley, P.J. Gallagher, A.F. Walls, Mast cell subpopulations in the synovial tissue of patients with osteoarthritis: Selective increase in numbers of tryptase-positive, chymase- negative mast cells, Journal of Pathology. 186 (1998) 67–74. https://doi.org/10.1002/(SICI)1096-9896(199809)186:1<67::AID-PATH132>3.0.CO;2-D.

[10] J.P. Kankkunen, I.T. Harvima, A. Naukkarinen, Quantitative analysis of tryptase and chymase containing mast cells in benign and malignant breast lesions, International Journal of Cancer. 72 (1997) 385–388. https://doi.org/10.1002/(SICI)1097-0215(19970729)72:3<385::AID-IJC1>3.0.CO;2-L.

[11] T. Ibaraki, M. Muramatsu, S. Takai, D. Jin, H. Maruyama, T. Orino, T. Katsumata, M. Miyazaki, The relationship of tryptase- and chymase-positive mast cells to angiogenesis in stage I non-small cell lung cancer, European Journal of Cardio-Thoracic Surgery. 28 (2005) 617–621. https://doi.org/10.1016/j.ejcts.2005.06.020.

[12] G. Varricchi, G. Marone, P.T. Kovanen, Cardiac Mast Cells: Underappreciated Immune Cells in Cardiovascular Homeostasis and Disease, Trends in Immunology. 41 (2020) 734–746. https://doi.org/10.1016/j.it.2020.06.006.

[13] M. Yamada, M. Ueda, T. Naruko, S. Tanabe, Y.S. Han, Y. Ikura, M. Ogami, S. Takai, M. Miyazaki, Mast cell chymase expression and mast cell phenotypes in human rejected kidneys,

Kidney International. 59 (2001) 1374–1381. https://doi.org/10.1046/j.1523-1755.2001.0590041374.x.

[14] S. Wernersson, G. Pejler, Mast cell secretory granules: armed for battle, Nature Reviews Immunology. 14 (2014) 478.

[15] J. Kalesnikoff, S.J. Galli, New developments in mast cell biology, Nature Immunology. 9 (2008) 1215–1223. https://doi.org/10.1038/ni.f.216.

[16] T.C. Moon, A. Dean Befus, M. Kulka, Mast cell mediators: Their differential release and the secretory pathways involved, Frontiers in Immunology. 5 (2014) 1–18. https://doi.org/10.3389/fimmu.2014.00569.

[17] N. di Girolamo, I. Indoh, N. Jackson, D. Wakefield, H.P. McNeil, W. Yan, C. Geczy, J.P. Arm, N. Tedla, Human Mast Cell-Derived Gelatinase B (Matrix Metalloproteinase-9) Is Regulated by Inflammatory Cytokines: Role in Cell Migration, The Journal of Immunology. 177 (2006) 2638–2650. https://doi.org/10.4049/jimmunol.177.4.2638.

[18] T. Inoue, Y. Suzuki, T. Yoshimaru, C. Ra, Reactive oxygen species produced up- or downstream of calcium influx regulate proinflammatory mediator release from mast cells: Role of NADPH oxidase and mitochondria, Biochimica et Biophysica Acta - Molecular Cell Research. 1783 (2008) 789–802. https://doi.org/10.1016/j.bbamcr.2007.12.004.

[19] T. Inoue, Y. Suzuki, C. Ra, Epigallocatechin-3-gallate induces cytokine production in mast cells by stimulating an extracellular superoxide-mediated calcium influx, Biochemical Pharmacology. 82 (2011) 1930–1939. https://doi.org/10.1016/j.bcp.2011.09.011.

[20] S.J. Galli, S. Nakae, M. Tsai, Mast cells in the development of adaptive immune responses, Nature Immunology. 6 (2005) 135.

[21] A.M. Gilfillan, C. Tkaczyk, Integrated signalling pathways for mast-cell activation, Nature Reviews Immunology. 6 (2006) 218–230. https://doi.org/10.1038/nri1782.

[22] T. Yoshimaru, Y. Suzuki, T. Inoue, S. Nishida, C. Ra, Extracellular superoxide released from mitochondria mediates mast cell death by advanced glycation end products, Biochimica et Biophysica Acta (BBA) - Molecular Cell Research. 1783 (2008) 2332–2343. https://doi.org/10.1016/j.bbamcr.2008.08.010.

[23] B.D. McNeil, P. Pundir, S. Meeker, L. Han, B.J. Undem, M. Kulka, X. Dong, Identification of a mast-cell-specific receptor crucial for pseudo-allergic drug reactions, Nature. 519 (2015) 237–241. https://doi.org/10.1038/nature14022.

[24] W. Manorak, C. Idahosa, K. Gupta, S. Roy, R. Panettieri, H. Ali, Upregulation of Mas-related G Protein coupled receptor X2 in asthmatic lung mast cells and its activation by the novel neuropeptide hemokinin-1, Respiratory Research. 19 (2018) 1–5.

[25] H. Subramanian, K. Gupta, H. Ali, Roles of Mas-related G protein–coupled receptor X2 on mast cell–mediated host defense, pseudoallergic drug reactions, and chronic inflammatory diseases, Journal of Allergy and Clinical Immunology. 138 (2016) 700–710.

[26] L. Lu, M.B. Parmar, M. Kulka, P. Kwan, L.D. Unsworth, Self-Assembling Peptide Nanoscaffold That Activates Human Mast Cells, ACS Applied Materials and Interfaces. 10 (2018) 6107–6117. https://doi.org/10.1021/acsami.7b14560.

[27] L.B. Schwartz, K.F. Austen, Enzymes of the mast cell granule, Journal of Investigative Dermatology. 74 (1980) 349–353.

[28] L.B. Schwartz, K.F. Austen, S.I. Wasserman, Immunologic release of β-hexosaminidase and β-glucuronidase from purified rat serosal mast cells, The Journal of Immunology. 123 (1979) 1445–1450.

[29] L.B. Schwartz, R.A. Lewis, D. Seldin, K.F. Austen, Acid hydrolases and tryptase from secretory granules of dispersed human lung mast cells., The Journal of Immunology. 126 (1981) 1290–1294.

[30] Z. Xiang, M. Block, C. Löfman, G. Nilsson, Ige-mediated mast cell degranulation and recovery monitored by time-lapse photography, Journal of Allergy and Clinical Immunology. 108 (2001) 116–121. https://doi.org/10.1067/mai.2001.116124.

[31] L.B. Schwartz, A.M. Irani, K. Roller, M.C. Castells, N.M. Schechter, Quantitation of histamine, tryptase, and chymase in dispersed human T and TC mast cells., The Journal of Immunology. 138 (1987) 2611–2615.

[32] L.B. Schwartz, H.-K. Min, S. Ren, H.-Z. Xia, J. Hu, W. Zhao, G. Moxley, Y. Fukuoka, Tryptase Precursors Are Preferentially and Spontaneously Released, Whereas Mature Tryptase Is Retained by HMC-1 Cells, Mono-Mac-6 Cells, and Human Skin-Derived Mast Cells, The Journal of Immunology. 170 (2003) 5667–5673. https://doi.org/10.4049/jimmunol.170.11.5667.

[33] S. Jogie-Brahim, H.K. Min, Y. Fukuoka, H.Z. Xia, L.B. Schwartz, Expression of α-tryptase and β-tryptase by human basophils, Journal of Allergy and Clinical Immunology. 113 (2004) 1086–1092. https://doi.org/10.1016/j.jaci.2004.02.032.

[34] S. Balzar, M.L. Fajt, S.A.A. Comhair, S.C. Erzurum, E. Bleecker, W.W. Busse, M. Castro, B. Gaston, E. Israel, L.B. Schwartz, D. Curran-Everett, C.G. Moore, S.E. Wenzel, Mast cell phenotype, location, and activation in severe asthma: Data from the Severe Asthma Research Program, American Journal of Respiratory and Critical Care Medicine. 183 (2011) 299–309. https://doi.org/10.1164/rccm.201002-0295OC.

[35] A. Zanini, A. Chetta, M. Saetta, S. Baraldo, R. D'Ippolito, A. Castagnaro, M. Neri, D. Olivieri, Chymase-positive mast cells play a role in the vascular component of airway remodeling in asthma, Journal of Allergy and Clinical Immunology. 120 (2007) 329–333. https://doi.org/10.1016/j.jaci.2007.04.021.

[36] C.K. Andersson, M. Mori, L. Bjermer, C.G. Löfdahl, J.S. Erjefält, Alterations in lung mast cell populations in patients with chronic obstructive pulmonary disease, American Journal of Respiratory and Critical Care Medicine. 181 (2010) 206–217. https://doi.org/10.1164/rccm.200906-0932OC.

[37] B. Hermes, I. Feldmann-Böddeker, P. Welker, B. Algermissen, M.U. Steckelings, J. Grabbe, B.M. Henz, Altered expression of mast cell chymase and tryptase and of c-Kit in human cutaneous scar tissue, Journal of Investigative Dermatology. 114 (2000) 51–55. https://doi.org/10.1046/j.1523-1747.2000.00837.x.

[38] R. Zhang, V.L.Y. Yip, S.G. Withers, Mechanisms of enzymatic glycosyl transfer, (2010).

[39] I.C. Koo, Y.M. Ohol, P. Wu, J.H. Morisaki, J.S. Cox, E.J. Brown, Role for lysosomal enzyme β-hexosaminidase in the control of mycobacteria infection, Proceedings of the National Academy of

Sciences of the United States of America. 105 (2008) 710–715. https://doi.org/10.1073/pnas.0708110105.

[40] N. Fukuishi, S. Murakami, A. Ohno, N. Yamanaka, N. Matsui, K. Fukutsuji, S. Yamada, K. Itoh, M. Akagi, Does β-Hexosaminidase Function Only as a Degranulation Indicator in Mast Cells? The Primary Role of β-Hexosaminidase in Mast Cell Granules, The Journal of Immunology. 193 (2014) 1886–1894. https://doi.org/10.4049/jimmunol.1302520.

[41] E. Trevisan, F. Vita, N. Medic, M.R. Soranzo, G. Zabucchi, V. Borelli, Mast Cells Kill Candida albicans in the Extracellular Environment but Spare Ingested Fungi from Death, Inflammation. 37 (2014) 2174–2189. https://doi.org/10.1007/s10753-014-9951-9.

[42] J.P. Lopes, M. Stylianou, G. Nilsson, C.F. Urban, Opportunistic pathogen Candida albicans elicits a temporal response in primary human mast cells, Scientific Reports. 5 (2015) 1–14. https://doi.org/10.1038/srep12287.

[43] W. Suginta, D. Chuenark, M. Mizuhara, T. Fukamizo, Novel β-N-acetylglucosaminidases from Vibrio harveyi 650: Cloning, expression, enzymatic properties, and subsite identification, BMC Biochemistry. 11 (2010). https://doi.org/10.1186/1471-2091-11-40.

[44] N. Konno, H. Takahashi, M. Nakajima, T. Takeda, Y. Sakamoto, Characterization of β-N-acetylhexosaminidase (LeHex20A), a member of glycoside hydrolase family 20, from Lentinula edodes (shiitake mushroom), AMB Express. 2 (2012) 1–7. https://doi.org/10.1186/2191-0855-2-29.

[45] Q. Yang, T. Liu, F. Liu, M. Qu, X. Qian, A novel β-N-acetyl-d-hexosaminidase from the insect Ostrinia furnacalis (Guenée), FEBS Journal. 275 (2008) 5690–5702. https://doi.org/10.1111/j.1742-4658.2008.06695.x.

[46] S. Katta, S. Ankati, A.R. Podile, Chitooligosaccharides are converted to N-acetylglucosamine by N-acetyl-β-hexosaminidase from stenotrophomonas maltophilia, FEMS Microbiology Letters. 348 (2013) 19–25. https://doi.org/10.1111/1574-6968.12237.

[47] N.O. Keyhani, S. Roseman, The chitin catabolic cascade in the marine bacterium vibrio furnissii: Molecular cloning, isolation, and characterization of a periplasmic β-N-acetylglucosaminidase, Journal of Biological Chemistry. 271 (1996) 33425–33432. https://doi.org/10.1074/jbc.271.52.33425.

[48] F. Nanjo, R. Katsumi, K. Sakai, Purification and characterization of an Exo-β-D-glucosaminidase, a novel type of enzyme, from nocardia orientalis, Journal of Biological Chemistry. 265 (1990) 10088–10094. https://doi.org/10.1016/s0021-9258(19)38783-6.

[49] L. Gushulak, R. Hemming, D. Martin, V. Seyrantepe, A. Pshezhetsky, B. Triggs-Raine, Hyaluronidase 1 and β-hexosaminidase have redundant functions in hyaluronan and chondroitin sulfate degradation, Journal of Biological Chemistry. 287 (2012) 16689–16697. https://doi.org/10.1074/jbc.M112.350447.

[50] S.M. Lim, D.K. Song, S.H. Oh, D.S. Lee-Yoon, E.H. Bae, J.H. Lee, In vitro and in vivo degradation behavior of acetylated chitosan porous beads, Journal of Biomaterials Science, Polymer Edition. 19 (2008) 453–466. https://doi.org/10.1163/156856208783719482.

[51] F. Liaqat, R. Eltem, Chitooligosaccharides and their biological activities: A comprehensive review, Carbohydrate Polymers. 184 (2018) 243–259.

[52] C. Chatelet, O. Damour, A. Domard, Influence of the degree of acetylation on some biological properties of chitosan films, Biomaterials. 22 (2001) 261–268. https://doi.org/10.1016/S0142-9612(00)00183-6.

[53] L.F. Boesel, R.L. Reis, J.S. Román, Innovative approach for producing injectable, biodegradable materials using chitooligosaccharides and green chemistry, Biomacromolecules. 10 (2009) 465–470. https://doi.org/10.1021/bm801332u.

[54] D.N. Gosalia, C.M. Salisbury, J.A. Ellman, S.L. Diamond, High throughput substrate specificity profiling of serine and cysteine proteases using solution-phase fluorogenic peptide microarrays, Molecular and Cellular Proteomics. 4 (2005) 626–636. https://doi.org/10.1074/mcp.M500004-MCP200.

[55] J.J. Perona, C.S. Craik, Structural basis of substrate specificity in the serine proteases, Protein Science. 4 (1995) 337–360.

[56] J.L. Harris, A. Niles, K. Burdick, M. Maffitt, B.J. Backes, J.A. Ellman, I. Kuntz, M. Haak-Frendscho, C.S. Craik, Definition of the Extended Substrate Specificity Determinants for β-Tryptases I and II, Journal of Biological Chemistry. 276 (2001) 34941–34947. https://doi.org/10.1074/jbc.M102997200.

[57] B. Spichalska, A. Lesner, M. Wysocka, M. Śledź, A. Łęgowska, A. Jaśkiewicz, H. Miecznikowska, K. Rolka, The influence of substrate peptide length on human β-tryptase

specificity, Journal of Peptide Science: An Official Publication of the European Peptide Society. 14 (2008) 917–923.

[58] S.T. Furlong, R.C. Mauger, A.M. Strimpler, Y.P. Liu, F.X. Morris, P.D. Edwards, Synthesis and physical characterization of a P1 arginine combinatorial library, and its application to the determination of the substrate specificity of serine peptidases, Bioorganic and Medicinal Chemistry. 10 (2002) 3637–3647. https://doi.org/10.1016/S0968-0896(02)00174-8.

[59] J.A. Cromlish, N.G. Seidah, M. Marcinkiewicz, J. Hamelin, D.A. Johnson, M. Chrétien, Human pituitary tryptase: Molecular forms, NH2-terminal sequence, immunocytochemical localization, and specificity with prohormone and fluorogenic substrates, Journal of Biological Chemistry. 262 (1987) 1363–1373. https://doi.org/10.1016/s0021-9258(19)75795-0.

[60] M. Wysocka, B. Spichalska, A. Lesner, M. Jaros, K. Brzozowski, A. Łęgowska, K. Rolka, Substrate specificity and inhibitory study of human airway trypsin-like protease, Bioorganic & Medicinal Chemistry. 18 (2010) 5504–5509.

[61] T. Tanaka, B.J. McRae, K. Cho, R. Cook, J.E. Fraki, D.A. Johnson, J.C. Powers, Mammalian Tissue Trypsin-like Enzymes, Journal of Biological Chemistry. 258 (1983) 13552–13557.

[62] M. Poe, C.D. Bennett, W.E. Biddison, J.T. Blake, G.P. Norton, J.A. Rodkey, N.H. Sigal, R. v. Turner, J.K. Wu, H.J. Zweerink, Human cytotoxic lymphocyte tryptase. Its purification from granules and the characterization of inhibitor and substrate specificity, Journal of Biological Chemistry. 263 (1988) 13215–13222. https://doi.org/10.1016/s0021-9258(18)37694-4.

[63] W.W. Raymond, S. Waugh Ruggles, C.S. Craik, G.H. Caughey, Albumin is a substrate, of human chymase: Prediction by combinatorial peptide screening and development of a selective inhibitor

based on the albumin cleavage site, Journal of Biological Chemistry. 278 (2003) 34517–34524. https://doi.org/10.1074/jbc.M304087200.

[64] M. Bastos, N.J. Maeji, R.H. Abeles, Inhibitors of human heart chymase based on a peptide library, Proceedings of the National Academy of Sciences of the United States of America. 92 (1995) 6738–6742. https://doi.org/10.1073/pnas.92.15.6738.

[65] A. Kinoshita, H. Urata, F.M. Bumpus, A. Husain, Multiple determinants for the high substrate specificity of an angiotensin II-forming chymase from the human heart, Journal of Biological Chemistry. 266 (1991) 19192–19197. https://doi.org/10.1016/s0021-9258(18)54981-4.

[66] S. Sanker, U.M. Chandrasekharan, D. Wilk, M.J. Glynias, S.S. Karnik, A. Husain, Distinct multisite synergistic interactions determine substrate specificities of human chymase and rat chymase-1 for angiotensin II formation and degradation, Journal of Biological Chemistry. 272 (1997) 2963–2968. https://doi.org/10.1074/jbc.272.5.2963.

[67] H. Urata, A. Kinoshita, K.S. Misono, F.M. Bumpus, A. Husain, Identification of a highly specific chymase as the major angiotensin II-forming enzyme in the human heart, Journal of Biological Chemistry. 265 (1990) 22348–22357. https://doi.org/10.1016/s0021-9258(18)45712-2.

[68] S. Ahmad, K.N. Wright, X. Sun, L. Groban, C.M. Ferrario, Mast cell peptidases (carboxypeptidase A and chymase)-mediated hydrolysis of human angiotensin-(1–12) substrate, Biochemical and Biophysical Research Communications. 518 (2019) 651–656. https://doi.org/10.1016/j.bbrc.2019.08.098.

[69] M.K. Andersson, M. Enoksson, M. Gallwitz, L. Hellman, The extended substrate specificity of the human mast cell chymase reveals a serine protease with well-defined substrate recognition profile, International Immunology. 21 (2009) 95–104. https://doi.org/10.1093/intimm/dxn128.

[70] J.C. Powers, T. Tanaka, J.W. Harper, Y. Minematsu, L. Barker, D. Lincoln, K. v Crumley, J.E. Fraki, N.M. Schechter, Mammalian chymotrypsin-like enzymes. Comparative reactivities of rat mast cell proteases, human and dog skin chymases, and human cathepsin G with peptide 4-nitroanilide substrates and with peptide chloromethyl ketone and sulfonyl fluoride inhibitors, Biochemistry. 24 (1985) 2048–2058.

[71] M.K. Andersson, M. Thorpe, L. Hellman, Arg143 and Lys192 of the human mast cell chymase mediate the preference for acidic amino acids in position P2′ of substrates, FEBS Journal. 277 (2010) 2255–2267. https://doi.org/10.1111/j.1742-4658.2010.07642.x.

[72] B. Korkmaz, G. Jégot, L.C. Lau, M. Thorpe, E. Pitois, L. Juliano, A.F. Walls, L. Hellman, F. Gauthier, Discriminating between the activities of human cathepsin G and chymase using fluorogenic substrates, The FEBS Journal. 278 (2011) 2635–2646.

[73] N. Lingwal, M. Padmasekar, B. Samikannu, R.G. Bretzel, K.T. Preissner, T. Linn, Inhibition of gelatinase B (matrix metalloprotease-9) activity reduces cellular inflammation and restores function of transplanted pancreatic islets, Diabetes. 61 (2012) 2045–2053. https://doi.org/10.2337/db11-1143.

[74] E. Kolaczkowska, B. Arnold, G. Opdenakker, Gelatinase B/MMP-9 as an inflammatory marker enzyme in mouse zymosan peritonitis: Comparison of phase-specific and cell-specific production

by mast cells, macrophages and neutrophils, Immunobiology. 213 (2008) 109–124. https://doi.org/10.1016/j.imbio.2007.07.005.

[75] C.N. Loynachan, A.P. Soleimany, J.S. Dudani, Y. Lin, A. Najer, A. Bekdemir, Q. Chen, S.N. Bhatia, M.M. Stevens, Renal clearable catalytic gold nanoclusters for in vivo disease monitoring, Nature Nanotechnology. 14 (2019) 883–890. https://doi.org/10.1038/s41565-019-0527-6.

[76] J. Pugin, M.C. Widmer, S. Kossodo, C.M. Liang, H.L. Preas, A.F. Suffredini, Human neutrophils secrete gelatinase B in vitro and in vivo in response to endotoxin and proinflammatory mediators, American Journal of Respiratory Cell and Molecular Biology. 20 (1999) 458–464. https://doi.org/10.1165/ajrcmb.20.3.3311.

[77] N. Kanbe, A. Tanaka, M. Kanbe, A. Itakura, M. Kurosawa, H. Matsuda, Human mast cells produce matrix metalloproteinase 9, European Journal of Immunology. 29 (1999) 2645–2649.

[78] H. Trøstrup, P. Holstein, T. Karlsmark, C. Moser, M.S. Ågren, Uncontrolled gelatin degradation in non-healing chronic wounds, Journal of Wound Care. 27 (2018) 724–734. https://doi.org/10.12968/jowc.2018.27.11.724.

[79] N. Lingwal, M. Padmasekar, B. Samikannu, R.G. Bretzel, K.T. Preissner, T. Linn, Inhibition of gelatinase B (matrix metalloprotease-9) activity reduces cellular inflammation and restores function of transplanted pancreatic islets, Diabetes. 61 (2012) 2045–2053.

[80] M. Santoro, A.M. Tatara, A.G. Mikos, Gelatin carriers for drug and cell delivery in tissue engineering, Journal of Controlled Release. 190 (2014) 210–218.

[81] D. Olsen, C. Yang, M. Bodo, R. Chang, S. Leigh, J. Baez, D. Carmichael, M. Perälä, E.-R. Hämäläinen, M. Jarvinen, Recombinant collagen and gelatin for drug delivery, Advanced Drug Delivery Reviews. 55 (2003) 1547–1567.

[82] U. Eckhard, P.F. Huesgen, O. Schilling, C.L. Bellac, G.S. Butler, J.H. Cox, A. Dufour, V. Goebeler, R. Kappelhoff, U. auf dem Keller, Active site specificity profiling of the matrix metalloproteinase family: Proteomic identification of 4300 cleavage sites by nine MMPs explored with structural and synthetic peptide cleavage analyses, Matrix Biology. 49 (2016) 37–60.

[83] B.I. Ratnikov, P. Cieplak, K. Gramatikoff, J. Pierce, A. Eroshkin, Y. Igarashi, M. Kazanov, Q. Sun, A. Godzik, A. Osterman, Basis for substrate recognition and distinction by matrix metalloproteinases, Proceedings of the National Academy of Sciences. 111 (2014) E4148–E4155.

[84] S.J. Kridel, E. Chen, L.P. Kotra, E.W. Howard, S. Mobashery, J.W. Smith, Substrate hydrolysis by matrix metalloproteinase-9, Journal of Biological Chemistry. 276 (2001) 20572–20578.

[85] N. Singh, A. Karambelkar, L. Gu, K. Lin, J.S. Miller, C.S. Chen, M.J. Sailor, S.N. Bhatia, Bioresponsive mesoporous silica nanoparticles for triggered drug release, Journal of the American Chemical Society. 133 (2011) 19582–19585. https://doi.org/10.1021/ja206998x.

[86] B. Grünwald, J. Vandooren, E. Locatelli, P. Fiten, G. Opdenakker, P. Proost, A. Krüger, J.P. Lellouche, L.L. Israel, L. Shenkman, M. Comes Franchini, Matrix metalloproteinase-9 (MMP-9) as an activator of nanosystems for targeted drug delivery in pancreatic cancer, Journal of Controlled Release. 239 (2016) 39–48. https://doi.org/10.1016/j.jconrel.2016.08.016.

[87] M.M. Nguyen, A.S. Carlini, M.P. Chien, S. Sonnenberg, C. Luo, R.L. Braden, K.G. Osborn, Y. Li, N.C. Gianneschi, K.L. Christman, Enzyme-Responsive Nanoparticles for Targeted

Accumulation and Prolonged Retention in Heart Tissue after Myocardial Infarction, Advanced Materials. 27 (2015) 5547–5552. https://doi.org/10.1002/adma.201502003.

[88] P. Sorlier, A. Denuzière, C. Viton, A. Domard, Relation between the degree of acetylation and the electrostatic properties of chitin and chitosan, Biomacromolecules. 2 (2001) 765–772. https://doi.org/10.1021/bm015531+.

[89] C. Wang, G. Li, R. Guo, Multiple morphologies from amphiphilic graft copolymers based on chitooligosaccharides as backbones and polycaprolactones as branches, Chemical Communications. 1 (2005) 3591–3593. https://doi.org/10.1039/b504428f.

[90] Y. Xu, L. Wang, Y.K. Li, C.Q. Wang, Reduction and pH dual-responsive nanoparticles based chitooligosaccharide-based graft copolymer for doxorubicin delivery, Colloids and Surfaces A: Physicochemical and Engineering Aspects. 497 (2016) 8–15. https://doi.org/10.1016/j.colsurfa.2016.01.049.

[91] J. Zhang, J. Han, X. Zhang, J. Jiang, M. Xu, D. Zhang, J. Han, Polymeric nanoparticles based on chitooligosaccharide as drug carriers for co-delivery of all-trans-retinoic acid and paclitaxel, Carbohydrate Polymers. 129 (2015) 25–34. https://doi.org/10.1016/j.carbpol.2015.04.036.

[92] C. Xin, X. Yao, B. Du, W. Yang, L. Wang, L. Ma, W. Weng, Stearic Acid-Grafted Chitooligosaccharide Nanomicelle System with Biocleavable Gadolinium Chelates as a Multifunctional Agent for Tumor Imaging and Drug Delivery, Pharmaceutical Research. 36 (2019). https://doi.org/10.1007/s11095-018-2530-2.

[93] J.S. Seong, M.E. Yun, S.N. Park, Surfactant-stable and pH-sensitive liposomes coated with N-succinyl-chitosan and chitooligosaccharide for delivery of quercetin, Carbohydrate Polymers. 181 (2018) 659–667. https://doi.org/10.1016/j.carbpol.2017.11.098.

[94] X. Hu, S. Chen, H. Yin, Q. Wang, Y. Duan, L. Jiang, L. Zhao, Chitooligosaccharides-modified PLGA nanoparticles enhance the antitumor efficacy of AZD9291 (Osimertinib) by promoting apoptosis, International Journal of Biological Macromolecules. 162 (2020) 262–272. https://doi.org/10.1016/j.ijbiomac.2020.06.154.

[95] X. Liu, L. Chen, Y. Zhang, X. Xin, L. Qi, M. Jin, Y. Guan, Z. Gao, W. Huang, Enhancing anti-melanoma outcomes in mice using novel chitooligosaccharide nanoparticles loaded with therapeutic survivin-targeted siRNA, European Journal of Pharmaceutical Sciences. 158 (2021) 105641. https://doi.org/10.1016/j.ejps.2020.105641.

[96] P. Chandika, G.W. Oh, S.Y. Heo, S.C. Kim, T.H. Kim, M.S. Kim, W.K. Jung, Electrospun porous bilayer nano-fibrous fish collagen/PCL bio-composite scaffolds with covalently cross-linked chitooligosaccharides for full-thickness wound-healing applications, Materials Science and Engineering C. 121 (2021) 111871. https://doi.org/10.1016/j.msec.2021.111871.

[97] M.M. Tomasiak, M. Tomasiak, Z. Zietkowski, R. Skiepko, A. Bodzenta-Lukaszyk, N-acetyl-beta-hexosaminidase activity in asthma, International Archives of Allergy and Immunology. 146 (2008) 133–137. https://doi.org/10.1159/000113516.

[98] A.K. Thakur, B. Kaundle, I. Singh, Mucoadhesive drug delivery systems in respiratory diseases, in: Targeting Chronic Inflammatory Lung Diseases Using Advanced Drug Delivery Systems, Elsevier, 2020: pp. 475–491.

[99] A.S. Balijepalli, R.C. Sabatelle, M. Chen, B. Suki, M.W. Grinstaff, A synthetic bioinspired carbohydrate polymer with mucoadhesive properties, Angewandte Chemie. 132 (2020) 714–720.

[100] S. Zhang, J. Ermann, M.D. Succi, A. Zhou, M.J. Hamilton, B. Cao, J.R. Korzenik, J.N. Glickman, P.K. Vemula, L.H. Glimcher, An inflammation-targeting hydrogel for local drug delivery in inflammatory bowel disease, Science Translational Medicine. 7 (2015) 300ra128-300ra128.

[101] K. Koss, C. Tsui, L.D. Unsworth, Induced Neural Differentiation of MMP-2 Cleaved (RADA)4 Drug Delivery Systems, Journal of Controlled Release. 243 (2016) 204–213. https://doi.org/10.1016/j.jconrel.2016.09.037.

[102] K.M. Koss, C. Tsui, L.D. Unsworth, Enzymatic Activity in Fractal Networks of Self-Assembling Peptides, Biomacromolecules. 20 (2019) 422–434. https://doi.org/10.1021/acs.biomac.8b01496.

[103] Y. Wang, Y. Luo, Q. Zhao, Z. Wang, Z. Xu, X. Jia, An Enzyme-Responsive Nanogel Carrier Based on PAMAM Dendrimers for Drug Delivery, ACS Applied Materials and Interfaces. 8 (2016) 19899–19906. https://doi.org/10.1021/acsami.6b05567.

[104] E. Secret, S.J. Kelly, K.E. Crannell, J.S. Andrew, Enzyme-responsive hydrogel microparticles for pulmonary drug delivery, ACS Applied Materials and Interfaces. 6 (2014) 10313–10321. https://doi.org/10.1021/am501754s.

[105] M. Najafi, H. Asadi, J. van den Dikkenberg, M.J. van Steenbergen, M.H.A.M. Fens, W.E. Hennink, T. Vermonden, Conversion of an Injectable MMP-Degradable Hydrogel into Core-Cross-Linked Micelles, Biomacromolecules. 21 (2020) 1739–1751. https://doi.org/10.1021/acs.biomac.9b01675.

[106] L. Massi, A. Najer, R. Chapman, C.D. Spicer, V. Nele, J. Che, M.A. Booth, J.J. Doutch, M.M. Stevens, Tuneable peptide cross-linked nanogels for enzyme-triggered protein delivery, Journal of Materials Chemistry B. 8 (2020) 8894–8907. https://doi.org/10.1039/d0tb01546f.

[107] C. Zhang, D. Pan, K. Luo, W. She, C. Guo, Y. Yang, Z. Gu, Peptide dendrimer-doxorubicin conjugate-based nanoparticles as an enzyme-responsive drug delivery system for cancer therapy, Advanced Healthcare Materials. 3 (2014) 1299–1308. https://doi.org/10.1002/adhm.201300601.

[108] C.E. Callmann, C. v. Barback, M.P. Thompson, D.J. Hall, R.F. Mattrey, N.C. Gianneschi, Therapeutic Enzyme-Responsive Nanoparticles for Targeted Delivery and Accumulation in Tumors, Advanced Materials. 27 (2015) 4611–4615. https://doi.org/10.1002/adma.201501803.

[109] L. Zhu, F. Perche, T. Wang, V.P. Torchilin, Matrix metalloproteinase 2-sensitive multifunctional polymeric micelles for tumor-specific co-delivery of siRNA and hydrophobic drugs, Biomaterials. 35 (2014) 4213–4222. https://doi.org/10.1016/j.biomaterials.2014.01.060.

[110] L. Zhu, T. Wang, F. Perche, A. Taigind, V.P. Torchilin, Enhanced anticancer activity of nanopreparation containing an MMP2-sensitive PEG-drug conjugate and cell-penetrating moiety, Proceedings of the National Academy of Sciences of the United States of America. 110 (2013) 17047–17052. https://doi.org/10.1073/pnas.1304987110.

[111] R. Dorresteijn, N. Billecke, M. Schwendy, S. Pütz, M. Bonn, S.H. Parekh, M. Klapper, K. Müllen, Polylactide-block-polypeptide-block-polylactide copolymer nanoparticles with tunable cleavage and controlled drug release, Advanced Functional Materials. 24 (2014) 4026–4033. https://doi.org/10.1002/adfm.201304074.

[112] N. Padmavathy, L. das Ghosh, S.R.K. Meka, K. Chatterjee, Synthesis of a Block Copolymer Exhibiting Cell-Responsive Phytochemical Release for Cancer Therapy, ACS Applied Materials & Interfaces. 10 (2018) 21816–21824. https://doi.org/10.1021/acsami.8b03521.

[113] C. Zhang, D. Pan, J. Li, J. Hu, A. Bains, N. Guys, H. Zhu, X. Li, K. Luo, Q. Gong, Z. Gu, Enzyme-responsive peptide dendrimer-gemcitabine conjugate as a controlled-release drug delivery vehicle with enhanced antitumor efficacy, Acta Biomaterialia. 55 (2017) 153–162. https://doi.org/10.1016/j.actbio.2017.02.047.

[114] H. Qi, Q. Chen, H. Ren, X. Wu, X. Liu, T. Lu, Electrophoretic deposition of dexamethasone-loaded gelatin nanospheres/chitosan coating and its dual function in anti-inflammation and osteogenesis, Colloids and Surfaces B: Biointerfaces. 169 (2018) 249–256. https://doi.org/10.1016/j.colsurfb.2018.05.029.

[115] A.A. Dongargaonkar, G.L. Bowlin, H. Yang, Electrospun blends of gelatin and gelatin-dendrimer conjugates as a wound-dressing and drug-delivery platform, Biomacromolecules. 14 (2013) 4038–4045. https://doi.org/10.1021/bm401143p.

[116] Z. Zou, D. He, X. He, K. Wang, X. Yang, Z. Qing, Q. Zhou, Natural gelatin capped mesoporous silica nanoparticles for intracellular acid-triggered drug delivery, Langmuir. 29 (2013) 12804–12810. https://doi.org/10.1021/la4022646.

[117] Z.X. Meng, X.X. Xu, W. Zheng, H.M. Zhou, L. Li, Y.F. Zheng, X. Lou, Preparation and characterization of electrospun PLGA/gelatin nanofibers as a potential drug delivery system, Colloids and Surfaces B: Biointerfaces. 84 (2011) 97–102. https://doi.org/10.1016/j.colsurfb.2010.12.022.

[118] L. Zhang, J. Liu, X. Zheng, A. Zhang, X. Zhang, K. Tang, Pullulan dialdehyde crosslinked gelatin hydrogels with high strength for biomedical applications, Carbohydrate Polymers. 216 (2019) 45–53. https://doi.org/10.1016/j.carbpol.2019.04.004.

[119] R.T. Annamalai, P.A. Turner, W.F. Carson, B. Levi, S. Kunkel, J.P. Stegemann, Harnessing macrophage-mediated degradation of gelatin microspheres for spatiotemporal control of BMP2 release, Biomaterials. 161 (2018) 216–227. https://doi.org/10.1016/j.biomaterials.2018.01.040.

[120] J.H. Xu, F.P. Gao, L.L. Li, H.L. Ma, Y.S. Fan, W. Liu, S.S. Guo, X.Z. Zhao, H. Wang, Gelatin-mesoporous silica nanoparticles as matrix metalloproteinases- degradable drug delivery systems in vivo, Microporous and Mesoporous Materials. 182 (2013) 165–172. https://doi.org/10.1016/j.micromeso.2013.08.050.

[121] S. Jain, P.U. Valvi, N.K. Swarnakar, K. Thanki, Gelatin coated hybrid lipid nanoparticles for oral delivery of Amphotericin B, Molecular Pharmaceutics. 9 (2012) 2542–2553. https://doi.org/10.1021/mp300320d.

[122] H. Blaser, C. Dostert, T.W. Mak, D. Brenner, TNF and ROS crosstalk in inflammation, Trends in Cell Biology. 26 (2016) 249–261.

[123] E.J. Swindle, D.D. Metcalfe, J.W. Coleman, Rodent and human mast cells produce functionally significant intracellular reactive oxygen species but not nitric oxide, Journal of Biological Chemistry. 279 (2004) 48751–48759. https://doi.org/10.1074/jbc.M409738200.

[124] H.S. Kuehn, E.J. Swindle, M.-S. Kim, M.A. Beaven, D.D. Metcalfe, A.M. Gilfillan, The Phosphoinositide 3-Kinase-Dependent Activation of Btk Is Required for Optimal Eicosanoid

Production and Generation of Reactive Oxygen Species in Antigen-Stimulated Mast Cells, The Journal of Immunology. 181 (2008) 7706–7712. https://doi.org/10.4049/jimmunol.181.11.7706.

[125] Y. Suzuki, T. Inoue, T. Yoshimaru, C. Ra, Galectin-3 but not galectin-1 induces mast cell death by oxidative stress and mitochondrial permeability transition, Biochimica et Biophysica Acta - Molecular Cell Research. 1783 (2008) 924–934. https://doi.org/10.1016/j.bbamcr.2008.01.025.

[126] E.J. Swindle, J.W. Coleman, F.R. DeLeo, D.D. Metcalfe, FcεRI- and Fcγ Receptor-Mediated Production of Reactive Oxygen Species by Mast Cells Is Lipoxygenase- and Cyclooxygenase-Dependent and NADPH Oxidase-Independent, The Journal of Immunology. 179 (2007) 7059–7071. https://doi.org/10.4049/jimmunol.179.10.7059.

[127] Y. Suzuki, T. Yoshimaru, T. Matsui, T. Inoue, O. Niide, S. Nunomura, C. Ra, FcεRI Signaling of Mast Cells Activates Intracellular Production of Hydrogen Peroxide: Role in the Regulation of Calcium Signals, The Journal of Immunology. 171 (2003) 6119–6127. https://doi.org/10.4049/jimmunol.171.11.6119.

[128] Y. Suzuki, T. Yoshimaru, T. Inoue, C. Ra, Discrete generations of intracellular hydrogen peroxide and superoxide in antigen-stimulated mast cells: Reciprocal regulation of store-operated Ca2+ channel activity, Molecular Immunology. 46 (2009) 2200–2209. https://doi.org/10.1016/j.molimm.2009.04.013.

[129] E.J. Swindle, J.A. Hunt, J.W. Coleman, A Comparison of Reactive Oxygen Species Generation by Rat Peritoneal Macrophages and Mast Cells Using the Highly Sensitive Real-Time Chemiluminescent Probe Pholasin: Inhibition of Antigen-Induced Mast Cell Degranulation by

Macrophage-Derived Hydrogen Pero, The Journal of Immunology. 169 (2002) 5866–5873. https://doi.org/10.4049/jimmunol.169.10.5866.

[130] T. Yoshimaru, Y. Suzuki, T. Inoue, O. Niide, C. Ra, Silver activates mast cells through reactive oxygen species production and a thiol-sensitive store-independent Ca2+ influx, Free Radical Biology and Medicine. 40 (2006) 1949–1959. https://doi.org/10.1016/j.freeradbiomed.2006.01.023.

[131] G. Saravanakumar, J. Kim, W.J. Kim, Reactive-Oxygen-Species-Responsive Drug Delivery Systems: Promises and Challenges, Advanced Science. 4 (2017). https://doi.org/10.1002/advs.201600124.

[132] W.C. Ballance, E.C. Qin, H.J. Chung, M.U. Gillette, H. Kong, Reactive oxygen species-responsive drug delivery systems for the treatment of neurodegenerative diseases, Biomaterials. 217 (2019) 119292. https://doi.org/10.1016/j.biomaterials.2019.119292.

[133] A.K. Shukla, M. Verma, K.N. Singh, Superoxide induced deprotection of 1,3-dithiolanes: A convenient method of dedithioacetalization, Indian Journal of Chemistry - Section B Organic and Medicinal Chemistry. 43 (2004) 1748–1752. https://doi.org/10.1002/chin.200449059.

[134] M.S. Shim, Y. Xia, A reactive oxygen species (ROS)-responsive polymer for safe, efficient, and targeted gene delivery in cancer cells, Angewandte Chemie - International Edition. 52 (2013) 6926–6929. https://doi.org/10.1002/anie.201209633.

[135] B. Liu, S. Thayumanavan, Mechanistic Investigation on Oxidative Degradation of ROS-Responsive Thioacetal/Thioketal Moieties and Their Implications, Cell Reports Physical Science. 1 (2020) 100271. https://doi.org/10.1016/j.xcrp.2020.100271.

[136] J. Li, C. Sun, W. Tao, Z. Cao, H. Qian, X. Yang, J. Wang, Photoinduced PEG deshielding from ROS-sensitive linkage-bridged block copolymer-based nanocarriers for on-demand drug delivery, Biomaterials. 170 (2018) 147–155. https://doi.org/10.1016/j.biomaterials.2018.04.015.

[137] D.S. Wilson, G. Dalmasso, L. Wang, S. v. Sitaraman, D. Merlin, N. Murthy, Orally delivered thioketal nanoparticles loaded with TNF-α-siRNA target inflammation and inhibit gene expression in the intestines, Nature Materials. 9 (2010) 923–928. https://doi.org/10.1038/nmat2859.

[138] Y. Yuan, J. Liu, B. Liu, Conjugated-polyelectrolyte-based polyprodrug: Targeted and image-guided photodynamic and chemotherapy with on-demand drug release upon irradiation with a single light source, Angewandte Chemie - International Edition. 53 (2014) 7163–7168. https://doi.org/10.1002/anie.201402189.

[139] C. Yue, Y. Yang, C. Zhang, G. Alfranca, S. Cheng, L. Ma, Y. Liu, X. Zhi, J. Ni, W. Jiang, J. Song, J.M. de la Fuente, D. Cui, ROS-responsive mitochondria-targeting blended nanoparticles: Chemo- and photodynamic synergistic therapy for lung cancer with on-demand drug release upon irradiation with a single light source, Theranostics. 6 (2016) 2352–2366. https://doi.org/10.7150/thno.15433.

[140] D. Chen, G. Zhang, R. Li, M. Guan, X. Wang, T. Zou, Y. Zhang, C. Wang, C. Shu, H. Hong, L.J. Wan, Biodegradable, Hydrogen Peroxide, and Glutathione Dual Responsive Nanoparticles for Potential Programmable Paclitaxel Release, Journal of the American Chemical Society. 140 (2018) 7373–7376. https://doi.org/10.1021/jacs.7b12025.

[141] J. Wang, X. He, S. Shen, Z. Cao, X. Yang, ROS-Sensitive Cross-Linked Polyethylenimine for Red-Light-Activated siRNA Therapy, ACS Applied Materials and Interfaces. 11 (2019) 1855–1863. https://doi.org/10.1021/acsami.8b18697.

[142] X. Ling, S. Zhang, P. Shao, P. Wang, X. Ma, M. Bai, Synthesis of a reactive oxygen species responsive heterobifunctional thioketal linker, Tetrahedron Letters. 56 (2015) 5242–5244. https://doi.org/10.1016/j.tetlet.2015.07.059.

[143] L. Xu, M. Zhao, W. Gao, Y. Yang, J. Zhang, Y. Pu, B. He, Polymeric nanoparticles responsive to intracellular ROS for anticancer drug delivery, Colloids and Surfaces B: Biointerfaces. 181 (2019) 252–260. https://doi.org/10.1016/j.colsurfb.2019.05.064.

[144] X. Xu, P.E. Saw, W. Tao, Y. Li, X. Ji, S. Bhasin, Y. Liu, D. Ayyash, J. Rasmussen, M. Huo, J. Shi, O.C. Farokhzad, ROS-Responsive Polyprodrug Nanoparticles for Triggered Drug Delivery and Effective Cancer Therapy, Advanced Materials. 29 (2017) 1–6. https://doi.org/10.1002/adma.201700141.

[145] H. Subramanian, K. Gupta, D. Lee, A.K. Bayir, H. Ahn, H. Ali, β-Defensins activate human mast cells via Mas-related gene X2, The Journal of Immunology. 191 (2013) 345–352.

[146] M. Kamohara, A. Matsuo, J. Takasaki, M. Kohda, M. Matsumoto, S. Matsumoto, T. Soga, H. Hiyama, M. Kobori, M. Katou, Identification of MrgX2 as a human G-protein-coupled receptor for proadrenomedullin N-terminal peptides, Biochemical and Biophysical Research Communications. 330 (2005) 1146–1152.

[147] H.-P. Nothacker, Z. Wang, H. Zeng, S.K. Mahata, D.T. O'Connor, O. Civelli, Proadrenomedullin N-terminal peptide and cortistatin activation of MrgX2 receptor is based on a common structural motif, European Journal of Pharmacology. 519 (2005) 191–193.

[148] L. Lu, M. Kulka, L.D. Unsworth, Peptide-mediated mast cell activation: ligand similarities for receptor recognition and protease-induced regulation, Journal of Leukocyte Biology. 102 (2017) 237–251.

[149] T.C. Theoharides, W.W. Douglas, Mast cell histamine secretion in response to somatostatin analogues: structural considerations, European Journal of Pharmacology. 73 (1981) 131–136.

[150] L. Lu, S. Raj, N. Arizmendi, J. Ding, G. Eitzen, P. Kwan, M. Kulka, L.D. Unsworth, Identification of short peptide sequences that activate human mast cells via mas-related g-protein coupled receptor member x2, Acta Biomaterialia. 136 (2021) 159–169.

[151] G. Varricchi, A. Pecoraro, S. Loffredo, R. Poto, F. Rivellese, A. Genovese, G. Marone, G. Spadaro, Heterogeneity of human mast cells with respect to MRGPRX2 receptor expression and function, Frontiers in Cellular Neuroscience. 13 (2019) 299.

[152] W. Manorak, C. Idahosa, K. Gupta, S. Roy, R. Panettieri, H. Ali, Upregulation of Mas-related G Protein coupled receptor X2 in asthmatic lung mast cells and its activation by the novel neuropeptide hemokinin-1, Respiratory Research. 19 (2018) 1–5. https://doi.org/10.1186/s12931-017-0698-3.

[153] S. Willows, M. Kulka, Harnessing the power of mast cells in unconventional immunotherapy strategies and vaccine adjuvants, Cells. 9 (2020) 2713.

[154] J.B. McLachlan, C.P. Shelburne, J.P. Hart, S. v Pizzo, R. Goyal, R. Brooking-Dixon, H.F. Staats, S.N. Abraham, Mast cell activators: a new class of highly effective vaccine adjuvants, Nature Medicine. 14 (2008) 536–541.

[155] E. Ruoslahti, Peptides as targeting elements and tissue penetration devices for nanoparticles, Advanced Materials. 24 (2012) 3747–3756. https://doi.org/10.1002/adma.201200454.

[156] F. Zhang, X. Huang, L. Zhu, N. Guo, G. Niu, M. Swierczewska, S. Lee, H. Xu, A.Y. Wang, K.A. Mohamedali, M.G. Rosenblum, G. Lu, X. Chen, Noninvasive monitoring of orthotopic glioblastoma therapy response using RGD-conjugated iron oxide nanoparticles, Biomaterials. 33 (2012) 5414–5422. https://doi.org/10.1016/j.biomaterials.2012.04.032.

[157] M. Lewin, N. Carlesso, C.H. Tung, X.W. Tang, D. Cory, D.T. Scadden, R. Weissleder, Tat peptide-derivatized magnetic nanoparticles allow in vivo tracking and recovery of progenitor cells, Nature Biotechnology. 18 (2000) 410–414. https://doi.org/10.1038/74464.

[158] X. Li, L. Xing, Y. Hu, Z. Xiong, R. Wang, X. Xu, L. Du, M. Shen, X. Shi, An RGD-modified hollow silica@Au core/shell nanoplatform for tumor combination therapy, Acta Biomaterialia. 62 (2017) 273–283. https://doi.org/10.1016/j.actbio.2017.08.024.

[159] F. Danhier, B. Vroman, N. Lecouturier, N. Crokart, V. Pourcelle, H. Freichels, C. Jérôme, J. Marchand-Brynaert, O. Feron, V. Préat, Targeting of tumor endothelium by RGD-grafted PLGA-nanoparticles loaded with Paclitaxel, Journal of Controlled Release. 140 (2009) 166–173. https://doi.org/10.1016/j.jconrel.2009.08.011.

[160] N. Yonenaga, E. Kenjo, T. Asai, A. Tsuruta, K. Shimizu, T. Dewa, M. Nango, N. Oku, RGD-based active targeting of novel polycation liposomes bearing siRNA for cancer treatment, Journal of Controlled Release. 160 (2012) 177–181. https://doi.org/10.1016/j.jconrel.2011.10.004.

[161] H.A. Kim, K. Nam, S.W. Kim, Tumor targeting RGD conjugated bio-reducible polymer for VEGF siRNA expressing plasmid delivery, Biomaterials. 35 (2014) 7543–7552. https://doi.org/10.1016/j.biomaterials.2014.05.021.

[162] C. Shu, R. Li, Y. Yin, D. Yin, Y. Gu, L. Ding, W. Zhong, Synergistic dual-targeting hydrogel improves targeting and anticancer effect of Taxol in vitro and in vivo, Chemical Communications. 50 (2014) 15423–15426. https://doi.org/10.1039/c4cc05614k.

[163] E.J. Kwon, J.S. Dudani, S.N. Bhatia, Ultrasensitive tumour-penetrating nanosensors of protease activity, Nature Biomedical Engineering. 1 (2017). https://doi.org/10.1038/s41551-017-0054.

[164] L.B. Schwartz, Diagnostic Value of Tryptase in Anaphylaxis and Mastocytosis, Immunology and Allergy Clinics of North America. 26 (2006) 451–463. https://doi.org/10.1016/j.iac.2006.05.010.

[165] E. Ordoqui, J.M. Zubeldia, A. Aranzábal, M. Rubio, T. Herrero, P. Tornero, V.M. Rodriguez, A. Prieto, M.L. Baeza, Serum tryptase levels in adverse drug reactions, Allergy: European Journal of Allergy and Clinical Immunology. 52 (1997) 1102–1105. https://doi.org/10.1111/j.1398-9995.1997.tb00182.x.

Chapter 3

[1] I.D.F.D. Atlas, 463 PEOPLE LIVING WITH DIABETES million, 2019.

[2] R. Shah, M. Patel, D. Maahs, V. Shah, Insulin delivery methods: Past, present and future, International Journal of Pharmaceutical Investigation. 6 (2016) 1. https://doi.org/10.4103/2230-973x.176456.

[3] H. Thabit, R. Hovorka, Coming of age: the artificial pancreas for type 1 diabetes, Diabetologia. 59 (2016) 1795–1805. https://doi.org/10.1007/s00125-016-4022-4.

[4] E. Latres, D.A. Finan, J.L. Greenstein, A. Kowalski, T.J. Kieffer, Navigating two roads to glucose normalization in diabetes: automated insulin delivery devices and cell therapy, Cell Metabolism. 29 (2019) 545–563.

[5] A.M.J. Shapiro, M. Pokrywczynska, C. Ricordi, Clinical pancreatic islet transplantation, Nature Reviews Endocrinology. 13 (2017) 268–277. https://doi.org/10.1038/nrendo.2016.178.

[6] B.J. Hering, W.R. Clarke, N.D. Bridges, T.L. Eggerman, R. Alejandro, M.D. Bellin, K. Chaloner, C.W. Czarniecki, J.S. Goldstein, L.G. Hunsicker, D.B. Kaufman, O. Korsgren, C.P. Larsen, X. Luo, J.F. Markmann, A. Naji, J. Oberholzer, A.M. Posselt, M.R. Rickels, C. Ricordi, M.A. Robien, P.A. Senior, A.M. James Shapiro, P.G. Stock, N.A. Turgeon, Phase 3 trial of transplantation of human islets in type 1 diabetes complicated by severe hypoglycemia, Diabetes Care. 39 (2016) 1230–1240. https://doi.org/10.2337/dc15-1988.

[7] A. Citro, E. Cantarelli, L. Piemonti, Anti-inflammatory strategies to enhance islet engraftment and survival, Current Diabetes Reports. 13 (2013) 733–744.

[8] D.C. Brennan, H.A. Kopetskie, P.H. Sayre, R. Alejandro, E. Cagliero, A.M.J. Shapiro, J.S. Goldstein, M.R. Desmarais, S. Booher, P.J. Bianchine, Long-Term Follow-Up of the Edmonton Protocol of Islet Transplantation in the United States, American Journal of Transplantation. 16 (2016) 509–517. https://doi.org/10.1111/ajt.13458.

[9] M.C. Vantyghem, M. Chetboun, V. Gmyr, A. Jannin, S. Espiard, K. le Mapihan, V. Raverdy, N. Delalleau, F. Machuron, T. Hubert, M. Frimat, E. van Belle, M. Hazzan, P. Pigny, C. Noel, R. Caiazzo, J. Kerr-Conte, F. Pattou, Erratum: Ten-year outcome of islet alone or islet after kidney transplantation in type 1 diabetes: A prospective parallel-arm cohort study.(Diabetes care(2019)42(2042–2049)Doi:10.2337/dc19-0401), Diabetes Care. 43 (2020) 1164. https://doi.org/10.2337/dc20er05.

[10] J.A. Emamaullee, A.M.J. Shapiro, Factors influencing the loss of β-cell mass in islet transplantation, Cell Transplantation. 16 (2007) 1–8.

[11] E.A. Ryan, J.R.T. Lakey, B.W. Paty, S. Imes, G.S. Korbutt, N.M. Kneteman, D. Bigam, R. v Rajotte, A.M.J. Shapiro, Successful islet transplantation: continued insulin reserve provides long-term glycemic control, Diabetes. 51 (2002) 2148–2157.

[12] N.R. Barshes, S. Wyllie, J.A. Goss, Inflammation-mediated dysfunction and apoptosis in pancreatic islet transplantation: implications for intrahepatic grafts, Journal of Leukocyte Biology. 77 (2005) 587–597.

[13] A. Miki, C. Ricordi, Y. Sakuma, T. Yamamoto, R. Misawa, A. Mita, R.D. Molano, N.D. Vaziri, A. Pileggi, H. Ichii, Divergent antioxidant capacity of human islet cell subsets: A potential cause

of beta-cell vulnerability in diabetes and islet transplantation, PLoS ONE. 13 (2018) 1–16. https://doi.org/10.1371/journal.pone.0196570.

[14] H.Q. Zhu, Y. Gao, H.R. Guo, Q.Z. Kong, Y. Ma, J.Z. Wang, S.H. Pan, H.C. Jiang, W.J. Dai, Pretreatment with bilirubin protects islet against oxidative injury during isolation and purification, in: Transplantation Proceedings, Elsevier, 2011: pp. 1810–1814.

[15] H. Chen, E.C. Carlson, L. Pellet, J.T. Moritz, P.N. Epstein, Overexpression of metallothionein in pancreatic β-cells reduces streptozotocin-induced DNA damage and diabetes, Diabetes. 50 (2001) 2040–2046.

[16] J.M. Barra, H.M. Tse, Redox-dependent inflammation in islet transplantation rejection, Frontiers in Endocrinology. 9 (2018) 175.

[17] M.J. Kim, Y. Lee, S. Jon, D.Y. Lee, PEGylated bilirubin nanoparticle as an anti-oxidative and anti-inflammatory demulcent in pancreatic islet xenotransplantation, Biomaterials. 133 (2017) 242–252. https://doi.org/10.1016/j.biomaterials.2017.04.029.

[18] H.S. Jung, K.S. Lim, M.J. Kim, Y.H. Hwang, C. Yoo, Y. Lee, Y.-H. Kim, D.Y. Lee, Hypoxic resistance of hypodermically transplanted pancreatic islets by using cell-absorbable antioxidant Tat-metallothionein, Journal of Controlled Release. 172 (2013) 1092–1101.

[19] A. Bruni, A.R. Pepper, R.L. Pawlick, B. Gala-Lopez, A. Gamble, T. Kin, A.J. Malcolm, C. Jones, J.D. Piganelli, J.D. Crapo, A.M.J. Shapiro, BMX-001, a novel redox-active metalloporphyrin, improves islet function and engraftment in a murine transplant model, American Journal of Transplantation. 18 (2018) 1879–1889. https://doi.org/10.1111/ajt.14705.

[20] A. Tovmasyan, C.G.C. Maia, T. Weitner, S. Carballal, R.S. Sampaio, D. Lieb, R. Ghazaryan, I. Ivanovic-Burmazovic, G. Ferrer-Sueta, R. Radi, A comprehensive evaluation of catalase-like activity of different classes of redox-active therapeutics, Free Radical Biology and Medicine. 86 (2015) 308–321.

[21] A.K. Shukla, M. Verma, K.N. Singh, Superoxide induced deprotection of 1,3-dithiolanes: A convenient method of dedithioacetalization, Indian Journal of Chemistry - Section B Organic and Medicinal Chemistry. 43 (2004) 1748–1752. https://doi.org/10.1002/chin.200449059.

[22] B. Liu, S. Thayumanavan, Mechanistic Investigation on Oxidative Degradation of ROS-Responsive Thioacetal/Thioketal Moieties and Their Implications, Cell Reports Physical Science. 1 (2020) 100271.

[23] G.S. Korbutt, J.F. Elliott, Z. Ao, D.K. Smith, G.L. Warnock, R. v Rajotte, Large scale isolation, growth, and function of porcine neonatal islet cells., The Journal of Clinical Investigation. 97 (1996) 2119–2129.

[24] K.K. Papas, A. Pisania, H. Wu, G.C. Weir, C.K. Colton, A stirred microchamber for oxygen consumption rate measurements with pancreatic islets, Biotechnology and Bioengineering. 98 (2007) 1071–1082.

[25] A.R. Pepper, B. Gala-Lopez, R. Pawlick, S. Merani, T. Kin, A.M.J. Shapiro, A prevascularized subcutaneous device-less site for islet and cellular transplantation, Nature Biotechnology. 33 (2015) 518–523.

[26] I.R. Sweet, G. Khalil, A.R. Wallen, M. Steedman, K.A. Schenkman, J.A. Reems, S.E. Kahn, J.B. Callis, Continuous measurement of oxygen consumption by pancreatic islets, Diabetes Technology & Therapeutics. 4 (2002) 661–672.

[27] D.L. Tribble, T.Y. Aw, D.P. Jones, The pathophysiological significance of lipid peroxidation in oxidative cell injury, Hepatology. 7 (1987) 377–386.

[28] D.S. Wilson, G. Dalmasso, L. Wang, S. v. Sitaraman, D. Merlin, N. Murthy, Orally delivered thioketal nanoparticles loaded with TNF-α-siRNA target inflammation and inhibit gene expression in the intestines, Nature Materials. 9 (2010) 923–928. https://doi.org/10.1038/nmat2859.

[29] L.A.H. van Bergen, G. Roos, F. de Proft, From thiol to sulfonic acid: Modeling the oxidation pathway of protein thiols by hydrogen peroxide, The Journal of Physical Chemistry A. 118 (2014) 6078–6084.

[30] X. Li, H. Chen, P.N. Epstein, Metallothionein Protects Islets from Hypoxia and Extends Islet Graft Survival by Scavenging Most Kinds of Reactive Oxygen Species, Journal of Biological Chemistry. 279 (2004) 765–771. https://doi.org/10.1074/jbc.M307907200.

[31] M.J. Kim, Y.H. Hwang, Y.H. Kim, D.Y. Lee, Immunomodulation of cell-penetrating tat-metallothionein for successful outcome of xenotransplanted pancreatic islet, Journal of Drug Targeting. 25 (2017) 350–359.

[32] Q. Yao, X. Jiang, Z.-W. Huang, Q.-H. Lan, L.-F. Wang, R. Chen, X.-Z. Li, L. Kou, H.-L. Xu, Y.-Z. Zhao, Bilirubin improves the quality and function of hypothermic preserved islets by its antioxidative and anti-inflammatory effect, Transplantation. 103 (2019) 2486–2496.

[33] A. Bruni, A.R. Pepper, B. Gala-Lopez, R. Pawlick, N. Abualhassan, J.D. Crapo, J.D. Piganelli, A.M.J. Shapiro, A novel redox-active metalloporphyrin reduces reactive oxygen species and inflammatory markers but does not improve marginal mass engraftment in a murine donation after circulatory death islet transplantation model, Islets. 8 (2016). https://doi.org/10.1080/19382014.2016.1190058.

[34] N.J. Abuid, K.M. Gattás-Asfura, E.A. Schofield, C.L. Stabler, Layer-by-Layer Cerium Oxide Nanoparticle Coating for Antioxidant Protection of Encapsulated Beta Cells, Advanced Healthcare Materials. 8 (2019) 1–10. https://doi.org/10.1002/adhm.201801493.

[35] A.A. Vernekar, D. Sinha, S. Srivastava, P.U. Paramasivam, P. D'Silva, G. Mugesh, An antioxidant nanozyme that uncovers the cytoprotective potential of vanadia nanowires, Nature Communications. 5 (2014). https://doi.org/10.1038/ncomms6301.

[36] S. Raj, S. Kumar, K. Chatterjee, Facile synthesis of vanadia nanoparticles and assessment of antibacterial activity and cytotoxicity, Materials Technology. 31 (2016) 562–573.

Chapter 4

[1] I.-T. Lee, C.-M. Yang, Role of NADPH oxidase/ROS in pro-inflammatory mediators-induced airway and pulmonary diseases, Biochemical Pharmacology. 84 (2012) 581–590.

[2] J.M. Barra, H.M. Tse, Redox-dependent inflammation in islet transplantation rejection, Frontiers in Endocrinology. 9 (2018) 175.

[3] E.J. Swindle, D.D. Metcalfe, The role of reactive oxygen species and nitric oxide in mast cell-dependent inflammatory processes, Immunological Reviews. 217 (2007) 186–205.

[4] C. Kohchi, H. Inagawa, T. Nishizawa, G.-I. Soma, ROS and innate immunity, Anticancer Research. 29 (2009) 817–821.

[5] E. Shekhova, Mitochondrial reactive oxygen species as major effectors of antimicrobial immunity, PLoS Pathogens. 16 (2020) e1008470.

[6] M.D. Kraaij, S.W. van der Kooij, M.E.J. Reinders, K. Koekkoek, T.J. Rabelink, C. van Kooten, K.A. Gelderman, Dexamethasone increases ROS production and T cell suppressive capacity by anti-inflammatory macrophages, Molecular Immunology. 49 (2011) 549–557.

[7] H. Blaser, C. Dostert, T.W. Mak, D. Brenner, TNF and ROS crosstalk in inflammation, Trends in Cell Biology. 26 (2016) 249–261.

[8] H.-U. Simon, A. Haj-Yehia, F. Levi-Schaffer, Role of reactive oxygen species (ROS) in apoptosis induction, Apoptosis. 5 (2000) 415–418.

[9] N.R. Barshes, S. Wyllie, J.A. Goss, Inflammation-mediated dysfunction and apoptosis in pancreatic islet transplantation: implications for intrahepatic grafts, Journal of Leukocyte Biology. 77 (2005) 587–597.

[10] G. Saravanakumar, J. Kim, W.J. Kim, Reactive-Oxygen-Species-Responsive Drug Delivery Systems: Promises and Challenges, Advanced Science. 4 (2017). https://doi.org/10.1002/advs.201600124.

[11] M.K. Gupta, T.A. Meyer, C.E. Nelson, C.L. Duvall, Poly (PS-b-DMA) micelles for reactive oxygen species triggered drug release, Journal of Controlled Release. 162 (2012) 591–598.

[12] P. Han, N. Ma, H. Ren, H. Xu, Z. Li, Z. Wang, X. Zhang, Oxidation-responsive micelles based on a selenium-containing polymeric superamphiphile, Langmuir. 26 (2010) 14414–14418.

[13] W. Cao, Y. Gu, T. Li, H. Xu, Ultra-sensitive ROS-responsive tellurium-containing polymers, Chemical Communications. 51 (2015) 7069–7071.

[14] D.S. Wilson, G. Dalmasso, L. Wang, S. v Sitaraman, D. Merlin, N. Murthy, Orally delivered thioketal nanoparticles loaded with TNF-α–siRNA target inflammation and inhibit gene expression in the intestines, Nature Materials. 9 (2010) 923–928.

[15] Y. Liu, Y. Liu, J. Zang, A.A.I. Abdullah, Y. Li, H. Dong, Design strategies and applications of ROS-responsive phenylborate ester-based nanomedicine, ACS Biomaterials Science & Engineering. 6 (2020) 6510–6527.

[16] C. Wei, Y. Zhang, H. Xu, Y. Xu, Y. Xu, M. Lang, Well-defined labile diselenide-centered poly (ε-caprolactone)-based micelles for activated intracellular drug release, Journal of Materials Chemistry B. 4 (2016) 5059–5067.

[17] B. Liu, S. Thayumanavan, Mechanistic Investigation on Oxidative Degradation of ROS-Responsive Thioacetal/Thioketal Moieties and Their Implications, Cell Reports Physical Science. 1 (2020) 100271.

[18] P.J. Barnes, How corticosteroids control inflammation: quintiles prize lecture 2005, British Journal of Pharmacology. 148 (2006) 245–254.

[19] A.E. Coutinho, K.E. Chapman, The anti-inflammatory and immunosuppressive effects of glucocorticoids, recent developments and mechanistic insights, Molecular and Cellular Endocrinology. 335 (2011) 2–13.

[20] M. Kadmiel, J.A. Cidlowski, Glucocorticoid receptor signaling in health and disease, Trends in Pharmacological Sciences. 34 (2013) 518–530.

[21] A.J. Giles, M.-K.N.D. Hutchinson, H.M. Sonnemann, J. Jung, P.E. Fecci, N.M. Ratnam, W. Zhang, H. Song, R. Bailey, D. Davis, Dexamethasone-induced immunosuppression: mechanisms and implications for immunotherapy, Journal for Immunotherapy of Cancer. 6 (2018) 1–13.

[22] K. Yamada, H. Sato, K. Sakamaki, M. Kamada, Y. Okuno, N. Fukuishi, K. Furuta, S. Tanaka, Suppression of IgE-independent degranulation of murine connective tissue-type mast cells by dexamethasone, Cells. 8 (2019) 112.

[23] M.V.M. Andrade, T. Hiragun, M.A. Beaven, Dexamethasone suppresses antigen-induced activation of phosphatidylinositol 3-kinase and downstream responses in mast cells, The Journal of Immunology. 172 (2004) 7254–7262.

[24] B.D. McNeil, P. Pundir, S. Meeker, L. Han, B.J. Undem, M. Kulka, X. Dong, Identification of a mast-cell-specific receptor crucial for pseudo-allergic drug reactions, Nature. 519 (2015) 237–241. https://doi.org/10.1038/nature14022.

[25] R.Z. Xiao, Z.W. Zeng, G.L. Zhou, J.J. Wang, F.Z. Li, A.M. Wang, Recent advances in PEG–PLA block copolymer nanoparticles, International Journal of Nanomedicine. 5 (2010) 1057.

[26] J. Li, C. Sun, W. Tao, Z. Cao, H. Qian, X. Yang, J. Wang, Photoinduced PEG deshielding from ROS-sensitive linkage-bridged block copolymer-based nanocarriers for on-demand drug delivery, Biomaterials. 170 (2018) 147–155. https://doi.org/10.1016/j.biomaterials.2018.04.015.

[27] O. Dechy-Cabaret, B. Martin-Vaca, D. Bourissou, Controlled ring-opening polymerization of lactide and glycolide, Chemical Reviews. 104 (2004) 6147–6176.

[28] R. Ghasemi, M. Abdollahi, E. Emamgholi Zadeh, K. Khodabakhshi, A. Badeli, H. Bagheri, S. Hosseinkhani, mPEG-PLA and PLA-PEG-PLA nanoparticles as new carriers for delivery of recombinant human Growth Hormone (rhGH), Scientific Reports. 8 (2018) 1–13.

[29] R. Gref, M. Lück, P. Quellec, M. Marchand, E. Dellacherie, S. Harnisch, T. Blunk, R.H. Müller, 'Stealth'corona-core nanoparticles surface modified by polyethylene glycol (PEG): influences of the corona (PEG chain length and surface density) and of the core composition on phagocytic uptake and plasma protein adsorption, Colloids and Surfaces B: Biointerfaces. 18 (2000) 301–313.

[30] Q. Wang, J. Jiang, W. Chen, H. Jiang, Z. Zhang, X. Sun, Targeted delivery of low-dose dexamethasone using PCL–PEG micelles for effective treatment of rheumatoid arthritis, Journal of Controlled Release. 230 (2016) 64–72.

[31] L. Lu, E.A. Armstrong, J.Y. Yager, L.D. Unsworth, Sustained Release of Dexamethasone from Sulfobutyl Ether β-cyclodextrin Modified Self-Assembling Peptide Nanoscaffolds in a Perinatal Rat Model of Hypoxia–Ischemia, Advanced Healthcare Materials. 8 (2019) 1900083.

[32] H. Gasmi, F. Siepmann, M.C. Hamoudi, F. Danede, J. Verin, J.-F. Willart, J. Siepmann, Towards a better understanding of the different release phases from PLGA microparticles: Dexamethasone-loaded systems, International Journal of Pharmaceutics. 514 (2016) 189–199.

[33] L. Zhang, W. Shen, J. Luan, D. Yang, G. Wei, L. Yu, W. Lu, J. Ding, Sustained intravitreal delivery of dexamethasone using an injectable and biodegradable thermogel, Acta Biomaterialia. 23 (2015) 271–281.

[34] D.-H. Kim, T.N. Nguyen, Y.-M. Han, P. Tran, J. Rho, J.-Y. Lee, H.-Y. Son, J.-S. Park, Local drug delivery using poly (lactic-co-glycolic acid) nanoparticles in thermosensitive gels for inner ear disease treatment, Drug Delivery. 28 (2021) 2268–2277.

[35] J. Urbańska, A. Karewicz, M. Nowakowska, Polymeric delivery systems for dexamethasone, Life Sciences. 96 (2014) 1–6.

[36] A. Yu, H. Shi, H. Liu, Z. Bao, M. Dai, D. Lin, D. Lin, X. Xu, X. Li, Y. Wang, Mucoadhesive dexamethasone-glycol chitosan nanoparticles for ophthalmic drug delivery, International Journal of Pharmaceutics. 575 (2020) 118943.

[37] N.M. Vacanti, H. Cheng, P.S. Hill, J.D.T. Guerreiro, T.T. Dang, M. Ma, S. Watson, N.S. Hwang, R. Langer, D.G. Anderson, Localized delivery of dexamethasone from electrospun fibers reduces the foreign body response, Biomacromolecules. 13 (2012) 3031–3038.

[38] K. Jiang, J.D. Weaver, Y. Li, X. Chen, J. Liang, C.L. Stabler, Local release of dexamethasone from macroporous scaffolds accelerates islet transplant engraftment by promotion of anti-inflammatory M2 macrophages, Biomaterials. 114 (2017) 71–81.

[39] X. Xu, L. Sun, L. Zhou, Y. Cheng, F. Cao, Functional chitosan oligosaccharide nanomicelles for topical ocular drug delivery of dexamethasone, Carbohydrate Polymers. 227 (2020) 115356.

[40] F.F. Sahle, C. Gerecke, B. Kleuser, R. Bodmeier, Formulation and comparative in vitro evaluation of various dexamethasone-loaded pH-sensitive polymeric nanoparticles intended for dermal applications, International Journal of Pharmaceutics. 516 (2017) 21–31.

[41] K. Rajes, K.A. Walker, S. Hadam, F. Zabihi, J. Ibrahim-Bacha, G. Germer, P. Patoka, B. Wassermann, F. Rancan, E. Rühl, Oxidation-sensitive core–multishell nanocarriers for the controlled delivery of hydrophobic drugs, ACS Biomaterials Science & Engineering. 7 (2021) 2485–2495.

[42] Q. Meng, H. Hu, X. Jing, Y. Sun, L. Zhou, Y. Zhu, B. Yu, H. Cong, Y. Shen, A modular ROS-responsive platform co-delivered by 10-hydroxycamptothecin and dexamethasone for cancer treatment, Journal of Controlled Release. 340 (2021) 102–113.

Chapter 5

[1] S.J. Galli, S. Nakae, M. Tsai, Mast cells in the development of adaptive immune responses, Nature immunology 6(2) (2005) 135-142.

[2] S. Wernersson, G. Pejler, Mast cell secretory granules: armed for battle, Nature Reviews Immunology 14(7) (2014) 478-494.

[3] J. Kalesnikoff, S.J. Galli, New developments in mast cell biology, Nature immunology 9(11) (2008) 1215.

[4] B.D. McNeil, P. Pundir, S. Meeker, L. Han, B.J. Undem, M. Kulka, X. Dong, Identification of a mast-cell-specific receptor crucial for pseudo-allergic drug reactions, Nature 519(7542) (2015) 237-241.

[5] K. Tatemoto, Y. Nozaki, R. Tsuda, S. Konno, K. Tomura, M. Furuno, H. Ogasawara, K. Edamura, H. Takagi, H. Iwamura, Immunoglobulin E-independent activation of mast cell is mediated by Mrg receptors, Biochemical and biophysical research communications 349(4) (2006) 1322-1328.

[6] H. Subramanian, K. Gupta, H. Ali, Roles of Mas-related G protein–coupled receptor X2 on mast cell–mediated host defense, pseudoallergic drug reactions, and chronic inflammatory diseases, Journal of Allergy and Clinical Immunology 138(3) (2016) 700-710.

[7] W. Manorak, C. Idahosa, K. Gupta, S. Roy, R. Panettieri, H. Ali, Upregulation of Mas-related G Protein coupled receptor X2 in asthmatic lung mast cells and its activation by the novel neuropeptide hemokinin-1, Respiratory research 19(1) (2018) 1-5.

[8] T. Karhu, K. Akiyama, O. Vuolteenaho, U. Bergmann, T. Naito, K. Tatemoto, K.-H. Herzig, Mast cell degranulation via MRGPRX2 by isolated human albumin fragments, Biochimica et Biophysica Acta (BBA)-General Subjects 1861(11) (2017) 2530-2534.

[9] M. Kamohara, A. Matsuo, J. Takasaki, M. Kohda, M. Matsumoto, S.-i. Matsumoto, T. Soga, H. Hiyama, M. Kobori, M. Katou, Identification of MrgX2 as a human G-protein-coupled receptor for proadrenomedullin N-terminal peptides, Biochemical and biophysical research communications 330(4) (2005) 1146-1152.

[10] N. Robas, E. Mead, M. Fidock, MrgX2 is a high potency cortistatin receptor expressed in dorsal root ganglion, Journal of Biological Chemistry 278(45) (2003) 44400-44404.

[11] Y. Yu, Y. Zhang, Y. Zhang, Y. Lai, W. Chen, Z. Xiao, W. Zhang, M. Jin, B. Yu, LL-37-induced human mast cell activation through G protein-coupled receptor MrgX2, International Immunopharmacology 49 (2017) 6-12.

[12] H. Subramanian, K. Gupta, D. Lee, A.K. Bayir, H. Ahn, H. Ali, β-Defensins activate human mast cells via Mas-related gene X2, The Journal of Immunology 191(1) (2013) 345-352.

[13] K. Gupta, A. Kotian, H. Subramanian, H. Daniell, H. Ali, Activation of human mast cells by retrocyclin and protegrin highlight their immunomodulatory and antimicrobial properties, Oncotarget 6(30) (2015) 28573.

[14] A. Navinés-Ferrer, E. Serrano-Candelas, A. Lafuente, R. Muñoz-Cano, M. Martín, G. Gastaminza, MRGPRX2-mediated mast cell response to drugs used in perioperative procedures and anaesthesia, Scientific reports 8(1) (2018) 1-11.

[15] A. Di Nardo, A. Vitiello, R.L. Gallo, Cutting edge: mast cell antimicrobial activity is mediated by expression of cathelicidin antimicrobial peptide, The Journal of Immunology 170(5) (2003) 2274-2278.

[16] N. Fukuishi, S. Murakami, A. Ohno, N. Yamanaka, N. Matsui, K. Fukutsuji, S. Yamada, K. Itoh, M. Akagi, Does β-hexosaminidase function only as a degranulation indicator in mast cells? The primary role of β-hexosaminidase in mast cell granules, The Journal of Immunology 193(4) (2014) 1886-1894.

[17] L. Lu, M. Kulka, L.D. Unsworth, Peptide-mediated mast cell activation: ligand similarities for receptor recognition and protease-induced regulation, Journal of Leukocyte Biology 102(2) (2017) 237-251.

[18] K. Lansu, J. Karpiak, J. Liu, X.-P. Huang, J.D. McCorvy, W.K. Kroeze, T. Che, H. Nagase, F.I. Carroll, J. Jin, In silico design of novel probes for the atypical opioid receptor MRGPRX2, Nature chemical biology 13(5) (2017) 529.

[19] V.B. Reddy, T.A. Graham, E. Azimi, E.A. Lerner, A single amino acid in MRGPRX2 necessary for binding and activation by pruritogens, Journal of Allergy and Clinical Immunology 140(6) (2017) 1726-1728.

[20] G. Grynkiewicz, M. Poenie, R.Y. Tsien, A new generation of Ca2+ indicators with greatly improved fluorescence properties, Journal of biological chemistry 260(6) (1985) 3440-3450.

[21] L. Lu, M.B. Parmar, M. Kulka, P. Kwan, L.D. Unsworth, Self-assembling peptide nanoscaffold that activates human mast cells, ACS applied materials & interfaces 10(7) (2018) 6107-6117.

[22] L. Lu, N. Arizmendi, M. Kulka, L.D. Unsworth, The Spontaneous Adhesion of BMMC onto Self-Assembled Peptide Nanoscaffold without Activation Inhibits Its IgE-Mediated Degranulation, Advanced Healthcare Materials 6(18) (2017) 1700334.

[23] G. Varricchi, A. Pecoraro, S. Loffredo, R. Poto, F. Rivellese, A. Genovese, G. Marone, G. Spadaro, Heterogeneity of human mast cells with respect to MRGPRX2 receptor expression and function, Frontiers in cellular neuroscience 13 (2019) 299.

[24] H.-P. Nothacker, Z. Wang, H. Zeng, S.K. Mahata, D.T. O'Connor, O. Civelli, Proadrenomedullin N-terminal peptide and cortistatin activation of MrgX2 receptor is based on a common structural motif, European journal of pharmacology 519(1-2) (2005) 191-193.

[25] K. Gupta, H. Subramanian, H. Ali, Modulation of host defense peptide-mediated human mast cell activation by LPS, Innate immunity 22(1) (2016) 21-30.

[26] K. Tatemoto, Y. Nozaki, R. Tsuda, S. Kaneko, K. Tomura, M. Furuno, H. Ogasawara, K. Edamura, H. Takagi, H. Iwamura, Endogenous protein and enzyme fragments induce immunoglobulin E-independent activation of mast cells via a G protein-coupled receptor, MRGPRX 2, Scandinavian journal of immunology 87(5) (2018) e12655.

[27] L. Malik, N.M. Kelly, J.-N. Ma, E.A. Currier, E.S. Burstein, R. Olsson, Discovery of non-peptidergic MrgX1 and MrgX2 receptor agonists and exploration of an initial SAR using solid-phase synthesis, Bioorganic & medicinal chemistry letters 19(6) (2009) 1729-1732.

[28] J. Grimes, S. Desai, N.W. Charter, J. Lodge, R. Moita Santos, A. Isidro-Llobet, A.M. Mason, Z. Wu, L.A. Wolfe III, L. Anantharaman, MrgX2 is a promiscuous receptor for basic peptides

causing mast cell pseudo-allergic and anaphylactoid reactions, Pharmacology research & perspectives 7(6) (2019) e00547.

[29] R. Malaviya, T. Ikeda, E. Ross, S.N. Abraham, Mast cell modulation of neutrophil influx and bacterial clearance at sites of infection through TNF-α, Nature 381(6577) (1996) 77-80.

[30] R. Malaviya, S.N. Abraham, Mast cell modulation of immune responses to bacteria, Immunological reviews 179(1) (2001) 16-24.

[31] A. Irani, T.R. Bradford, C.L. Kepley, N.M. Schechter, L.B. Schwartz, Detection of MCT and MCTC types of human mast cells by immunohistochemistry using new monoclonal anti-tryptase and anti-chymase antibodies, Journal of Histochemistry & Cytochemistry 37(10) (1989) 1509-1515.

[32] A.L. Christy, M.E. Walker, M.J. Hessner, M.A. Brown, Mast cell activation and neutrophil recruitment promotes early and robust inflammation in the meninges in EAE, Journal of autoimmunity 42 (2013) 50-61.

[33] K.S.H. Blatman, N. Gonsalves, I. Hirano, P.J. Bryce, Expression of mast cell–associated genes is upregulated in adult eosinophilic esophagitis and responds to steroid or dietary therapy, The Journal of allergy and clinical immunology 127(5) (2011) 1307.

[34] C.V. Velasquez, A.D. Roman, N.T.P. Lan, N.T. Huy, E.S. Mercado, F.E. Espino, M.L.M. Perez, V.T.Q. Huong, T.T. Thuy, V.D. Tham, Alpha tryptase allele of tryptase 1 (TPSAB1) gene associated with dengue hemorrhagic fever (DHF) and dengue shock syndrome (DSS) in Vietnam and Philippines, Human immunology 76(5) (2015) 318-323.

Chapter 6

[1] L. Lu, S. Raj, N. Arizmendi, J. Ding, G. Eitzen, P. Kwan, M. Kulka, L.D. Unsworth, Identification of short peptide sequences that activate human mast cells via mas-related g-protein coupled receptor member x2, Acta Biomaterialia. 136 (2021) 159–169.

[2] C. Yue, Y. Yang, C. Zhang, G. Alfranca, S. Cheng, L. Ma, Y. Liu, X. Zhi, J. Ni, W. Jiang, J. Song, J.M. de la Fuente, D. Cui, ROS-responsive mitochondria-targeting blended nanoparticles: Chemo- and photodynamic synergistic therapy for lung cancer with on-demand drug release upon irradiation with a single light source, Theranostics. 6 (2016) 2352–2366. https://doi.org/10.7150/thno.15433.

[3] D. Chen, G. Zhang, R. Li, M. Guan, X. Wang, T. Zou, Y. Zhang, C. Wang, C. Shu, H. Hong, L.J. Wan, Biodegradable, Hydrogen Peroxide, and Glutathione Dual Responsive Nanoparticles for Potential Programmable Paclitaxel Release, Journal of the American Chemical Society. 140 (2018) 7373–7376. https://doi.org/10.1021/jacs.7b12025.

[4] J. Wang, X. He, S. Shen, Z. Cao, X. Yang, ROS-Sensitive Cross-Linked Polyethylenimine for Red-Light-Activated siRNA Therapy, ACS Applied Materials and Interfaces. 11 (2019) 1855–1863. https://doi.org/10.1021/acsami.8b18697.

[5] X. Ling, S. Zhang, P. Shao, P. Wang, X. Ma, M. Bai, Synthesis of a reactive oxygen species responsive heterobifunctional thioketal linker, Tetrahedron Letters. 56 (2015) 5242–5244. https://doi.org/10.1016/j.tetlet.2015.07.059.

[6] D.S. Wilson, G. Dalmasso, L. Wang, S. v. Sitaraman, D. Merlin, N. Murthy, Orally delivered thioketal nanoparticles loaded with TNF-α-siRNA target inflammation and inhibit gene expression in the intestines, Nature Materials. 9 (2010) 923–928. https://doi.org/10.1038/nmat2859.

[7] P.J. Barnes, How corticosteroids control inflammation: quintiles prize lecture 2005, British Journal of Pharmacology. 148 (2006) 245–254.

Appendix

Supplementary tables for Chapter 5

Table 1. Primer and probes sequences for Tryptase and HPRT1

Target	Primer/probe	Sequence	Assay ID
TPSAB1, HOMO_SAPIENS	Forward primer	CAG TGG TGT TTT GGA CAG C	Hs.PT.58.19121290.g
	Reverse primer	CGG CCT GGC ATC TAC AC	
	Probe	/56-FAM/TGA CTC ACG /ZEN/GCT TTT TGG GGA CAT /3IABkFQ/	
HPRT1, HOMO_SAPIENS	Forward primer	GCG ATG TCA ATA GGA CTC CAG	Hs.PT.58v.45621572
	Reverse primer	TTG TTG TAG GAT ATG CCC TTG A	
	Probe	/5HEX/AGC CTA AGA /ZEN/TGA GAG TTC AAG TTG AGT TTG G/3IABkFQ	

Table 2. Truncated PAMP-12 peptide sequences

Peptide	Sequence	Net charge at pH 7.0	Iso-electric point (pH)
PAMP-12	FRKKWNKWALSR	+5	14
N-truncated peptides			
TS-N1	RKKWNKWALSR	+5	14
TS-N2	KKWNKWALSR	+4	14
TS-N3	KWNKWALSR	+3	14
TS-N4	WNKWALSR	+2	14
TS-N5	NKWALSR	+2	14
C-truncated peptides			
TS-C1	FRKKWNKWALS	+4	14
TS-C2	FRKKWNKWAL	+4	14
TS-C3	FRKKWNKW	+4	14
TS-C4	FRKKW	+3	14
TS-C5	FRKK	+3	14
TS-C6	FRK	+2	14
TS-C7	FR	+1	14
N+C-truncated peptides			
TS-N4C1	WNKWAL	+1	14
TS-N4C2	WNKWA	+1	14
TS-N4C3	WNKW	+1	14
TS-N4C4	WNK	+1	14
Net charges at pH 7.0 and iso-electric points were calculated by online tool: http://pepcalc.com/			

Table 3. Peptide library created through alanine scanning of PAMP-12

Peptide	Sequence	Net charge at pH 7.0	Iso-electric point (pH)
PAMP-12	FRKKWNKWALSR	+5	14
AS1	**A**RKKWNKWALSR	+5	14
AS2	F**A**KKWNKWALSR	+4	14
AS3	FR**A**KWNKWALSR	+4	14
AS4	FRK**A**WNKWALSR	+4	14
AS5	FRKK**A**NKWALSR	+5	14
AS6	FRKKW**A**KWALSR	+5	14
AS7	FRKKWN**A**WALSR	+4	14
AS8	FRKKWNK**A**ALSR	+5	14
AS10	FRKKWNKWA**A**SR	+5	14
AS11	FRKKWNKWAL**A**R	+5	14
AS12	FRKKWNKWALS**A**	+4	14
Net charges at pH 7.0 and iso-electric points were calculated by online tool: http://pepcalc.com/			

Table 4. Custom peptides used to test the generalized structure for mast cell activation *via* the MRGPRX2 receptor

Peptide	Sequence	Net charge at pH 7.0	Iso-electric point (pH)
CST1	KKW	+2	14
CST2	WKK	+2	14
CST3	KWKW	+2	14
CST4	WKKW	+2	14
CST5	FKKF	+2	14
CST6	YKKY	+2	10.38
CST7	YKKKY	+3	10.64
CST8	WKKKW	+3	14
CST9	FKKKF	+3	14
CST10	KWKWK	+3	14
CST11	KYKYK	+3	10.64
Net charges at pH 7.0 and iso-electric points were calculated by online tool: http://pepcalc.com/			

Table 5. Peptide sequences with generalized motifs that activates mast cell *via* MRGPRX2

Name	**Sequence**	**Functions**	**Net charge at pH 7.0**	**Iso-electric point**	**Reference**	**EC_{50}**
Mastoparan-B	LKLKSIVSWAKKVL-NH_2	Peptide toxin	+5.0	14	[1]	
Somatostatin	AGCKNFFWKTFTSC-OH	Neuro-peptides	+1.9	9.04	[2, 3]	
Cortistatin-14	PCKNFFWKTFSSCK-OH		+2.9	10.15	[1-3]	$MRGPRX_2$: 107 nM [1] Mrgprb2: 21 μM [1]
VIP	HSDAVFTDNYTRLRQMAVKKYLNSILN		+2.1	9.93	[3]	
PACAP	HSDGIFTDSYSRYRKQMAVKKYLAAVLGKRYKQRVKNK-NH_2		+10.1	11.08	[3]	
LL-37	LLGDFFRKSKEKIGKEFKRIVQRIKDFLRNLVPRTES	Antimicrobial peptides	+6.0	11.15	[4]	

Indolicidin	ILPWKWPWWPWRR-NH_2		+4.0	14	[3]	
β-defensin 2	GIGDPVTCLKSGAICHPVFCPRRYKQIGTCGLPGTKCCKKP		+5.7	9.16	[5]	
β-defensin 3	GIINTLQKYYCRVRGGRCAVLSCLPKEEQIGKCSTRGRKCCRRKK		+10.6	10.52	[5],	
PAMP -12	FRKKWNKWALSR-NH_2	Endogenous peptide	+6.0	14	[1]	MRGPRX$_2$: 166 nM [1] Mrgprb2: 12 μM [1]
Cetrorelix	Ac-D-Nal-D-Cpa-D-Pal-Ser-Tyr-D-Cit-Leu-Arg-Pro-D-Ala-NH_2	Peptide drugs			[1]	MRGPRX$_2$: 155 nM [1] Mrgprb2: 16.4 μM [1]
Octreotide	D-Phe-Cys-Phe-D-Trp-Lys-Thr-Cys-				[1]	MRGPRX$_2$:

	Thr-ol [Disulfide bridge: 2-7]					7 μM [1] Mrgprb2: 10 μM [1]
Leuprolide	Pyr-His-Trp-Ser-Tyr-D-Leu-Leu-Arg-Pro-NHEt				[1]	$MRGPRX_2$: 7 μM [1] Mrgprb2: 120 μM [1]
Underlined: X_a-$(Y)_{(n \geq 3)}$-X_b, or its reversed motifs: (i) X_a is a hydrophobic residue with an aromatic ring (F, Y and W, or unnatural Thi, Tic, D-Nal, D-Cpa, D-Pal); (ii) X_b is any hydrophobic residue (aromatic: F, Y and W, or unnatural Thi, Tic, D-Nal, D-Cpa, D-Pal, and aliphatic: A, V, I, L, M, or unnatural Oic, etc.); and (iii) Y must have a minimum of one positively charged residue (R and K) with the remainder being uncharged residues; Net charges at pH 7.0 and Iso-electric points were calculated by online tool: http://pepcalc.com/						

Table 6. Non-peptide stimuli for MRGPRX2 in bearing physiochemical properties in accordance with the generalized motif

Name	**Structures**	**Category**	**"Y"**	**"X_a" & "X_b"**
Compound 48/80 [1]	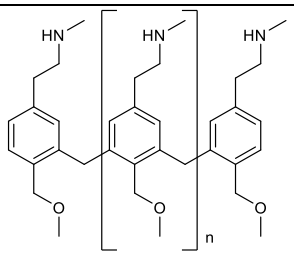	Polymer	Secondary amines	Benzene rings and saturated hydrocarbon
Atracurium [1]	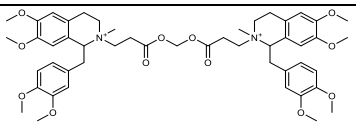	Drugs	Quaternary ammoniums	Benzene rings and saturated hydrocarbon
Tubocurarine[1]	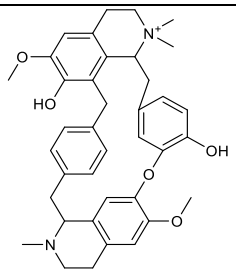		Quaternary ammonium and tertiary amine	Benzene rings and saturated hydrocarbon
Ciprofloxacin [1]	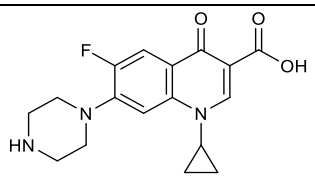		Secondary amine and tertiary amines	Benzene ring, fluorine and saturated hydrocarbon
Morphine [6]	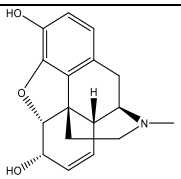		Tertiary amine	Benzene ring and saturated hydrocarbon
Dextrorphan [6]	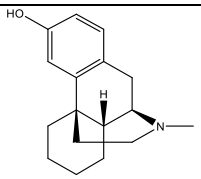		Tertiary amine	Benzene ring and saturated hydrocarbon

X_a and X_b are hydrophobic motifs including at least an aromatic ring; Y is positively charged motif.

References

[1] B.D. McNeil, P. Pundir, S. Meeker, L. Han, B.J. Undem, M. Kulka, X. Dong, Identification of a mast-cell-specific receptor crucial for pseudo-allergic drug reactions, Nature. 519 (2015) 237–241. https://doi.org/10.1038/nature14022.

[2] N. Robas, E. Mead, M. Fidock, MrgX2 Is a High Potency Cortistatin Receptor Expressed in Dorsal Root Ganglion, Journal of Biological Chemistry. 278 (2003) 44400–44404. https://doi.org/10.1074/jbc.M302456200.

[3] K. Tatemoto, Y. Nozaki, R. Tsuda, S. Konno, K. Tomura, M. Furuno, H. Ogasawara, K. Edamura, H. Takagi, H. Iwamura, M. Noguchi, T. Naito, Immunoglobulin E-independent activation of mast cell is mediated by Mrg receptors, Biochemical and Biophysical Research Communications. 349 (2006) 1322–1328. https://doi.org/10.1016/j.bbrc.2006.08.177.

[4] H. Subramanian, K. Gupta, Q. Guo, R. Price, H. Ali, Mas-related gene X2 (MrgX2) is a novel G protein-coupled receptor for the antimicrobial peptide LL-37 in human mast cells: Resistance to receptor phosphorylation, desensitization, and internalization, Journal of Biological Chemistry. 286 (2011) 44739–44749. https://doi.org/10.1074/jbc.M111.277152.

[5] H. Subramanian, K. Gupta, D. Lee, A.K. Bayir, H. Ahn, H. Ali, β-Defensins Activate Human Mast Cells via Mas-Related Gene X2, The Journal of Immunology. 191 (2013) 345–352. https://doi.org/10.4049/jimmunol.1300023.

[6] K. Lansu, J. Karpiak, J. Liu, X.P. Huang, J.D. McCorvy, W.K. Kroeze, T. Che, H. Nagase, F.I. Carroll, J. Jin, B.K. Shoichet, B.L. Roth, In silico design of novel probes for the atypical opioid

receptor MRGPRX2, Nature Chemical Biology. 13 (2017) 529–536. https://doi.org/10.1038/nchembio.2334.